BIOLOGICAL CHARACTERIZATION OF ARSENITE OXIDIZING BACTERIA FROM TERRESTRIAL ECONICHES OF GOA

Thesis submitted to Goa University

For the Award of the Degree of

DOCTOR OF PHILOSOPHY

In

MICROBIOLOGY

By

Ms. MUJAWAR SAJIYA YUSUF

Under the guidance of

Prof. Santosh Kumar Dubey
(Research Guide)
Department of Microbiology,
Goa University, Goa, India

Prof. Sandeep Garg
(Co-Guide)
Department of Microbiology,
Goa University, Goa, India

July 2020

CERTIFICATE

This is to certify that **Miss Mujawar Sajiya Yusuf** has worked on the thesis entitled "**Biological characterization of arsenite oxidizing bacteria from terrestrial econiches of Goa**" under my supervision and guidance.

This thesis, being submitted to the Goa University, Goa, India, for the award of the degree of Doctor of Philosophy in Microbiology is an original record of research work carried out by the candidate herself and has not been submitted for the award of any other degree or diploma of this or any other university in India or abroad.

Prof. Santosh Kumar Dubey

Research Guide

Department of Microbiology

Goa University

Prof. Sandeep Garg

Co-Guide

Department of Microbiology

Goa University

DECLARATION

I hereby state that the present thesis entitled “Biological characterization of arsenite oxidizing bacteria from terrestrial econiches of Goa” is my original contribution, and the same has not been previously submitted for the award of degree/diploma to any Institute or University. To the best of my knowledge, the present study is the first comprehensive work of its kind from this area.

Sajiya Yusuf Mujawar
Department of Microbiology
Goa University
July 2020

STATEMENT

As required under the Goa University Ordinance OA-19.8 (viii), I hereby state that the present thesis entitled “Biological Characterization of Arsenite Oxidizing Bacteria from Terrestrial Econiches of Goa” is my original contribution, and the same has not been previously submitted for the award of degree/diploma to any institute or University.

To the best of my knowledge, the existing study is the first comprehensive work of its kind from this area. The literature related to the problem investigated has been cited. Due acknowledgement has been made wherever facilities and suggestions have been availed of. All the suggestions made by honourable examiner (s) have been incorporated in the thesis.

Sajiya Yusuf Mujawar	**Prof. Santosh Kumar Dubey**	**Prof. Sandeep Garg**
(Student)	(Research Guide)	(Co-Guide)
Department of Microbiology	Department of Microbiology	Department of Microbiology
Goa University	Goa University	Goa University

ACKNOWLEDGEMENT

Completion of my research work and thesis would not have been possible without the support of number of people. I would like to extend my sincere appreciation and gratitude to all who have helped me in this study.

First of all, I am thankful to Almighty Allah for blessing me with enough strength, good health and determination to complete this research work.

I would like to express my deep and sincere gratitude to my supervisor **Prof. Santosh Kumar Dubey** for his immense encouragement, guidance and continuous support throughout my Ph. D. tenure. I am highly obliged for his valuable scientific inputs, discussions, constructive comments, suggestions and guidance throughout the study. I also express my sincere thanks to my Co-guide **Prof. Sandeep Garg** for his kind support, guidance and comments on my research.

I would like to thank **Prof. Varun Sahni**, the Vice Chancellor of Goa University and **Prof. P.K. Sharma**, Dean of Life Sciences and Environment for providing necessary infrastructure and resources to accomplish my research work. I am thankful to **Prof. Sandeep Garg**, Head of Department of Microbiology for giving me necessary permissions, resources and infrastructural facilities to accomplish my research work and also for his help in administrative procedure during my study.

I greatly acknowledge the University Grants Commission, New Delhi, for financial assistance through the UGC-MANF fellowship program. I also thank my V.C.'s nominee **Prof. Sanjeev Ghadi** and **Dr. Rakhee Khandeparker** for their review, valuable advice and comments, which helped me to improve Ph.D. work.

My sincere thanks also go to all the Faculty members of Department of Microbiology Prof. Irene Furtado, Prof. Sarita Nazareth, Dr. Lakshangy, Dr. Milind, Dr. Priya, Dr. Trelita, Dr. Bhakti, Dr. Gauri, Dr. Meghnath, Dr. Sanika, Dr. Shyamalina, Dr. Varada, Dr. Trupti, Dr. Delicia, Ms. Snigdha and Dr. Pooja for their encouragement and feedback all through . I would like to offer my special thanks to **Dr. Shyamalina Haldar**, **Dr. Milind Mohan Naik** and **Dr. Priya D'costa** for their friendly support, encouragement and guidance during the Ph.D. tenure.

I want to extend my appreciation to my colleagues **Ashwini, Aarti, Dr. Kashif, Dr. Jaya, Kiran, Richard, Rahul, Alisha, Sulochana, Dr. Neha, Dr. Jyothi, Dviti, Komal and Aabha** for their suggestions, help and support.

I thank Mr. M. G. Lanjewar from the University Science Instrumentation Centre, Goa University for SEM analysis. I would like to thank Mr. Areef Sardar from the National Institute of Oceanography, Goa for EDX analysis and AIRF, Jawaharlal Nehru University, New Delhi for TEM-EDX analysis. I am also thankful to Prof. B.R. Srinivasan, Head and Mr. Rahul Kerkar from the Department of Chemistry, Goa University for FTIR analysis. I am grateful to Dr. Santhakumari and Ms. Reema Banerjee from the National Chemical Laboratory, Pune, for carrying out the proteomic analysis.

I am deeply grateful to all Non-teaching staff of our Department Mrs. Saraswati, Ms. Deepashri, Mrs. Afra, Mr. Buddhaji, Mr. Dominic, Mr. Narayana, Mr. Tanu, Mr. Rajesh, Mr. Gajanan, Mr. Bhushan, Mrs. Prathana, Ms. Vandana and Mrs. Yojana for their support during my candidature.

I would like to express my greatest appreciation to my family and friends for their endless support throughout my journey. I express my heartfelt gratitude to my father **Mr. Yusuf A.R Mujawar**, my mother **Mrs. Aktari Mujawar**, my brothers **Mr. Jikriya Mujawar**

and **Mr. Suhail Mujawar** for their never-ending love, encouragement and unconditional support throughout my life. They have been selfless in giving me the best of everything and I express my deep gratitude for their love. I could complete this extensive journey indeed due to their constant blessings, support and love.

It is said that "Good Friends are Hard to Find," but I was blessed to have them. I would like to express my heartfelt gratitude to **Ms. Diviya Vaigankar** and **Mr. Sanket Gaonkar** for their constant help, support, and encouraging me whenever I lost hope and confidence. I genuinely thank them for sticking by my side, even when I was irritable and depressed. This journey would not have been possible without two of you all. Thank you for everything.

Lastly, I would like to thank everybody who has any kind of contribution to this thesis in some way or other.

Sajiya Mujawar

ABBREVIATIONS

DCIP	2,6-dichlorophenolindophenol
ADP	Adenosine diphosphate
ATP	Adenosine triphosphate
APS	Ammonium persulphate
As(V)	Arsenate
As	Arsenic
Ars	Arsenic resistance system
As (III)	Arsenite
Aio	Arsenite oxidase
aioA	Arsenite oxidase large subunit
aioB	Arsenite oxidase small subunit
bp	Base pair
BLAST	Basic local alignment search tool
BSA	Bovine serum albumin
Cd	Cadmium
Cm	Centimetre
Cu	Copper
Conc.	Concentration
CFU	Colony forming unit
°C	Degree celsius
DNA	Deoxyribonucleic acid
DTT	Dithiothreitol
EDAX	Energy dispersive X-ray spectroscopy
EDTA	Ethylenediaminetetraacetic acid
FDR	False discovery rate
FTIR	Fourier-transform infrared spectroscopy
g	Gram
GMO	Genetically modified microorganisms
h	Hour
Fe	Iron
kb	Kilobase pair
kDa	Kilodalton

KEGG Kyoto encyclopedia of genes and genomes

Pb Lead

L Litre

LC-MS Liquid chromatography mass spectrometry

MTC Maximum tolerance concentration

µm Micro meter

µg Microgram

µL Microlitre

mg Milligram

mL Millilitre

mm Millimetre

mM Millimolar

MSM Mineral salt medium

MIC Minimum inhibitory concentration

Min Minute

M Molar

MES Morpholinoethelene diol sulfonic acid

ng Nanogram

ng/m3 Nanogram per cubic meter

nm Nanometre

Ni Nickel

NCBI National centre for biotechnology information

OD Optical density

min^{-1} Per minute

% Percentage

PMSF Phenylmethylsulfonyl fluoride

PBS Phosphate buffer saline

PCR Polymerase chain reaction

pit phosphate inorganic transport system

pst phosphate specific transport system

KBr Potassium bromide

rpm Revolutions per minute

RNA Ribonucleic acid

SEM Scanning electron microscopy

sec Second

$AgNO_3$ Silver nitrate

$NaAsO_2$ Sodium arsenite

SDS-PAGE Sodium dodecyl sulphate-Polyacrylamide gel electrophoresis

Na_2MoO_4 Sodium molybdate

sp. Species

H_2SO_4 Sulfuric acid

TOF Time of flight

TEM Transmission electron microscopy

TAE Tris acetate EDTA

TE Tris-EDTA

US-EPA United States Environmental Protection agency

V Volts

WHO World health organisation

Zn Zinc

LIST OF TABLES

Chapter V

LIST OF FIGURES

Chapter IV

Chapter V

CONTENTS

	2.4 Determination of arsenite oxidizing ability of bacterial isolates	
	2.5 Isolation of plasmid DNA	
	2.6 Extraction of chromosomal DNA	
	2.7 PCR amplification of arsenite oxidase (*aioA*) and transporter (*ACR3*) genes	
	2.8 Identification of selected arsenite oxidizing bacterial isolates	
	2.8.1 Morphological and biochemical characterization	
	2.8.2 PCR amplification and DNA sequencing of 16S rRNA gene	
	2.9 Determination of Minimum Inhibitory Concentration (MIC) of sodium (meta) arsenite for bacterial isolates	
	2.10 Determination of optimal growth conditions for selected arsenite oxidizing bacterial isolates	
	2.11 Study of growth behaviour of selected arsenite oxidizing bacterial isolates in the presence of arsenite	
	2.12 Fourier transformed infrared (FTIR) spectroscopic analysis of selected arsenite oxidizing bacterial isolates	
	2.13 SEM-EDAX analysis of selected arsenite oxidizing bacterial isolates	
	2.14 TEM-EDAX analysis of selected arsenite oxidizing bacterial isolates	
	2.15 Quantitative analysis of arsenate	
	2.16 Arsenite oxidase enzyme assay	
	2.16.1 Preparation of cell-free extract	

Chapter I

Introduction

1.1 Introduction

Heavy metals are defined as metals with a density above 5 g/cm^3 and are widely distributed in the environment due to natural as well as anthropogenic activities (Nies, 1999). Contamination of environment with heavy metals and metalloids is a matter of great concern because they tend to persist indefinitely, circulating and accumulating throughout the food chain, thus posing a severe threat to the entire biota along with human beings (Ali et al., 2019). Among the metalloids, arsenic is the most significant environmental concern due to its hazardous nature (Gebel, 2000; Hughes et al., 2011).

Arsenic enters into the environment via natural viz. volcanic eruptions, weathering of rocks and leaching processes as well as anthropogenic viz. mining, industrial and agricultural activities (Smedley and Kinniburgh, 2002; Stolz et al., 2010; Khoei et al., 2018). Environmental exposure to arsenic is associated with soil, water and air. The adverse health effects of arsenic on humans depend strongly on the dose, species and duration of exposure. Acute effects of exposure to high levels of arsenic range from gastrointestinal distress viz. nausea, diarrhoea, abdominal pain leading to death. Chronic exposure to arsenic is associated with irritation of the skin and mucous membranes, cancer, neurological and cardiovascular disorders (Meliker et al., 2007; Zhu et al., 2008; Hughes et al., 2011; Mazumder and Dasgupta, 2011).

Numerous Physico-chemical processes have been used to remove arsenic from contaminated environments. However, due to the several disadvantages associated with the use of these processes has led to the development of microbe mediated transformation processes, which are environmentally friendly and economically viable (Kumari and Jagadevan, 2016). Microbial transformations such as reduction, oxidation and

methylation help in mobilization and biogeocycling of arsenic in the environment (Lloyd and Lovely, 2001; Chang et al., 2011). Moreover, microorganisms have also adopted various strategies such as extracellular precipitation, chelation, intracellular sequestration, transporter proteins and metal-specific efflux pumps as a means to detoxify arsenic toxicity in the environment (Chang et al., 2011; Kruger et al., 2013). Thus, it is crucial to isolate bacteria which possess mechanisms to resist arsenite stress followed by its biotransformation into arsenate, hence, leading to its bioremediation.

1.2 Review of Literature

1.2.1 Arsenic

Arsenic (As) with atomic number 33 ranks 20th element in abundance and is present at concentrations of 1.5-2.0 ppm in the earth's crust (National Research Council, 1977). It was first documented by Albertus Magnus in 1250 and occurs in both organic as well as inorganic forms (Rosen et al., 1999; Mandal and Suzuki, 2002). In nature, inorganic arsenic exists in several oxidation states such as arsine [As (-III)], elemental arsenic [As (0)], arsenite [As (III)] and arsenate [As (V)] but latter two are most commonly found in the environment (Oremland and Stolz, 2003; 2005). The organic forms of arsenic also known as organo-arsenicals include monomethylarsonic acid (MMMA), dimethylarsinic acid (DMAA), trimethylarsine oxide (TMAO), arsenobetaine and arsenocholine (Grund et al., 2000; Páez-Espino et al., 2009).

Arsenic has been widely used in paints, metal alloys for electronic circuitry, wood preservative, insecticides, pesticides, optical glass and also as an anti-cancer agent to treat lymphoma and leukaemia (Novick and Warrell, 2000; Rahman et al., 2004; Sadaf et al., 2018). For example, monosodium arsenate, disodium arsenate and diethyl arsenic

acid were used in the agriculture sector as insecticides, herbicides and larvicides, respectively, while chromated copper arsenate was used as a wood preservative. Roxarsone was used as a nutritional supplement for poultry, whereas various arsenic compounds viz. gallium arsenide, indium arsenide and aluminum arsenide were used as semiconductor alloy in computer hardware and electronic chips to modify connectivity and plasticity (Palma-Lara et al., 2020). Although arsenic has medicinal, industrial and agricultural applications, at higher concentrations it exhibits toxicity to plants and carcinogenicity to humans and animals (Niazi et al., 2017; Shakoor et al., 2018).

1.2.2 Arsenic in the environment

Arsenic contamination results due to both natural geogenic and anthropogenic activities (Fig. 1.1). Geogenic sources include natural weathering of rocks and minerals, volcanic dust fluxes, hydrothermal ore deposits and fossil fuels (Smedley and Kinniburgh, 2002; Fendorf et al., 2010). Anthropogenic sources of arsenic include arsenic-based pesticides (herbicides, fungicides, insecticides), wood preservatives, pigments, anti-fouling paints, dyes and food additives (Cheng et al., 2009; Hughes et al., 2011; Khoei et al., 2018). The primary anthropogenic input derives from mining, storage batteries, combustion of municipal solid waste, industrial waste, fossil fuels and release from metal smelters (Mondal et al., 2006; Bundschuh et al., 2011). The estimated global average level of arsenic in soil is 5 mg kg^{-1}, in open seawater is 1-2 μg L^{-1} and in air in the range of 1-3 ng m^{-3} for low anthropogenic activity areas, whereas 20-30 ng m^{-3} for high anthropogenic activity areas and 100-300 ng m^{-3} in industrial zones (ATSDR, 2013; Chakrabarti et al., 2018).

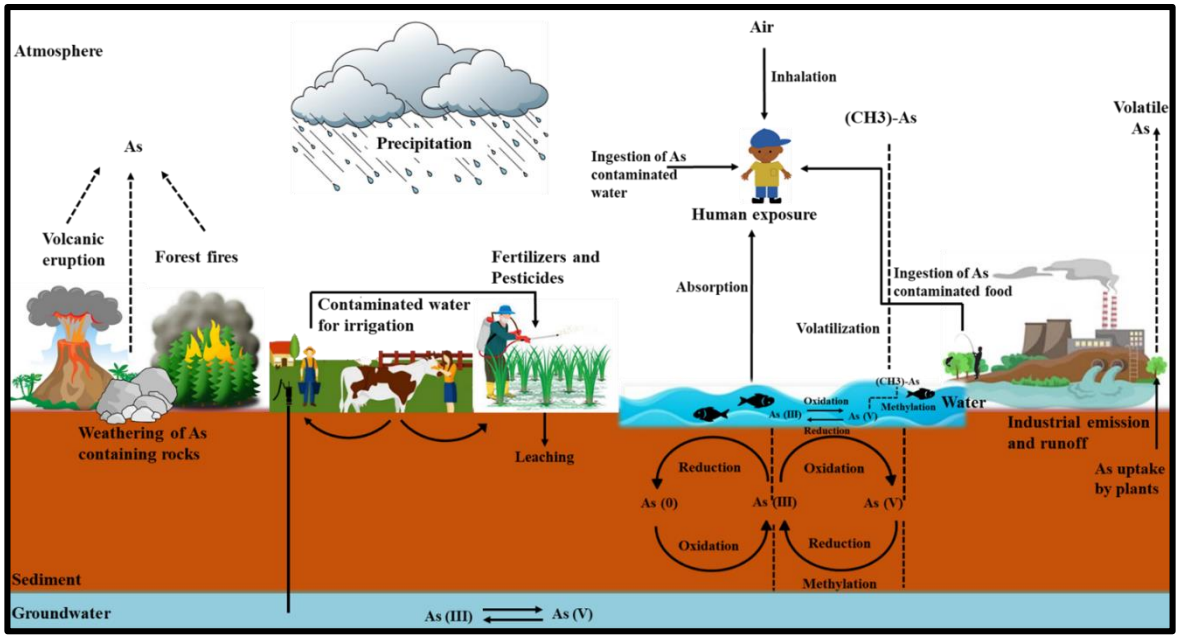

Fig. 1.1: Arsenic cycle in the environment.

Microbes play a vital role in the geocycling of arsenic in the environment (Fig. 1.2) (Mukhopadhyay et al., 2002). Arsenite can be released by arsenate respiring bacteria from sediments containing arsenate resulting in contamination of groundwater (Stolz et al., 2006). Further, the released arsenite can be oxidized by certain bacteria to arsenate (Santini et al., 2000; Stolz et al., 2006). These inorganic arsenicals are taken up by phytoplankton and macroalgae, get transformed to methyl-arsenicals and complex organo-arsenicals inside the cells followed by cell lysis resulting in their release back to the aquatic environment. These marine organisms are also an important food source for animals of higher trophic level in the food chain in the aquatic ecosystem, thus resulting in accumulation of arsenic (Rahman et al., 2012). Among marine organisms, crustaceans and molluscs accumulate higher concentrations of arsenic as compared to fish in their soft tissues. Moreover, arsenosugars and arsenolipids are transformed into arsenobetaine by marine organisms, which are further converted into inorganic arsenic species from

coastal water as well as sediments. These complete the biological cycle of arsenic in the marine ecosystem (Mukhopadhyay et al., 2002; Dembitsky et al., 2004).

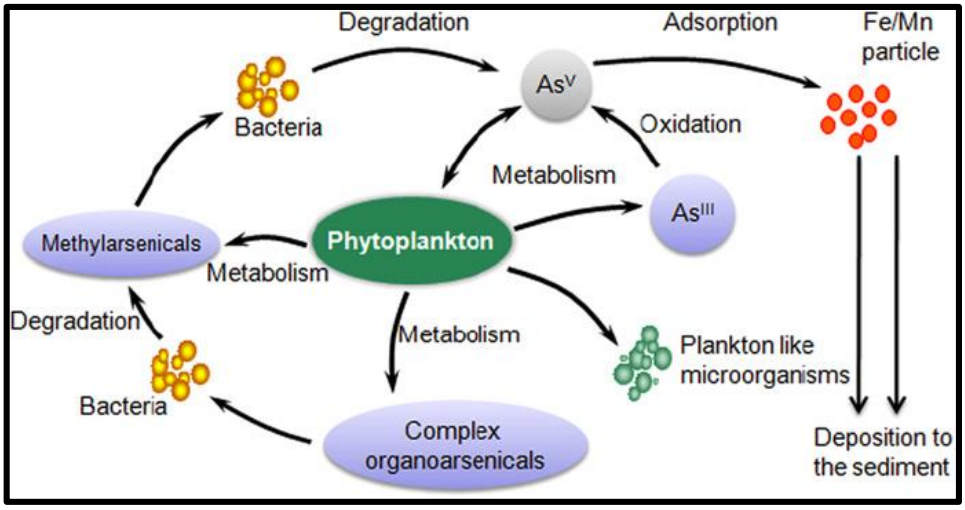

Fig. 1.2: The biotransformation and biogeochemical cycle of arsenic species in the aquatic ecosystem (Rahman et al., 2012).

1.2.3 Toxicity and health hazards of arsenic

Arsenic is classified as Group-I human carcinogen by WHO (Nidheesh and Singh, 2017). Exposure routes of arsenic in humans commonly include ingestion, inhalation of dust containing arsenic, dermal contact and through drinking water (Khairul et al., 2017; Shakoor et al., 2017). Its toxicity depends on the oxidation state, bioavailability, intake rate/exposure time, frequency and route of intake (Rosen and Liu, 2009). The inorganic forms of arsenic species are known to be more toxic than organic forms, and toxicity of inorganic arsenicals decreases with increasing oxidation state (Nriagu, 1984; Hughes et al., 2011). Furthermore, arsenite is 100 times more toxic than arsenate, as it is a more soluble and mobile form (Rosen, 2002; Quéméneur et al., 2010).

Arsenite has a very high affinity for thiol groups and reacts with thiol groups present on active sites of many enzymes resulting in its inhibition (Hughes, 2002). Similarly, it also inhibits cellular glucose uptake, gluconeogenesis, fatty acid oxidation and further production of acetyl CoA (Hughes, 2002). Effect of arsenate partially occurs because it gets transformed into arsenite and its toxicity proceeds after that. The toxicity of arsenate lies in its ability to resemble inorganic phosphate and substitutes phosphate in glycolytic and cellular pathways. Because of its similarity to phosphate in size and valency, it gets preferably incorporated into ADP to form ADP-arsenate instead of ATP (Fig. 1.3). This molecule of ADP-arsenate undergoes a futile cycle of hydrolysis where the cleavage of ADP-arsenate bond yields no energy required for the cellular metabolic activities (Anderson et al., 1992; Ali et al., 2012).

The majority of arsenic enters the body in the trivalent inorganic form (arsenite) via simple diffusion mechanism, and only a small amount of arsenate can cross cell membranes through an energy-dependent transport system, after which it is immediately reduced to arsenite that subsequently binds to DNA or protein molecules (Jomova et al., 2011; Shakoor et al., 2017). In the body, arsenite is taken in a protein-bound form having successive reductive methylation by arsenic methyltransferase to less toxic pentavalent intermediates in the presence of cofactor glutathione (GSH) and S-adenosylmethionine (SAM). These end products are finally excreted in the urine (Fig. 1.3) (Jomova et al., 2011; Khairul et al., 2017; Shakoor et al., 2017) while some portion of it gets accumulated in hair and nails at concentrations higher than 1 μg g^{-1} and 1.5 μg g^{-1} respectively (Marchiset-Ferlay et al., 2012).

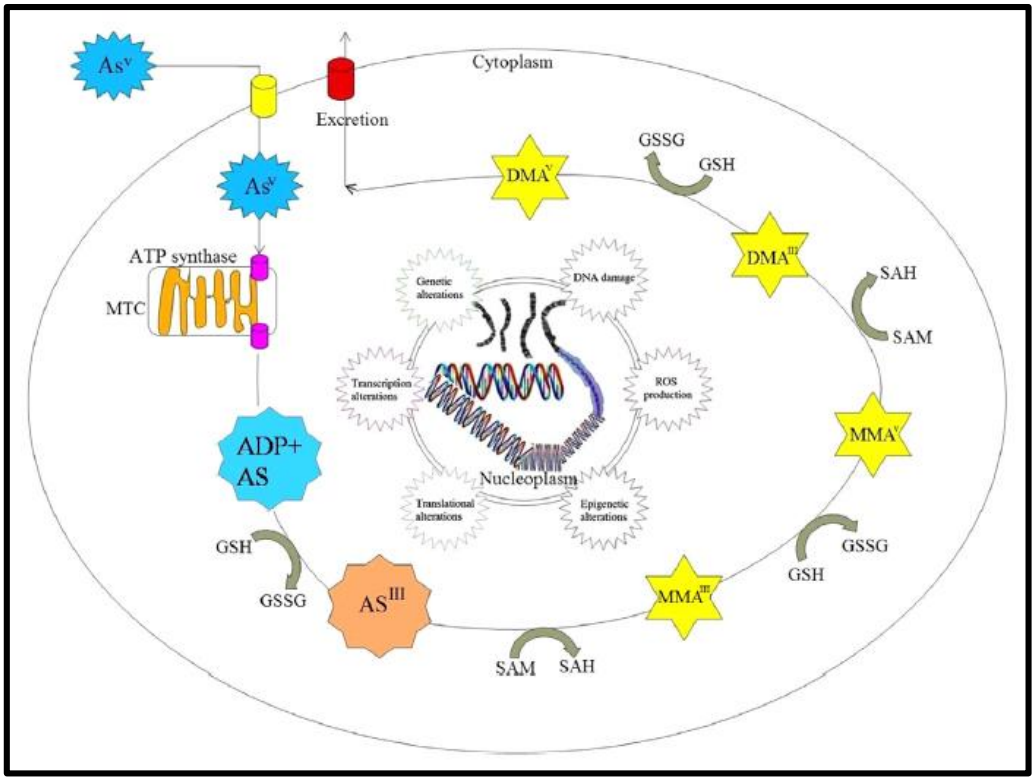

Fig. 1.3: Mechanism of arsenic toxicity (Sodhi et al., 2019).

Arsenic is known to cause several severe diseases in humans by interfering/ altering different mechanisms viz. cell signalling, cell cycle control, oxidative stress, mitochondrial damage, DNA methylation, DNA repair, proliferation of cell and tumour development (Hughes, 2002; Ebele, 2009; Naujokas et al., 2013) (Fig. 1.4). It is also carcinogenic and has been reported to cause skin, lung, uterus, liver and bladder cancer (Mandal and Suzuki, 2002; Rahman et al., 2009; Mazumder and Dasgupta, 2011; Shakoor et al., 2017; Palma-Lara et al., 2020). Chronic arsenic poisoning can also cause melanosis (hyper-pigmentation/ hypopigmentation or white spots), hyperkeratosis (harden skin), restrictive lung disease, peripheral heart disease, black foot disease, gangrene, diabetes mellitus, hypertension and ischemic heart disease (Dani, 2010; Jomova et al., 2011; Khairul et al., 2017). Exposures to high concentrations of inorganic arsenic can also cause infertility and miscarriages in women, declining resistance to

infections, brain damage and cardiovascular diseases including hypertension, coronary artery disease, peripheral vascular disease and atherosclerosis (Walton et al., 2004; Rahman et al., 2009).

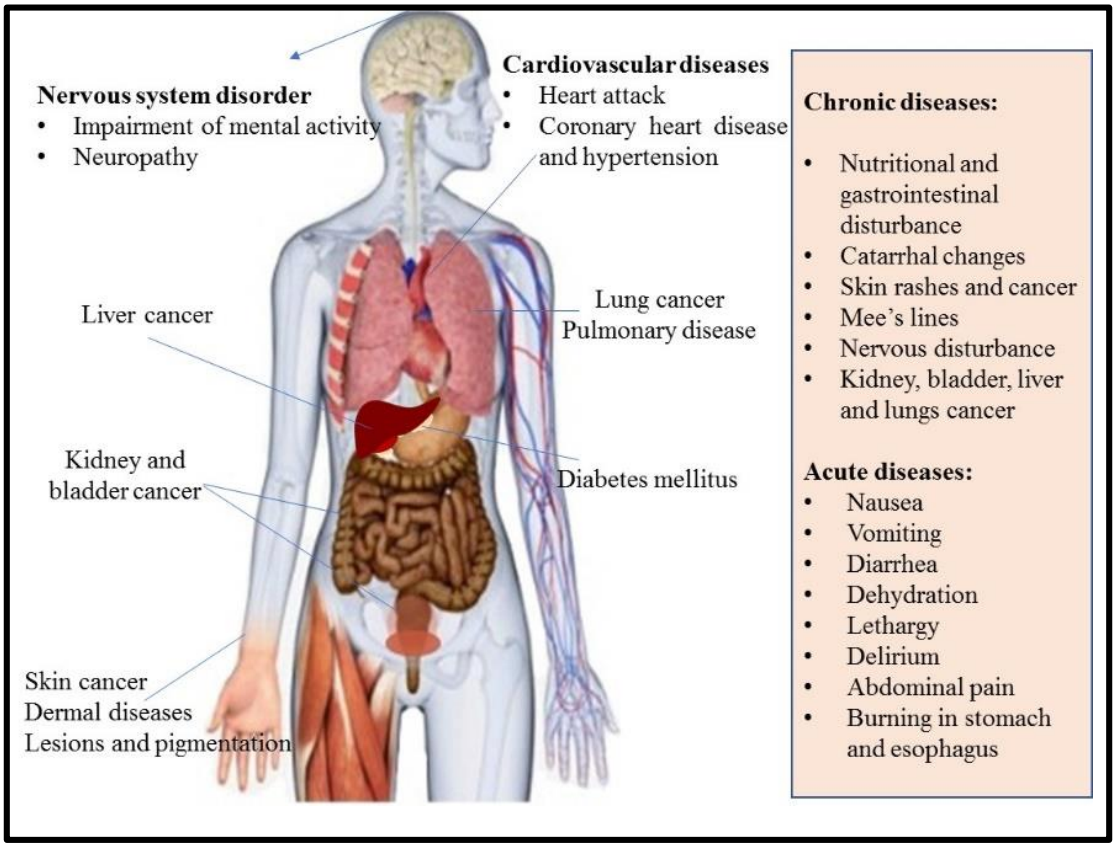

Fig. 1.4: Effects of arsenic toxicity on human health (Shahid et al., 2018).

1.2.4 Status of arsenic contamination around the world

The presence of arsenic in the environment has become a major concern in many countries around the world. The contamination of groundwater with arsenic has been reported from several countries including Argentina, Bangladesh, Chile, China, India, Japan, Mexico, Mongolia, Nepal, Poland, Taiwan and Vietnam (Tuli et al., 2010; Singh and Kumar, 2012; Rahman et al., 2014). However, in South Asian countries namely, Bangladesh, Cambodia, India and Vietnam, the problem of arsenic contamination in

groundwater is extreme (Argos et al., 2010; Singh and Kumar et al., 2012). Additionally, the use of arsenic-contaminated groundwater for irrigation of agricultural soils must have significantly contributed to the accumulation of arsenic in both soils and plants (Zhao et al., 2010). The transfer of arsenic to the food chain will ultimately remain a long-term risk to humans and the ecosystem (Tuli et al., 2010; Bhowmick et al., 2018).

The United States Environmental Protection Agency (US EPA) and Agency for Toxic Substances and Disease Registry (ATSDR) has ranked arsenic at the first position on the list of hazardous materials (Zhu et al., 2014). Taking into account the toxicity of arsenic compounds, the World Health Organization (2014) has set the permissible limit of arsenic in drinking water up to 10 μg L^{-1} while in Australia it is set up to 7 μg L^{-1} (Singh et al., 2015; Shewale et al., 2017). Nearly 200 million people are estimated to suffer from health problems in many countries in the world through drinking of arsenic-contaminated water with a level above 50 μg L^{-1} (Nicomel et al., 2016). It has been reported that about 79.9 million and 42.7 million people in Bangladesh and India, respectively, are exposed to arsenic-contaminated groundwater with concentrations above 50 μg L^{-1} (Zhu et al., 2014). In India, Assam, Bihar, Chhattisgarh, Jharkhand, Manipur, Uttar Pradesh, and West Bengal were also found exposed to arsenic-contaminated tube-well drinking water above 50 μg L^{-1} (Singh and Singh, 2015; Alam et al., 2016; Shewale et al., 2017).

1.2.5 Techniques of arsenic remediation

Arsenic contaminated drinking water and soil is a major threat to humanity. Various physical, chemical and biological methods have been used to remove arsenic from the environment under both laboratory and field conditions (Fig. 1.5). The physical

methods include soil washing by acids, immobilization of soluble arsenite using cement, filtration, use of surfactants, co-solvents, osmosis and cyclodextrin to assist soil flushing (Lim et al., 2014). The chemical methods involve strategies such as ion exchange, adsorption with activated alumina and activated carbon, reverse osmosis, complexation with metal ions followed by coagulation, immobilization and modified coagulation along with filtration and precipitation. Other alternative methods to reduce arsenic toxicity include nanofiltration, distillation, vacuum-UV irradiation and ultrafiltration of drinking water (Das et al., 2009; Dabrowska et al., 2012). The major drawbacks of these physicochemical processes are that they require high energy inputs, intensive labour, use of chemical treatments which generate secondary wastes altering soil characteristics posing a severe threat to native soil microflora (Ali et al., 2013).

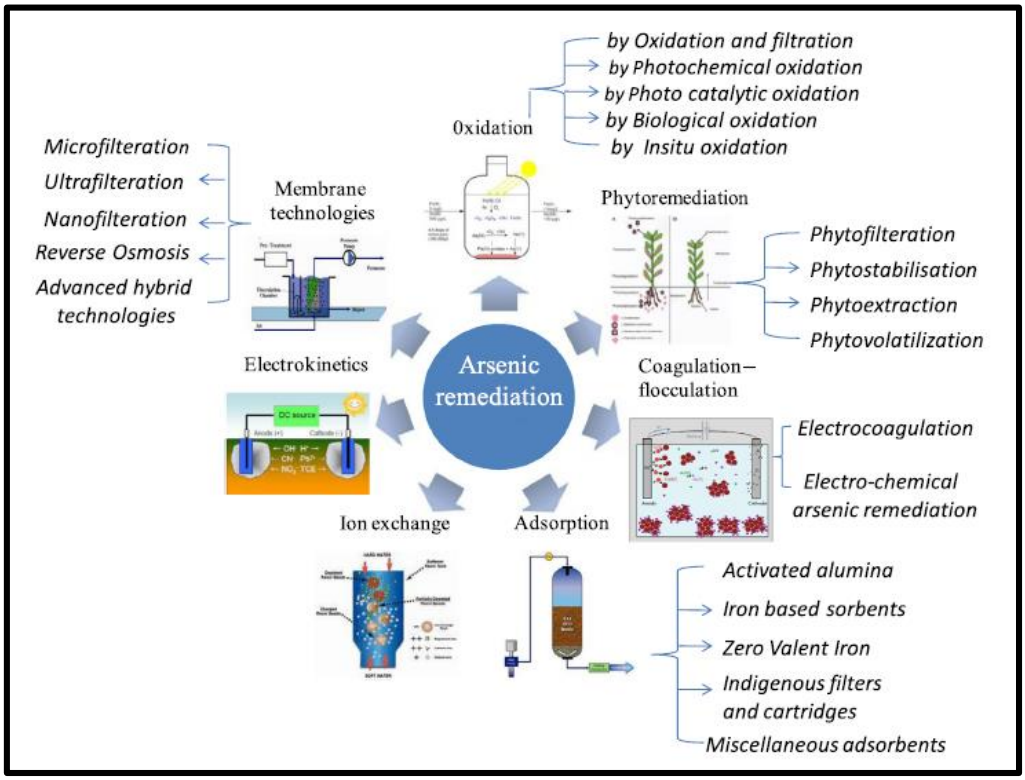

Fig. 1.5: Schematic diagram showing various techniques used for the removal of arsenic from soil and water (Singh et al., 2015).

The biological detoxification is a potentially cost-effective alternative over physicochemical methods for removal of organic and inorganic arsenic from contaminated environments (Battaglia-Brunet et al., 2002). The process of bioremediation involves the use of algae, fungi, bacteria, archaea and plants to remove arsenic from the air, soil and water (Singh and Singh, 2015; Ahmad et al., 2017). Bioremediation through plants is known as phytoremediation and includes phytoextraction, phytofiltration, phytostabilization and phytovolatization processes (Singh et al., 2015). Biological treatment includes biosorption and bioaccumulation, which involves intracellular mechanisms such as metal binding, methylation, oxidation-reduction reactions and intracellular precipitation (Malik et al., 2009; Ahmad et al., 2017). Sometimes, the biological treatment process can work exclusively or may be followed by other conventional treatment processes. Various aspects like metal uptake, sequestration, detoxification mechanism and resistance in the biological system have been studied at the molecular level in bacteria, but they still require extensive research to explore the potential of microbes in arsenic bioremediation (Ali et al., 2013).

1.2.6 Arsenic resistance in bacteria and it's biotransformation

The biogeochemical cycle of arsenic strongly depends on the microbial transformation that affects its mobility and distribution in the environment (Tamaki and Frankenberger, 1992). Despite arsenic toxicity, bacteria have evolved with several resistance mechanisms such as arsenate reduction, extrusion of arsenite from the cell interior, arsenite oxidation and methylation of arsenic to transform arsenic to less toxic forms (Silver and Phung, 2005; Páez-Espino et al., 2009) (Fig. 1.6, Table 1.1). These redox reactions are mostly carried out by microorganisms either for detoxification or for the generation of energy to support cellular growth.

1.2.6.1 Uptake of arsenic by bacterial cells

Arsenic uptake by prokaryotic cells is catalysed by various existing transporter proteins due to the structural similarity of arsenite and arsenate to their substrates (Rosen and Liu, 2009). Arsenate enters into the cells through phosphate transporter proteins such as pit (phosphate inorganic transport system) and pst (phosphate specific transport system). Studies in *Escherichia coli* has confirmed that pit plays an important role in arsenate uptake (Willsky and Malamy, 1980 a, b; Rosen, 2002). Pit is a constitutive transmembrane protein, and the uptake of ion is driven by proton motive force performing bidirectional flow of divalent ions. In contrast, pst is an ABC type periplasmic transporter protein responsible for the influx of ions such as phosphate and arsenate. Arsenite enters into the cell via glycerol transporters such as GlpF (Tsai et al., 2009). The mechanism of arsenite transport by GlpF has been identified and studied in *E. coli* (Meng et al., 2004). Similar GlpF homologues have also been identified in other organisms such as *Leishmania major* and *Pseudomonas putida* (Gourbal et al., 2004; Páez-Espino et al., 2009).

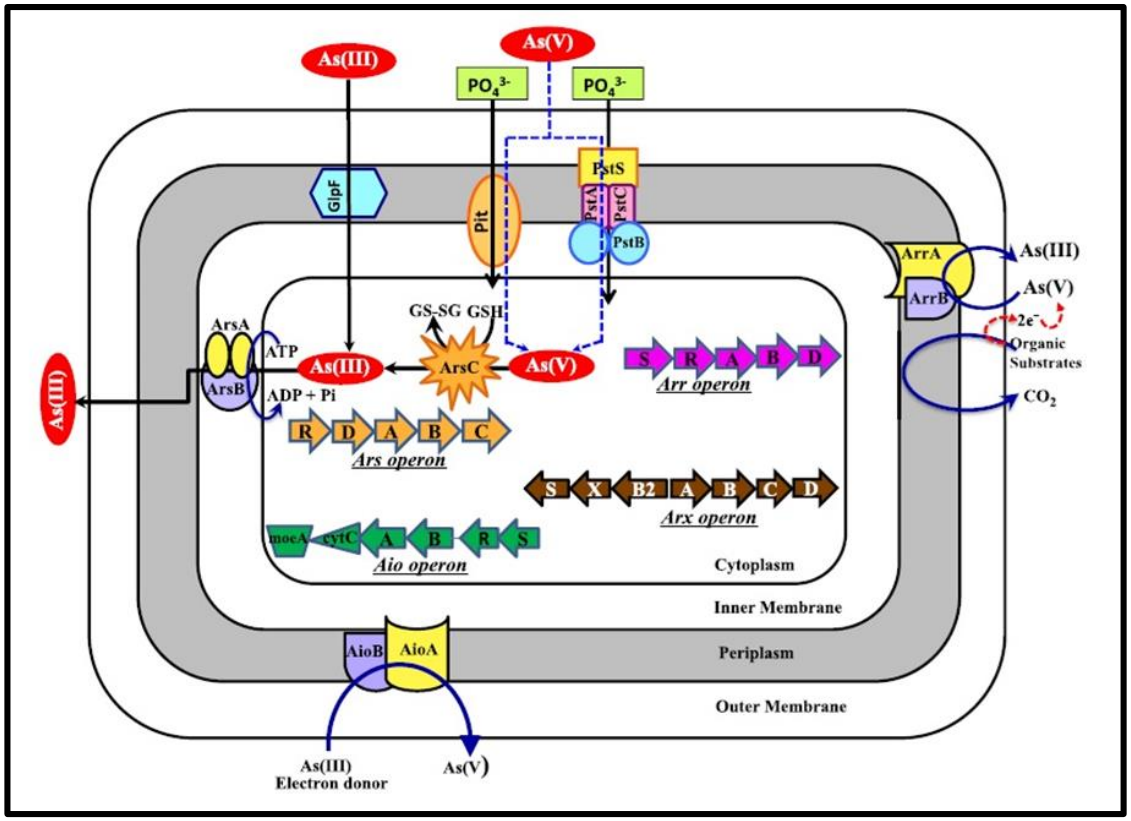

Fig. 1.6: Schematic representation of microbial redox processes that take place in arsenic metabolizing bacteria (Kumari et al., 2016).

Table 1.1: List of arsenic resistant microorganisms.

Organisms	Isolation sites	Mechanism of resistance	References
Pseudomonas arsenicoxydans VC-1	Sediment samples, Chile	Arsenite oxidation	Campos et al., 2010
Stenotrophomonas sp. MM-7	Lead smelter plant, South Australia	Arsenite oxidation	Bahar et al., 2012

Staphylococcus sp. NBRIEAG-8	Arsenic contaminated site, West Bengal	Volatilization	Srivastava et al., 2012
Anaeromyxobacter Dehalogenans PSR-1	Contaminated soil, Japan	Arsenate reduction	Kudo et al., 2013
Geobacter sp. OR-1	Paddy field, Japan	Arsenate reduction	Ohtsuka et al., 2013
Enterobacter sp., *Klebsiella pneumoniae*	Pakistan	Arsenite oxidation	Abbas et al., 2014
Halomonas sp. ANAO-440	Alkaline saline lake, Mongolia	Arsenite oxidation	Hamamura et al., 2014
Micrococcus sp. MS-AsIII-49	Metal-polluted stream sediment, Brazil	Arsenate reduction	Costa et al., 2015
Aliihoeflea sp. 2WW	Arsenic contaminated groundwater	Arsenite oxidation	Corsini et al., 2015
Bacillus sp. M17-15, *Pseudomonas* sp. M17-1	Arsenic aquifers of Hetao basin, Mongolia	Arsenate reduction	Guo et al., 2015
Acinetobacter soli IBL-1, *Acinetobacter junii*	Contaminated water-bodies, West Bengal, India	Arsenite oxidation	Goswami et al., 2015

IBL-3, *Acinetobacter baumannii* IBL-4			
Bacillus selenatarsenatis SF-1T	Effluent drain sediments from glass manufacturing plant	Arsenate reduction	Kuroda et al., 2015
Azospirillum sp. MM-17	Soil sample, South Australia	Arsenite oxidation	Bahar et al., 2016
Roseomonas sp. L-159a, *Nocardioides* sp. L-37a,	Lonar lake soil	Arsenite oxidation, Arsenate reduction	Bagade et al., 2016
Bacillus aryabhattai	Rice rhizosphere, Uttar Pradesh	Intracellular accumulation and volatilization of arsenic	Singh et al., 2016
Shewanella oneidensis MR-1	Oak Ridge National Laboratory	Biotransformation and biomethylation	Wang et al., 2016
Bacillus sp., *Aneurinibacillus aneurinilyticus*	West Bengal, India	As accumulation, Arsenite oxidation	Dey et al., 2017
Citrobacter sp. RPT	Kolli Hills, Tamil Nadu, India	Arsenite oxidation, Arsenate reduction	Selvankumar et al., 2017

Bosea sp. As-1	Central China	Arsenite oxidation	Lu et al., 2018
Micrococcus sp. KUMAs15	Nadia, West Bengal, India	Arsenite oxidation	Tanmoy et al., 2018
Bacillus, *Micrococcus*, *Kytococcus*, *Staphylococcus*	West Bengal, India	Arsenite oxidation, As absorption	Roychowdhury et al., 2018
Pseudomonas sp.	Gangetic plains, Bihar, India	Arsenite oxidation, Arsenate reduction	Satyapal et al., 2018
Bacillus sp. BAR1,	Groundwater sample, Bhojpur, Bihar	Arsenate reduction	Biswas et al., 2019a
Delftia spp. BAs29	Shallow aquifer, Bihar, India	Arsenite oxidation	Biswas et al., 2019b
Leclercia adecarboxylata strain As3-1	As-mine, China	Arsenate reduction	Han et al., 2019
Bacillus sp. PVR-YHB1-1	Roots of As-hyperaccumulator *Pteris vittata*	Arsenate reduction	Jia et al., 2019
Citrobacter sp. A99	Arsenic contaminated soils, Central China	Arsenate reduction	Kawa et al., 2019

Rhodococcus sp.	MTCC Chandigarh, India	Arsenite bioaccumulation, biotransformation and biosorption	Kumari et al., 2019
Achromobacter sp. KAs 3-5^{T}	As-contaminated groundwater, West Bengal	Arsenate reduction	Mohapatra et al., 2019
Bacillus cereus, *Lysinibacillus boronitolerans*	Soil samples, Rico Stream, Brazil	Arsenate reduction, Arsenite oxidation	Aguilar et al., 2020
Bacillus firmus L-148	Soil samples, Maharashtra, India	Arsenite oxidation	Bagade et al., 2020
Bacillus XZM	Core samples of sand	Arsenate reduction	Wang et al., 2020
Pantoea sp. IMH, *Achromobacter* sp. SY8	-	Arsenate reduction, Arsenite oxidation	Ye et al., 2020

1.2.6.2 Mechanism of arsenic resistance

1.2.6.2.1 Arsenic resistance operon

Arsenic resistance genes in bacteria are very well organised in *ars* operon, which is located either on the chromosomal genome or plasmid (Rosen, 2002; Bhat et al., 2011). The constitution of *ars* operon varies in different microorganisms as it may possess either three genes viz. *ars R, B, C* or five genes viz. *ars R, D, A, B, C,* (Mukhopadhyay et al.,

2002; Tsai et al., 2009). The core genes of the system include the *arsR* (transcriptional regulator), *arsB* (arsenite efflux pump) and *arsC* encoding arsenate reductase enzyme (Xu et al., 1998). *ArsA* is an ATPase that provides energy to *arsB* for extrusion of arsenite while *arsD* transfers arsenite from glutathione-bound complexes to the arsA subunit and activates it (Lin et al., 2007; Yang et al., 2010). In addition to arsB several other arsenic efflux pumps are present in bacteria to protect cells from arsenic toxicity. This includes acr3, arsP, arsK, arsJ and aqpS that confer resistance to arsenite, arsenate and methylarsenite (Fig. 1.7). *ArsB* genes are mostly found in Firmicutes and γ-proteobacteria, while *acr3* are commonly present in actinobacteria and α-proteobacteria (Achour et al., 2007). Till date, arsJ is the sole permease identified for efflux of arsenate. Additionally, arsP permease was first reported in *Campylobacter jejuni* to efflux methylarsenite and was found to be encoded by an *ars* operon (Wang et al., 2009; Shen et al., 2014). Similarly, arsK was also identified as methylarsenite selective permease in the chromosome of *Agrobacterium tumefaciens* GW4 and *Bacillus* sp. (Shi et al., 2018; Jia et al., 2019).

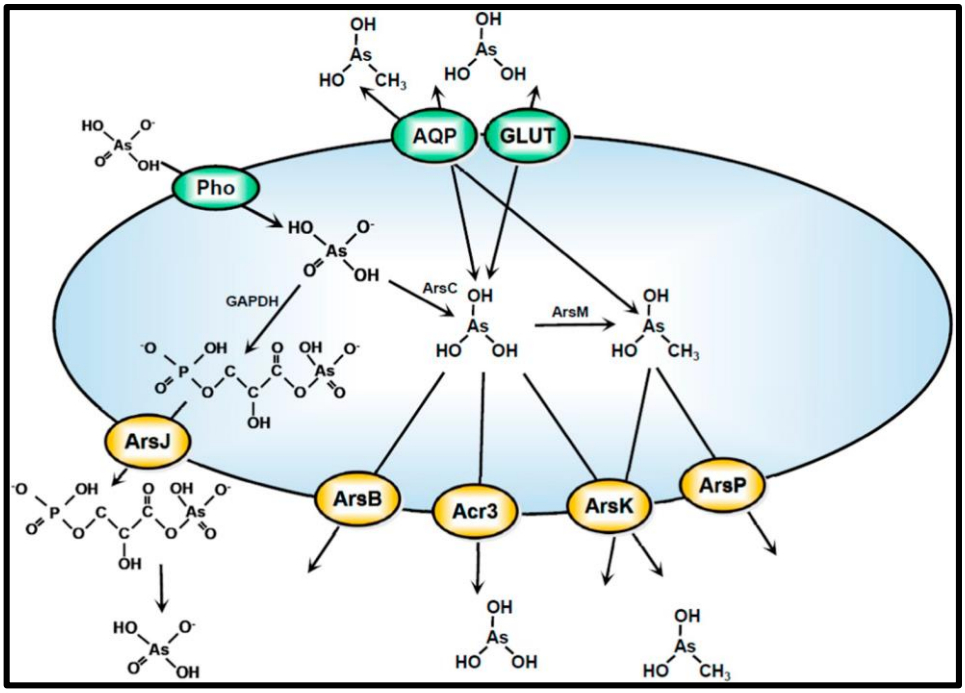

Fig. 1.7: Model of arsenic transporter system (Luis et al., 2019).

The three-gene operon arranged as *arsRBC* gene cluster has been found in the chromosome of *E. coli*, *P. fluorescens* MSP3, *Staphylococcus aureus* plasmids pI258 and *Staphylococcus xylosus* pSX267 (Fig. 1.8) (Carlin et al., 1995; Silver, 1998; Prithivirajsingh et al., 2001). The presence of extended five-gene operon arranged in *arsRDABC* has been reported in *E. coli* plasmid R773 (Fig. 1.8) (Chen et al., 1986). Furthermore, the occurrence of both operons in one strain along with other *ars* genes related to arsenic resistance has also been observed in *T. arsenitoxidans* 3As (Muller et al., 2007; Chauhan et al., 2009; Páez-Espino et al., 2009; Arsène-Ploetze et al., 2010).

Few microorganisms also utilise arsenate as an electron acceptor during respiration and reduction is carried out by respiratory arsenate reductase (arr) enzyme having a catalytic subunit arrA and smaller subunit arrB of *arrSRABD* operon (Malasarn et al., 2008; Richey et al., 2009). Also, arsenate can be reduced and methylated by

enzyme S-adenosylmethionine (SAM) methyltransferase enzyme encoded by *arsM*, involving the addition of methyl groups generating intermediates such as monomethyl arsenite (MMAs (III)), dimethyl arsenate (DMA-V), dimethyl arsenite (DMAs (III)) and trimethyl arsine (TMAs) (Dombrowski et al., 2005; Kruger et al., 2013). Arsenic methylation has been found in both aerobic and anaerobic bacteria including *Clostridium collagenovorans*, *Desulfovibrio vulgaris*, *Desulfovibrio gigas*, *Rhodopseudomonas palustris* and *Methanobacterium formicium*, *Staphylococcus* sp. NBRIEAG-8 (Michalke et al., 2000; Bentley and Chasteen, 2002; Qin et al., 2006; Srivastava et al., 2012).

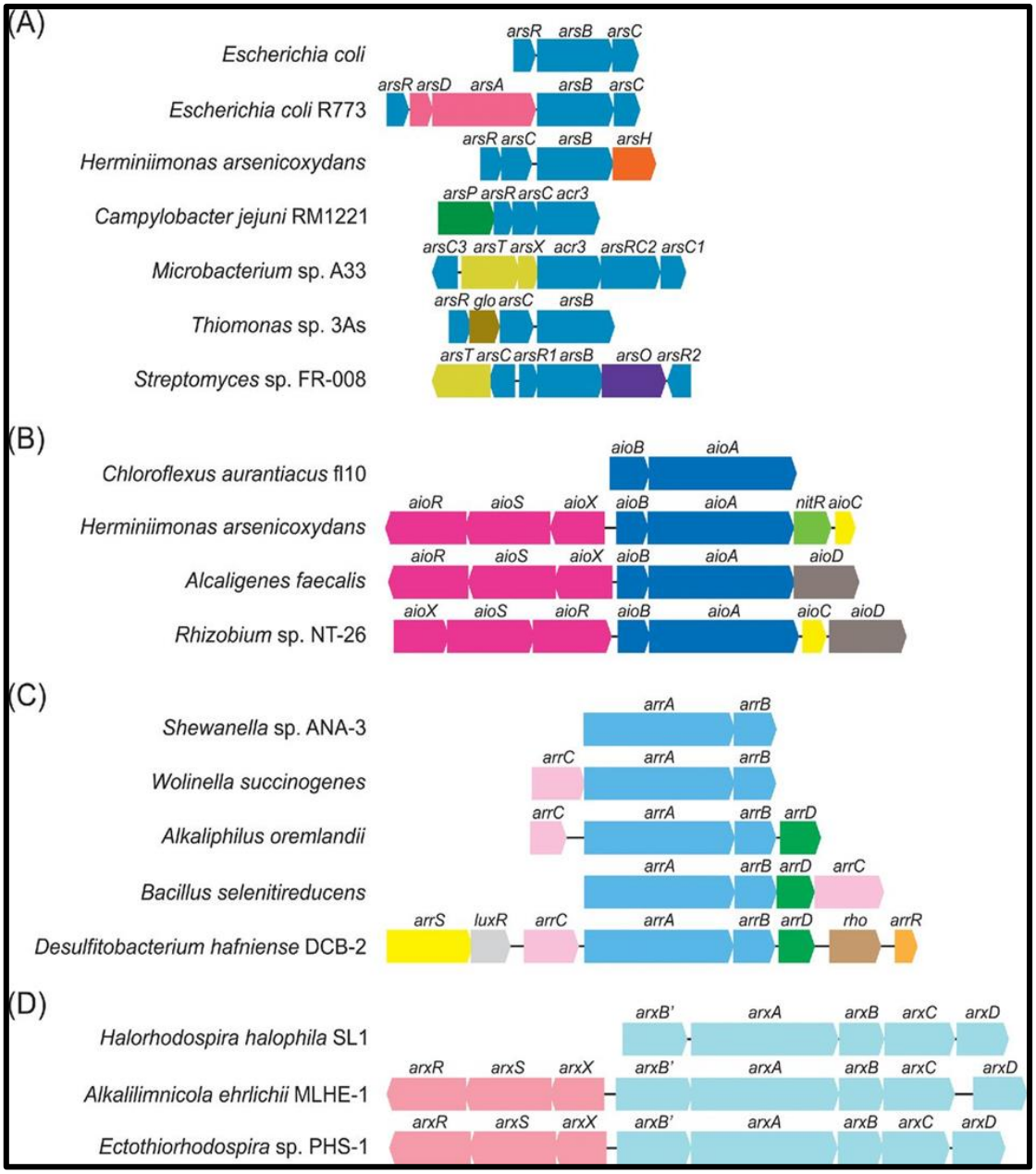

Fig. 1.8: Organisation of gene clusters: (A) *ars*, (B) *aio*, (C) *arr* and (D) *arx* for arsenic resistance in bacteria (Andres and Bertin, 2016).

1.2.6.2.2 Arsenite oxidation

The oxidation of arsenite to arsenate is carried out by arsenite oxidase enzyme encoded by *aio* gene belonging to *aioSRABcytC* operon which confers complete resistance to arsenic (Kashyap et al., 2006; Muller et al., 2007). This operon comprises of arsenite oxidase enzyme encoded by *aioAB* gene, regulator gene (*aioR*), c-type

cytochrome (*cytc2*/*aioC*), sensor kinase (*aioS*) and molybdopterin biosynthesis (*chlE*/*aioD*) gene (Santini and vanden Hoven, 2004; Kashyap et al., 2006; Koechler et al., 2010). The *Rhizobium* sp. strain NT-26 has an operon consisting of *aioRSABC* genes (Santini and vanden Hoven, 2004). Studies on *Agrobacterium tumefaciens* 5A and *Herminiimonas arsenicoxydans* have shown the presence of *aioR, aioS* as well as sigma factor *rpoN* to be associated with regulation of arsenic oxidation (Koechler et al., 2010; Sardiwal et al., 2010; Kang et al., 2012). Additionally, a flagellar protein encoded by gene *dnaJ* and periplasmic arsenite binding protein, aioX has been found to regulate arsenic oxidation which has been characterised in diverse bacteria (Koechler et al., 2010; Kruger et al., 2013). In *Achromobacter* sp. SY8 *aio* operons containing *aioX-aioS-aioR* and *aioB-aioA-aioC-aioD* genes were found responsible for arsenite oxidation (Cai et al., 2009 a; b).

AioA gene-mediated oxidation of arsenite has been identified in genomes of several bacteria including *Acinetobacter junii*, *Pseudomonas stutzeri* strain GIST-BDan 2, *Acinetobacter baumannii*, *Geobacillus stearothermophilus*, *Herminiimonas arsenicoxydans* and *Thiomonas* sp.3As (Muller et al., 2007; Arsène-Ploetze et al., 2010; Chang et al., 2010; Majumder et al., 2013). Some bacterial strains, viz. *Brevibacillus* sp. KUMAs2, *Acinetobacter calcoaceticus* are reported to possess plasmid-borne *aioA* genes while in strains like *Acinetobacter soli*, the gene was present on chromosomal and plasmid DNA (Mallick et al., 2014; Goswami et al., 2015).

Arx enzyme carries out the oxidation of arsenite under anaerobic conditions coupled with nitrate reduction or CO_2 fixation which is encoded by *arx* gene which is constituent of *arxSXB2ABCD* operon (Páez-Espino et al., 2009, Kumari et al., 2016).

ArxA capable of oxidizing arsenite has been identified in *Ectothiorhodospira* sp. strain PHS-1 and *Alkalilimnicola ehrlichii* strain MLHE-1 (Kulp et al., 2008; Zargar et al., 2010).

1.2.6.2.2.1 Structure of arsenite oxidase enzyme

The oxidation of toxic [As(III)] to less toxic [As(V)] is carried out by arsenite oxidase enzyme and consists of two subunits: large molybdopterin containing catalytic subunit aioA with MW∼90 kDa and a small iron-sulfur cluster containing subunit aioB with MW ∼14 kDa (Oremland et al., 2009; Lett et al., 2012) (Fig. 1.9). The large subunit aioA comprises of two pyranopterin cofactors binding the Mo atom in the active site and a [3Fe-4S] cluster for electron transport and acts as a functional marker for aerobic arsenite oxidizing bacteria (Quéméneur et al., 2008). The large subunit of aioA contains four domains; domain I bind to the [3Fe-4S] cluster and the rieske-subunit of the smaller subunit while II and IV domains are linked through a pseudo-two-fold axis of symmetry, and both possess homologous dinucleotide binding folds which help in binding molybdenum. Domain III that binds the molybdenum centre is constituted of two parallel β sheets (Ellis et al., 2001). The aioA and aioB subunits are held together in the heterodimer structure by a network of hydrogen bonds at the interface between the two subunits and also by aioA's C- and N- terminal stretches that entwine the aioB protein. The small subunit (aioB) contains a Rieske-type [2Fe-2S] cluster and transfers the electrons to coupling proteins of the respiratory chain (Anderson et al., 1992; Ellis et al., 2001).

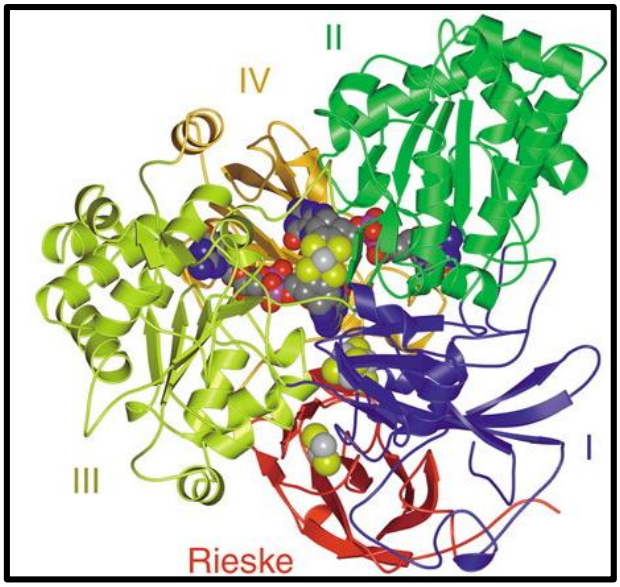

Fig. 1.9: Crystal structure of arsenite oxidase enzyme from *Alcaligenes faecalis*. Domains I-IV of the large subunits of arsenite oxidase enzyme are drawn in blue, green, yellow and orange, respectively. The rieske subunit is drawn in red and the molybdenum cofactor, [3Fe-4S] and [2Fe-2S] cluster are also shown (Ellis et al., 2001).

Arsenite oxidase enzyme was first characterised in *Alcaligenes faecalis*, and the crystal structure was studied (Anderson et al., 1992). Studies on the structure of arsenite oxidase enzyme in *Rhizobium* sp. strain NT-26 also showed the presence of enzyme similar to that of *Alcaligenes faecalis* containing molybdenum and a rieske type subunit (Santini and vanden Hoven, 2004). In both these organisms, aioA consists of conserved motif Cys-X_2-Cys-X_3-Cys-X_{70}-Ser that binds to [3Fe-4S] cluster in a subunit (Santini and vanden Hoven, 2004). The similar conserved motif was also identified in *Stenotrophomonas* sp. MM7 (Bahar et al., 2012). Likewise, several other arsenite oxidizing bacterial strains have been studied for their enzyme structure, and some of them are outlined in Table 1.2.

Table 1.2: Enzyme structure of several arsenic oxidizing bacteria.

Bacteria	Location of Enzyme	Native molecular weight (k Da)	Molecular weight of subunits	References
Alcaligenes faecalis NCIB 8687	Membrane fraction	100	85 kDa aoxB; 15 kDa aoxA	Anderson et al., 1992; Ellis et al., 2001
Herminiimonas arsenicoxydans ULPAs1	Membrane fraction	-	826 aas aoxB; 134 aas aoxA	Muller et al., 2003
Rhizobium NT-26	Periplasmic	219	98 kDa aroA; 14 kDa aroB	Santini and vanden Hoven, 2004
Hydrogenophaga sp. str. NT-14	Periplasmic	306	86 kDa aroA; 16 kDa aroB	vanden Hoven and Santini., 2004
Ochrobactrum triticii SCII24	Periplasmic	-	846 aas aoxB; 175 aas aoxA	Branco et al., 2009
Arthrobacter sp. 15b	Membrane fraction	100	85 k Da aioA; 14 kDa aioB	Prasad et al., 2009
*Ralstonia S*22	Membrane fraction	110	97 kDa aroA; 16 kDa aroB	Lieutaud et al., 2010

*The genes of large and small subunits of arsenite oxidase enzyme are named as *aoxB-aoxA, aroA-aroB, asoA-asoB and aioA-aioB* respectively (Lett et al., 2012).

1.2.6.2.2.2 Microbial arsenite oxidation

Microbial resistance to arsenite has been extensively studied from various arsenic-contaminated sources such as soil (Bahar et al., 2013; 2016; Das et al., 2016), agricultural fields (Tanmoy et al., 2018), lake (Bagade et al., 2016), aquifer (Biswas et al., 2019a), groundwater (Dey et al., 2016; Jebeli et al., 2017; Jebelli et al., 2018), mines (Fahy et al., 2015; Debiec et al., 2017) and industrial effluents (Rehman et al., 2010; Jain et al., 2014) suggesting the extensive distribution of arsenite oxidizers in the environment. Arsenite oxidizing bacteria are classified either as heterotrophs or chemolithoautotrophs based on their preferred growth substrates. Heterotrophic arsenite oxidizing bacteria acquire energy from organic carbon and is designated as detoxification mechanism involving oxidation of arsenite [As (III)] to less toxic arsenate [As (V)] (vanden Hoven and Santini, 2004; Stolz et al., 2010), whereas chemolithoautotrophic arsenite oxidizing bacteria obtain energy by oxidizing arsenite to arsenate using nitrate as their terminal electron acceptor during inorganic carbon fixation (Oremland et al., 2002; Battaglia-Brunet et al., 2006).

Microbial oxidation of arsenite was first reported in *Bacillus arsenoxydans* isolated from cattle dipping tank in South Africa by Green (1918). Subsequently, many arsenite oxidizing bacterial strains have been reported which include *Alcaligenes faecalis*, *Acinetobacter sp.*, *Flavobacterium sp.*, *Sinorhizobium sp.*, *Sphingomonas sp.*, *Pseudomonas lubricans*, *Bacillus flexus* strain As-12, *Agrobacterium tumefaciens* 5A, *Microbacterium oxydans*, *Aeromonas* sp., *Bacillus firmus* L-148, *Agrobacterium* sp., *Comamonas* sp., *Enterobacter* sp., *Pseudomonas chengduensis* As-11, *Pantoea* sp., *Bacillus cereus*, *Lysinibacillus boronitolerans*, *Pseudomonas* sp., *Rhizobium sp*. and *Microbacterium* sp. (Philips and Taylor, 1976; Santini et al., 2002; Kashyap et al., 2006;

Aksornchu et al., 2008; Chang et al., 2010; Rehman et al., 2010; Paul et al., 2015; Jebeli et al., 2017; Jebelli et al., 2018; Aguilar et al., 2020; Bagade et al., 2020).

The arsenite oxidation efficiency significantly varies among the strains depending on their physiological attributes and growth conditions. Arsenite oxidizing strain *Alcaligenes* sp. strain RS19 isolated from mine soil could oxidize 0.042 mM arsenite min^{-1} while *Bosea* sp. strain AR-11 isolated from contaminated groundwater could oxidize 0.25 mM of arsenite in 12 h (Yoon et al., 2009; Liao et al., 2011). Similarly, arsenite oxidation capacity of several bacterial isolates such as *Pseudomonas stutzeri* (1 mM within 25-30 h), *Stenotrophomonas panacihumi* (500 µM within 12 h), *Variovorax* sp. MM-1 (500 µM within 3 h), *Bacillus megaterium* AMO-10 (30 mM within 24 h), *Bacillus flexus* strain As-12 (45% after 48 h) and *Pseudomonas chengduensis* As-11 (48% after 72h) have also been studied (Chang et al., 2010; Bahar et al., 2012; 2013; Majumder et al., 2013; Jebeli et al., 2017; Jebelli et al., 2018). Recently Aguilar et al. (2020) showed that *Bacillus cereus* and *Lysinibacillus boronitolerans* could oxidize 69.38 % and 71.88 % of arsenite, respectively from the culture medium. Additionally, *Bacillus firmus* L-148 was also reported to tolerate 3300 mM arsenite and oxidized 75 mM arsenite in 14 days (Bagade et al., 2020).

1.2.6.3 Genetic engineering of bacteria for bioremediation of arsenic

The development of genetically engineered bacteria for the conversion of toxic arsenite to arsenate via enzyme-mediated redox reactions is one practical option for bioremediation of arsenite (Singh et al., 2011). Several types of genetically modified microorganisms (GMOs) have been developed which bioaccumulate high levels of arsenic via arsenic binding proteins (Table 1.3). For instance, a genetically engineered

(GE) strain of *E. coli* over-expressing ars*R* has been shown to accumulate 5 to 60-fold more arsenic than the wild type (Kostal et al., 2004). This regulatory protein (arsR) offers immense potential for bioremediation by genetic engineering due to its high-affinity transport system and selectivity towards arsenite. Thus, overexpression of arsR in bacteria by strain could be a promising strategy to increase the cellular accumulation and removal of arsenic. Recently, Liu et al. (2011) demonstrated that arsenic could be removed by overexpression of *arsM* genes through volatilization from the contaminated soil by GE bacterial strains such as *Sphingomonas desiccabilis* and *Bacillus idriensis*. Hence, volatilization of arsenic by using the genetically engineered bacteria with numerous copies of *arsM* gene may be highly useful in bioremediation of arsenic.

Additionally, studies have shown that inactivation or deletion of genes encoding arsenic efflux proteins can increase the intracellular accumulation of arsenic (Sousa et al., 2015). For example, genetically engineered *E. coli* strains lacking arsenic efflux transporter demonstrated 10.39 % higher arsenic volatilization rate (Ke et al., 2019). However, there are several problems associated with the application of genetically engineered bacteria in the field which needs to be addressed.

Table 1.3: Genetically engineered bacteria showing enhanced arsenic tolerance.

Bacteria	**Modifications**	**Tolerance (Fold increase)**	**References**
E. coli	Over-expression *of arsR*	60	Kostal et al., 2004
E. coli	Expression of *fMT* and *GlpF*	26-30	Singh et al., 2008

E. coli	Mutation in *GlpF*	10	Tsai et al., 2009
E. coli	Over-expression *of* PC Synthase	50	Páez-Espino et al., 2009
E. coli (without arsenic efflux)	Expression of *SpPCS, GshI, GlpF*	80	Singh et al., 2010
Sphingomonas desiccabilis	Expression of *arsM*	10	Liu et al., 2011
Bacillus idriensis	Expression of *arsM*	10	Liu et al., 2011

* *arsR*- regulator gene, *GlpF*- aquaglyceroporin, *arsM*- arsenic methyltransferase gene

Unlike organic contaminants, arsenite cannot be degraded, but it can be transformed into less toxic forms. The most commonly used physicochemical techniques for removal of arsenic are expensive, time-consuming and hazardous to the environment. Therefore, the bacterial oxidation of arsenite to arsenate may contribute to a natural reduction of arsenic contamination in the environment. Thus, it is imperative and highly desirable to characterize arsenite oxidizing bacterial isolates in order to explore genes and encoded proteins which confer arsenite resistance. Therefore, keeping in view these crucial facts and findings following objectives were proposed:

1. ***Screening and isolation of arsenite oxidizing bacteria from terrestrial econiches of Goa.***
2. ***Identification of selected arsenite oxidizing bacterial isolates.***
3. ***PCR mediated characterization of arsenite resistant bacterial isolates.***
4. ***Proteomic analysis of selected arsenite oxidizing bacterial isolates.***

Chapter II

Materials and methods

2.1 Sampling

Soil samples were collected from different locations across Goa, India, in sterile zip-locked bags. These samples were stored in the cold room until analysed. The physiological parameters of samples viz. pH and temperature were determined using pH meter and thermometer, respectively.

2.2 Isolation of arsenite resistant bacteria

Collected soil samples were serially diluted in 0.85 % saline and spread plated on nutrient agar (NA) and mineral salt medium (MSM) agar plates amended with 10 mM of sodium (meta) arsenite (Appendix-A & B). The plates were incubated at 28 ºC for 24 h and checked for the appearance of bacterial colonies. Morphologically distinct bacterial colonies were selected, purified by repeated streaking and maintained on nutrient agar with 2 mM sodium (meta) arsenite for further characterization.

2.3 Determination of Maximum Tolerance Concentration (MTC) of bacterial isolates for sodium (meta) arsenite

Selected bacterial isolates were spot inoculated on MSM agar plates supplemented with increasing concentration of $NaAsO_2$ (range: 0-45 mM). These plates were incubated at 28 ºC for 24-48 h and observed for visible bacterial colonies.

2.4 Determination of arsenite oxidizing ability of bacterial isolates

Bacterial isolates were spot inoculated on MSM agar plates containing 10 mM sodium (meta) arsenite and incubated at 28 ºC for 4-5 days. Subsequently, the agar plates

were flooded with solution of 0.1 M $AgNO_3$ (Appendix-B) and observed for colour change.

2.5 Isolation of plasmid DNA

The bacterial isolates were grown in Luria Bertani (LB) broth (Appendix-A) at 28 ºC, 150 rpm for 16-18 h and plasmid DNA was extracted using Gen Elute Plasmid Miniprep kit (Sigma-Aldrich, USA). Plasmid DNA was electrophoresed in 0.8 % agarose gel containing ethidium bromide with a final concentration of 0.5 μg mL^{-1} (Appendix-C) and visualized using G: BOX Gel documentation system (Syngene, UK).

2.6 Extraction of chromosomal DNA

Bacterial isolates were inoculated in Luria Bertani (LB) broth and culture flasks were incubated at 28 ºC, 150 rpm for 16-18 h. Cell pellets were obtained by centrifugation at 8000 rpm, 4 ºC for 10 min and chromosomal DNA was extracted using Dneasy® Blood and Tissue Kit (Qiagen, Hilden, Germany). The DNA sample was analysed using 0.8 % agarose gel electrophoresis, visualized under G: BOX Gel documentation system (Syngene, UK) and was further quantified using Nanodrop 2000c (Thermo Scientific, USA).

2.7 PCR amplification of arsenite oxidase (*aioA*) and transporter (*acr3*) genes

The *aioA* and *acr3* genes were PCR amplified using Jump Start Red Taq Ready Mix (Sigma-Aldrich, USA) and gene-specific primers (Appendix-E). Both plasmid and chromosomal DNA samples were separately used as templates for PCR reactions. Each 50 μL PCR reaction contained: 50 ng template DNA, 1μL of each set of primers, 25 uL

of 2X master mix and sterile Milli Q water to bring the final volume to 50 uL. The thermal cycler program for each gene amplification is listed as used (Appendix-E). The PCR reaction was performed in a Nexus Gradient Mastercycler (Eppendorf, Germany) and 5 uL of PCR product was analysed by gel electrophoresis using 1 % agarose gel and visualized under G: BOX gel documentation system (Syngene, UK). The 100 bp and 1 kb DNA marker (Sigma-Aldrich, USA; Promega, USA) was loaded in the parallel lane during electrophoresis to determine the size of the gene amplicons.

2.8 Identification of selected arsenite oxidizing bacterial isolates

2.8.1 Morphological and biochemical characterization

The Gram characteristics of selected arsenite oxidizing bacterial isolates were determined using microscopy (Nikon H600L, Japan) and specific biochemical tests were performed in order to tentatively identify the selected bacterial isolates based on Bergey's Manual of Systematic Bacteriology (Holt et al., 1994).

2.8.2 PCR amplification and DNA sequencing of 16S rRNA gene

PCR amplification of the 16S rRNA gene was done using Jump Start Red Taq Ready Mix (Sigma - Aldrich, USA) and universal eubacterial primers: 27F and 1495R (Appendix-E). The thermal cycler programme used is tabulated (Appendix-E) and was carried out using Nexus Gradient Mastercycler (Eppendorf, Germany). The resulting amplicon was analysed on 1 % agarose gel and visualized using G: Box gel documentation system (Syngene, UK). The PCR amplicon was purified using a PCR clean-up kit (Promega, USA) and sequenced at Eurofins Genomics (Bangalore, India). The nucleotide sequence obtained was analysed by BLAST using the NCBI database and

the sequence was submitted to GenBank. The phylogenetic tree was constructed using the neighbour-joining method with MEGA 7 package (Kumar et al., 2016).

2.9 Determination of Minimum Inhibitory Concentration (MIC) of sodium (meta) arsenite for bacterial isolates

The overnight grown bacterial cultures (0.25 mL) were inoculated in culture flasks with 25 mL MSM broth supplemented with increasing concentration of sodium (meta) arsenite (1-30 mM) and incubated at 28 ºC, 150 rpm for 24-48 h. The MIC for each bacterial strain was determined by taking absorbance at 600 nm using Biospectrometer (Eppendorf, Germany). The lowest concentration of sodium (meta) arsenite at which the growth of bacteria ceases was considered it's MIC.

2.10 Determination of optimal growth conditions for selected arsenite oxidizing bacterial isolates

To determine the optimum pH for growth of the selected bacterial isolates, the strains SSAI1 and SSSW7 were inoculated in a series of conical flasks containing MSM broth (25 mL) with a varying range of pH (5-11) separately, and flasks were incubated at 28 ºC at 150 rpm for 24 h. To find the optimal temperature, the strains were inoculated in series of flasks containing MSM broth (25 mL) and the flasks were incubated at different temperatures (20-45 ºC) separately. The absorbance was recorded at 600 nm using Biospectrometer (Eppendorf, Germany) in order to determine the growth.

2.11 Study of growth behaviour of selected arsenite oxidizing bacterial isolates in the presence of arsenite

The selected bacterial isolates were grown in MSM broth amended with different concentrations of sodium (meta) arsenite in a range of 5-25 mM along with 0.2 % glucose. The flask containing MSM broth with 0.2 % glucose without sodium (meta) arsenite served as a control. The culture flasks were incubated at 28 ºC, 150 rpm for 24-40 h. The cultures aliquots were taken at 2 h intervals and absorbance was recorded at 600 nm using Biospectrometer (Eppendorf, Germany).

2.12 Fourier transformed infrared (FTIR) spectroscopic analysis of selected arsenite oxidizing bacterial isolates

The bacterial isolates were grown in the presence (10 & 15 mM) or absence of arsenite were centrifuged at 10,000 rpm for 10 min, followed by washing with 0.1 M phosphate buffer saline (PBS), pH 7.4 (Appendix-B). The cell pellet was dried in incubator at 45 °C for 24 h and was ground to fine powder in the presence of KBr using mortar and pestle. The IR spectrum was recorded on an IR Prestige-21 instrument (Shimadzu, Japan) in the region of 4000-400 cm^{-1}.

2.13 SEM-EDAX analysis of selected arsenite oxidizing bacterial isolates

The selected bacterial isolates were inoculated in MSM broth supplemented with (10 & 15 mM) and without arsenite as test and control. The flasks were incubated at 28 ºC, 150 rpm for 24 h. The bacterial cells in exponential growth phase were harvested at 8,000 rpm for 10 min from both control and arsenite stressed conditions and were

subjected to washing with 0.1 M PBS (pH 7.4). Bacterial cells were evenly spread on a grease-free coverslip followed by overnight fixation with 2.5 % glutaraldehyde at room temperature. The cells were incubated with different concentrations of acetone, i.e. 20-100 % for 10 min at each concentration. The samples were coated with gold using a coater and then subjected to SEM-EDAX analysis (Carl-Ziess, Germany).

2.14 TEM-EDAX analysis of selected arsenite oxidizing bacterial isolates

The bacterial isolates were grown in the presence (10 &15 mM) and absence of arsenite and cells in exponential phase were harvested by centrifugation at 8,000 rpm for 10 min, followed by washing the pellet with 0.1M sodium phosphate buffer pH 7.2 (Appendix-B). The pellet obtained was fixed in a mixture of 2.5 % glutaraldehyde and 2 % paraformaldehyde prepared in 0.1 M sodium phosphate buffer (pH 7.2) for 2-3 h at 4 °C. The fixed cells were further incubated in 1 % OsO_4 and propylene oxide for 1 h followed by a graded series of dehydration in ethanol. The samples were then embedded in Epon 812 resins, sectioned (60 nm) and analysed using transmission electron microscope (TEM-JEOL 2100F, Germany) followed by EDAX to determine elemental content.

2.15 Quantitative analysis of arsenate

The quantification of arsenate was done by using molybdene blue method with some slight modifications (Lenoble et al., 2003; Cai et al., 2009b). Bacterial cultures were grown in the presence (10 & 15 mM) of sodium (meta) arsenite and centrifuged at 8000 rpm for 10 min. The resulting cell pellet was disrupted by sonication (Vibronics, three times for 2 min with 10 min cool-down intervals). The supernatant (0.3 mL) was

added to a mixture of 4 mL Milli Q water, 0.4 mL 50 % H_2SO_4 (v/v), 0.4 mL of 3 % Na_3MoO_4 (w/v) and 0.2 mL of 2 % ascorbic acid (w/v) and incubated at 90 ºC in water bath for 20 min. The samples were cooled and final volume was adjusted to 10 mL using Milli Q water. The same protocol was also followed for the control samples and the absorbance of the samples at 838 nm was determined using Biospectrometer (Eppendorf, Germany). The standard curve of arsenate was used to determine the concentration of arsenate in the test samples.

2.16 Arsenite oxidase enzyme assay

2.16.1 Preparation of cell-free extract

The bacterial cells were grown in MSM broth and centrifuged at 8000 rpm at 4 °C for 10 min (Eppendorf, Germany). The resulting cell pellet was washed thrice with washing buffer (Appendix-B) and was resuspended in 10 mL suspension buffer (Appendix-B). The cell suspension was incubated with 1 mg mL^{-1} lysozyme at 28 °C for 2 h with occasional stirring followed by addition of magnesium sulphate (20 mM), magnesium acetate (100 mM), DNase (100 µg) and RNase (500 µg) and incubated at 28 °C for 30 min. The cell suspension was then sonicated thrice with 2 min bursts and 10 min cool-down intervals followed by incubation at 60 °C for 1 min. Subsequently, the suspension was cooled on ice, centrifuged at 8000 rpm for 10 min and the pH of the clear supernatant was adjusted to 8.4 with 2 M NaOH (Appendix-B) (Prasad et al., 2009).

2.16.2 Preparation of periplasmic and spheroplast fractions

Bacterial cells grown in MSM broth were harvested by centrifugation at 8000 rpm for 10 min and the resulting cell pellet was suspended in 20 mM Tris-HCl buffer, 0.1 mM PMSF, 10 mM EDTA pH 8.4 along with 20 % sucrose. The outer membrane

was lysed using 0.5 mg mL^{-1} lysozyme (Appendix-B) and incubated at 28 °C for 40 min. After incubation, the suspension was centrifuged at 8000 rpm for 10 min. The supernatant was collected and cell pellet containing spheroplast was washed twice in the above buffer and assayed for arsenite oxidase activity.

2.16.3 Enzyme assay

The arsenite oxidase enzyme activity was determined in the cell-free extract, periplasmic and spheroplast fractions following standard method (Anderson et al., 1992). The enzyme sample was mixed with 1 mL of assay buffer containing 60 µM 2,6-dichlorophenol indophenol (DCIP), 200 µM sodium arsenite and 50 mM morpholinoethelene diol sulfonic acid (MES) buffer (pH 6.0). The change in absorbance due to the reduction of DCIP per minute was monitored at 600 nm for 5 min using Biospectrometer (Eppendorf, Germany). The specific activity of the enzyme was expressed as µmol of DCIP reduced min^{-1} mg^{-1} of protein. The protein concentration in the supernatants was determined by Bradford assay (Bradford, 1976) using bovine serum albumin (Himedia, Mumbai, India) as a standard.

2.17 Cross tolerance to other heavy metals

The chosen bacterial isolates were grown in MSM broth containing 5 mM sodium (meta) arsenite and 0.2 % glucose as carbon source along with different concentration of various heavy metals/ metalloids viz. Zn, Cr, As (V), Pb, Ni, Cu, Fe, Mn and Cd (Appendix-B). The flasks were incubated at 28 ºC, 150 rpm for 24 h and growth was monitored by recording absorbance at 600 nm using Biospectrometer (Eppendorf, Germany). The lowest concentration of the metal/metalloid that inhibited the bacterial growth completely was considered the MIC for that metal.

2.18 Antibiotic susceptibility test

Overnight grown bacterial cultures were spread plated on Mueller-Hinton agar (Appendix-A) followed by overlaying with the octa-discs containing eight different antibiotics (Himedia, India). The plates were incubated at 28 ºC for 24 h and the zone of inhibition (diameter in mm) caused by each antibiotic was measured. Sensitivity or resistance of the bacterial isolates to several antibiotics was determined using the Kirby-Bauer chart (Bauer et al., 1966).

2.19 Proteomic analysis

2.19.1 Extraction of whole-cell proteins

Bacterial cells were grown up to mid-log phase in the presence (5 mM) and absence of sodium (meta) arsenite and then centrifuged at 8000 rpm for 10 min at 4 ℃. The resulting cell pellet was washed twice with PBS (0.1 M, pH 7.4) and resuspended in 0.1 % *Rapi*GestSF buffer (Waters, USA) prepared in 50 mM ammonium bicarbonate containing 2 mg mL^{-1} lysozyme. The bacterial cells were sonicated for 30 sec on ice followed by centrifugation at 10,000 rpm at 4 ℃ for 30 min. The resultant supernatant was collected in clean microfuge tubes, and proteins from the control and arsenite exposed cells were quantified by Bradford assay using bovine serum albumin as a standard (Bradford, 1976).

2.19.2 Qualitative analysis of protein

Whole-cell protein samples from control and test were mixed, heated with 6X sample solubilizing buffer (Appendix-D) and analysed using 12 % sodium dodecyl sulphate-polyacrylamide gel electrophoresis (SDS-PAGE) at a constant voltage of 90 V using BIORAD Mini-PROTEAN Tetra System (BIO-RAD, USA). The gel was stained

overnight using Coomassie Brilliant blue R250 (0.05 %) followed by de-staining in de-staining solution (Appendix-D; Sambrook et al., 1989).

2.19.3 In- Solution digestion

The extracted proteins from the control and arsenite exposed cells were subsequently subjected to in-solution digestion using trypsin (Deshmukh et al., 2017). The protein sample (50 µg) was heated at 80 °C for 20 min, followed by reduction using 3 µL of 100 mM dithiothreitol (DTT) at 65 °C for 15 min. The solution was then alkylated by adding 3 µL of 200 mM iodoacetamide and incubated in the dark at room temperature for 30 min. Further 2 µL of 1 µg μL^{-1} trypsin was added and incubated overnight at 37 °C under mild shaking conditions. The trypsin was inactivated and *Rapi*Gest was precipitated by adding 2 µL formic acid. The sample was then incubated on ice for 15 min followed by centrifugation at 14000 rpm at 4 °C for 15 min and peptides were desalted using Sep Pak C18 cartridges (Waters, USA) as per supplier's instructions.

2.19.4 LC-MS/MS analysis

One µg of protein digest was loaded on to a Hypersil Gold reverse phase C18 column (150 mm x 2.1 mm, 1.9 µm) connected to an Accela 1250 UHPLC system (Thermo Fischer Scientific, USA) in line with a Q-Exactive Hybrid Quadrupole-Orbitrap Mass Spectrometer (Thermo Fischer Scientific, USA). All the samples were acquired by Data Dependent Acquisition (DDA) in full MS/ddMS2 mode. A 90-minute gradient of 3-40 % acetonitrile in water containing 0.1 % formic acid was used as mobile phase for separation at 350 µL min^{-1} flow rate. The temperature of column was maintained at 40 °C and instrument tune parameters viz. spray voltage (4.20 kV), capillary temperature

(320 °C), auxiliary gas heater temperature (320 °C), sheath gas flow (45), auxiliary gas flow (12) and S-lens RF value (50) were optimized. The acquisition was performed primarily in full scan mode (MS) at resolution 70000 at 200 m/z followed by ddMS2 wherein top 15 precursors were selected for MS/MS by HCD and analysed at resolution 17500 at 200 m/z. MS data were acquired in a scan range from 200-1800 m/z. The automatic gain control (AGC) and maximum IT value were 1×10^6 ions and 100 ms. ddMS2 was acquired at normalized collision energy value of 30, AGC value of 1×10^5 ion, maximum IT of 50 ms and isolation window of 4 m/z. The dynamic exclusion was set to 10 seconds. All the samples were acquired in technical triplicates.

2.19.5 Identification and quantification of proteins

The proteins were identified and quantified using MaxQuant software with Uni Prot database restricted to *Bacillus flexus* and *Klebsiella pneumonia* for SSAI1 and SSSW7 isolates. False discovery rate analysis (FDR) was set to 1 % and proteins identified with at least 2 unique peptides were selected for further analysis. Label-free quantification (LFQ) was performed using default parameters of MaxQuant and fold change between control and test was calculated based on the LFQ intensities.

2.20 Statistical analysis

All experiments in the present study were performed in triplicates; the standard error was calculated and incorporated in the thesis.

Chapter III

Isolation, identification and characterization of arsenite resistant bacterial isolates

(Results & Discussion)

3.1 Sampling

The sediment samples were collected from 8 different sites of Goa viz. agro industry waste, battery waste, ceramic waste, metal industry waste, mine rejects, shipyard waste and municipal waste dump (Fig. 3.1). These sampling sites were selected based on the possible sources of arsenic contamination. The temperature of sediment samples ranged between 27-30 ℃, whereas pH ranged between 6.5 to 8.4 (Table 3.1). The sediment sample from mine reject, Piligao showed pH 8.4 and temperature 30 ℃. Whereas the sediment sample from battery waste, Corlim had a temperature of 28 ℃ and pH 6.5 due to the abundance of acids.

Previously several bacterial strains have been isolated from various arsenic contaminated sources such as soil (Bahar et al., 2016; Das et al., 2016), agricultural fields (Tanmoy et al., 2018), aquifer (Biswas et al., 2019a), lake (Bagade et al., 2016), groundwater (Jebeli et al., 2017; Jebelli et al., 2018), industrial effluents (Rehman et al., 2010; Jain et al., 2014) and mines (Fahy et al., 2015; Debiec et al., 2017) signifying the wide distribution of arsenite resistant bacteria in the environment. The occurrence of arsenite resistant bacterial strains has also been reported in water and sediment samples of estuarine environments of Goa (Nagvenkar and Ramaiah, 2010). However, there are no reports on isolation of arsenite resistant bacterial isolates from terrestrial econiches of Goa making this first report.

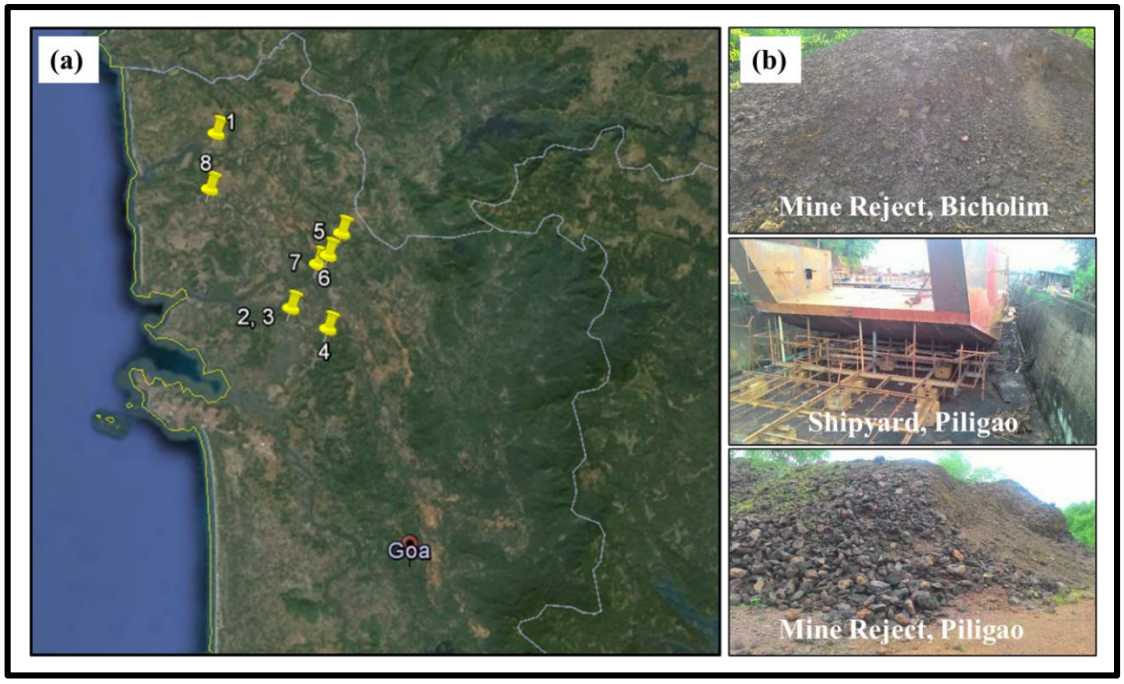

Fig. 3.1: (a) Map of Goa showing locations of eight sampling sites. 1- Agro industry waste, Tuem; 2-Battery waste, Corlim; 3-Ceramic waste, Corlim; 4-Metal industry waste, Kundaim; 5- Mine reject, Bicholim; 6- Mine reject, Piligao; 7- Shipyard waste, Piligao; 8-Municipal waste dump, Mapusa. **(b) Photographs of three sampling sites:** Mine reject, Bicholim; Shipyard waste, Piligao and Mine reject, Piligao.

Table 3.1: Physiological characteristics of sediment samples collected from different sites of Goa.

S. N.	Sampling sites	Sample Designation	Temperature (°C)	pH
1	Agro industry waste, Tuem	AI	27	7.6
2	Battery waste, Corlim	BW	28	6.5
3	Ceramic waste, Corlim	CW	28	7.3
4	Metal industry waste, Kundaim	MI	30	7.96

5	Mine reject, Bicholim	MB	28	7.1
6	Mine reject, Piligao	MP	30	8.4
7	Shipyard waste, Piligao	SW	27	7.66
8	Municipal waste dump, Mapusa	MW	29	6.68

3.2 Isolation of arsenite resistant bacteria

All the environmental samples showed the presence of arsenite resistant bacteria with higher viable counts on nutrient agar as compared to mineral salts medium. The highest viable count of arsenite resistant bacteria was obtained in the battery waste sample on both Nutrient and MSM agar, followed by agro industry waste (Table 3.2). Arsenic has been widely used in lead-acid batteries, electronics, corrosion-resistant materials and agriculture industry (Jang et al., 2016). Hence this could be the possible reason for the occurrence of a large number of arsenite resistant bacterial isolates in these samples. Total 34 morphologically different arsenite resistant bacterial isolates obtained from different environmental samples were selected and purified for further characterization.

Table 3.2: Viable count of arsenite resistant bacteria from sediment samples on Nutrient agar and MSM agar.

S. N.	Samples	Viable Count (cfu mL^{-1})	
		Nutrient Agar + 10 mM $NaAsO_2$	**Mineral Salts Media agar + 10 mM $NaAsO_2$**
1	Agro industry waste	48.5×10^5	13.8×10^5
2	Battery waste	22.4×10^6	7.13×10^6
3	Ceramic waste	24.7×10^4	12.79×10^4
4	Metal industry waste	30.2×10^5	9.33×10^5
5	Mine reject, Bicholim	29×10^4	3×10^4
6	Mine reject, Piligao	10.7×10^5	6.867×10^5
7	Shipyard waste	47.3×10^5	4.86×10^5
8	Municipal waste dump	22.1×10^4	2.6×10^4

3.3 Determination of Maximum Tolerance Concentration (MTC) of sodium (meta) arsenite

The arsenite resistant bacterial isolates obtained showed arsenite tolerance in the range of 10-45 mM on MSM agar (Fig. 3.2). Out of these, 26 isolates could tolerate arsenite within a range of 27 to 45 mM, which is significantly very high concentration. Several studies have shown the potential of bacteria to tolerate arsenite in different solid medium. For instance, bacterial strains isolated from arsenic contaminated groundwater exhibited MIC of 2.5 mM for *Pseudomonas* sp. strain AR-1, 5 mM for *Psychrobacter* sp. strain AR-5, 2 mM for *Vibrio* sp. strain AR-6, 5 mM for *Citrobacter* sp. strain AR-7, 5 mM for *Enterobacter* sp. strain AR-8, 5 mM for *Bacillus* sp. strain AR-9 and 2 mM for

Bosea sp. strain AR-11 (Liao et al., 2011). Similarly, *Bacillus* sp. strain As-14 and *Exiguobacterium* sp. strain As-9 were reported to tolerate 10 mM and 180 mM of arsenite, respectively (Pandey and Bhatt, 2015). Recently *Delftia* spp strain BAs29 isolated from aquifer exhibited MIC value of 70 mM for arsenite (Biswas et al., 2019b).

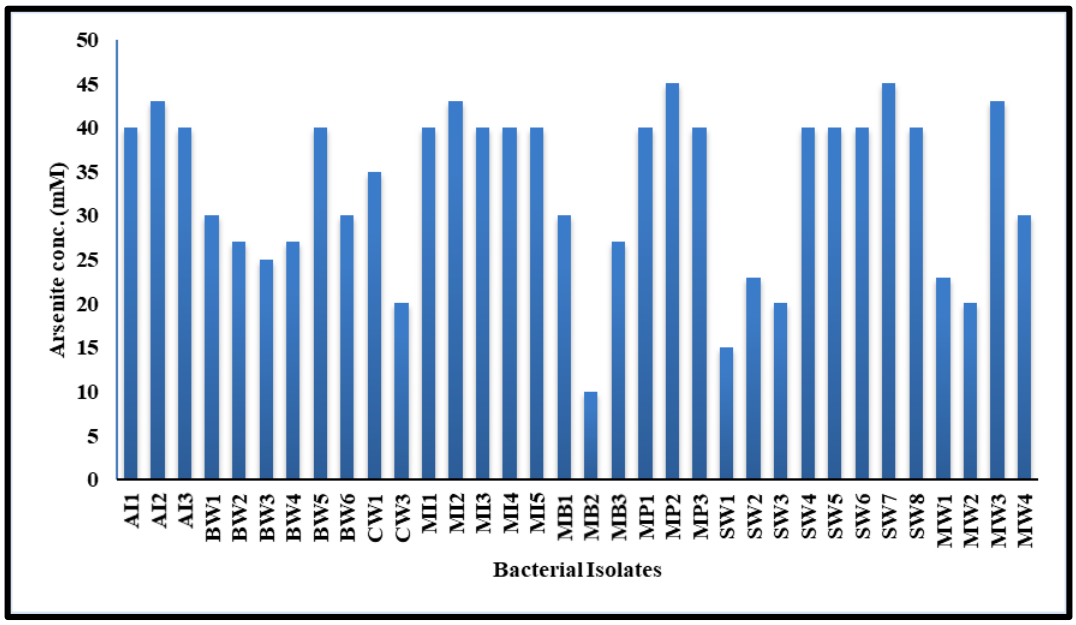

Fig. 3.2: MTC of arsenite resistant bacteria for sodium (meta) arsenite.

3.4 Determination of arsenite oxidizing ability

The ability of selected arsenite resistant bacterial isolates to oxidize arsenite to arsenate was determined by using qualitative silver nitrate screening technique. Arsenite reacts with silver nitrate to give a yellow precipitate of silver-orthoarsenite while arsenate generates a brown coloured precipitate of silver-orthoarsenate indicating arsenite oxidation. According to $AgNO_3$ test, 15 arsenite resistant bacterial isolates (Fig. 3.3; Table 3.3) were positive, demonstrating arsenite oxidizing ability while the rest of the

isolates were found to be negative. These positive isolates were selected for further characterization.

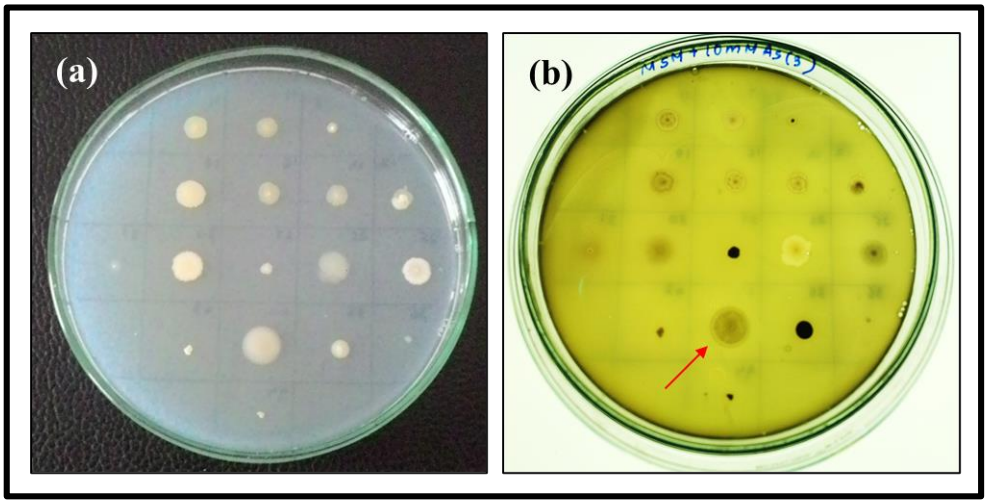

Fig. 3.3: Arsenite oxidation potential of bacterial isolates. (a) MSM agar plate with 10 mM arsenite (before staining) and (b) MSM agar plate with 10 mM arsenite (after staining with 0.1M $AgNO_3$). Red arrow indicates a colony showing positive arsenite oxidase test.

Table 3.3: Bacterial isolates showing positive $AgNO_3$ test.

S. N.	Bacterial Isolates	Silver nitrate test
1	AI1	+
2	BW1	+
3	BW2	+
4	BW5	+
5	BW6	+
6	CW1	+
7	MI2	+

8	MB3	+
9	MP1	+
10	MP2	+
11	SW4	+
12	SW5	+
13	SW6	+
14	SW7	+
15	SW8	+

3.5 Isolation of plasmid DNA

Arsenic resistance encoding genes in bacteria are known to be present on both chromosomal and/ plasmid genome depending on the bacterial strains (Silver and Phung, 2005; Wang et al., 2009). Therefore arsenite oxidizing bacterial isolates were screened for the presence of plasmids. Interestingly out of 15 bacterial isolates, one arsenite oxidizing bacterial strain SW7 showed the presence of a supercoiled plasmid (Fig. 3.4). Earlier studies on *Acinetobacter soli* strain IBL-1, *Acinetobacter venetianus* strain IBL-2, *Acinetobacter junii* strain IBL-3, *Acinetobacter baumannii* strain IBL-4, *Acinetobacter calcoaceticus* strain IBL-5, *Microbacterium oleivorans* strain Ransu-1 and *Brevibacillus* sp. KUMAs2 have been reported to possess plasmid which contains various genes viz. *arsR*, *arsB*, *arsC* and *aroA*/*aoxB* conferring resistance to arsenic (Mallick et al., 2014, Goswami et al., 2015). Therefore, the plasmid present in isolate SW7 may also be responsible for resistance to high concentrations of arsenite.

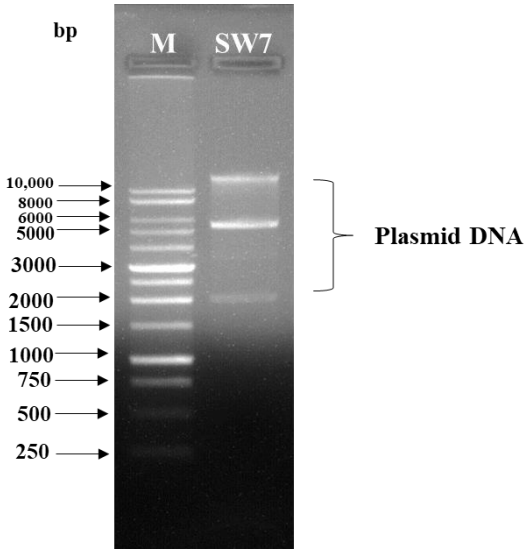

Fig. 3.4: Plasmid profile of bacterial isolate SW7. M: 1 kb DNA marker.

3.6 Extraction of chromosomal DNA

Agarose gel electrophoresis of DNA samples extracted from arsenite oxidizing bacterial isolates revealed a distinct band of chromosomal DNA which were then used for further analysis (Fig. 3.5).

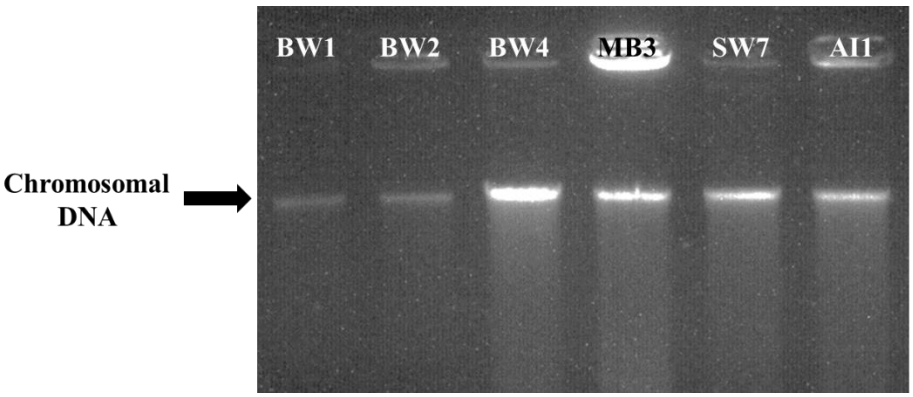

Fig. 3.5: Chromosomal DNA isolated from arsenite oxidizing bacterial isolates.

3.7 PCR amplification of arsenite oxidase (*aioA*) and transporter (*acr3*) genes

The presence of arsenite resistance genes (*aioA* and *acr3*) in plasmid and chromosomal DNA were detected by PCR using gene specific primers. An amplicon of approximately 1100 bps corresponding to *aioA* gene was obtained from bacterial isolates BW1, BW2, BW5, MB3, SW4 and AI1 using chromosomal DNA (Fig. 3.6). These strains did not possess any plasmid indicating that the arsenite resistance may be solely governed by the genes located on the chromosomal genome. Interestingly, in case of strain SW7 *aioA* gene was found to be present on both chromosomal as well as plasmid DNA (Figs. 3.6 & 3.7). This suggested that both chromosomal and plasmid DNA plays an important role in conferring arsenite resistance in this strain. Similar results were also obtained in *Acinetobacter soli* which showed the presence of *aioA* gene on both plasmid and genomic DNA (Goswami et al., 2015). Numerous studies on arsenite transforming bacteria have shown the occurrence of arsenite oxidizing gene (*aoxB*) located either on chromosomal or plasmid genome (Majumder et al., 2013; Mallick et al., 2014; Goswami et al., 2015).

The PCR mediated amplification of transporter gene (*acr3*(1)) with gene specific primers revealed a positive amplicon of approximately 750 bps in BW1, BW2, BW5, MB3 and SW4 isolates using chromosomal DNA as a template (Fig. 3.8). In contrast, no PCR amplicon was obtained for isolates AI1 and SW7 with chromosomal and/ plasmid DNA. All the bacterial isolates were found to be negative for *acr3*(2) set of primers. The absence of PCR amplicon for *aioA* and *acr3* genes in other arsenite oxidizing bacterial isolates could be due to failure of primer sets to amplify a particular gene used in the current study, or the genes might be absent (Sun et al., 2004). Many bacterial strains,

such as *Bacillus* sp. A17, *Microbacterium* sp. A33, *Arthrobacter* sp. A03, *Micrococcus* sp., *Paracoccus* sp. A10 and *Pseudomonas* sp. are reported to possess *acr3*(1) subset only and not *acr3*(2) subset (Achour et al., 2007). Conversely, the bacterial strains, namely *Sinorhizobium* sp. A16, *Phyllobacterium myrsinacearum* A26, *Aminobacter aminovorans* A27, *Ensifer adhaerens* B04, *Pseudomonas* sp. A07, *Shewanella* sp. ANA-3 and *S. oneidensis* MR-1 showed the presence of *acr3*(2) subset; while no PCR amplicon was obtained for *acr3*(1) subset (Achour et al., 2007). Out of 15 bacterial isolates, seven were found positive for *aioA* gene and were selected for identification by biochemical tests and 16S rRNA gene sequencing.

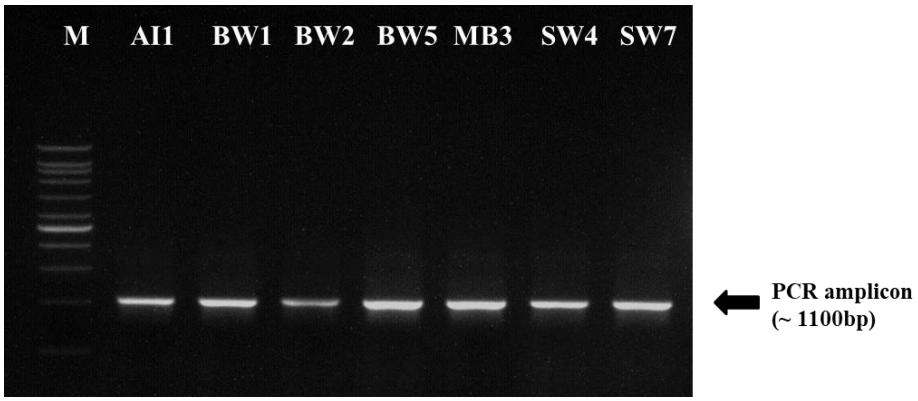

Fig. 3.6: PCR amplification of *aioA* gene from arsenite oxidizing bacterial isolates using chromosomal DNA as a template. (M - 1kbps DNA Marker).

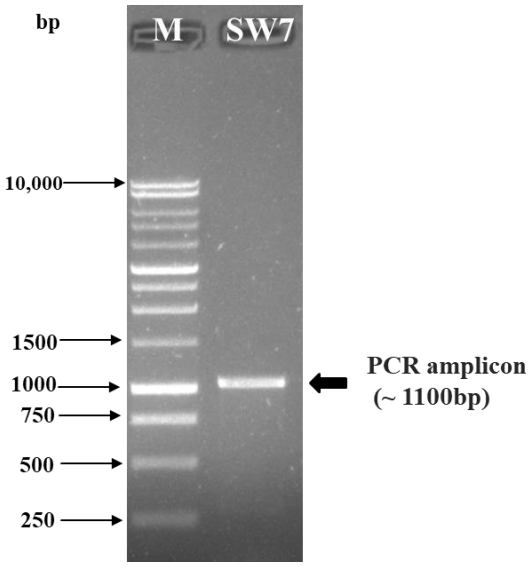

Fig. 3.7: PCR amplification of *aioA* gene using plasmid DNA of strain SW7 as a template. (M- 1kbps DNA marker)

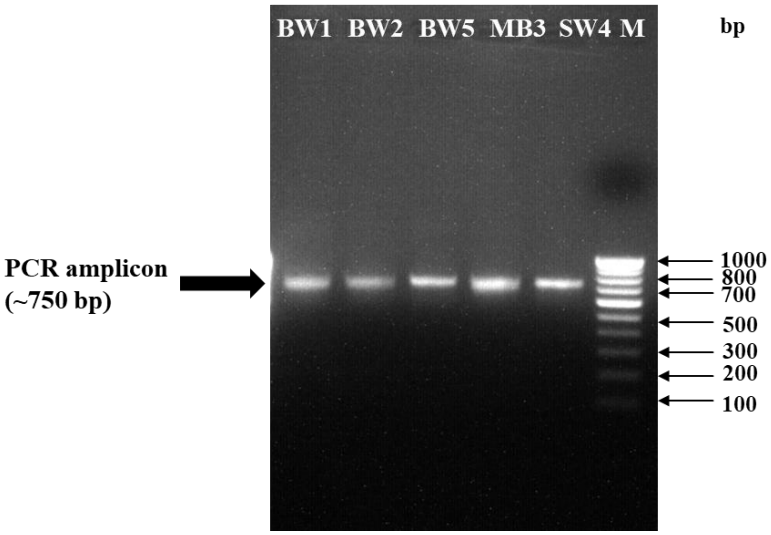

Fig. 3.8: PCR amplification of *acr3* gene of arsenite oxidizing bacterial isolates using chromosomal DNA as a template. (M: 100 bps DNA Marker)

3.8 Identification of selected arsenite oxidizing bacterial isolates

3.8.1 Morphological and biochemical characterization

Among the 7 arsenite oxidizing bacterial isolates, the isolates BW1, BW2, BW5, SW4 and AI1 were Gram-positive while SW7 and MB3 were Gram-negative. Subsequently, based on biochemical tests all the seven bacterial isolates BW1, BW2, BW5, SW4, SW7, AI1 and MB3 were tentatively identified as *Microbacterium* sp., *Corynebacterium* sp., *Paenarthrobacter* sp., *Micrococcus* sp., *Klebsiella* sp., *Bacillus* sp. and *Stenotrophomonas* sp. respectively (Table 3.4).

Table 3.4: Biochemical characteristics of selected arsenite oxidizing bacterial isolates.

S. N.	Biochemical tests	Bacterial isolates						
		BW1	BW2	BW5	SW4	SW7	AI1	MB3
1	Indole test	+	-	-	-	-	-	+
2	Methyl red test	+	-	-	-	-	-	-
3	Voges-Proskauer test	-	+	+	-	+	-	-
4	Citrate utilization test	-	+	+	+	+	+	+
5	Nitrate reduction test	+	-	-	+	+	+	+
6	Urease test	-	+	+	+	+	-	-
7	Motility	-	-		-	-	+	-
8	Oxidase	-	+	-	+	-	+	-

9	Catalase	+	+	+	+	+	+	+
10	Gelatinase	-	+	+	+	-	+	+
11	Morphology	Rods	Rods	Short rods	Cocci	Short rods	Rods	Rods
Sugar fermentation test								
	Sugars	**Fermentative activity**						
12	Arabinose	-	-	+	+	+	+	-
13	Xylose	-	-	+	-	+	+	+
14	Rhamnose	-	+	-	-	+	-	-
15	Raffinose	-	+	+	+	+	+	-
16	Trehalose	-	+	+	+	+	-	-
17	Glucose	+	+	+	+	+	+	+
18	Lactose	+	+	+	-	+	-	-
19	Maltose	+	+	+	+	+	+	-
20	Fructose	+	+	+	+	+	+	+
21	Mannitol	+	+	+	-	+	+	-
22	Sucrose	+	+	+	+	+	+	+
23	Galactose	+	+	+	+	+	+	+

*Key: + Positive ; - Negative

3.8.2 PCR amplification and DNA sequencing of 16S rRNA gene

PCR amplicon of approximately 1500 bps was obtained for 16S rRNA gene on 1 % agarose gel (Fig. 3.9). Based on 16S rRNA gene sequencing and BLAST analysis the bacterial isolates have been identified as *Microbacterium* sp. strain SSBW1 (accession

no. MG430348), *Corynebacterium* sp. strain SSBW2 (accession no. MH031689), *Paenarthrobacter* sp. strain SSBW5 (accession no. MN640912), *Micrococcus* sp. strain SSSW4 (accession no. MG430350), *Klebsiella* sp. strain SSSW7 (accession no. MG430351), *Bacillus* sp. strain SSAI1 (accession no. MH031690) and *Stenotrophomonas* sp. strain SSMB3 (accession no. MG430349). The phenogram of strains SSBW1, SSBW2 and SSBW5 showed its closest match to *Microbacterium hydrocarbonoxydans*, *Corynebacterium ilicis* and *Paenarthrobacter nicotinovorans* respectively (Fig. 3.10 a, b & c). Similarly, the dendrogram analysis of strains SSSW4, SSSW7, SSAI1 and SSMB3 revealed phylogenetic relatedness to *Micrococcus endophyticus*, *Klebsiella pneumoniae*, *Bacillus flexus* and *Stenotrophomonas pavanii* respectively (Fig. 3.10 d, e, f & g).

Earlier studies have shown the potential of bacterial isolates such as *Stenotrophomonas panacihumi*, *Microbacterium lacticum*, *Microbacterium oxydans*, *Micrococcus* sp., *Bacillus aryabhattai*, *Bacillus megaterium* AMO-10, *Enterobacter* sp., *Klebsiella pneumoniae*, *Bacillus* sp., *Bacillus flexus* strain As-12, *Bacillus cereus* and *Bacillus firmus* L-148 in arsenite resistance (Mokashi and Paknikar, 2002; Bahar et al., 2012; Abbas et al., 2014; Singh et al., 2016; Jebeli et al., 2017; Roychowdhury et al., 2018; Bagade et al., 2020; Aguilar et al., 2020). Even though there is a report available on arsenite resistant *Klebsiella pneumoniae* and *Bacillus flexus* strain As-12 (Abbas et al., 2014; Jebeli et al., 2017) but, the present study showed a higher level of arsenite oxidation potential as compared to the above reported ones. Moreover, rest bacterial species identified in the present study have not been previously reported.

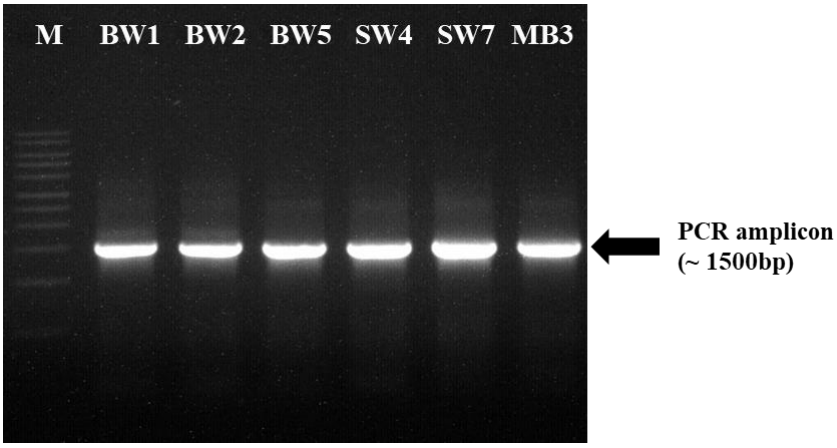

Fig. 3.9: 16S rRNA gene amplicon of arsenite oxidizing bacterial isolates.

(M- 1 kbps DNA Marker)

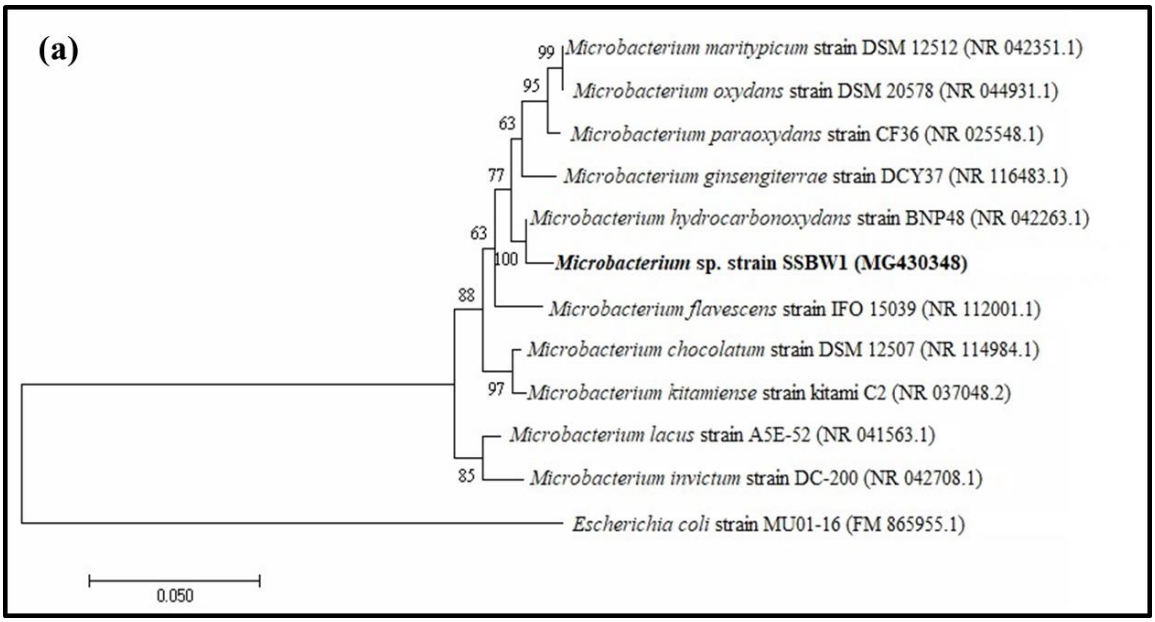

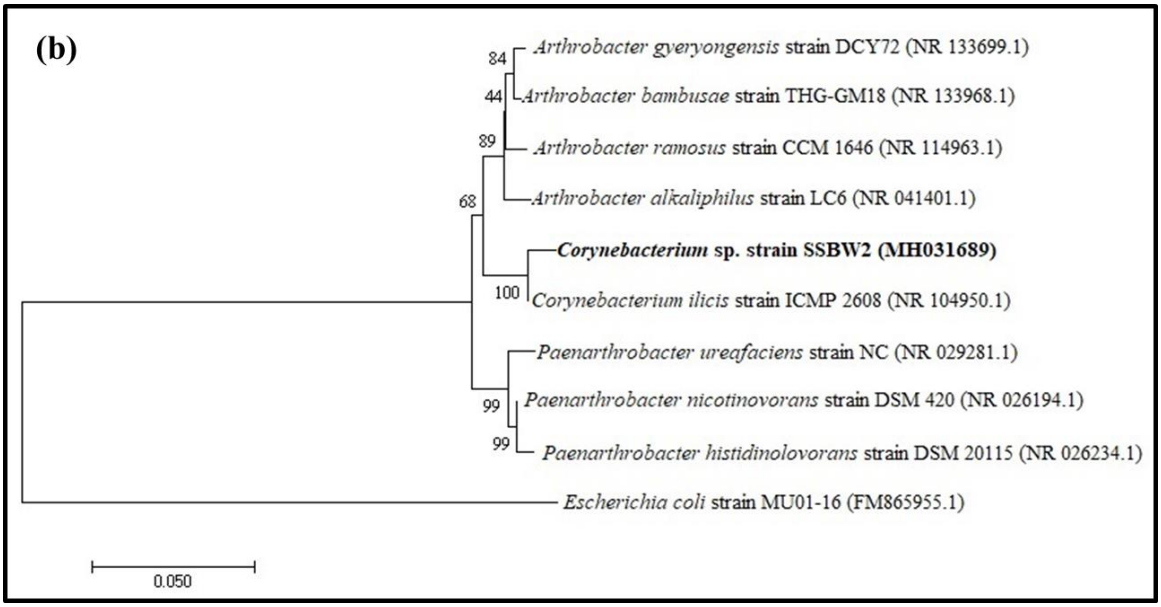
(b)
84
44
89
68
100
99
99
Arthrobacter gyeryongensis strain DCY72 (NR 133699.1)
Arthrobacter bambusae strain THG-GM18 (NR 133968.1)
Arthrobacter ramosus strain CCM 1646 (NR 114963.1)
Arthrobacter alkaliphilus strain LC6 (NR 041401.1)
Corynebacterium sp. strain SSBW2 (MH031689)
Corynebacterium ilicis strain ICMP 2608 (NR 104950.1)
Paenarthrobacter ureafaciens strain NC (NR 029281.1)
Paenarthrobacter nicotinovorans strain DSM 420 (NR 026194.1)
Paenarthrobacter histidinolovorans strain DSM 20115 (NR 026234.1)
Escherichia coli strain MU01-16 (FM865955.1)
0.050

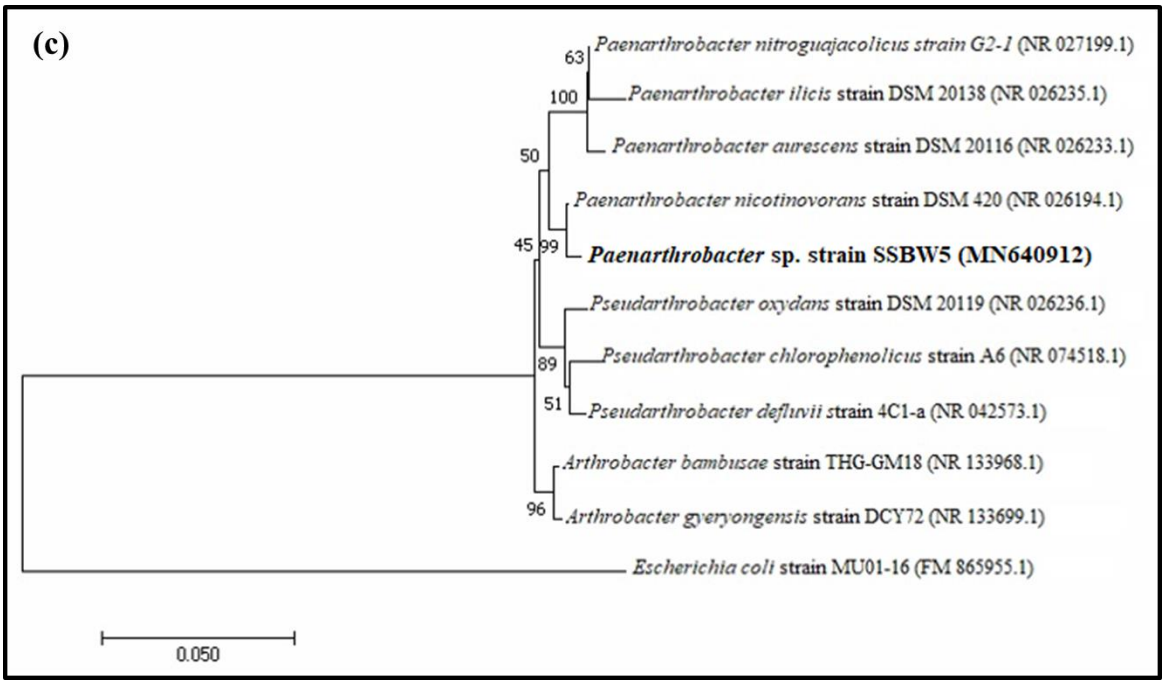
(c)
63
100
50
45
99
89
51
96
Paenarthrobacter nitroguajacolicus strain G2-1 (NR 027199.1)
Paenarthrobacter ilicis strain DSM 20138 (NR 026235.1)
Paenarthrobacter aurescens strain DSM 20116 (NR 026233.1)
Paenarthrobacter nicotinovorans strain DSM 420 (NR 026194.1)
Paenarthrobacter sp. strain SSBW5 (MN640912)
Pseudarthrobacter oxydans strain DSM 20119 (NR 026236.1)
Pseudarthrobacter chlorophenolicus strain A6 (NR 074518.1)
Pseudarthrobacter defluvii strain 4C1-a (NR 042573.1)
Arthrobacter bambusae strain THG-GM18 (NR 133968.1)
Arthrobacter gyeryongensis strain DCY72 (NR 133699.1)
Escherichia coli strain MU01-16 (FM 865955.1)
0.050

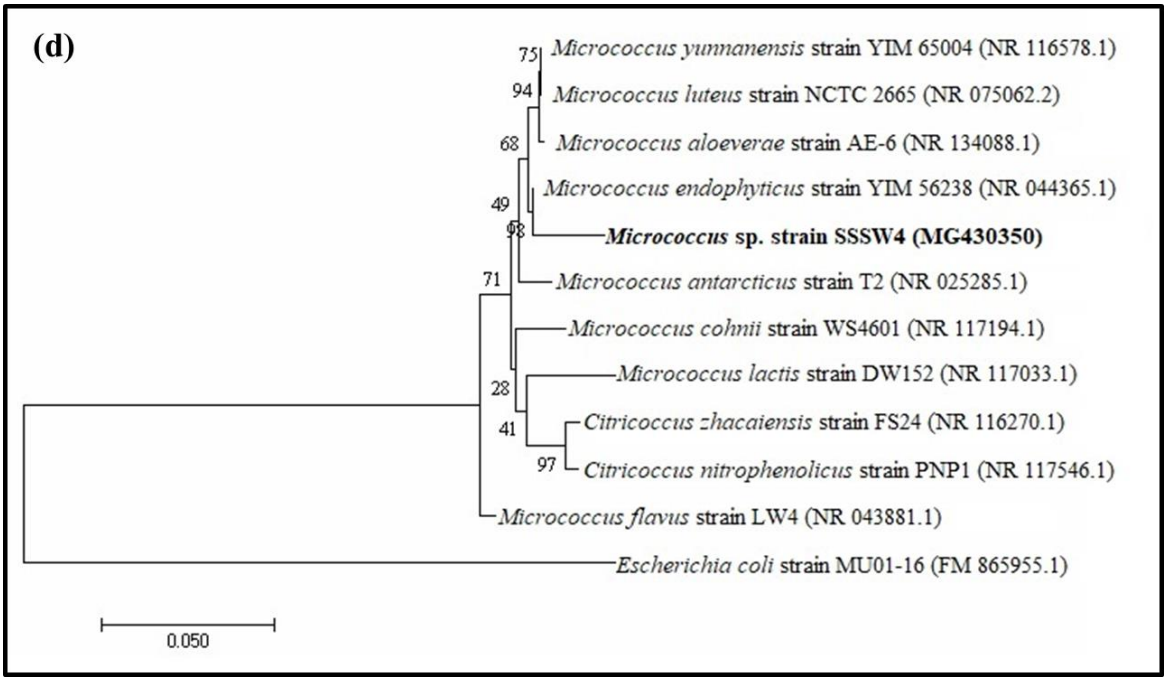
(d)
75
94
68
49
98
71
28
41
97
Micrococcus yunnanensis strain YIM 65004 (NR 116578.1)
Micrococcus luteus strain NCTC 2665 (NR 075062.2)
Micrococcus aloeverae strain AE-6 (NR 134088.1)
Micrococcus endophyticus strain YIM 56238 (NR 044365.1)
Micrococcus sp. strain SSSW4 (MG430350)
Micrococcus antarcticus strain T2 (NR 025285.1)
Micrococcus cohnii strain WS4601 (NR 117194.1)
Micrococcus lactis strain DW152 (NR 117033.1)
Citricoccus zhacaiensis strain FS24 (NR 116270.1)
Citricoccus nitrophenolicus strain PNP1 (NR 117546.1)
Micrococcus flavus strain LW4 (NR 043881.1)
Escherichia coli strain MU01-16 (FM 865955.1)
0.050

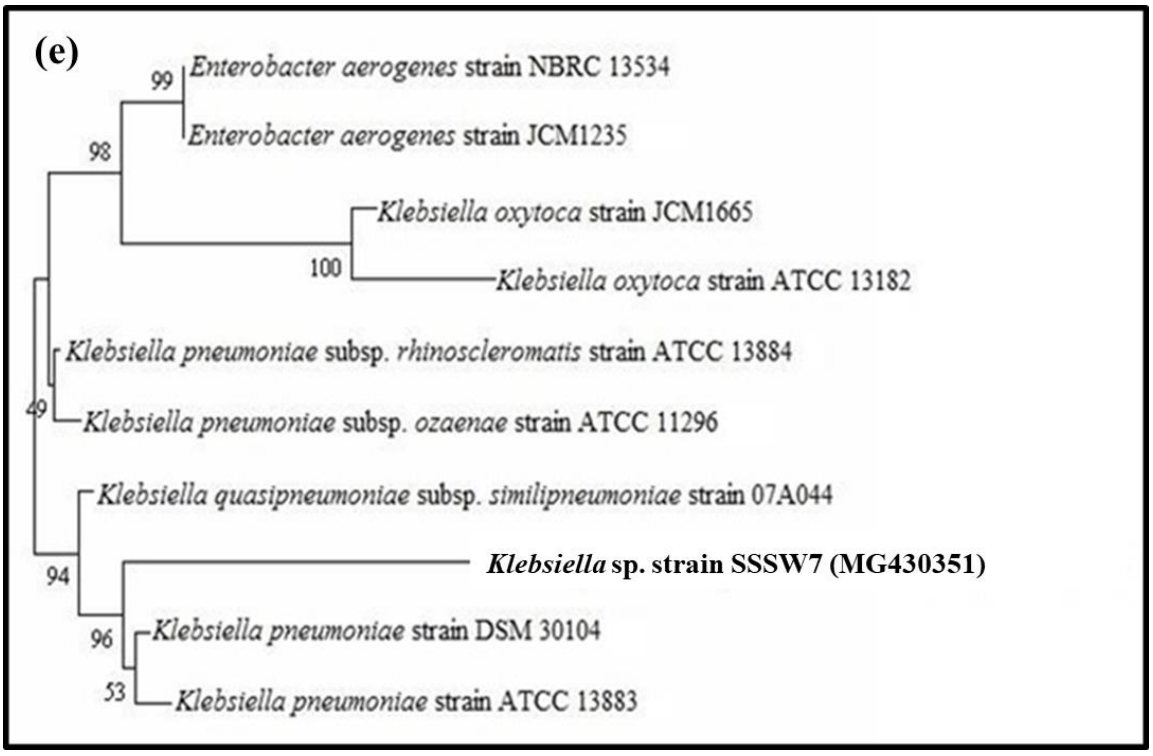
(e)
99
98
100
49
94
96
53
Enterobacter aerogenes strain NBRC 13534
Enterobacter aerogenes strain JCM1235
Klebsiella oxytoca strain JCM1665
Klebsiella oxytoca strain ATCC 13182
Klebsiella pneumoniae subsp. rhinoscleromatis strain ATCC 13884
Klebsiella pneumoniae subsp. ozaenae strain ATCC 11296
Klebsiella quasipneumoniae subsp. similipneumoniae strain 07A044
Klebsiella sp. strain SSSW7 (MG430351)
Klebsiella pneumoniae strain DSM 30104
Klebsiella pneumoniae strain ATCC 13883

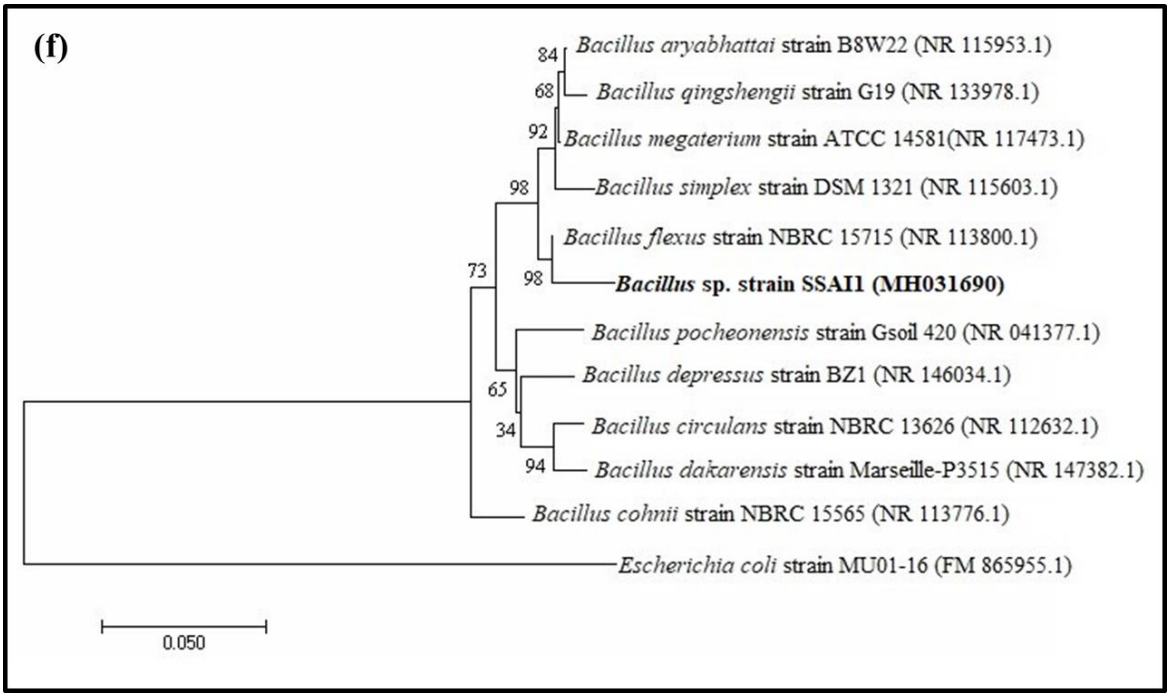

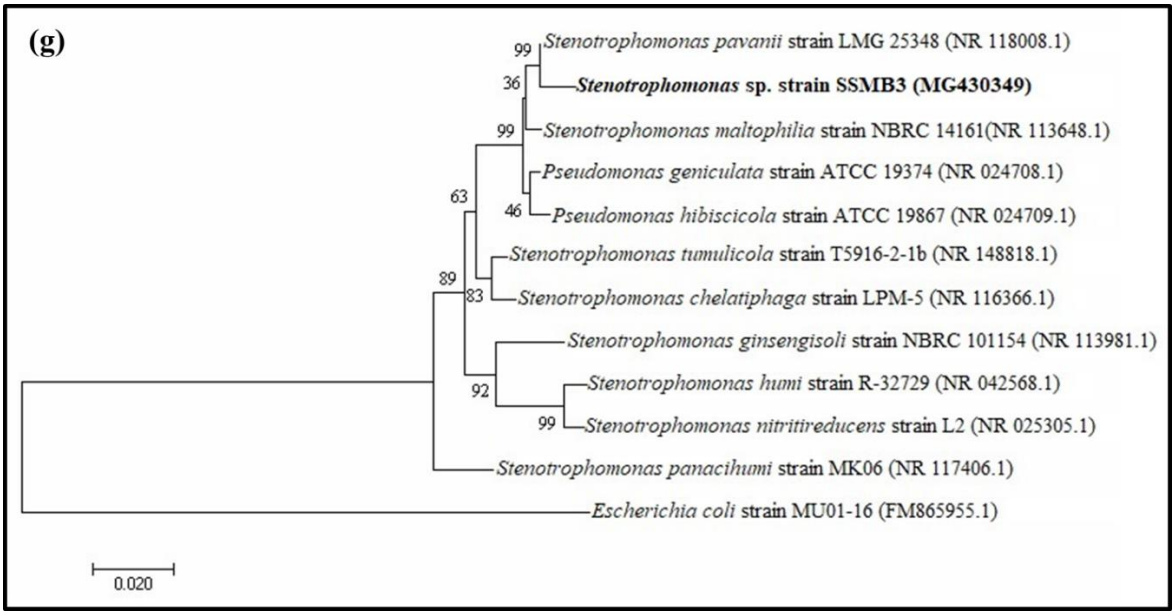

Fig. 3.10: Neighbour-joining phylogenetic tree of arsenite oxidizing bacterial isolates with closely related species of bacteria. (a) SSBW1, (b) SSBW2, (C) SSBW5, (d) SSSW4, (e) SSSW7, (f) SSAI1 and (g) SSMB3. The bootstrap values are based on 1000 replicates and are shown next to the branches.

3.9 Determination of minimum inhibitory concentration (MIC) of sodium (meta) arsenite

The MIC of arsenite for selected arsenite oxidizing bacterial strains ranged from 8-25 mM in MSM broth (Fig. 3.11). The isolates *Paenarthrobacter* sp. strain SSBW5, *Microbacterium* sp. strain SSBW1, *Micrococcus* sp. strain SSSW4 and *Corynebacterium* sp. strain SSBW2 showed MIC at 18, 17, 15 and 12 mM respectively. Two isolates *Bacillus* sp. strain SSAI1 and *Klebsiella* sp. strain SSSW7 exhibited the highest MIC at 25 and 21 mM respectively while the lowest MIC of 8 mM was obtained for *Stenotrophomonas* sp. strain SSMB3. The toxicity of arsenite was found to be higher in the liquid medium than solid because of its uniform distribution throughout the liquid medium, resulting in higher bioavailability of arsenite to the bacterial cells.

Several bacterial strains have been reported to tolerate arsenite at varying concentration. This includes *Stenotrophomonas panacihumi* MM-7 (60 mM), *K. pneumoniae* strains MNZ4 and MNZ6 (2.3 mM and 2.9 mM), *K. pneumoniae* strain MR4 (5 mM), *Alishewanella* sp. GIDC-5 (18 mM), *Brevibacillus* sp. KUMAs2 (17 mM), *Bacillus flexus* strain As-12 (5 mM) and *Pseudomonas chengduensis* As-11 showed a MIC of 25 mM (Daware et al., 2012; Bahar et al., 2012; Abbas et al., 2014; Mallick et al., 2014; Jain et al., 2014; Jebeli et al., 2017; Jebelli et al., 2018). However, it is inappropriate to compare the MIC values obtained in the present study with previous reports as the media composition varies the availability of arsenite in the medium.

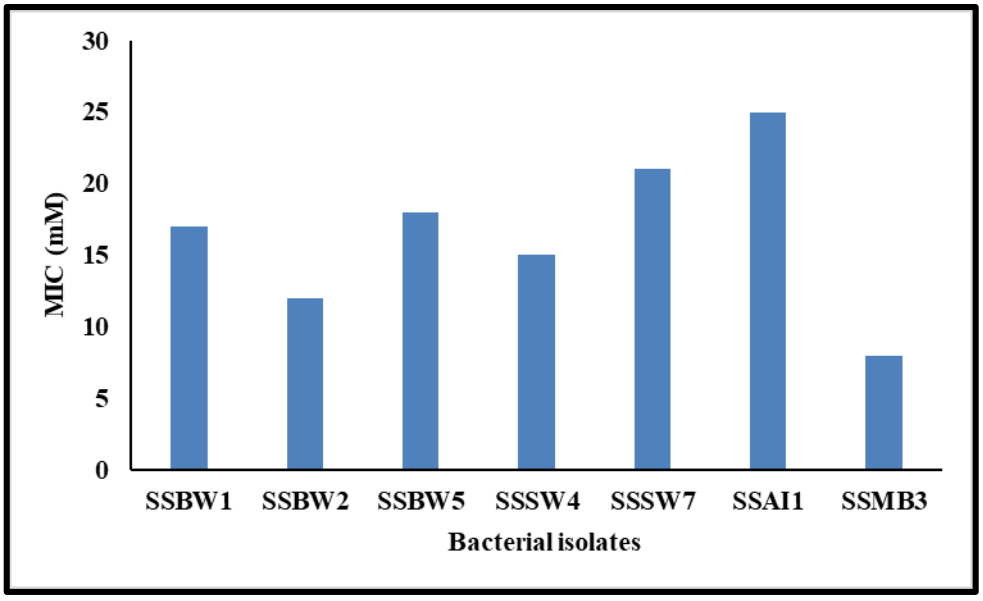

Fig. 3.11: MIC of sodium arsenite for arsenite oxidizing bacterial isolates.

Summary

Arsenite resistant bacterial strains were isolated from 8 different terrestrial sites of Goa. Among all the sampling sites, battery waste sample showed the highest viable count of 22.4 x 10^6 and 7.13 x 10^6 cfu mL^{-1} on Nutrient and MSM agar, respectively. The maximum tolerance concentration for these bacterial strains ranged from 10 to 45 mM on MSM agar. Out of 27 isolates, 15 were positive for arsenite oxidase test. The bacterial strain SW7 showed the presence of supercoiled plasmid DNA. Interestingly, strains BW1, BW2, BW5, SW4, MB3 and AI1 showed a positive PCR amplicon for *aioA* gene using chromosomal DNA as a template while SW7 showed the presence of this gene on chromosomal as well as plasmid DNA. Moreover, bacterial strains BW1, BW2, BW5, SW4 and MB3 also showed a positive amplicon for arsenite transporter gene (*acr3*) while the same was absent in isolates AI1 and SW7. Subsequently, the potential arsenite oxidizing bacterial isolates SSBW1, SSBW2, SSBW5, SSSW4, SSSW7, SSAI1 and SSMB3 were tentatively identified as *Microbacterium* sp., *Corynebacterium* sp., *Paenarthrobacter* sp., *Micrococcus* sp., *Klebsiella* sp., *Bacillus* sp. and *Stenotrophomonas* sp. respectively based on biochemical tests and 16S rDNA sequencing. Furthermore, these bacterial strains exhibited MIC in the range of 8-25 mM for arsenite in MSM broth and two isolates SSAI1 and SSSW7 showing the highest MIC values (25 & 21 mM) were selected for further studies.

Chapter IV

Response of *Bacillus* sp. strain SSAI1 and *Klebsiella* sp. strain SSSW7 to arsenite

(Results & Discussion)

4.1 Determination of optimal growth condition

The selected *Bacillus* sp. strain SSAI1 exhibited growth between pH range of 7-11 while *Klebsiella* sp. strain SSSW7 showed growth at wider pH ranging from 5-11, while the optimal growth was observed at pH 7 for both the strains (Fig. 4.1a). The strain SSAI1 showed growth at 28, 37 and 45 ℃ with highest growth at 28 ℃ whereas, strain SSSW7 could grow at 20, 28, 37 and 45 ℃ with optimum of 28 ℃ (Fig. 4.1b). Therefore the optimal pH of 7 and temperature 28 ℃ was kept constant during the entire study.

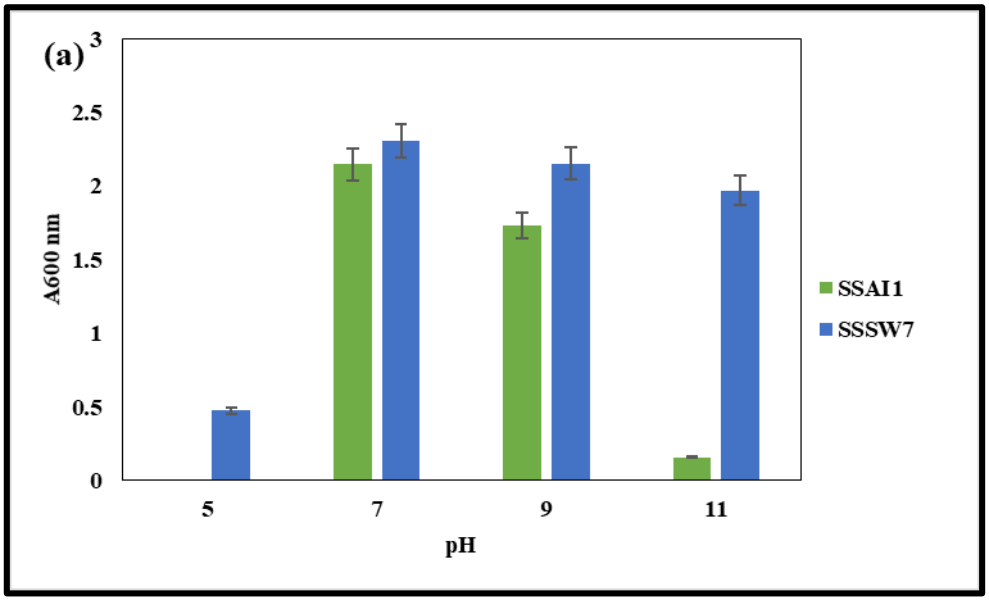

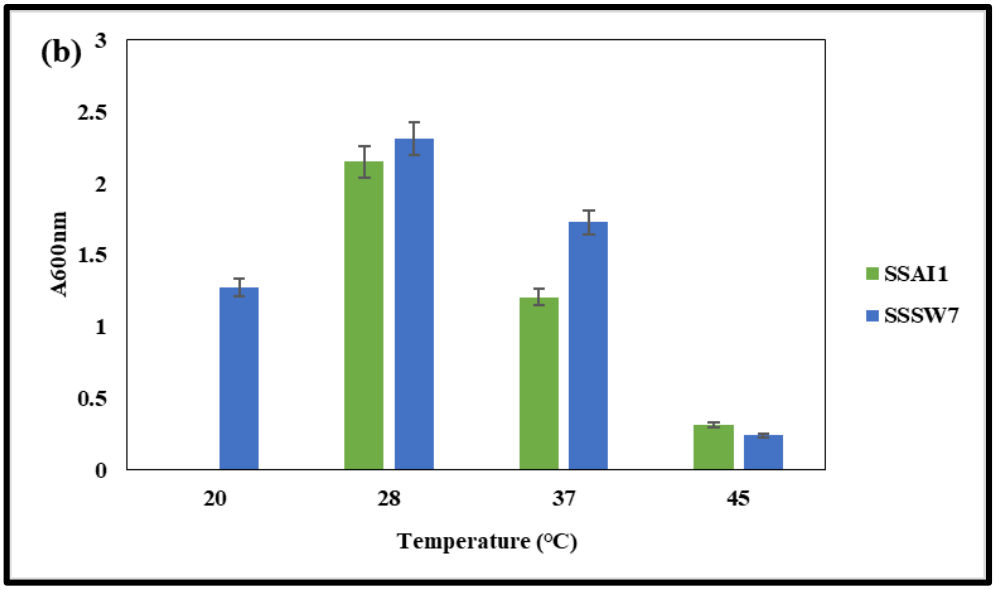

Fig. 4.1: Growth of *Bacillus* sp. strain SSAI1 and *Klebsiella* sp. strain SSSW7 at various growth conditions : (a) pH and (b) temperature.

4.2 Growth behaviour of bacterial isolates in the presence of arsenite

Both SSAI1 and SSSW7 strains followed a typical sigmoidal pattern of growth, but the presence of arsenite significantly repressed bacterial growth with increasing arsenite concentration as lag phase was found to be extended (Fig. 4.2). In *Bacillus* sp. strain SSAI1 shift in the initiation of log phase was observed from 4 h to 6 h, 12 h, 16 h, 20 h and 24 h when exposed to 5 mM, 10 mM, 15 mM, 20 mM and 24 mM arsenite respectively. A similar shift was also observed from 2 h to 6 h, 12 h and 20 h in *Klebsiella* sp. strain SSSW7 exposed to 10 mM, 15 mM and 20 mM arsenite respectively. No growth was observed in isolates SSAI1 and SSSW7 in the presence of 25 mM and 21 mM arsenite respectively, thus confirming their minimum inhibitory concentration (MIC) for arsenite.

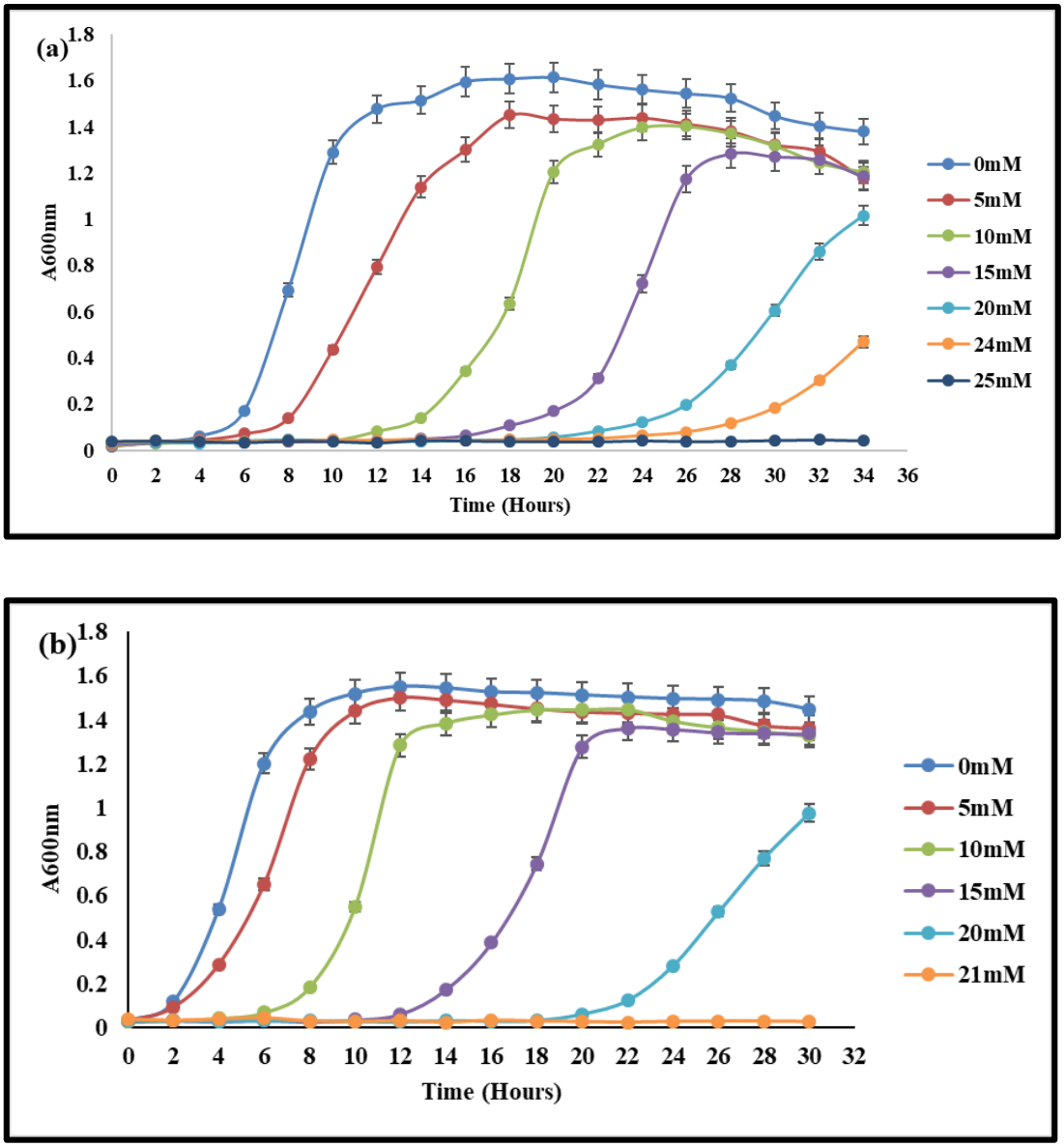

Fig. 4.2: Growth curves of bacterial strains in the presence and absence of arsenite: (a) *Bacillus* sp. strain SSAI1 and (b) *Klebsiella* sp. strain SSSW7.

4.3 Mechanism of arsenite resistance in selected bacterial isolates

4.3.1 FTIR analysis

FTIR spectroscopy of *Bacillus* sp. strain SSAI1 and *Klebsiella* sp. strain SSSW7 cells led to the identification of probable functional groups involved in arsenite resistance

(Figs. 4.3 & 4.4). The IR spectrum analysis of bacterial cells (SSAI1 & SSSW7) exposed to arsenite indicated shifting and sharpening of several peaks which could be assigned to various functional groups present on the bacterial cells involved in arsenite binding and accumulation (Table 4.1 & 4.2). Spectral changes in the region of 3300 cm^{-1} - 2800 cm^{-1} was observed which was attributed to N-H stretch of amide, O-H stretch of the carboxylic acids and hydroxyl groups. Shifting of FTIR peaks was also observed in the regions from 1750-1500 cm^{-1} and 1500-1200 cm^{-1}, demonstrating the interaction of amide linkages from proteins and peptides (Oust et al., 2004). Sharpening and peak changes were perceived in the band region of 1200-1000 cm^{-1} of arsenite exposed cells which can be attributed to a C-N stretching of aliphatic amine and C-O stretching of alcohols, carboxylic acids, esters and ethers. Peak changes observed in the region 900-700 cm^{-1} were attributed to =C-H bending of alkenes and C-H bending of aromatics. The spectral changes observed in the region 700-500 cm^{-1} were associated with alkyl halide stretching. Therefore, IR analysis revealed that functional groups viz. carboxyl, hydroxyl, amino, amide and amine were involved in the interaction of this toxic metalloid.

In earlier studies, functional groups such as amino, carboxyl and hydroxyl are reported to interact with metal ions (Bueno et al., 2008; Pandi et al., 2009). Similarly, FTIR analysis of arenite exposed *Escherichia coli* displayed involvement of C-H of alkane, amino, amine and amide group in arsenite binding (Wu et al., 2010). Likewise, Singh et al. (2016) also showed changes in the spectrum of *Bacillus aryabhattai* strain NBRI014 grown in the presence of arsenic indicating that amino, alkyl halides and hydroxyl group present on the bacterial surface may be involved in arsenic binding.

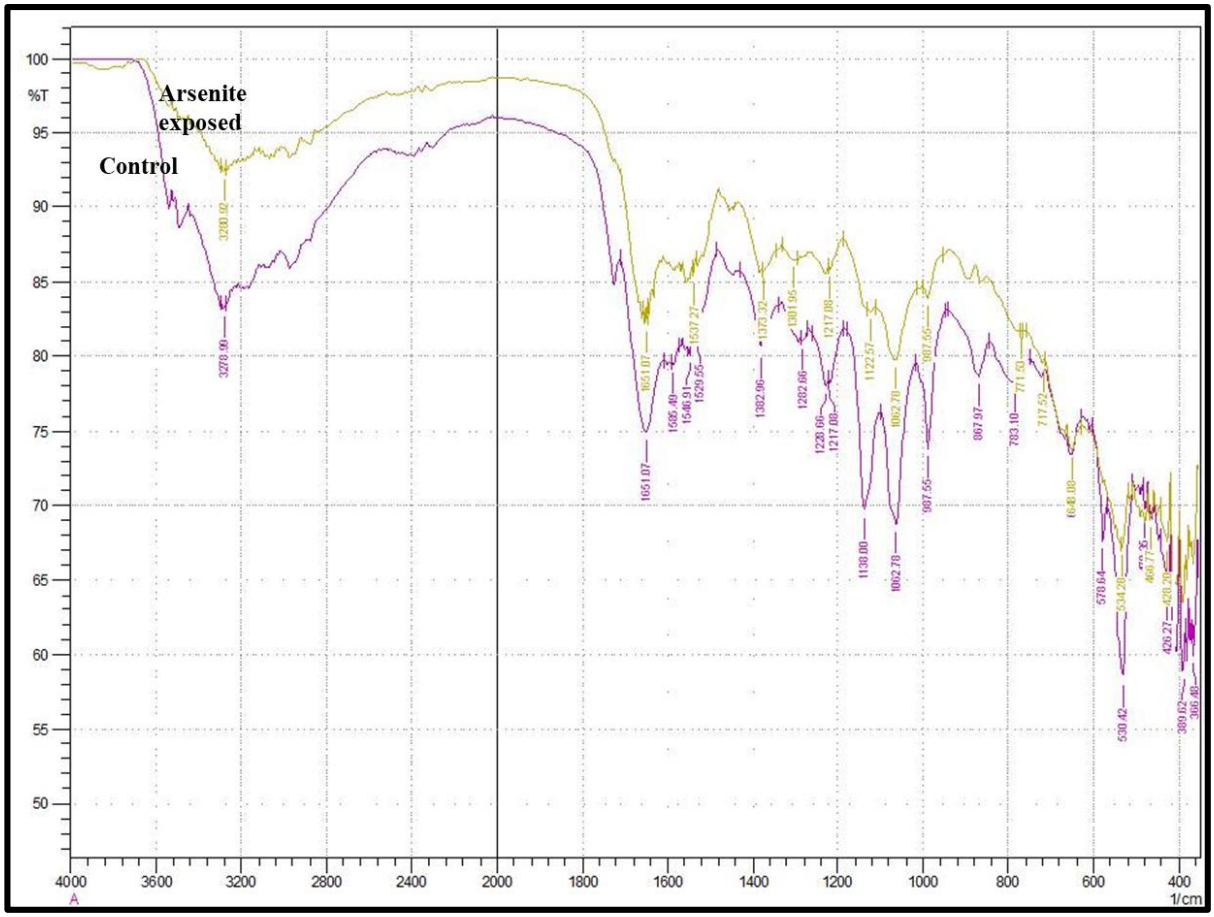

Fig. 4.3: FTIR spectrum of *Bacillus* sp. strain SSAI1. Purple-Bacterial cells in the absence of arsenite (control), Golden - Bacterial cells exposed to 10 mM arsenite (exposed).

Table 4.1: IR peak changes observed in *Bacillus* sp. strain SSAI1 indicating different functional groups present on the cell surface.

Control cells (cm^{-1})	Arsenite exposed cells (cm^{-1})	Functional groups
3278.99	3280.92	O-H stretch of carboxylic acids
1651.07	1651.07	-C=C- stretch of alkenes
1529.55	1537.27	N-O asymmetric stretch of nitro compounds

1382.96	1373.32	-C-H bend of alkane
1282.66	1301.96	C-N stretch of aromatic amines, C-O stretch of alcohols, carboxylic acids, esters, ethers
1217.08	1217.08	C-N stretch of aliphatic amines
1138	1122.57	C-N stretch of aliphatic amines
1062.78	1062.78	C-N stretch of aliphatic amines
987.55	987.55	=C-H bend of alkenes
867.97	891.11	C-H bend of aromatics
530.42	534.28	C-Br stretch of alkyl halides

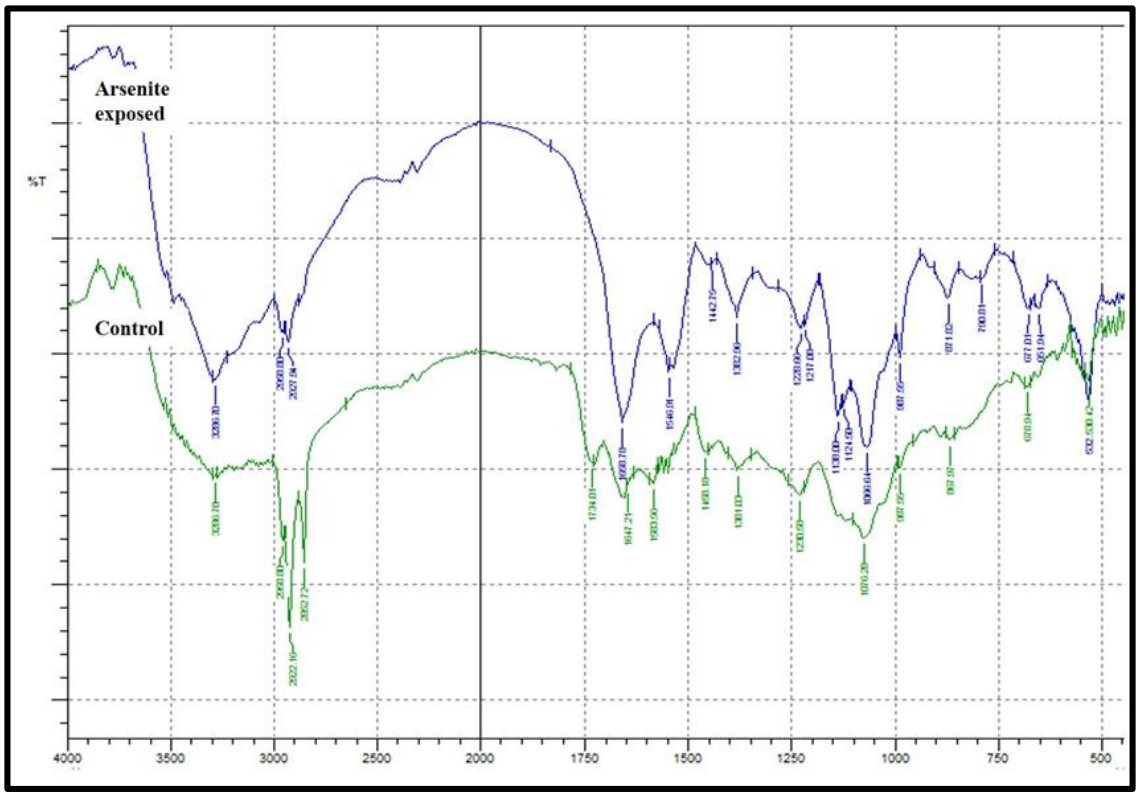

Fig. 4.4: FTIR spectrum of *Klebsiella* sp. strain SSSW7. Green - Bacterial cells without arsenite (control), Blue - Bacterial cells exposed to 15 mM arsenite.

Table 4.2: IR peak changes observed in *Klebsiella* sp. strain SSSW7 indicating different functional groups present on the cell surface.

Control cells (cm^{-1})	Arsenite exposed cells (cm^{-1})	Functional groups
3296.70	3296.70	N-H stretch of amides and O-H stretch of hydroxyl groups
2922.16	2927.94	C-H stretch of alkanes and O-H stretch of carboxylic acids
2852.72	-	C-H stretch of alkanes, O-H stretch of carboxyl acids
1734.01	1658.78	–C=C- stretch of alkenes
1647.21	1546.91	N-O asymmetric stretch of nitro compounds
1583.56	-	N-H bend of 1º amine
1458.10	1442.75	C-C stretch of aromatics
1381.03	1382.96	-C-H bend of alkane
1230.58	1228.86	C-O stretch of alcohols, carboxylic acids, esters ethers
-	1138.00	C-N stretch of aliphatic amine and C-O stretch of alcohol carboxylic acids, esters, ethers
1076.28	1066.64	C-O stretch of alcohol carboxylic acids, esters, ethers
987.56	987.56	=C-H bend of alkenes
867.97	871.82	=C-H, bend of alkenes, C-H bend, aromatics

678.94	677.01	C-Br stretch of alkyl halide
651.94	651.94	C-Cl and C-Br stretch of alkyl halides
530.42	532.35	C-Br stretch of alkyl halide

4.3.2 SEM-EDAX analysis

Unique morphological alterations in *Bacillus* sp. strain SSAI1 and *Klebsiella* sp. strain SSSW7 were observed on exposure to arsenite. In the presence of arsenite cells of strain SSAI1 showed clumping (Fig. 4.5 a,c), while strain SSSW7 demonstrated the formation of long interconnected chains of cells (Fig. 4.6 a,c). This could be one of the strategies used by bacterial cells to alleviate toxicity of arsenite as decrease in cell to volume ratio reduces the toxicity of the metal or metalloid. Similar morphological changes have been observed in *Acinetobacter lwoffii*, *Lysinibacillus* sp. B2A1 *Pseudomonas resinovorans* and *Acinetobacter calcoaceticus* and exposed to arsenite (Banerjee et al., 2011; Rathod et al., 2019).

Interestingly, electron dispersive X-ray spectroscopy (EDAX) did not show any adsorption peak of arsenic on the bacterial cell surface (Figs. 4.5 and 4.6 b,d). This clearly suggested intracellular accumulation of arsenite in *Bacillus* sp. strain SSAI1 and *Klebsiella* sp. strain SSSW7.

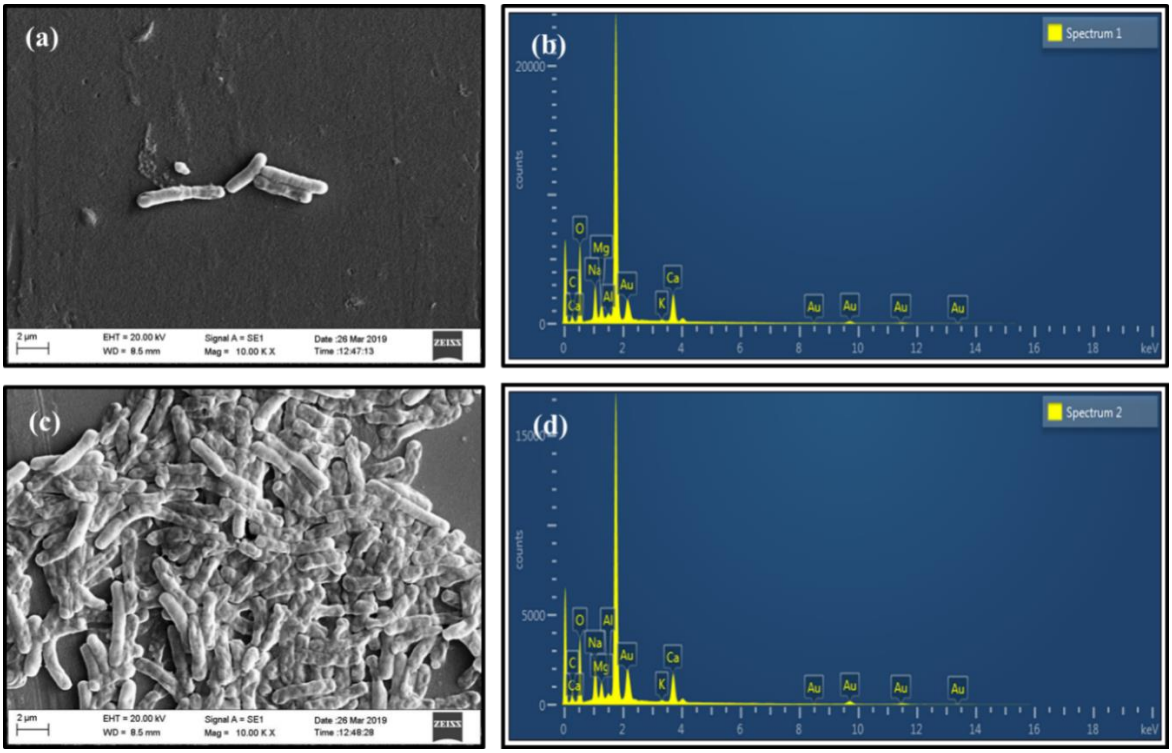

Fig. 4.5: Scanning electron micrograph demonstrating the effect of arsenite on the morphology of *Bacillus* sp. strain SSAI1. (a) Bacterial cells without arsenite exposure, (b) EDAX spectrum of bacterial cells without arsenite exposure, (c) Bacterial cells exposed to 10 mM arsenite (d) EDAX spectrum of bacterial cells presence exposed to 10 mM arsenite.

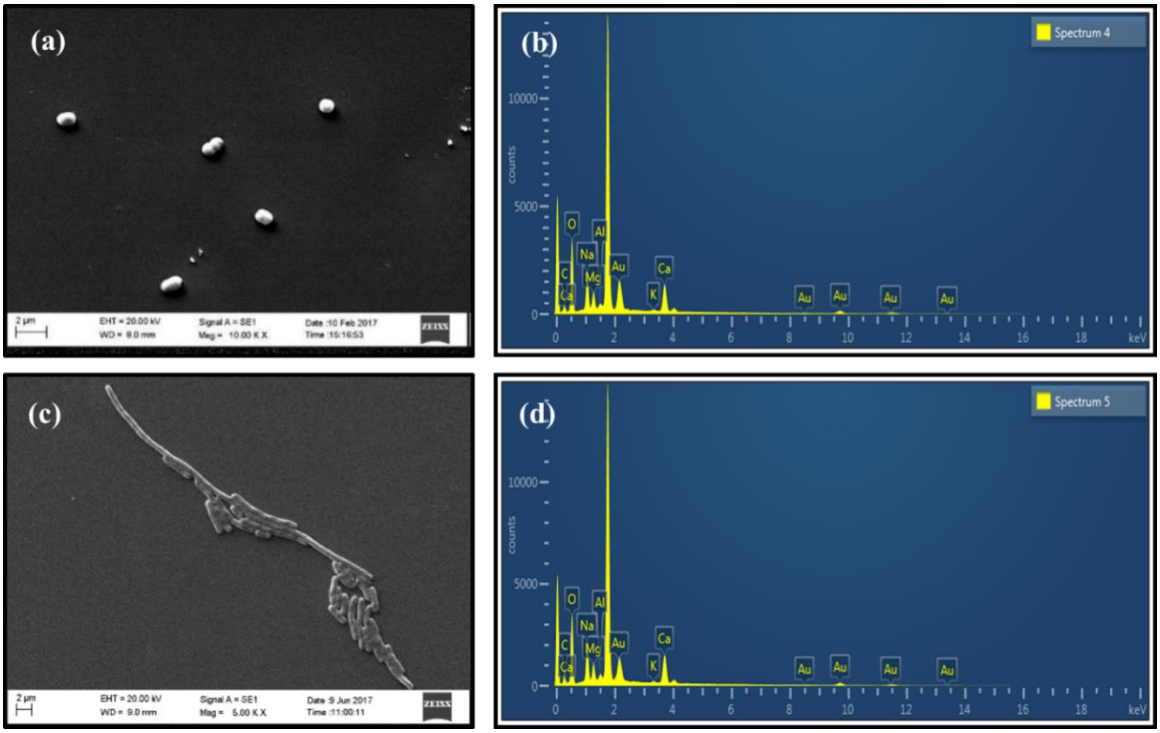

Fig. 4.6: Scanning electron micrograph demonstrating the effect of arsenic on the morphology of *Klebsiella* sp. strain SSSW7. (a) Bacterial cells without arsenite exposure, (b) EDAX spectrum of bacterial cells without arsenite exposure, (c) Bacterial cells exposed to 15 mM arsenite, (d) EDAX spectrum of bacterial cells exposed to 15 mM arsenite.

4.3.3 TEM-EDAX analysis

TEM analysis of *Bacillus* sp. strain SSAI1 and *Klebsiella* sp. strain SSSW7 exposed to arsenite revealed that arsenite severely affected the integrity of the plasma membrane and caused condensation of cytoplasm (Figs. 4.7 a,b & 4.8 a,b). The presence of electron-dense deposits throughout the cytoplasm was observed in the strain SSAI1 (Fig. 4.7 a,b) while in case of SSW7 strain electron-dense deposits were found in the periplasmic space (Fig. 4.8 a, b). The unexposed cells of SSAI1 and SSSW7 strains did not show any such depositions. Thus indicating the arsenic accumulation in the

cytoplasmic and periplasmic spaces of exposed SSAI1 and SSSW7 cells which corroborated with SEM results. The presence of arsenic peaks in EDAX spectrum of SSAI1 and SSSW7 cells treated with 10 and 15 mM arsenite respectively further confirmed that arsenite is not adsorbed at the cell surface, but accumulated intracellularly (Fig. 4.7 c,d & 4.8 c,d).

Previously TEM studies of arsenite exposed bacterial isolates viz. *Microbacterium oleivorans* strain Ransu-1, *Acinetobacter soli* strain IBL-1, *Acinetobacter venetianus* strain IBL-2, *Acinetobacter junii* strain IBL-3, *Acinetobacter baumannii* strain IBL-4 and *Acinetobacter calcoaceticus* strain IBL-5 demonstrated that arsenite affected the integrity of the plasma membrane. Additionally strains IBL-1, IBL-2, IBL-3 and IBL-5 also showed condensation of cytoplasm on exposure to 1 mg L^{-1} of arsenite (Goswami et al., 2014). Likewise, the presence of intracellular electron-dense deposits and arsenic has been reported in *Acinetobacter lwoffii* strain, RJB-2, *Kocuria flava* AB402 and *Bacillus vietnamensis* AB403 (Banerjee et al., 2011; Mallick et al., 2018).

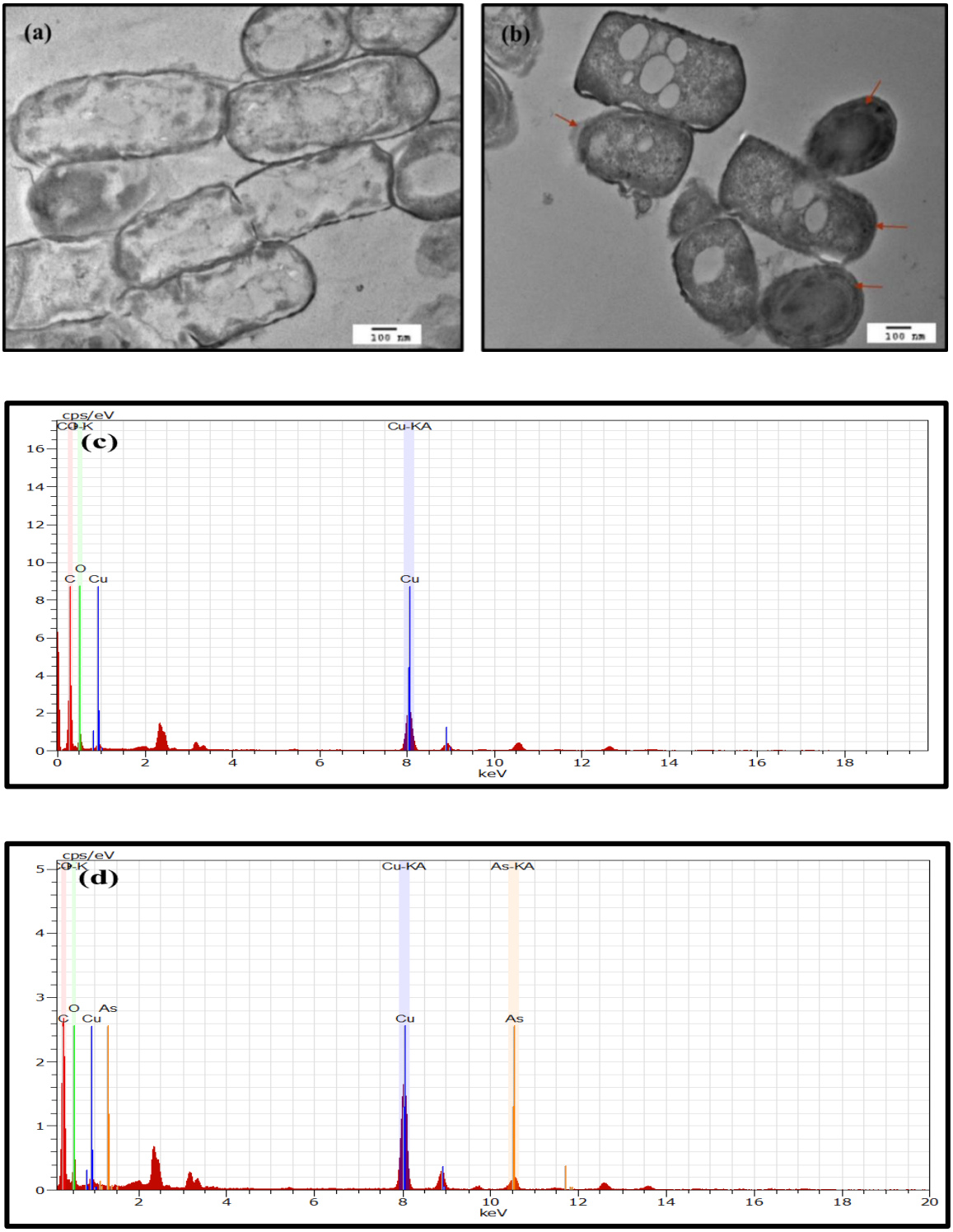

Fig. 4.7: Transmission electron micrograph of *Bacillus* sp. strain SSAI1. (a) Bacterial cells in the absence of arsenite, (b) Bacterial cells exposed to 10 mM arsenite: red arrows indicate the damaged plasma membrane, condensed cytoplasm and presence of electron-

dense deposits, (c) EDAX spectrum of bacterial cells in the absence of arsenite, (d) EDAX spectrum of bacterial cells in the presence of 10 mM arsenite.

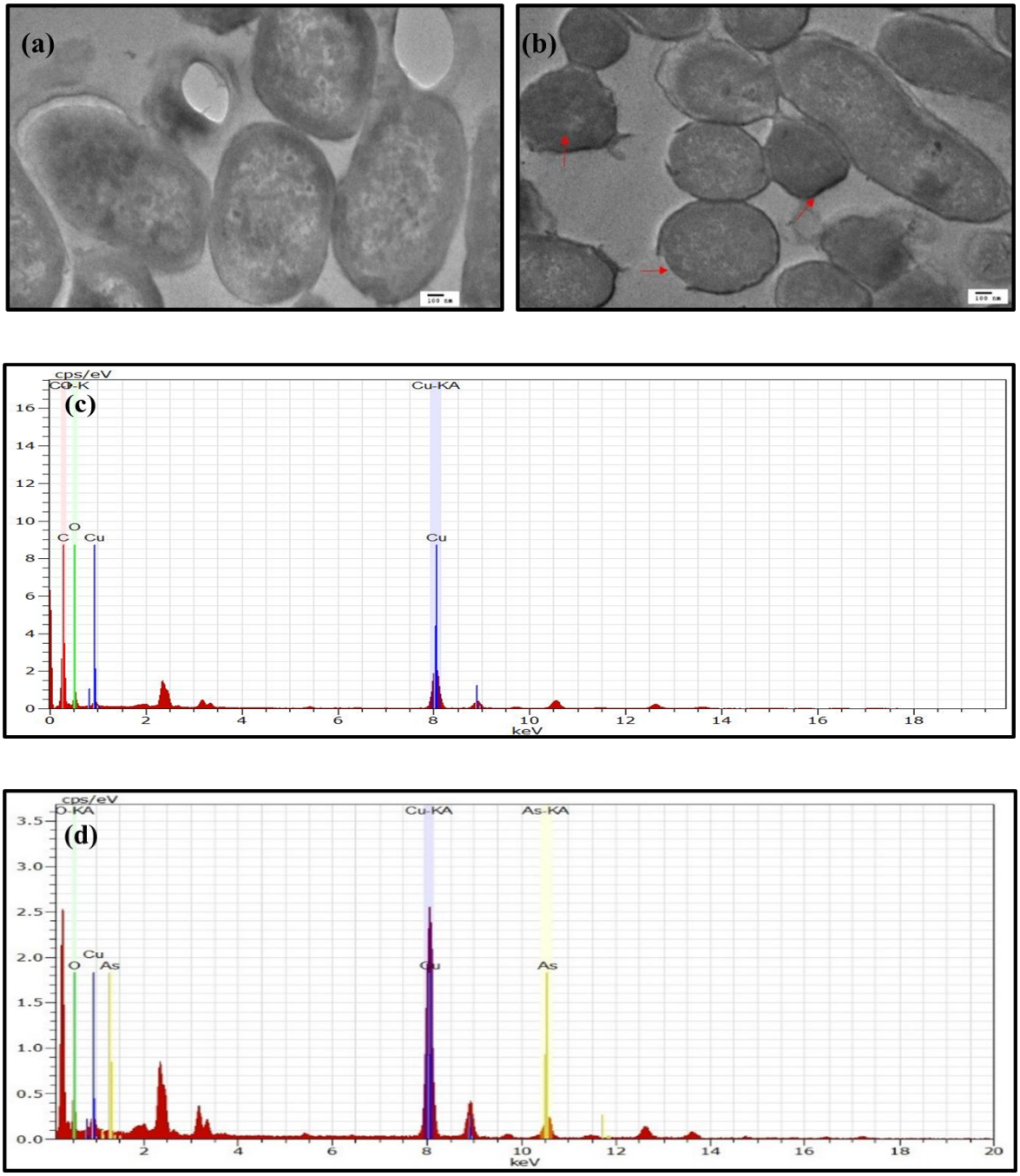

Fig. 4.8: Transmission electron micrograph of *Klebsiella* sp. strain SSSW7. (a) Bacterial cells in the absence of arsenite, (b) Bacterial cells exposed to 15 mM arsenite: red arrows indicate the damaged plasma membrane, condensed cytoplasm and electron-

dense deposits at periplasm, (c) EDAX spectrum of bacterial cells in the absence of arsenite, (d) EDAX spectrum of bacterial cells in the presence of 15 mM arsenite.

4.3.4 Quantitative analysis of arsenate

Quantitative estimation of arsenate through molybdene blue method revealed that the cells of bacterial strain SSAI1 and SSSW7 internalized 7 mM and 10 mM of arsenate respectively after transformation of arsenite within 24 h. This studies confirmed intracellular uptake of arsenic in strain SSAI1 and SSSW7 further corroborating our previous results of FTIR, SEM, TEM and EDAX analysis. Several studies have shown the potential of bacterial strains such as *Pseudomonas stutzeri* (1 mM within 25-30 h), *Stenotrophomonas panacihumi* (500 µM within 12 h), *Variovorax* sp. MM-1 (500 µM within 3 h), *Bacillus flexus* strain As-12 (45 % after 48 h), *Pseudomonas chengduensis* As-11 (48 % after 72 h) and *Pseudomonas extremorientalis* (25 % after 72 h) to oxidize arsenite (Chang et al., 2010; Bahar et al., 2012; 2013; Majumder et al., 2013; Jebeli et al., 2017; Jebelli et al., 2018; Satyapal et al., 2018). However, the strains (SSAI1 & SSSW7) isolated in the present study were found to be much more efficient in the oxidation of arsenite as compared to previously reported strains. Thus, making them economically viable candidates for future arsenite detoxification application.

4.3.5 Assay of arsenite oxidase activity

Arsenite oxidase activity was determined using three fractions, i.e. cell-free extract, periplasmic and spheroplast from both *Bacillus* sp. strain SSAI1 and *Klebsiella* sp. strain SSSW7 (Table 4.3). The arsenite oxidase enzyme activity of SSAI1 cells was

found to be highest in periplasmic fraction (i.e. 2.168 µmol DCIP min^{-1} mg^{-1} protein) followed by cell-free extract (i.e. 0.574 µmol DCIP min^{-1} mg^{-1} protein) and spheroplast fractions (i.e. 0.338 µmol DCIP min^{-1} mg^{-1} protein). Whereas in case of strain SSSW7 highest enzyme activity was obtained in periplasmic fraction (i.e. 1.328 µmol DCIP min^{-1} mg^{-1} protein) as compared to cell-free extract (i.e. 0.577 DCIP min^{-1} mg^{-1} protein) and spheroplast fractions (i.e. 0.059 µmol DCIP min^{-1} mg^{-1} protein). The above observations clearly demonstrated that arsenite oxidase enzyme is predominant in the periplasmic space of the isolates. Previously several bacterial strains viz. *Rhizobium* NT-26, *Hydrogenophaga* sp strain NT-14 and *Ochrobactrum triticii* SCII24 are reported to carryout arsenite oxidation mediated by periplasmic arsenite oxidase enzyme (Santini and Vanden Hoven, 2004; Vanden Hoven and Santini, 2004; Branco et al., 2009). These reports further strengthen our findings that *Bacillus* sp. strain SSAI1 and *Klebsiella* sp. strain SSSW7 also posses periplasmic arsenite oxidase enzyme.

Table 4.3: Arsenite oxidase activity of *Bacillus* sp. strain SSAI1 and *Klebsiella* sp. strain SSSW7

S. N.	Fractions	Specific arsenite oxidase activity (µM DCIP min^{-1} mg^{-1} protein)	
		SSAI1	SSSW7
1	Cell free extract	0.574	0.577
2	Spheroplast fraction	0.338	0.059
3	**Periplasmic fraction**	**2.168**	**1.328**

4.4 Cross tolerance to other heavy metals

The *Bacillus* sp. strain SSAI1 and *Klebsiella* sp. strain SSSW7 showed cross-tolerance to several heavy metals and metalloids (Fig. 4.9). The strain SSAI1 exhibited highest cross-tolerance to arsenate (60 mM) followed by chromium (12 mM), iron (12 mM), manganese (10 mM), zinc (6 mM), lead (4 mM) while least for cadmium, nickel and copper (2 mM each). Similarly, in case of strain SSSW7 highest tolerance was obtained for arsenate (160 mM) followed by chromium (15 mM), iron (15.5 mM), cadmium (14.5 mM), manganese (14 mM), copper (12 mM), zinc (11 mM), nickel (10 mM) and least for lead (5 mM). Several resistance mechanisms involving efflux pumps, surface adsorption, intra as well as extracellular sequestration and redox reactions are usually present in microorganisms to reduce metal/metalloid toxicity (Ianeva, 2009; Özdemir et al., 2012). These mechanisms are usually non-specific and therefore results in cross-tolerance to various heavy metals and metalloids (Naik et al., 2012). This could be the possible reason for cross-tolerance in strain SSAI1 and SSSW7. Additionally, it was also observed that *Klebsiella* sp. strain SSSW7 showed higher tolerance to heavy metals/ metalloids as compared to SSAI1 isolate, which could be due to the presence of plasmid in this strain. The previous study on arsenic resistant *Bacillus flexus* strain As-12 showed resistance to heavy metals such as zinc, chromium, lead, nickel, copper, mercury and cadmium (Jebeli et al., 2017). Similarly, *Escherichia coli* Cont-1 was reported to show resistance to several heavy metals viz. As^{5+}, Fe^{3+}, Co^{2+}, Cu^{2+}, Se^{6+}, Zn^{2+} and Cd^{2+} (Mohapatra and Sar, 2018). However, it will be inappropriate to compare the MTC values of the current study with previous reports as the media composition and experimental set up is different.

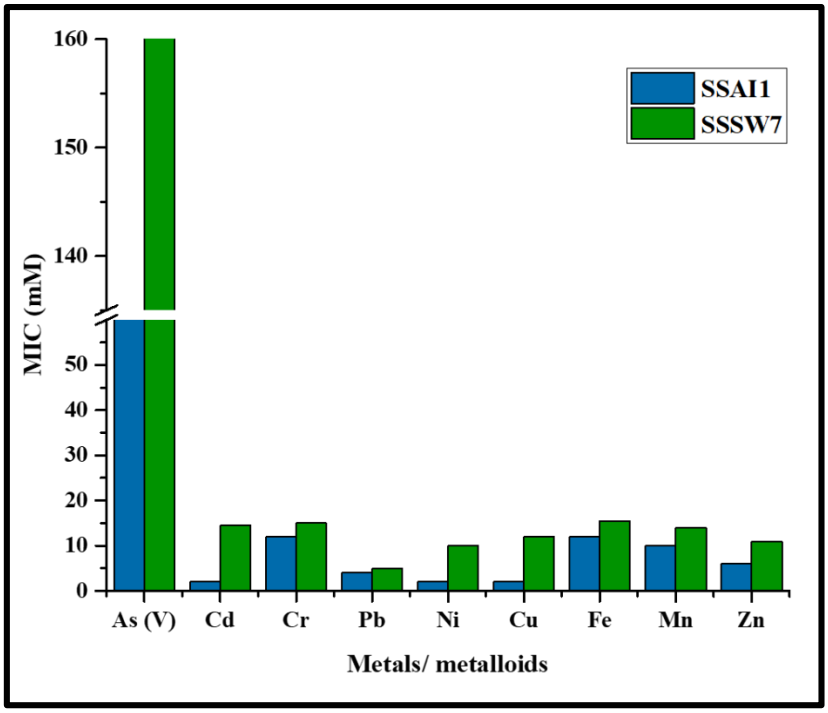

Fig. 4.9: Cross tolerance of *Bacillus* sp. strain SSAI1 and *Klebsiella* sp. strain SSSW7 to other heavy metals/ metalloids.

4.5 Antibiotic susceptibility

It is interesting to note that both the isolates showed resistance to different antibiotics (Table 5.3). The isolate SSAI1 was found resistant to penicillin-G (10 Units), erythromycin (15µg), clindamycin (2 µg), bacitracin (10 Units) and sulphatriad (200 Units). In contrast, it was found to be susceptible to cloxacillin (5 µg), gentamicin (10 µg), oxytetracycline (30 µg), co-trimoxazole (25 µg), cephalothin (30 µg), chloramphenicol (30 µg), polymyxin-B (300 Units), tetracycline (30 µg), ciprofloxacin (10 µg), kanamycin (30 µg), amikacin (10 µg), ampicillin (10 µg) and colistin sulphate (25 µg).

On the other hand, the isolate SSSW7 carrying plasmid demonstrated resistance to several antibiotics viz. cloxacillin (5 µg), penicillin-G (10 Units), erythromycin (15 µg), clindamycin (2 µg), bacitracin (10 Units), carbenicillin (100 µg), nitrofurantoin (300 µg), ampicillin (10 µg) and sulphatriad (200 Units). In comparison, it was found susceptible to gentamicin (10 µg), oxytetracycline (30 µg), co-trimoxazole (25 µg), cephalothin (30 µg), chloramphenicol (30 µg), polymyxin-B (300 Units), tetracycline (30 µg), ciprofloxacin (10 µg), kanamycin (30 µg), amikacin (10 µg), streptomycin (10 µg) and colistin sulphate (25 µg) which was evident from the zone of clearance surrounding the respective antibiotic disc (Fig. 4.10). It is a well-known fact that genes encoding heavy metal/ metalloid resistance and various antibiotics coexist on the chromosomal or plasmid genome in bacteria (Silver and Phung, 1996; Lupo et al., 2012). A similar observation was also reported in *Escherichia coli* Cont-1, which showed resistance to several antibiotics, heavy metals and metalloids (Mohapatra and Sar, 2018).

Table 4.4: Susceptibility of *Bacillus* sp. strain SSAI1 and *Klebsiella* sp. strain SSSW7 to various antibiotics.

Antibiotics	Amount of different antibiotics on respective discs (µg)	Response of isolates	
		SSAI1	SSSW7
Cloxacillin	5	S	R
Gentamicin	10	S	S
Oxytetracycline	30	S	S
Penicillin-G	10 Units	R	R
Co-trimoxazole	25	S	S
Erythromycin	15	R	R

Cephalothin	30	S	S
Clindamycin	2	R	R
Bacitracin	10 Units	R	R
Chloramphenicol	30	S	S
Polymyxin B	300	S	S
Tetracycline	30	S	S
Carbenicillin	100	I	R
Ciprofloxacin	10	S	S
Kanamycin	30	S	S
Nitrofurantoin	300	I	R
Streptomycin	10	I	S
Amikacin	10	S	S
Ampicillin	10	S	R
Colistin methane sulphonate	25	S	S
Sulphatriad	200 Units	R	R

* R - Resistant, I - Intermediate, S - Susceptible

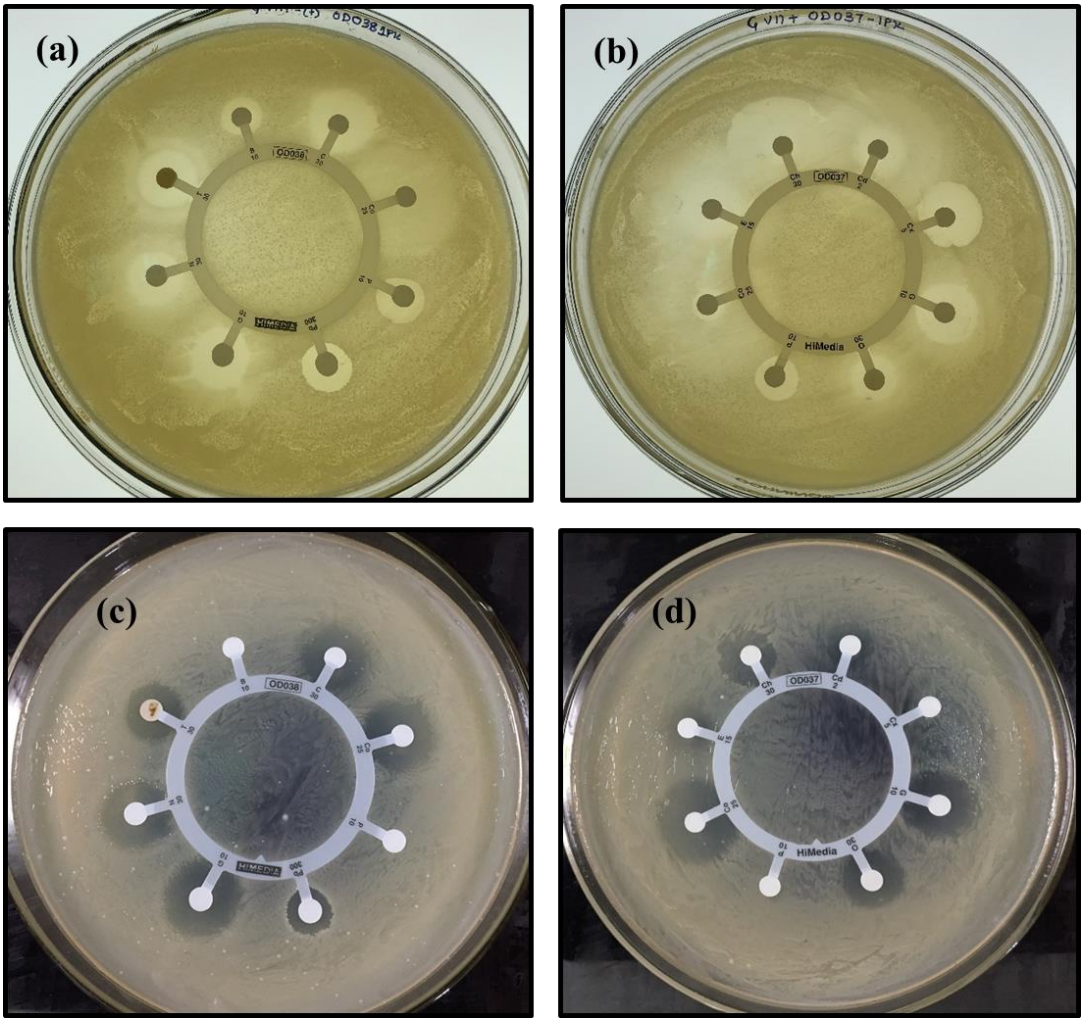

Fig. 4.10: Antibiotic susceptibility of the *Bacillus* sp. strain SSAI1 (a, b) and *Klebsiella* sp. strain SSSW7 (c, d) against various antibiotics.

Summary

The optimum growth of the bacterial isolates *Bacillus* sp. SSAI1 and *Klebsiella* sp. SSSW7 was observed at pH 7 and temperature 28 ℃. Growth studies of strains SSAI1 and SSSW7 revealed an extended lag phase with increasing arsenite concentration in the medium. FTIR analysis of both the isolates indicated interactions of arsenite with the functional groups present on the bacterial cells due to arsenic accumulation. Furthermore, SEM analysis of *Bacillus* sp. strain SSAI1 showed clumping of cells on exposure to arsenite while *Klebsiella* sp. strain SSSW7 revealed morphology changes from short rods to long chains of cells. EDAX spectrum showed no significant arsenite adsorption at the cell surface. Subsequently TEM-EDAX analysis of *Bacillus* sp. strain SSAI1 and *Klebsiella* sp. strain SSSW7 demonstrated severe disruption of the plasma membrane, condensation of cytoplasm and intracellular accumulation of arsenic. The bacterial isolates SSAI1 and SSSW7 were found to internalize 7 and 10 mM arsenate respectively within 24 hours as revealed by molybdene blue method. Enzyme assay further confirmed that the arsenite oxidase enzymes of *Bacillus* sp. strain SSAI1 and *Klebsiella* sp. strain SSSW7 were periplasmic. Additionally the isolates SSAI1 and SSSW7 also showed cross-tolerance to several heavy metals/ metalloids and resistance to the majority of common antibiotics.

Chapter V

Proteomic analysis of *Bacillus* sp. strain SSAI1 and *Klebsiella* sp. strain SSSW7 exposed to arsenite

(Results & Discussion)

5.1 LC-MS/MS Analysis

SDS-PAGE analysis of the whole-cell protein extracted from control and arsenite exposed cells of *Bacillus* sp. strain SSAI1 (Fig. 5.1) and *Klebsiella* sp. strain SSSW7 revealed differential expression of several proteins in response to arsenite which were further analyzed using LC-MS/MS. There are very few reports on proteomic analysis of bacteria exposed to arsenic (Carapito et al., 2006; Li et al., 2010; Daware et al., 2012; Shah and Damare, 2018); therefore these reports prompted us to explore arsenite responsive specific proteins in arsenite resistant bacterial isolates.

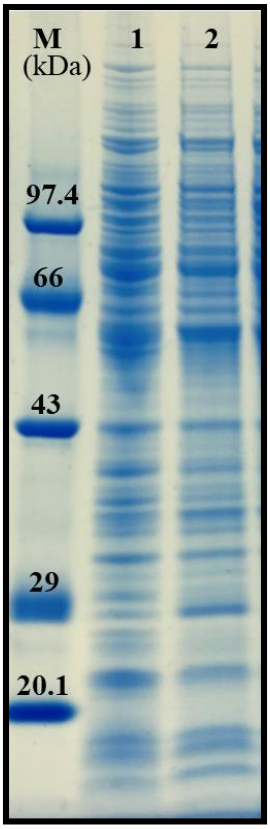

Fig. 5.1: SDS-PAGE analysis of *Bacillus* sp. strain SSAI1. Lane 1: Protein profile of cells without arsenite exposure**,** Lane 2: Protein profile of cells exposed to 5 mM arsenite**,** M: Medium range protein molecular weight marker.

5.1.1 Proteomic analysis of *Bacillus* sp. strain SSAI1

Protein profile of *Bacillus* sp. strain SSAI1 revealed the identification of total 642 and 631 proteins in control and arsenite exposed cells, respectively. All the proteins identified in control and test samples were divided into various categories based on their functional processes using KEGG pathway (Figs. 5.2 & 5.3). Majority of these proteins were related to metabolic processes; (e.g. carbohydrate, energy, lipid, nucleotide, amino acid, cofactor and vitamins, terpenoid, polyketides, xenobiotics); cellular processes and environmental as well as genetic information processing.

Out of 631, 128 proteins were up-regulated and 122 were down-regulated as compared to control (Figs. 5.4 & 5.5). It was observed that most of the up-regulated proteins (Fig. 5.4) were involved in carbohydrate metabolism (27 %), amino acid metabolism (12 %), transport (7 %), transcription and translation (6 %), cell growth (5 %), nucleotide metabolism (4 %), energy metabolism (3 %) and lipid metabolism (3 %) followed by the metabolism of cofactor and vitamins (2 %), xenobiotic biodegradation and metabolism (2 %), signal transduction (2 %), **peptidoglycan biosynthesis (2 %)**, peptidases and inhibitors (2 %), chromosome and associated proteins (2 %), **chaperones and folding catalysts (1 %)**, **stress response (1 %),** metabolism of terpenoid and polyketides(1 %), drug resistance (1 %), uncharacterized/ hypothetical proteins (3 %) and others (16 %). The arsenite up-regulated proteins identified in the strain SSAI1 along with their fold change value has also been expressed clearly (Table 5.1).

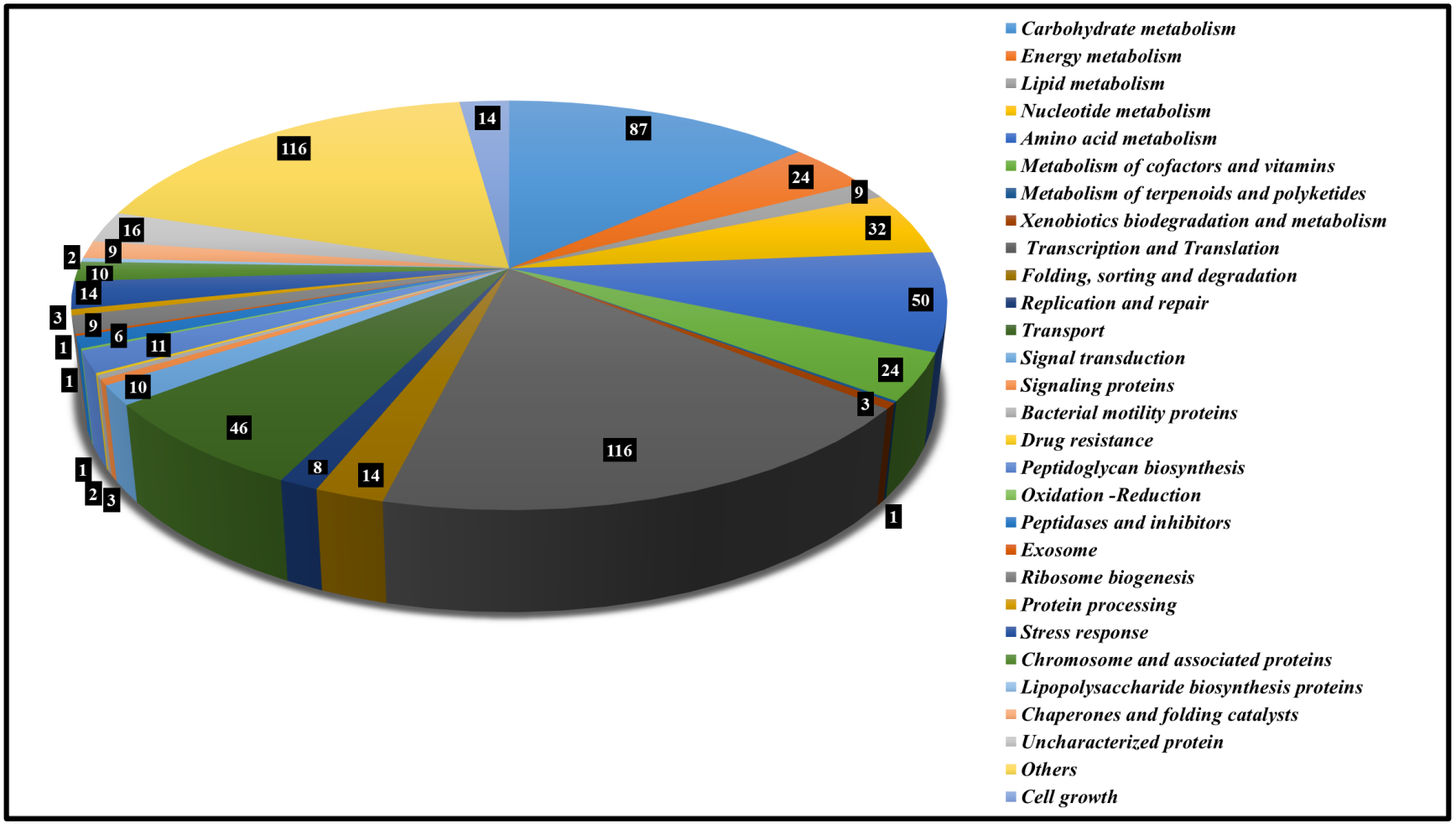

Fig. 5.2: Graphical representation depicting the classification of proteins identified in *Bacillus* sp. strain SSAI1 (control). The numbers denote the total proteins identified for each category

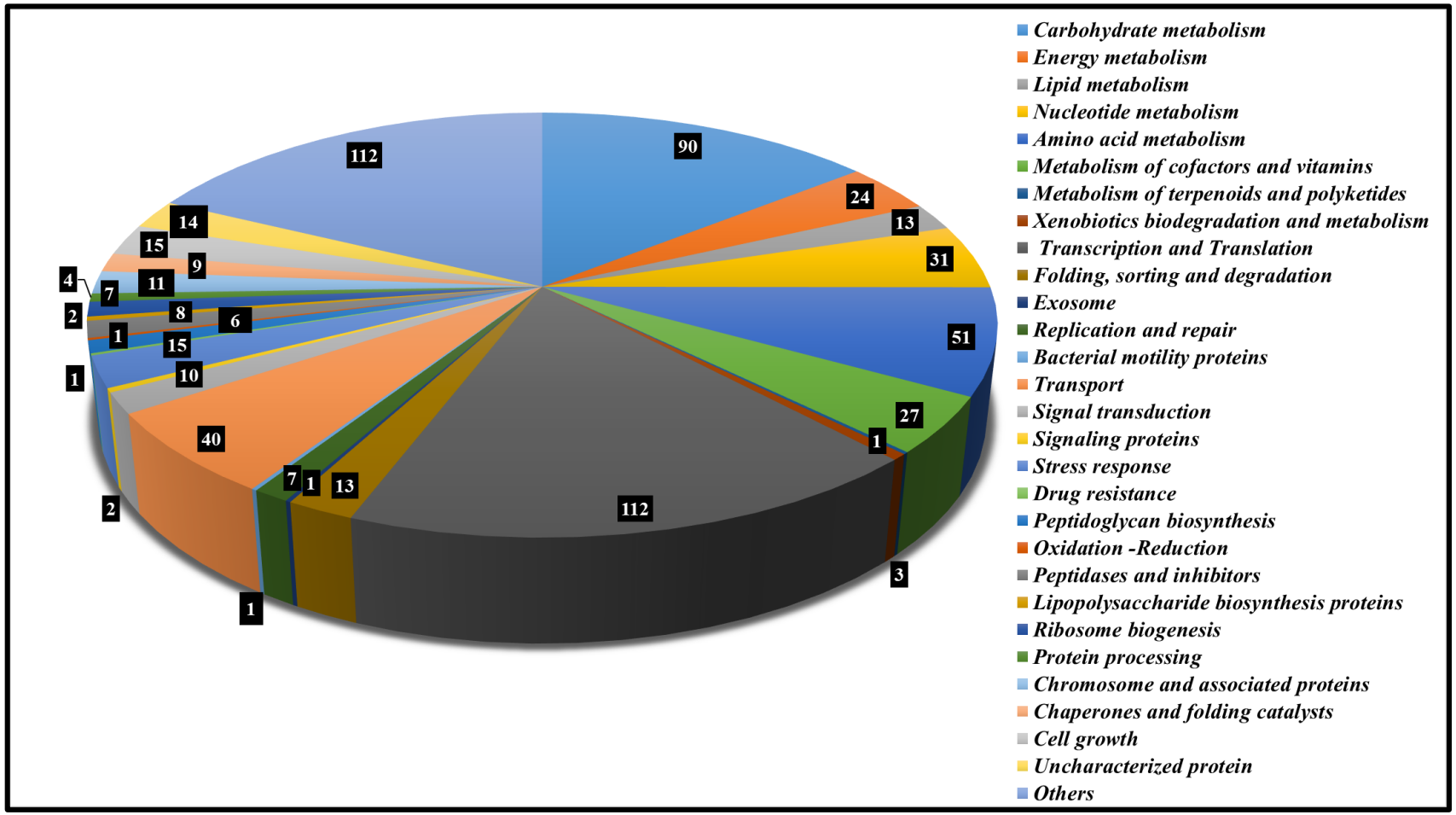

Fig. 5.3: Graphical representation depicting the classification of proteins identified in *Bacillus* sp. strain SSAI1 exposed to 5 mM arsenite (Test). The numbers denote the total proteins identified for each category.

5.1.1.1 Proteins involved in metabolism

Proteins involved in carbohydrate metabolisms such as glycolysis, pentose phosphate pathway and TCA cycle were found to be upregulated under arsenite stress. Similar observations were also observed in *C. testosterone*, CNB-1, *K. pneumoniae*, *T. arsenivorans*, *Y. enterolitica* 1A, *Exiguobacterium* strains S17 and *Staphylococcus* sp. NIOSBK35 on exposure to arsenic (Zhang et al., 2007; Bryan et al., 2009; Mallik et al., 2012; Belfiore et al., 2013; Shah and Damare, 2018). The strain SSAI1 also showed up-regulation of several proteins involved in energy and fatty acid metabolism. In addition, phospholipase protein involved in the maintenance of membrane and regulation of cellular mechanisms was highly upregulated with fold change value of 11.08 on exposure to arsenite.

5.1.1.2 Proteins involved in membrane integrity and transport

Many proteins involved in peptidoglycan biosynthesis and outer membrane lipoprotein carrier protein were found to be up-regulated on exposure to arsenite indicating probable involvement of these proteins in arsenite resistance. Modification of permeability of membrane or changing composition of cell envelope is one of the strategies commonly used by microorganisms to combat heavy metals stress (Andres and Bertin, 2016). Previous studies on *L. ferriphilum*, *Staphylococcus* sp. NBRIEAG-8, *Thiomonas arsenivorans* and *Rhizobium* sp. NT-26 have shown differential expression of genes involved in the synthesis of cell envelope, peptidoglycan and lipopolysaccharide (Bryan et al., 2009; Li et al., 2010; Srivastava et al., 2012; Andres et al., 2013). Additionally, strain SSAI1 also showed upregulation of several transport-related proteins

which could be a mechanism for coping with metal stress. Cleiss-Arnold et al. (2010) observed a similar expression of genes involved in transport.

5.1.1.3 Proteins involved in sporulation

Several proteins involved in the formation of spores viz. SpoIIIAH-like family protein (4.16-fold), spore coat assembly protein (2.17-fold), sporulation protein (1.97-fold), stage 0 sporulation protein A (1.85-fold), stage IV sporulation protein A (1.49 -fold), stage V sporulation protein (1.43-fold) and stage VI sporulation protein D (1.38-fold) were also found to be up-regulated in the presence of 5 mM arsenite indicating the possible involvement of these proteins in arsenite resistance in the strain SSAI1. Recently a study on *Bacillus firmus* L-148 reported 1.15-fold upregulation of stage IV sporulation protein in the presence of 10 mM arsenite (Bagade et al., 2020). However, the fold change values obtained for strain SSAI1 were found to be significantly high as compared to previously reported strain L-148.

5.1.1.4 Proteins involved in oxidative stress responses

The strain SSAI1 also demonstrated upregulation of proteins such as dps, thioredoxin, thioredoxin reductase, catalase and redoxin domain-containing protein involved in maintaining oxidative stress. The upregulation of thioredoxins, thioredoxin reductases, thiol peroxidases and glutaredoxins was also observed in *H. arsenicoxydans* and *F. acidarmanus* Fer1 on exposure to arsenic (Baker-Austin et al., 2007; Cleiss-Arnold et al., 2010). Also, studies on *H. arsenicoxydans*, *C. metallidurans* and *Rhizobium* sp. NT-26 showed the presence and upregulation of catalase enzyme involved in scavenging and decomposition of hydrogen peroxide (Zhang et al., 2009; Cleiss-Arnold

et al., 2010; Andres et al., 2013). Thus, the above observations suggest that these antioxidant enzymes may be involved in protecting strain SSAI1 from oxidative stress caused by arsenite.

5.1.1.5 Proteins involved in transcription, DNA repair and metal homeostasis

Several transcriptional regulators viz. FadR family transcriptional regulator, MerR family transcriptional regulator and RsfA family transcriptional regulator were found to be up-regulated under arsenite stress. This changes in expression of regulators reflect the setting up of arsenic responses and are in agreement with previous reports (Andres and Bertin, 2016). The strain SSAI1 also exhibited upregulation of (Fe-S)-binding protein (3.41-fold) involved in gene regulation, RNA modification, DNA replication and repair (Mettert and Kiley, 2015). Moreover, it also showed 2.12-fold upregulation of copper resistance protein (CopC) which is a periplasmic copper-binding protein involved in copper homeostasis in bacteria.

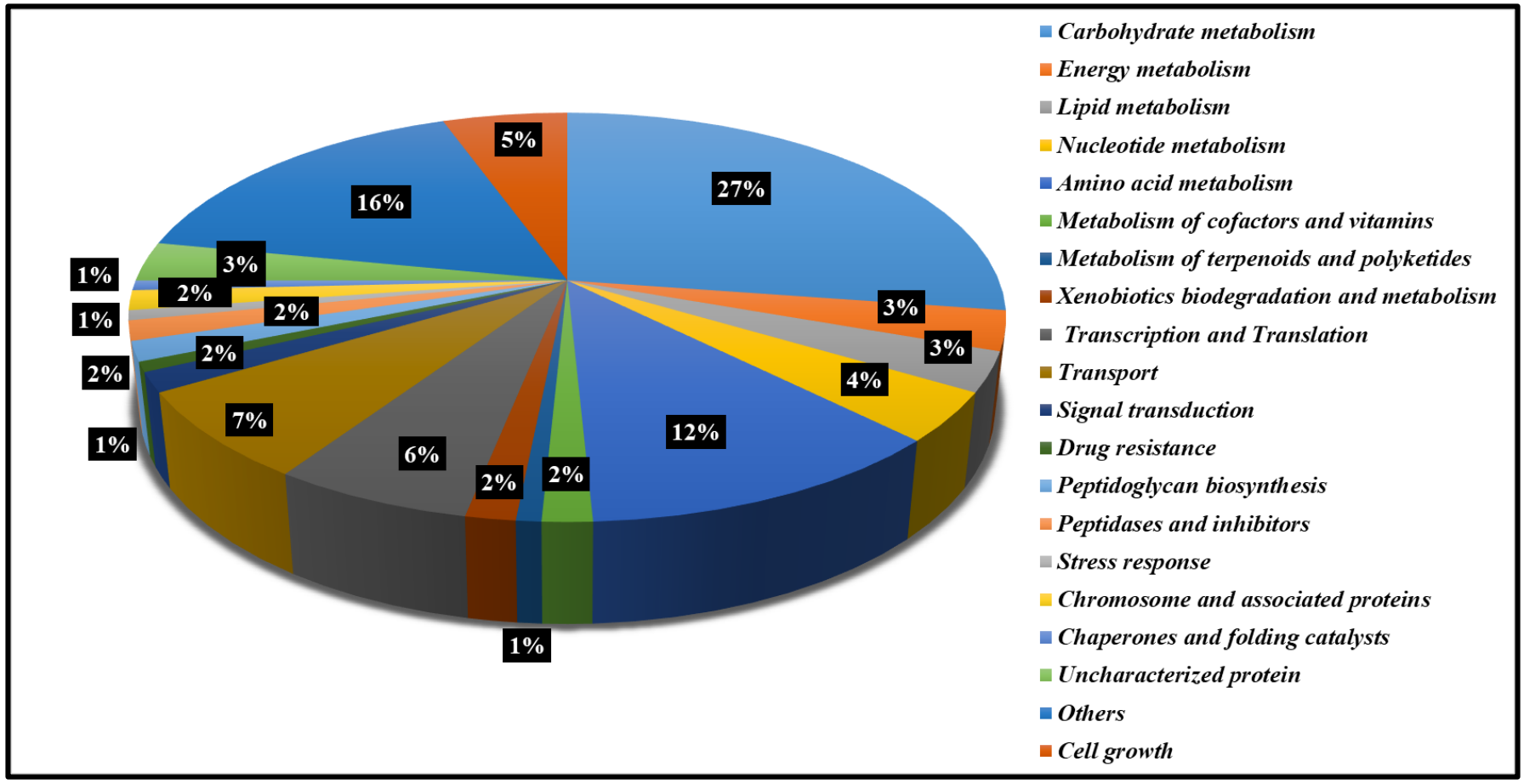

Fig. 5.4: Graphical representation depicting the classification of the up-regulated proteins identified in *Bacillus* sp. strain SSAI1 on exposure to 5 mM arsenite.

Table 5.1: List of up-regulated proteins identified in *Bacillus* sp. strain SSAI1 exposed to 5mM arsenite and the fold change in expression.

Reference Accession number	Proteins	Fold change
Metabolism		
Carbohydrate metabolism		
A0A4P8X7B4	3-hydroxyacyl-CoA dehydrogenase	1.54
A0A4P8X4K8	6-phosphogluconate-dehydrogenase, decarboxylase	2.96
A0A4P8XCU6	Acetate–CoA ligase	1.67
A0A4P8X8J2	Acetyl-CoA C-acetyltransferase	1.63
A0A4P8XCA9	Acetyl-CoA carboxylase biotin carboxylase subunit	4.1
A0A4P8X8T2	Aconitate hydratase	1.53
A0A4P8X8Y0	Acyl-CoA carboxylase subunit beta	4.09
A0A4P8X634	Acyl-CoA dehydrogenase	2.07
A0A4P8X517	Acyl-CoA dehydrogenase	2.16
A0A4P8XCW9	Aldehyde dehydrogenase family protein	4.29
A0A4P8XDR3	Bifunctional-2-methylcitrate dehydratase/aconitate hydratase	1.6
A0A4V1G333	Citrate synthase	2.23
A0A4P8XER0	Fumarate hydratase class I	1.6
A0A4P8X596	Glucose-1-phosphate adenylyltransferase	1.5

A0A4P8XAZ1	Glucose-1-phosphate adenylyltransferase	1.68
A0A4P8XB30	Malate synthase G	1.91
A0A4P8X444	Phosphate acetyltransferase	1.63
A0A4P8X7M6	Phosphoenolpyruvate carboxykinase (ATP)	3.59
A0A4P8XF63	Phosphoglucosamine mutase	1.55
A0A4P8X4Z8	Triosephosphate isomerase	1.59
Energy metabolism		
A0A4P8X556	Electron transfer flavoprotein subunit alpha/ FixB family protein	1.56
A0A4P8X7Z4	Electron transfer flavoprotein subunit beta/ FixA family protein	1.54
A0A4P8X4N8	SUF system NifU family Fe-S cluster assembly protein	2.61
Lipid metabolism		
A0A4P8XBC7	3-oxoacyl-[acyl-carrier-protein] synthase 3	2.07
A0A4P8XHE2	Long-chain fatty acid–CoA ligase	4.39
A0A4P8X4K0	Acetyl-CoA C-acetyltransferase	5.07
A0A4P8XCV1	Phospholipase	11.09
Nucleotide metabolism		
A0A4V1G339	Adenine deaminase	1.62
A0A4P8XCC2	Adenylate kinase	1.71
A0A4P8X490	CTP synthase	1.6
Amino acid metabolism		
A0A4P8XAJ4	3-deoxy-7-phosphoheptulonate synthase	1.7

A0A4P8X8Q7	Dihydroxy-acid dehydratase	1.86
A0A4P8XBU7	Glutamate-1-semialdehyde 2,1-aminomutase	1.52
A0A4V1G2F2	Histidinol-phosphate aminotransferase	1.73
A0A4P8X4L3	Homoserine dehydrogenase	2.45
A0A4P8X4W6	L-glutamate gamma-semialdehyde dehydrogenase	1.55
A0A4P8X732	Thioredoxin reductase	1.57
A0A4P8X635	Tryptophan synthase beta chain	2.15
Metabolism of cofactors and vitamins		
A0A4P8X805	6-carboxyhexanoate–CoA ligase	2.05
Xenobiotics biodegradation and metabolism		
A0A4P8XC33	Enoyl-CoA hydratase	1.83
Genetic Information Processing		
Transcription and Translation		
A0A4P8X4P4	50S ribosomal protein L31	1.7
A0A4P8X836	FadR family transcriptional regulator	1.91
A0A4V1G2S4	MerR family transcriptional regulator	2.45
A0A4V1G2A5	Phenylalanine–tRNA ligase beta subunit	2.16
A0A4V1G273	RsfA family transcriptional regulator	3.33
Environmental Information Processing		
Transport		
A0A4P8XEE8	ABC transporter substrate-binding protein	1.65
A0A4P8XBB9	Carbohydrate ABC transporter substrate-binding protein	1.46

A0A4P8X7R7	Copper resistance protein CopC	2.12
A0A4P8X4G0	HPr family phosphocarrier protein	1.61
A0A4P8XAN7	Phosphocarrier protein HPr	1.63
A0A4P8XDG3	PTS sugar transporter subunit IIB	1.49
Signal transduction		
A0A4P8XBD2	Sporulation protein	1.97
A0A4P8X6B1	Stage 0 sporulation protein A	1.85
Drug resistance		
A0A4P8X8A2	N-acetylmuramoyl-L-alanine amidase	1.57
Peptidoglycan biosynthesis		
A0A4P8X516	UDP-N-acetylmuramate–L-alanine ligase	1.33
A0A4P8XCB6	UDP-N-acetylmuramoyl-L-alanyl-D-glutamate–2,6-diaminopimelate ligase	1.59
Peptidases and inhibitors		
A0A4P8X4A0	M23 family metallopeptidase	4.48
A0A4V1G308	Oligoendopeptidase F	1.63
Cell growth		
A0A4P8XIS2	Anti-sigma F factor	2.62
A0A4V1G2E5	Anti-sigma F factor antagonist	1.5
A0A4P8XBI6	SafA/ExsA family spore coat assembly protein	2.17
A0A4P8X5R6	SpoIIIAH-like family protein	4.16
A0A4P8X623	Stage IV sporulation protein A	1.49
A0A4V1G2H2	Stage V sporulation protein SpoVS	1.43
A0A4P8X588	Stage VI sporulation protein D	1.38

Chromosome and associated proteins		
A0A4P8X4U8	DNA starvation/ stationary phase protection protein (dps)	1.5
Chaperones and folding catalysts		
A0A4P8X5N5	Thioredoxin	1.72
Uncharacterized/Hypothetical protein		
A0A4P8X6R9	Uncharacterized protein	1.7
A0A4V1G2Y7	Uncharacterized protein	1.73
Others		
A0A4P8XAW1	(Fe-S)-binding protein	3.41
A0A4P8X8B4	Catalase	1.51
A0A4P8XD31	Dicarboxylate/amino acid:cation symporter	1.84
A0A4P8XBL0	FAD-binding oxidoreductase	3.44
A0A4P8XBA5	FAD-binding protein	3.57
A0A4P8X4I3	HPr kinase/phosphorylase	1.66
A0A4P8X721	Insulinase family protein	1.57
A0A4P8X6M2	Insulinase family protein	1.62
A0A4P8XG76	Multifunctional fusion protein	1.65
A0A4V1G330	NAD(P)H-dependent oxidoreductase	1.5
A0A4V1G350	Outer membrane lipoprotein carrier protein LolA	2.37
A0A4V1G2L6	Peptidase	2.72
A0A4P8X9H2	Redoxin domain-containing protein	2.13

5.1.1.6 Proteins downregulated under arsenite stress

Numerous proteins were found to be down-regulated under arsenite stress (Fig. 5.5, Table 5.2). These include proteins involved in carbohydrate metabolism (10 %), energy metabolism (2 %), lipid metabolism (1 %), nucleotide metabolism (3 %), amino acid metabolism (5 %), metabolism of cofactor and vitamins (4 %), transcription and translation (18 %), cell growth (3 %), peptidoglycan biosynthesis (2 %), **stress response (5 %)**, transport (11 %), exosome (1 %), replication and repair (1 %), oxidation-reduction (1 %), ribosome biogenesis (1 %), chaperones and folding catalysts (2 %), uncharacterized protein (3 %) and others (23 %).

Some proteins involved in translation processes and ribosomal biogenesis in strain SSAI1 were found to be downregulated under arsenic stress which is in agreement with previous reports on *C. testosteroni* CNB-1, *Exiguobacterium* sp. PS and *Staphylococcus* sp. NBRIEAG-8 (Zhang et al., 2007; Srivastava et al., 2012; Sacheti et al., 2013). Proteins like heat shock proteins and chaperones are known to be up-regulated under stress conditions (Visioli et al., 2010). However, it is quite interesting to note that in *Bacillus* sp. strain SSAI1 general stress proteins, 60 kDa chaperonin, chaperones and Asp23/ Gls24 family envelope stress response proteins were found to be down-regulated indicating that they may not be playing any role in arsenite resistance. Similar observations were also reported in *S. cohnii* #NIOSBK35 exposed to arsenite (Shah and Damare, 2018).

Furthermore, alpha/beta-type small acid-soluble spore proteins involved in double-stranded DNA binding and DNA topological change was found to be highly

down-regulated (13.5, 6.89, 4.75-fold) in the presence of arsenite. Likewise, two proteins of unknown functions DUF2653 family protein (9.82-fold) and DUF3243 domain-containing protein (4.08-fold) were found to be highly down-regulated. Also, arsenite is known to bind sulfhydryl groups of proteins, thereby affecting their activity (Zhao et al., 2010). This could be the possible reason for the downregulation of several sulfur-containing proteins such as adenylyl-sulfate kinase, cysteine synthase etc. Furthermore, many transport proteins such as phosphate-specific transport system were found to be downregulated, which could be due to the interference of arsenic. A similar observation was also seen in *Staphylococcus* sp. NIOSBK35 (Shah and Damare, 2018).

Hence above observations indicate that the proteins found to be either up or down-regulated on exposure to arsenite probably help *Bacillus* sp. strain SSAI1 in survival under arsenite stress. This is the first detailed study on *Bacillus* sp. showing the role of several proteins involved in arsenite resistance using the proteomic approach.

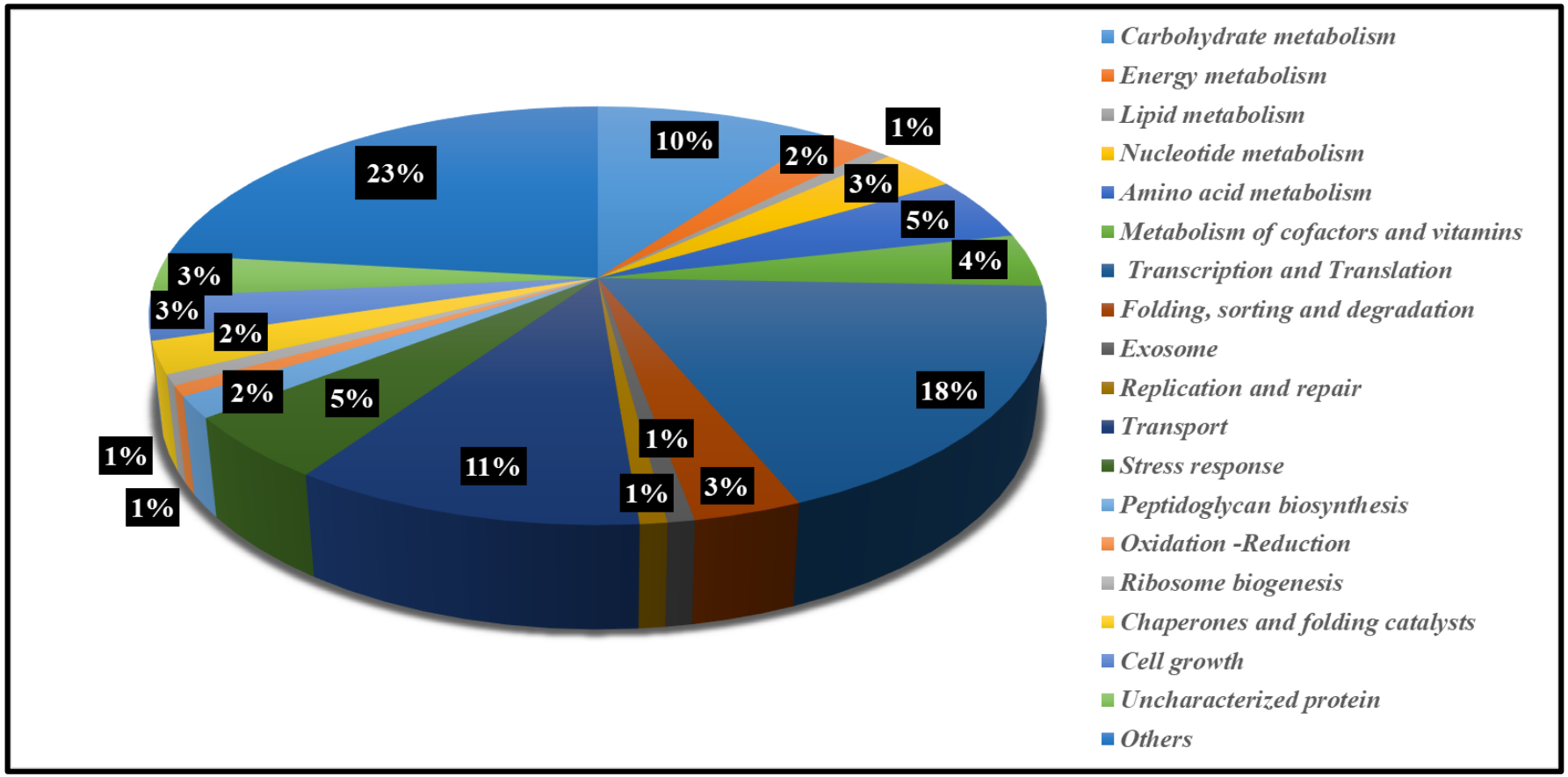

Fig. 5.5: Graphical representation depicting the classification of the down-regulated proteins identified in *Bacillus* sp. strain SSAI1 on exposure to 5 mM arsenite.

Table 5.2: List of down-regulated proteins identified in *Bacillus* sp. strain SSAI1 exposed to 5 mM arsenite and the fold change in expression.

Reference Accession number	Proteins	Fold change
Metabolism		
Carbohydrate metabolism		
A0A4V1G288	2,3-bisphosphoglycerate-independent phosphoglycerate mutase	2.28
A0A4V1G2Q0	Acyl-CoA ligase	2.19
A0A4P8XEV5	Glutamine–fructose-6-phosphate aminotransferase [eroxidise]	1.65
A0A4P8X6E9	Ribulose-phosphate 3-epimerase	2.43
Energy metabolism		
A0A4P8X7I8	Adenylyl-sulfate kinase	2.29
A0A4P8XD81	Cysteine synthase	2.25
Nucleotide metabolism		
A0A4P8X5X4	Pyrimidine-nucleoside phosphorylase	1.57
A0A4P8X9K3	Thymidylate synthase	1.57
Amino acid metabolism		
A0A4P8XA86	Acireductone dioxygenase	1.91
A0A4P8X9F2	Gamma-glutamyl phosphate reductase	1.51
A0A4V1G2B6	Ketol-acid reductoisomerase (NADP (+))	1.51
A0A4P8X8B2	Pyrroline-5-carboxylate reductase	1.5

A0A4P8X7L8	S-ribosylhomocysteine lyase	2.92
Metabolism of cofactors and vitamins		
A0A4P8X4N2	NAD(P)/FAD-dependent oxidoreductase	1.71
A0A4P8XD29	NAD(P)-dependent oxidoreductase	6.73
A0A4P8X9I9	NAD(P)H:eroxid oxidoreductase	6.04
Genetic Information Processing		
Transcription and Translation		
A0A4P8XCR0	30S ribosomal protein S14 type Z	1.88
A0A4P8XD38	50S ribosomal protein L14	1.75
A0A4P8X4T3	50S ribosomal protein L31 type B	3.98
A0A4V1G355	50S ribosomal protein L36	2.49
A0A4P8X7G2	Carbonic anhydrase	1.85
A0A4V1G2C4	Rrf2 family transcriptional regulator	1.84
A0A4P8X4S3	Sporulation transcriptional regulator SpoIIID	1.99
A0A4P8XDC9	Stage V sporulation protein T	3.86
A0A4P8X5X0	Transcriptional repressor	1.46
Stress response		
A0A4P8XF14	**60 kDa chaperonin**	1.39
A0A4P8XCF6	**Asp23/Gls24 family envelope stress response protein**	1.37
A0A4P8XGR5	**Cold-shock protein**	1.49
A0A4P8X829	**Cold-shock protein**	1.41
A0A4P8X910	**General stress protein**	2.28
A0A4P8X985	**General stress protein**	1.68

Environmental Information Processing		
Transport		
A0A4P8XCB1	Amino acid ABC transporter substrate-binding protein	2.2
A0A4P8X7C6	Lipoprotein	2.58
A0A4P8X838	Lipoprotein	2.13
A0A4P8XAQ5	Methionine import ATP-binding protein MetN	3.17
A0A4P8XDP0	Methionine import ATP-binding protein MetN	2.94
A0A4P8X564	Potassium:proton antiporter	2.93
A0A4P8XFQ8	Siderophore ABC transporter substrate-binding protein	1.63
A0A4P8X5B7	Zinc ABC transporter substrate-binding protein	5.47
Exosome		
A0A4P8X4I7	Alkyl hydroperoxide reductase C	1.7
Cell growth		
A0A4P8XAA0	Alpha/beta-type small acid-soluble spore protein	13.5
A0A4P8XCA3	Alpha/beta-type small acid-soluble spore protein	6.89
A0A4P8X5I1	Alpha/beta-type small acid-soluble spore protein	4.75
Folding, sorting and degradation		
A0A4V1G2C9	Chaperone protein DnaJ	1.55
Chaperones and folding catalysts		
A0A4V1G2T2	Foldase protein PrsA	1.54
A0A4P8XD67	Hsp20/alpha crystallin family protein	3.5
Uncharacterized protein/ Hypothetical protein		

A0A4P8X9D3	Uncharacterized protein	3.08
A0A4P8XBS8	Uncharacterized protein	2.36
Others		
A0A4P8XAP3	Acyl-CoA dehydrogenase family protein	1.58
A0A4P8XBZ7	Aminopyrimidine aminohydrolase	2.17
A0A4P8X9J1	Bacillithiol biosynthesis deacetylase BshB2	1.76
A0A4P8X607	Bifunctional cystathionine gamma-lyase/ homocysteine desulfhydrase	5.72
A0A4P8XA36	Carbon-nitrogen family hydrolase	1.85
A0A4P8X903	DUF2653 family protein	9.82
A0A4P8X6L0	DUF3243 domain-containing protein	4.08
A0A4P8X9L2	DUF4397 domain-containing protein	2.27
A0A4V1G2J9	Ferredoxin--NADP reductase	2.03
A0A4P8X7L4	Metal-sensitive transcriptional regulator	2.37
A0A4P8X4A1	Nucleotide sugar dehydrogenase	2.05
A0A4P8XFP8	PspA/IM30 family protein	1.54
A0A4P8X9D7	Putative competence-damage inducible protein	1.52
A0A4P8X4C7	Ribosome hibernation promoting factor	1.49
A0A4P8XAN6	SPFH domain-containing protein	1.51
A0A4P8XES9	STAS domain-containing protein	1.75
A0A4V1G2A8	Thiol peroxidase	1.34

5.1.2 Proteomic analysis of *Klebsiella* sp. strain SSSW7

In *Klebsiella* sp. strain SSSW7, total 579 and 360 proteins were identified in control and arsenite exposed cells respectively, out of which 196 were found to be up-regulated and 168 were down-regulated proteins. The proteins identified in the control and test were classified into different functional categories viz. metabolism, cellular processes, environmental and genetic information processing using KEGG pathway (Figs. 5.6 & 5.7).

The classification of up-regulated proteins in SSSW7 revealed that most of the proteins were involved in transcription and translation (24 %), transport (12 %), carbohydrate metabolism (7 %), energy metabolism (6 %), **chaperones and folding catalysts (5 %)**, amino acid metabolism (5 %), nucleotide metabolism (4 %) followed by lipid metabolism (2 %), metabolism of cofactor and vitamins (2 %), **stress response (2 %),** chromosome and associated proteins (2 %), drug resistance (2 %), oxidation-reduction (1 %), signal transduction (1 %), **peptidoglycan biosynthesis (1 %)**, **lipopolysaccharide biosynthesis (1 %)**, peptidases and inhibitors (1 %), folding sorting and degradation (1 %), replication repair (1 %), secretion system (1 %), exosome (1 %), ribosome biogenesis (1 %), RNA biogenesis (1 %), uncharacterized protein (3 %) and others (18 %) (Fig. 5.8). All the up-regulated proteins along with their fold change values obtained under arsenite stress conditions have been shown in Table 5.3.

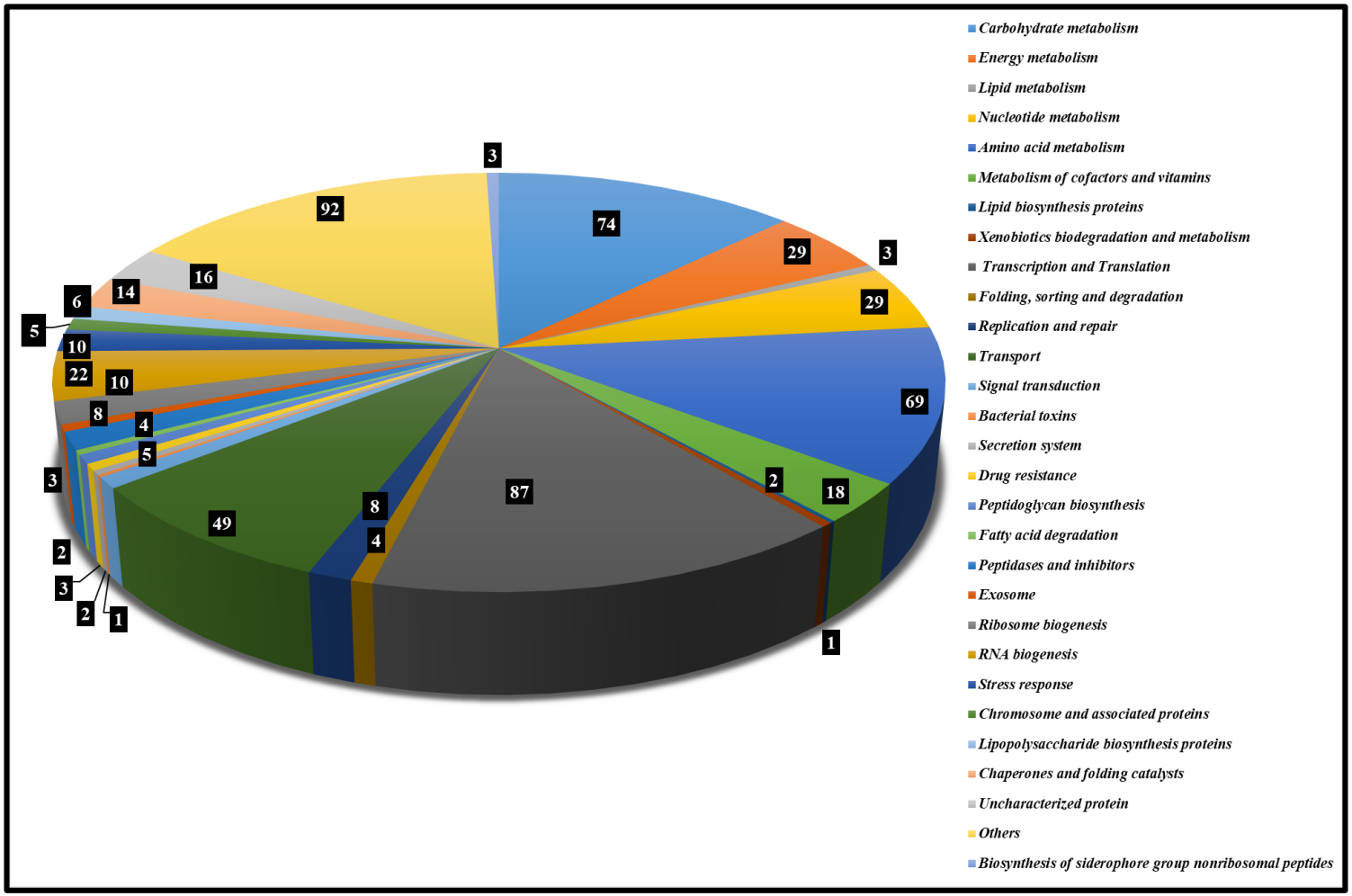

Fig. 5.6: Graphical representation depicting the classification of the proteins identified in *Klebsiella* sp. strain SSSW7 (Control). The numbers denote the total proteins identified for each category.

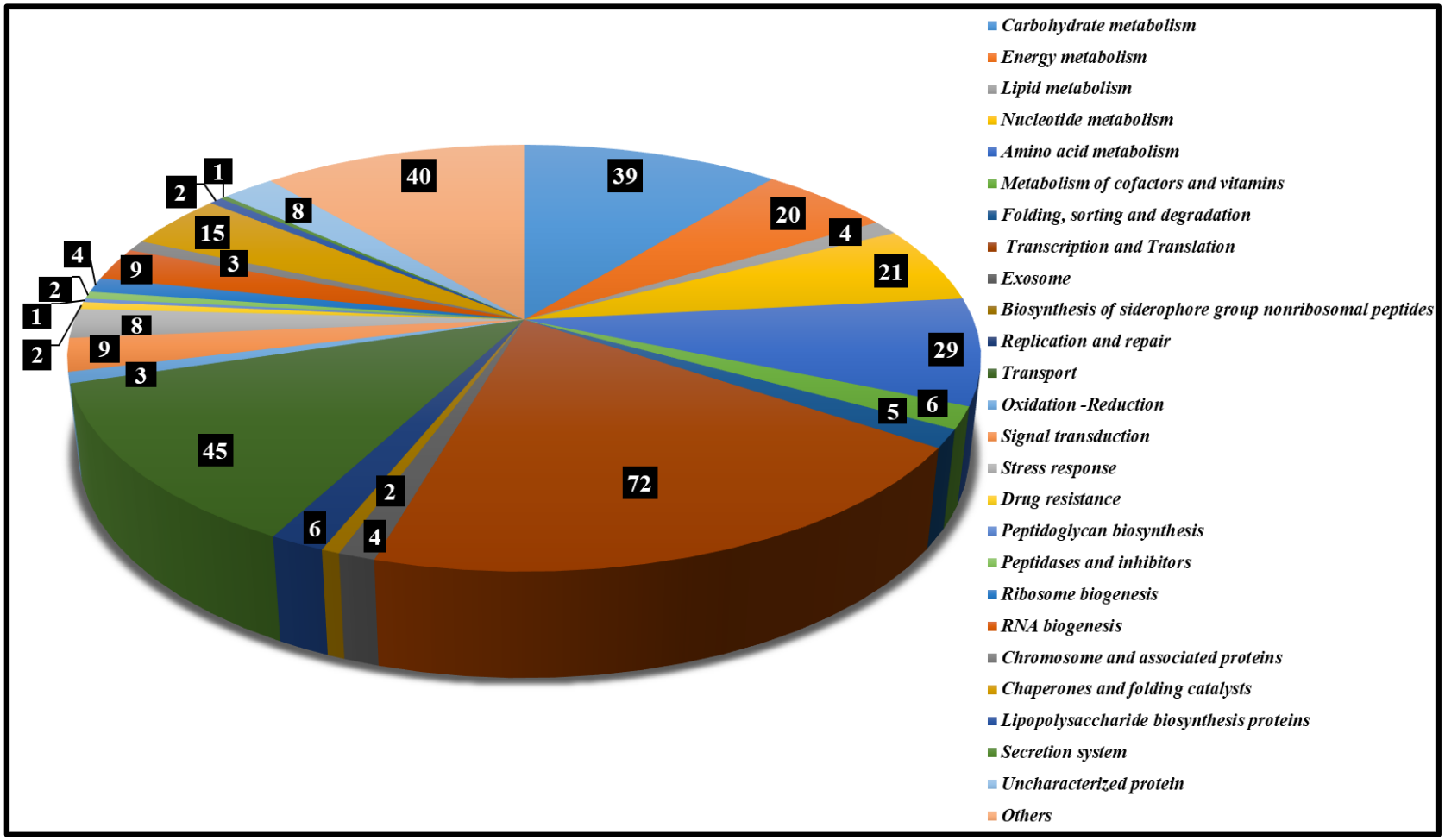

Fig. 5.7: Graphical representation depicting the classification of the proteins identified in *Klebsiella* sp. strain SSSW7 exposed to 5 mM arsenite (Test). The numbers denote the total proteins identified for each category.

5.1.2.1 Proteins involved in metabolism

Several proteins involved in various metabolism-related processes viz. glycolysis, pentose phosphate pathway, pyruvate metabolism, nucleotide metabolism, amino acid metabolism and fatty acid biosynthesis showed upregulation of proteins on exposure to 5mM arsenite. Similar findings were also reported in *Herminiimonas arsenicoxydans* (Cleiss-Arnold et al., 2010), *K. pneumoniae* (Daware et al., 2012), *Exiguobacterium* strains S17 (Belfiore et al., 2013), *Exiguobacterium* sp. PS (Sacheti et al., 2013) and *Staphylococcus cohnii* (Shah and Damare, 2018) showing the expression of proteins involved in metabolic pathways. Additionally, proteins such as ATP synthase subunit b (4.64-fold), inorganic pyrophosphatase (3.66-fold) and ATP synthase subunit delta (2.02-fold) involved in oxidative phosphorylation were found to be highly upregulated in the presence of arsenite. The above results suggest that in *Klebsiella* sp. strain SSSW7 upregulation of energy providing metabolic pathways may be are necessary to overcome cellular stress caused by arsenite. Upregulation of proteins involved in oxidative phosphorylation has been observed in many studies (Andres et al., 2013).

5.1.2.2 Proteins involved in membrane integrity and transport

Microorganisms are also known to modify cell envelope or membrane permeability as a resistance mechanism (Andres and Bertin, 2016). Interestingly strain SSSW7 also showed upregulation of many proteins like murein lipoprotein (6.54-fold), outer membrane lipoprotein (6.29-fold) and 3-deoxy-manno-octulosonate cytidylyltransferase (2.88-fold) involved in peptidoglycan and lipopolysaccharide biosynthesis. Other membrane proteins such as outer membrane protein A (10.41-fold),

outer membrane protein assembly factor (5.93-fold) and peptidoglycan-associated protein (7.92-fold) were found to be highly upregulated suggesting alterations in peptidoglycan and lipopolysaccharide layer at 5 mM arsenite concentrations. Similar observations were seen in *Thiomonas arsenivorans*, *Staphylococcus* sp. NBRIEAG-8, *H. arsenicoxydans*, *L. ferriphilum* and *Rhizobium* sp. NT-26 demonstrating expression of proteins involved in the synthesis of peptidoglycan and lipopolysaccharide in the presence of arsenic (Bryan et al., 2009; Cleiss-Arnold et al., 2010; Li et al., 2010; Srivastava et al., 2012; Andres et al., 2013).

The strain SSSW7 also showed up-regulation of several transport proteins such as ABC transporters on exposure to 5 mM arsenite. Proteins like MotA/TolQ/ExbB proton channel family protein (6.68-fold), export protein (8.37-fold) and outer membrane transporter (8.62-fold) involved in protein transport, export of extracellular polysaccharide and transport of vitamin B12 respectively were found to be highly upregulated. Likewise, TonB-dependent receptors responsible for substrate specific transport across the outer membrane was found to be highly upregulated with fold change value of 10.11 and 8.32. These may be a way of effluxing out toxic substances from the cell under arsenite stress. Similar expression of transporters in the presence of arsenic was observed in *Herminiimonas arsenicoxydans* and *Staphylococcus cohnii* #NIOSBK35 (Cleiss-Arnold et al., 2010; Shah and Damare, 2018).

5.1.2.3 Proteins involved in oxidative stress responses

Several proteins such as alkyl hydroperoxide reductase subunit C-like protein (3.32-fold), glutathione reductase (3.19-fold), glutaredoxin (2.87-fold), thioredoxin

(2.84-fold), thioredoxin reductase (2.79-fold), superoxide dismutase (1.77-fold) and thiol peroxidase (1.73-fold) were found to be up-regulated on exposure to arsenite. These proteins are known to keep the intracellular redox concentrations at a low level generated during metal stress, thereby minimizing oxidative stress (Meyer et al., 2009). Thus, the above observations suggest that these antioxidant enzymes may be required to protect strain SSSW7 from oxidative damage resulting from exposure to 5 mM arsenite. Studies on *H. arsenicoxydans* and *F. acidarmanus* Fer1 also showed upregulation of thiol peroxidases, thioredoxin reductases, thioredoxins and glutaredoxins in the presence of arsenic (Baker-Austin et al., 2007; Cleiss-Arnold et al., 2010). Furthermore, the presence and upregulation of superoxide dismutase were observed in *Klebsiella pneumonia* MR4 and *Bacillus firmus* L-148 with fold change value of 0.37 and 0.9 in arsenite treated cells respectively (Daware et al., 2012; Bagade et al., 2020). However, the fold change values obtained in the present study were higher than the previously reported strains.

5.1.2.4 Chaperones and stress response proteins

Production of molecular chaperones and heat shock or stress response proteins have been extensively implicated in overcoming heavy metal stress. This strain also showed expression of several chaperones and stress response proteins viz. universal stress protein F (1.59-fold), 10 kDa chaperonin (4.62-fold), ATP-dependent clp protease ATP-binding subunit clpA (1.71-fold), chaperone protein DnaK (3.49-fold), chaperone protein Skp (2.25-fold), hsp 60 family chaperone GroEL (2.23-fold), peptidyl-prolyl cis-trans isomerase (2.17-fold), protein GrpE (2.01-fold), thiol: disulfide interchange protein (2.94-fold), osmotically inducible protein Y (3.68-fold) and trigger factor (3.56-fold). The up-regulation of molecular chaperone DnaK, GroEL and GroES involved in protein

folding, renaturation or degradation has been previously reported in *F. acidarmanus* Fer1 and *K. pneumonia* MR4 under arsenic stress (Baker-Austin et al., 2007; Daware et al., 2012). Other chaperones such as Clp ATPases and trigger factor were identified in *L. ferriphilum* and *K. pneumoniae* MR4 respectively and were found to be up-regulated by arsenite (Li et al., 2010; Daware et al., 2012). The fold change values obtained for strain SSSW7 in the present study were higher than previously reported *K. pneumoniae* MR4. Also, the strain in the present study showed upregulation of several other chaperones and stress response proteins which were not identified in MR4. Interestingly the strain SSSW7 exposed to arsenite also showed upregulation of many cold shock proteins (2.57, 1.86, 1.89-fold change). Similar observations were also seen in *Exiguobacterium* sp. S17 and *Exiguobacterium* sp. PS in response to arsenic (Belfiore et al., 2013; Sacheti et al., 2013). Thus, from all above observations, it can be concluded that chaperones, chaperonins, universal proteins and cold shock proteins play a vital role in *K. pneumoniae* strain SSSW7 protecting cells during arsenite stress.

5.1.2.5 Proteins involved in arsenic resistance and metabolism

Interestingly, this strain showed the presence of arsenic specific proteins such as arsenate reductase, arsenical pump-driving ATPase and arsenite efflux transporter metallochaperone (ArsD) which were highly up-regulated with fold change value of 169.67, 160.74 and 167.12 under 5 mM arsenite stress indicating their possible involvement in arsenite resistance. The presence and upregulation of these proteins indicate the reduction of arsenate by arsenate reductase enzyme to arsenite followed by extrusion of arsenite by efflux pump. Besides, overexpression of arsenical pump and arsD protein explicate the enhanced arsenite tolerance in this strain. The previous study

on *Staphylococcus cohnii* #NIOSBK35 showed upregulation of arsenate reductase and arsenical pump-driving ATPase with fold change value of 2.0 and 19.49-fold respectively (Shah and Damare, 2018). Recently Bagade et al. (2020) reported up-regulation of arsenate reductase in *Bacillus firmus* L-148 by 1.5-fold on exposure to 10 mM arsenite. However, the fold change values obtained in the present study on SSSW7 showed higher values as compared to previously reported strains. Also, the presence of arsenic specific proteins with such high fold change values have not been reported previously, making this first report of its kind.

5.1.2.6 Proteins involved in transcription, translation, DNA repair and metal homeostasis

Several proteins involved in transcriptional and translation processes are reported to express differentially in the presence of toxic arsenic in prokaryotes. A similar observation was also seen in strain SSSW7. Previously studies on *T. arsenivorans*, *Rhizobium* sp. NT-26, *H. arsenicoxydans*, *Y. enterolitica* 1A, *K. pneumoniae*, *L. ferriphilum* and *Exiguobacterium* sp. S17 have also shown similar upregulation in translation processes (Bryan et al., 2009; Cleiss-Arnold et al., 2010; Li et al., 2010; Daware et al., 2012; Mallik et al., 2012; Andres et al., 2013; Belfiore et al., 2013).

Additionally, strain SSSW7 also displayed 3.4-fold upregulation of ssDNA-binding protein involved in DNA repair processes. Arsenic is known to cause DNA damages viz. single strand or double-strand DNA breaks, inhibition of DNA repair processes etc. (Flora, 2011; Bustaffa et al., 2014). Functional studies have shown that proteins and transcripts involved in DNA repair mechanisms are differentially expressed

in the presence of arsenic. For instance, upregulation of proteins associated with DNA repair mechanisms were observed in *H. arsenicoxydans*, *Thiomonas* sp. 3As and *L. ferriphilum* on exposure to arsenite (Bryan et al., 2009; Cleiss-Arnold et al., 2010; Li et al., 2010). Furthermore, proteins such as NfuA (4.16-fold), iron-sulfur cluster assembly scaffold protein (6.93-fold), colicin I receptor (10.37-fold) and ferric aerobactin receptor (13.67-fold) involved in gene regulation, Fe^{3+} transport and iron homeostasis were found to be highly upregulated under arsenite stress. Previously studies have shown that up-regulation of genes involved in iron transport play a role in protecting the cell from oxidative damage and also help *S. xylosus* to tolerate higher concentrations of chromium (Henne et al., 2009; Pereira et al., 2018). Thus, the up-regulation of transport and iron homeostasis proteins in the presence of arsenite demonstrated that these proteins might have a role in aiding strain SSSW7 to tolerate higher concentrations of arsenite.

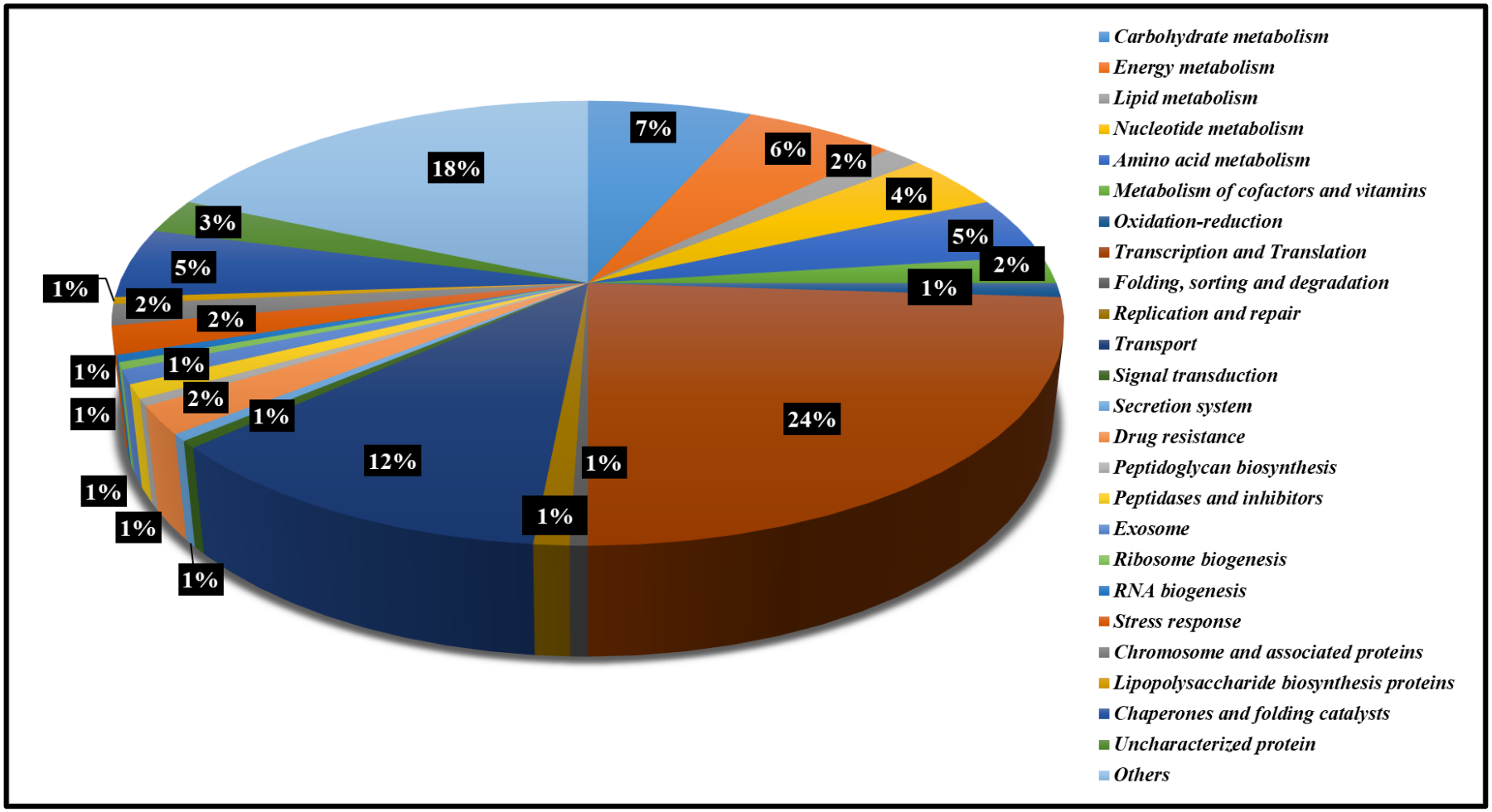

Fig. 5.8: Graphical representation depicting the classification of the up-regulated proteins identified in *Klebsiella* sp. strain SSSW7 on exposure to 5 mM arsenite.

Table 5.3: List of up-regulated proteins identified in *Klebsiella* sp. strain SSSW7 exposed to 5mM arsenite and the fold change in expression.

Reference Accession number	Proteins	Fold change
Metabolism		
Carbohydrate metabolism		
A0A5E3A6L6	3-isopropylmalate dehydratase small subunit	1.88
A0A447RZN0	Acetolactate synthase 3 catalytic subunit	1.58
A0A377ZHK3	Acid phosphatase	1.52
A0A087FRS7	Bifunctional 4-hydroxy-2-oxoglutarate aldolase/ 2-dehydro-3-deoxy-phosphogluconate aldolase	2.81
A0A1Y0PU72	Biotin carboxyl carrier protein of acetyl-CoA carboxylase	2.12
A0A0E1CC44	Fructose-bisphosphate aldolase	1.89
A0A4U9DJ85	Mannose-6-phosphate isomerase	1.94
A0A2A5PMG2	Phosphoglycolate phosphatase (Fragment)	1.61
W1EP24	PTS system, glucose-specific IIB component / PTS system, glucose-specific IIC component	3.42
A0A0E1CCD6	PTS system, mannose-specific IIAB component	2.05
A0A0E1C7G8	Ribulose-phosphate 3-epimerase	1.91
Energy metabolism		
A0A377UWE9	ATP synthase epsilon chain	1.71
ATPG	ATP synthase gamma chain	1.76

W1I1N3	ATP synthase subunit b	4.64
ATPD	ATP synthase subunit delta	2.02
A0A2A2SUW6	Cysteine synthase	3.91
A0A377XBQ8	Cysteine synthase	2.19
A0A0E1CE79	Enolase	2.61
A0A378E8F6	Inorganic pyrophosphatase	3.66
A0A378BDW3	Respiratory nitrate reductase subunit beta	1.5
A0A378E7S5	Sulfate-binding protein Sbp	2.44
A0A377X5P1	Ubiquinol oxidase subunit 2	1.62
Lipid metabolism		
A0A087FQL5	3-oxoacyl-(Acyl-carrier-protein) reductase	1.81
A0A0E1CKI5	3-oxoacyl-[acyl-carrier-protein] synthase 2	2.06
ACP	Acyl carrier protein	3.02
Nucleotide metabolism		
A0A0E1CKY2	Aspartate carbamoyltransferase	1.59
A0A2N4W4D4	Deoxyuridine 5-triphosphate nucleotidohydrolase	1.92
PYRC	Dihydroorotase	2.77
A0A0E1CB16	Inosine-5-monophosphate dehydrogenase	2.09
A0A4V4RRF6	Phosphoribosylformylglycinamidine cyclo-ligase	1.74
A0A377VNS2	Purine nucleoside phosphorylase DeoD-type	2.03
A0A0J2GCT6	Pyrimidine/purine nucleoside phosphorylase	3.16
Amino acid metabolism		
A0A0E1CJL4	3-isopropylmalate dehydrogenase	1.78

DAPA	4-hydroxy-tetrahydrodipicolinate synthase	1.5
C8TB42	5-methylthioadenosine/S-adenosylhomocysteine nucleosidase	2.17
W1ERN8	Agmatinase	3.33
A0A5E3C022	Imidazole glycerol phosphate synthase cyclase subunit	1.5
A0A5D6NKJ7	Ornithine carbamoyltransferase	2.7
A0A5E2RGB3	S-ribosylhomocysteine lyase	1.36
W1I0E5	Thioredoxin reductase	2.79
Metabolism of cofactors and vitamins		
W1HQ42	Glutathione reductase	3.19
GCH1	GTP cyclohydrolase 1	1.74
A0A5E3DWI0	NAD(P) transhydrogenase subunit alpha	2.39
Genetic Information Processing		
Translation and Transcription		
A0A087FR93	30S ribosomal protein S1	3.36
A0A5C2LI57	30S ribosomal protein S10	2.09
W1ASV5	30S ribosomal protein S11	1.79
A0A5D8RS19	30S ribosomal protein S13 (Fragment)	1.66
A0A3S4GE18	30S ribosomal protein S16	3.52
RS18	30S ribosomal protein S18	3.18
RS2	30S ribosomal protein S2	2.18
A0A0E1C8C7	30S ribosomal protein S21	4.22
A0A0G3S1N1	30S ribosomal protein S3	1.94

RS4	30S ribosomal protein S4	2.18
A0A0H3GQP2	30S ribosomal protein S6	2.31
A0A0E1CC51	30S ribosomal protein S7	3.35
A0A0B7GDW9	50S ribosomal protein L10	1.95
W8UBP9	50S ribosomal protein L13	1.65
RL15	50S ribosomal protein L15	2.27
A0A485H895	50S ribosomal protein L16	2.29
RL17	50S ribosomal protein L17	3.85
RL18	50S ribosomal protein L18	4.19
A0A483LQT7	50S ribosomal protein L20	3.38
RL22	50S ribosomal protein L22	1.64
RL24	50S ribosomal protein L24	4.09
RL28	50S ribosomal protein L28	1.46
W8UTK0	50S ribosomal protein L29	2.81
R4YBE6	50S ribosomal protein L30	1.5
A0A5C2LHL1	50S ribosomal protein L31	2.66
RL32	50S ribosomal protein L32	6.19
RL4	50S ribosomal protein L4	1.71
RL6	50S ribosomal protein L6	1.79
A0A0H3GH99	50S ribosomal protein L7/L12	3.62
A0A0J2FQI9	DNA-directed RNA polymerase subunit alpha	2.43
A0A486TUL5	DNA-directed RNA polymerase subunit omega	3.26
A0A0H3GIJ5	Elongation factor Ts	1.56
FUR	Ferric uptake regulation protein	3.56

A0A0H3GTV2	Regulator of nucleoside diphosphate kinase	1.79
J2XCH1	Ribosomal protein S20	2.47
J2LN93	RNA polymerase sigma factor RpoD	1.93
A0A0E1C9P5	RNA polymerase sigma factor RpoS	4.31
A0A377V8U9	Transcription elongation factor GreA	3.63
W1H193	Transcription termination/ antitermination protein NusA	2.35
A0A4P1KLH1	Translation initiation factor IF-1	2.79
Stress response		
A0A0E1CCA0	**Cold shock protein**	1.86
A0A0E1CMC7	**Cold shock protein**	2.57
A0A087FU55	**Cold-shock protein**	1.89
A0A2X1Q9T8	**Universal stress protein F**	1.59
Environmental Information Processing		
Transport		
A0A377ZHT4	Amino acid ABC transporter periplasmic amino acid-binding protein	1.5
G7RUZ1	**Arsenical pump-driving ATPase**	**160.74**
A0A5C8GF08	**Arsenite efflux transporter metallochaperone ArsD (Fragment)**	**167.12**
A0A430IE90	Cystine ABC transporter substrate-binding protein	1.92
A0A378F898	Deferrochelatase/peroxidase	1.965
A0A1C1EYS9	Flavodoxin	3.14

A0A087FJ81	Histidine ABC transporter substrate-binding protein HisJ	2.65
A0A4S4UZU8	Lipoprotein	1.68
W1EG70	Lipoprotein	2.07
A0A1C3Q0R4	Mechanosensitive channel MscS	1.87
A0A060VJP4	MotA/TolQ/ExbB proton channel family protein	6.68
A0A0H3YGJ3	Outer membrane protein A	10.41
A0A378EBK0	Outer membrane protein assembly factor BamB	5.93
A0A0E1CM48	Peptidoglycan-associated protein	7.92
PTHP	Phosphocarrier protein HPr	3.08
A0A193SH17	Polysaccharide export protein Wza	8.37
A0A485VLI4	Putative TonB-dependent receptor	10.11
A0A377VXJ2	Sulfate and thiosulfate binding protein CysP	2.6
A0A367P3P4	Thiamine ABC transporter substrate-binding protein (Fragment)	2.89
A0A485WBU4	TonB-dependent receptor	8.32
A0A2X3CS15	Vitamin B12/ cobalamin outer membrane transporter	8.62
Signal transduction		
A0A333FPM0	Copper-sensing two-component system response regulator CpxR	1.69
Drug resistance		
A0A0E1CIT3	Acriflavin resistance periplasmic protein	2.29
A0A447RWL8	Peptidyl-prolyl cis-trans isomerase	1.68

A0A087FQ75	Peptidyl-prolyl cis-trans isomerase	3.09
V0AVR5	Peptidyl-prolyl cis-trans isomerase	3.77
Peptidoglycan biosynthesis		
A6TAE1	**Murein lipoprotein**	6.54
Lipopolysaccharide biosynthesis proteins		
A0A2G5BZV7	**3-deoxy-manno-octulosonatecytidylyltransferase**	2.88
Peptidases and inhibitors		
A0A0E1CJ09	Lon protease	1.73
A0A4S4WAM1	Periplasmic serine endoprotease DegP-like	1.8
Ribosome biogenesis		
A0A2L0KGW1	Ribonuclease E	1.72
Transfer RNA biogenesis		
A0A486TNC6	Ribonuclease R	1.63
Oxidation-reduction		
A0A422WG35	**Arsenate reductase**	**169.67**
A0A080T0K7	Chromate reductase	1.31
Replication and repair		
A0A086I6S5	DNA-binding protein	2.0
A0A5E2EAS1	**SsDNA-binding protein**	3.4
Chromosome and associated proteins		
A0A2S7SJN3	Cell division protein FtsZ	2.89
A0A378E9F9	Cell division protein ZapB	2.65
A0A4V6Z3U8	Integrase	1.78

Folding, sorting and degradation		
A0A377Y2R0	Polyribonucleotide nucleotidyltransferase	1.93
Chaperones and folding catalysts		
CH10	**10 kDa chaperonin**	4.62
A0A0E1CL18	**ATP-dependent clp protease ATP-binding subunit clpA**	1.71
A0A4S5VSQ4	**Chaperone protein DnaK**	3.49
A0A060VDA9	**Chaperone protein Skp**	2.25
A0A377WJ25	**Glutaredoxin**	2.87
A0A5E1Q5N9	**Heat shock protein 60 family chaperone GroEL**	**2.23**
A0A377XWN3	Peptidyl-prolyl cis-trans isomerase	2.17
A0A378GC92	**Protein GrpE**	2.01
A0A2S6EHE6	Thiol: disulfide interchange protein	2.94
A0A0H3GLK1	**Thioredoxin**	2.84
Uncharacterized protein/ Hypothetical protein		
W1EJX3	Uncharacterized protein	2.58
A0A377XQJ6	Uncharacterized protein	2.86
A0A4S4UFZ6	Uncharacterized protein	5.03
Exosome		
A0A087FNR9	Alkyl hydroperoxide reductase C	1.92
Others		
A0A1C1EWN6	2-iminobutanoate/2-iminopropanoate deaminase	2.7

R4Y729	3-hydroxydecanoyl-[acyl-carrier-protein] dehydratase	2.71
W1DMF6	Alkyl hydroperoxide reductase subunit C-like protein	3.33
A0A0E1CGM6	Arginine-binding protein	3.43
A0A0E1CLH7	Arginine-binding protein	2.51
A0A4S7KNF7	Autonomous glycyl radical cofactor	2.05
J2E284	Colicin I receptor	10.37
A0A422XUR5	Cytosol nonspecific dipeptidase	1.78
A0A0E1C6Z4	Dipeptide-binding protein	3.56
A0A0E1C7Z2	ElaB protein	2.22
A0A377V0Z4	Exported protein	2.45
NFUA	Fe/S biogenesis protein NfuA	4.16
A0A0E1CKH1	Ferric aerobactin receptor	13.67
A0A0C7KAE5	Glucans biosynthesis protein G	2.39
A0A0E1CHC2	Glutamate/aspartate-binding protein	2.07
W1DIM4	Iron-chelator utilization protein	1.74
A0A087FSF3	Iron-sulfur cluster assembly scaffold protein IscU	6.94
A0A5E3BEL5	LysM domain/BON superfamily protein	2.64
A0A378EBU5	Multifunctional fusion protein	3.05
A0A0J2GSR3	NADP-dependent malic enzyme	1.78
A0A2X3H720	Osmotically inducible lipoprotein E	1.68
A0A0E1CK02	Osmotically inducible protein Y	3.68
A0A0W8AUH6	Outer membrane lipoprotein SlyB	6.29

W1HV56	Probable cytosol aminopeptidase	5.55
A0A5C2LHQ7	Protein-export chaperone SecB	1.73
R4Y7K4	PTS EIIB type-3 domain-containing protein	1.52
A0A0E1CF19	PTS system, glucose-specific IIA component	3.86
A0A378E8S0	Superoxide dismutase	1.77
A0A377VZX4	Thiol peroxidase	1.73
V0AVN8	Trigger factor	3.56
A0A0J4W3X6	UPF0234 protein BANRA	2.39
A0A377UXZ5	UPF0255 protein NCTC13443	2.99
A0A087FUP6	UPF0325 protein CWM98	1.67

5.1.2.7 Proteins downregulated under arsenite stress

Moreover, several proteins were found to be down-regulated under arsenic stress (Fig. 5.9, Table 5.4). These include proteins involved in carbohydrate metabolism (20 %), energy metabolism (7 %), lipid metabolism (2 %), nucleotide metabolism (7 %), amino acid metabolism (17 %), metabolism of cofactor and vitamins (2 %), transcription and translation (4 %), folding sorting and degradation (1 %), biosynthesis of siderophore group and nonribosomal peptides (1 %), signal transduction (2 %), stress response (1 %), transport (4 %), peptidoglycan biosynthesis (1 %), peptidases and inhibitors (2 %), RNA biogenesis (7 %), replication and repair (1 %), lipopolysaccharide biosynthesis proteins (1 %), ribosome biogenesis (1 %), chaperones and folding catalysts (1 %), uncharacterized protein (2 %) and others (18 %).

Differential expression of proteins involved in metabolism, transcription and translation has been reported to occur under arsenic stress in bacteria (Shen et al. 2013; Andres and Bertin, 2016). A similar observation was also observed in strain SSSW7, indicating that metabolic functions of the cell were affected in the presence of arsenite. Earlier studies on bacterial isolates such as *C. testosteroni* CNB-1, *Exiguobacterium* sp. and *Staphylococcus* sp. NBRIEAG-8 also showed repression in proteins involved in translation processes on exposure to arsenic (Zhang et al., 2007; Srivastava et al., 2012; Sacheti et al., 2013).

Many ABC transporter proteins involved in the transport of dipeptides, sugars etc. were found to downregulated on exposure to arsenite. Previously Daware et al. (2012) have reported downregulation of dipeptide and oligopeptide transport binding protein as a mechanism of arsenite resistance in *K. pneumoniae*. Thus, it is likely that in our study, the down-regulation of various ABC transporter proteins could be a mechanism of arsenite resistance.

Similarly, some proteins with unknown functions such as uncharacterized protein and YodA were found to be highly downregulated with fold change value of 9.79 and 6.7, respectively. Additionally, the strain SSSW7 also showed downregulation of several proteins involved in ribosomal biogenesis. Bacterial strains, such as *Staphylococcus* sp. NBRIEAG-8, *Exiguobacterium* sp. PS and *C. estosterone* CNB-1 also demonstrated repressed ribosomal biogenesis and translation on exposure to arsenic (Zhang et al., 2007; Srivastava et al., 2012; Sacheti et al., 2013) indicating the involvement of other resistance processes such as chaperones etc. which was also evident in the present study.

Hence all the above facts indicated that up or down-regulation of several proteins involved in various processes enable *Klebsiella* sp. strain SSSW7 to maintain arsenite stress. This is the first study showing the involvement of several arsenite specific proteins imparting resistance in *Klebsiella* sp. through the proteomic approach.

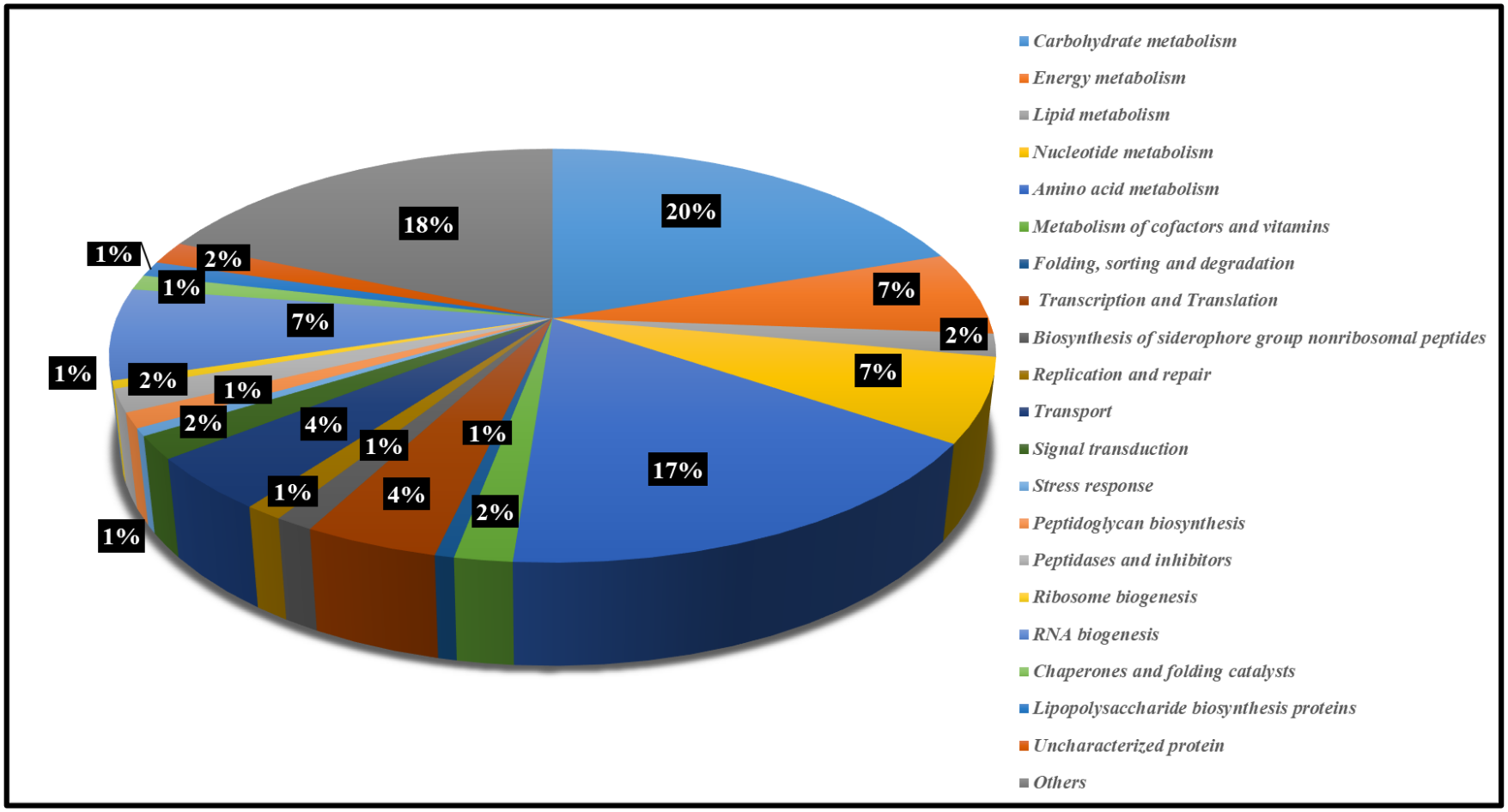

Fig. 5.9: Graphical representation depicting the classification of the down-regulated proteins identified in *Klebsiella* sp. strain SSSW7 on exposure to 5 mM arsenite.

Table 5.4: List of down-regulated proteins identified in *Klebsiella* sp. strain SSSW7 exposed to 5 mM arsenite and the fold change in expression.

Accession number	Proteins	Fold change
Metabolism		
Carbohydrate metabolism		
A0A0H3GMJ2	3-isopropylmalate dehydratase large subunit	2.06
A0A193SEV3	6-phosphogluconate dehydrogenase, decarboxylating	1.84
A0A087FJ69	Acetate kinase	1.89
A6T4R3	Aconitate hydratase B	1.73
W1E6E6	Aldehyde dehydrogenase	6.69
A0A3S5DIA1	Aldehyde-alcohol dehydrogenase	1.68
PFKA	ATP-dependent 6-phosphofructokinase	3.74
A0A378E671	Biotin carboxylase	1.93
J2DN50	Citrate synthase	1.39
A0A0E1CIH6	Citrate synthase	2.93
A0A1Y0Q3I7	Fructose-1,6-bisphosphatase class 1	1.59
A0A0E1C8T2	Fructose-bisphosphate aldolase	2.3
GLK	Glucokinase	1.95
A0A0E1CCS1	Glucose-6-phosphate 1-dehydrogenase	2.42
A0A0E1CL24	Glucose-6-phosphate isomerase	4.31
A0A087FN25	Glutamine synthetase	2.39

A0A378B829	Glyoxylate/ hydroxypyruvate reductase	1.69
A0A5E3KD25	Isocitrate dehydrogenase	1.96
A0A483IRT4	Isocitrate lyase	5.56
A0A5E1PGL4	Phosphate acetyltransferase	1.59
A0A486EHY6	Phosphoenolpyruvate carboxykinase	1.63
A0A0E1CEL7	Short chain dehydrogenase	2.33
A0A377Z8L8	Succinate--CoA ligase [ADP-forming] subunit alpha	1.82
W1E946	Triosephosphate isomerase	1.77
A0A0E1CHP2	UDP-glucose 4-epimerase	2.4
A0A193SH34	UDP-glucose 6-dehydrogenase	1.75
A0A5E2JR56	UTP-glucose-1-phosphate uridylyltransferase	4.39
A0A336IHT3	UTP--glucose-1-phosphate uridylyltransferase	1.59
Energy metabolism		
A0A331MVR4	ATP synthase subunit beta	1.99
A0A0E1CHH8	D-3-phosphoglycerate dehydrogenase	2.23
A0A5E1S4Q8	Glutamate synthase subunit alpha	1.59
METAS	Homoserine O-succinyltransferase	4.12
A0A2X3CXG3	Nitrite reductase subunit NirD	2.13
A0A4S5W2J2	Phosphoglycerate dehydrogenase	1.72
W1BBE5	Phosphoserine aminotransferase	1.99
A0A5D1MNC0	Sulfateadenylyltransferase subunit	1.99
CYSD	Sulfateadenylyltransferase subunit 2	2.83
Nucleotide metabolism		

A0A5E2S832	Bifunctional purine biosynthesis protein PurH	2.17
A0A5E3A6D9	Carbamoyl-phosphate synthase large subunit	1.97
A0A5D4KET1	CTP synthase (Glutamine hydrolyzing)	2.51
GUAA	GMP synthase [glutamine-hydrolyzing]	2.49
NDK	Nucleoside diphosphate kinase	1.55
A0A0E1CLT7	Phosphoglucomutase	2.41
PUR7	Phosphoribosylaminoimidazole-succinocarboxamide synthase	2.37
A0A5E1RZ62	Ribose-phosphate pyrophosphokinase	1.61
A0A2J4VE84	Uridylate kinase	1.83
Amino acid metabolism		
V0AQQ9	1-(5-phosphoribosyl)-5-[(5-phosphoribosylamino) methylideneamino] imidazole-4-carboxamide isomerase	1.51
AROA	3-phosphoshikimate 1-carboxyvinyltransferase	2.24
A0A2N4W7Z0	4-hydroxy-tetrahydrodipicolinate reductase	1.89
A0A0E1CDI0	5-methyltetrahydropteroyltriglutamate--homocysteine methyltransferase	1.55
A0A5D0ZP75	5-methyltetrahydropteroyltriglutamate--homocysteine S-methyltransferase	2.89
W1AUH9	Acetylornithine/succinyldiaminopimelate aminotransferase	2.55
C8TD88	Aminotransferase	2.37
A0A0B7GBC3	Aminotransferase	2.15

A0A060VRU8	Anthranilate phosphoribosyltransferase	7.36
A0A486BFT0	Anthranilate synthase component 1	2.29
W9BJ69	Argininosuccinate lyase	2.31
W8UBU9	Argininosuccinate synthase	1.85
A0A0J4LGA3	Aspartokinase	2.58
A0A2N5AHC6	Diaminopimelate decarboxylase	2.82
A0A0E1CHG3	Enolase-phosphatase E1	1.97
A0A080SSI8	Glutamine--fructose-6-phosphate aminotransferase [isomerizing]	2.3
A0A0C7KFT9	Glutathione synthetase	3.02
A0A2V3K1Z7	Histidinol-phosphate aminotransferase	1.57
A0A5E3LWV6	Homocysteine S-methyltransferase	1.52
ILVC	Ketol-acid reductoisomerase (NADP (+))	1.6
A0A370YJT0	Methionine synthase	1.79
A0A3F3BCP9	Methylthioribulose-1-phosphate dehydratase	1.6
A0A2N4W5R8	Phospho-2-dehydro-3-deoxyheptonate aldolase	1.94
A0A0E1CNK1	Pyrroline-5-carboxylate reductase	3.59
A0A235PX33	SAM-dependent methyltransferase	1.79
TRPB	Tryptophan synthase beta chain	2.16
Metabolism of cofactors and vitamins		
A0A060VFS0	Aldo/keto reductase	2.25
A0A0E1CG99	NAD(P)H dehydrogenase (quinone)	1.64
Genetic Information Processing		
Translation and Transcription		

A0A5C2LKJ9	30S ribosomal protein	1.66
RS8	30S ribosomal protein S8	2.06
A0A0E1CC61	50S ribosomal protein L2	1.56
A0A0E1CBD0	50S ribosomal protein L25	3.95
A0A5D1MVR3	Histidyl-tRNA synthetase	2.48
A0A181Y230	Stringent starvation protein A	3.92
RNA biogenesis		
SYR	Arginine--tRNA ligase	1.64
A0A087FQF5	Glutamate--tRNA ligase	2.08
A0A5D1QC64	Glutaminyl-tRNA synthetase	1.56
A0A060VDM5	Isoleucine--tRNA ligase	1.95
A0A486SRK5	Serine--tRNA ligase	1.66
A0A0E1CDI2	Tyrosine--tRNA ligase	1.79
Environmental Information Processing		
Transport		
A0A422XPA4	ABC transporter substrate-binding protein	2.49
A0A0C4MI82	Dipeptide-binding ABC transporter, periplasmic substrate-binding component	1.52
W8UIA3	High-affinity zinc uptake system protein znuA	3.3
A0A060VMZ3	Hydroxymethylpyrimidine ABC transporter substrate-binding protein	1.63
A0A0E1C6L6	Lipoprotein	1.67
A0A377UZB8	Sugar ABC transporter	1.65
Lipopolysaccharide biosynthesis proteins		

KDSA	2-dehydro-3-deoxyphosphooctonate aldolase	1.95
A0A181VYK8	ADP-L-glycero-D-manno-heptose-6-epimerase	2.19
Peptidoglycan biosynthesis		
A0A2X3E7L8	D-alanyl-D-alanine carboxypeptidase	2.74
Replication and repair		
A0A485TFU7	DNA polymerase	1.63
Peptidases and inhibitors		
A0A2L0KHD8	Aminopeptidase N	2.83
A0A1Y5CDI2	Methionine aminopeptidase	1.51
A0A422ZBW2	Oligopeptidase A	3.19
Signal transduction		
A0A1C1EPK5	DNA-binding response regulator	1.56
A0A087FRB0	DNA-binding transcriptional dual regulator, leucine-binding	2.24
Chaperones and folding catalysts		
A6T5I0	ATP-dependent Clp protease proteolytic subunit	3.57
Uncharacterized protein/ Hypothetical protein		
R4Y5V0	Uncharacterized protein	9.79
A0A5E3SSR0	Uncharacterized protein	1.78
Biosynthesis of siderophore group nonribosomal peptides		
A0A0J4XXY1	Enterobactin synthase component F	2.4
A0A483H0F6	Isochorismate synthase EntC	2.14
Others		
A0A377VXX3	1,4-dihydroxy-2-naphthoyl-CoA synthase	3.59

W1B0C1	Acetyltransferase component of pyruvate dehydrogenase complex	2.19
A0A378BST9	Alkanesulfonates-binding protein	2.81
A0A5D6AEA6	D-hexose-6-phosphate mutarotase	1.64
A0A0E1CM50	Dipeptide-binding protein	2.65
A0A0W8AM03	GTP-binding protein TypA	1.57
A0A485YMQ0	Hemin transport protein HmuS	2.99
A0A4S3AY45	Maltodextrin-binding protein	1.83
A0A483GEK9	Multifunctional fusion protein	3.49
A0A378F8S4	Multifunctional fusion protein	2.61
A0A377TW07	Multifunctional fusion protein	1.73
A0A486F1F8	Periplasmic hemin-binding protein	3.47
A0A378E6M1	Phosphatase YidA	1.62
W1DY13	Protein ydjA	1.63
A0A0E1C9K5	Rossmann fold nucleotide-binding protein	2.57
A0A5E3A7S7	Serine protein kinase (PrkA protein)	2.08
W9BJG9	Thiamine-phosphate synthase	2.24
A0A060VE16	T-protein	2.27
A0A193SEU6	UDP-glucose pyrophosphorylase	2.45
A0A377ZC34	UPF0265 protein	1.67
C8T794	UPF0304 protein HMPREF0484	2.34
V0AL84	YodA	6.7

Summary

The arsenic resistant bacterial isolates in the present study showed differential expression of several proteins under arsenite stress. In *Bacillus* sp. strain SSAI1, 631 proteins were identified in arsenite exposed cells out of which 128 proteins were found to be up-regulated and 122 were down-regulated. Proteins like transporter proteins, cell division proteins, sporulation proteins, antioxidant enzymes, lipoproteins and peptidoglycan biosynthesis proteins were found up-regulated on exposure to 5 mM arsenite. Moreover, numerous proteins involved in the metabolism of carbohydrates, amino acids, lipids, nucleotides, cofactors, vitamins and stress proteins, along with transcriptional and translational proteins were also differentially expressed. Whereas in case of *Klebsiella* sp. strain SSSW7, 360 proteins were identified in arsenite (5 mM) exposed cells, of which 196 were found to be up-regulated and 168 were down-regulated proteins. **Arsenic specific proteins viz. arsenate reductase, arsenical pump-driving ATPase and arsenite efflux transporter metallo-chaperone were found highly up-regulated**. Likewise, several proteins involved in the metabolism of carbohydrates, energy, amino acids, nucleotides, lipids, cofactors, vitamins, along with transport, stress proteins, hypothetical proteins, antioxidant enzymes, DNA repair processes, lipopolysaccharide and peptidoglycan biosynthesis proteins were significantly expressed.

SALIENT FEATURES OF THE RESEARCH

- Arsenite resistant *Bacillus* sp. strain SSAI1 and *Klebsiella* sp. strain SSSW7 isolated in the present study exhibited the highest MIC of 25 and 21 mM for arsenite respectively.
- The presence of *aioA* gene in chromosomal and/ plasmid DNA in strain SSAI1 and SSSW7 has been first time reported.
- Morphological changes were observed as resistance strategies in both strains and also demonstrated intracellular and periplasmic accumulation of arsenic in strain SSAI1 and SSSW7, respectively.
- The strains also exhibited rapid oxidation potential converting toxic arsenite to arsenate.
- This is the first report showing the effect of arsenite on protein profile of *Bacillu*s sp. strain SSAI1 and *Klebsiella* sp. strain SSSW7.

APPENDICES

Appendix-A

Media

A.1 Nutrient Agar	g L^{-1}
Peptone	10.0
Beef extract	10.0
Sodium chloride	5.0
Agar agar	15.0
pH	7.3±0.2

A.2 Mineral Salt Medium Agar	g L^{-1}
Ferrous sulphate	0.06 g
Dipotassium hydrogen ortho phosphate (12.6 %)	100 mL
Potassium dihydrogen ortho phosphate (18.2 %)	20 mL
Ammonium nitrate (10 %)	20 mL
Magnesium sulphate (1 %)	20 mL
Manganese sulphate (0.6 %)	0.2 mL
Sodium molybdate (0.6 %)	0.2 mL
Calcium chloride (1 %)	15 mL
Agar agar	15.0

pH	7.3±0.2

A.3 Luria Bertani (L.B) Broth	g L^{-1}
Tryptone	10.0
Yeast extract	5.0
Sodium Chloride	10.0
pH	7.3±0.2

A.4 Mueller Hinton Agar	g L^{-1}
Meat infusion	2.0
Casein acid hydrolysate	17.5
Starch	1.5
Agar agar	15.0
pH	7.3±0.2

Appendix-B

Other Chemicals

B.1 Metal/ Metalloid stock solutions

B.1.1 Sodium (meta) arsenite

Stock solution (1 M): 12.991 g was dissolved in 100 mL of deionized water. The solution was filter sterilized through a 0.22-micron membrane and stored at 4 °C in a dark place.

B.1.2 Silver nitrate

Stock solution (0.1 M): 1.6987 g was dissolved in 100 mL of deionized water. The solution was filter sterilized through a 0.22-micron membrane and stored at 4 °C in a dark place.

B.1.3 Sodium arsenate

Stock solution (1 M): 31.201 g was dissolved in 100 mL of deionized water. The solution was filter sterilized through a 0.22-micron membrane and stored at 4 °C in a dark place.

B.1.4 Zinc chloride

Stock solution (1 M): 13.6286 g was dissolved in 100 mL of deionized water. The solution was filter sterilized through a 0.22-micron membrane and stored at 4 °C in a dark place.

B.1.5 Chromium nitrate

Stock solution (1 M): 23.8011 g was dissolved in 100mL of deionized water. The solution was filter sterilized through a 0.22-micron membrane and stored at 4 °C in a dark place.

B.1.6 Lead nitrate

Stock solution (1 M): 33.12 g was dissolved in 100 mL of deionized water. The solution was filter sterilized through a 0.22-micron membrane and stored at 4 °C in a dark place.

B.1.7 Nickel chloride

Stock solution (1 M): 12.95994 g was dissolved in 100 mL of deionized water. The solution was filter sterilized through a 0.22-micron membrane and stored at 4 °C in a dark place.

B.1.8 Copper sulphate

Stock solution (1 M): 15.9609 g was dissolved in 100 mL of deionized water. The solution was filter sterilized through a 0.22-micron membrane and stored at 4 °C in a dark place.

B.1.9 Ferrous sulphate

Stock solution (1 M): 15.1908 g was dissolved in 100 mL of deionized water. The solution was filter sterilized through a 0.22-micron membrane and stored at 4 °C in a dark place.

B.1.10 Manganese sulphate

Stock solution (1 M): 15.1001 g was dissolved in 100 mL of deionized water. The solution was filter sterilized through a 0.22-micron membrane and stored at 4 °C in a dark place.

B.1.11 Cadmium nitrate

Stock solution (1 M): 23.642 g was dissolved in 100 mL of deionized water. The solution was filter sterilized through a 0.22-micron membrane and stored at 4 °C in a dark place.

B.2 Phosphate buffered saline (PBS)

137 mM NaCl

2.7 mM KCl

10 mM Na2HPO4

2 mM KH2PO4

Adjust the pH to 7.4

B.3 Sodium phosphate buffer

Stock solution A: 0.2 M monobasic sodium phosphate, monohydrate (27.6 g L^{-1})

Stock solution B: 0.2 M dibasic sodium phosphate (28.4 g L^{-1})

Mix 28 mL of A and 72 mL of B and make total volume to 200 mL with deionized water to make 0.1M sodium phosphate buffer pH 7.2.

B.4 Enzyme Assay Buffers

B.4.1 Washing Buffer

20 mM Tris-HCl

0.1 mM phenylmethylsulfonyl fluoride (PMSF)

0.6 mM EDTA (pH 8.4)

0.9 % NaCl (pH 8.4)

B.4.2 Suspension Buffer

20 mM Tris-HCl buffer (pH 8.0)

0.6 mM PMSF

0.6 mM EDTA (pH 8.4)

B.4.3 10mg mL^{-1} Lysozyme

Dissolve 10.0 mg of lysozyme in 1 mL of 0.1 M Tris-HCl buffer (pH 8.0) and store at -20.

B.4.4 NaOH

Stock solution (2 M). 8 g was dissolved in 100 mL of Deionized water. The solution was filter sterilized through a 0.22-micron membrane and stored at 4 °C.

Appendix-C

Agarose Gel Electrophoresis

C.1 0.8 % and 1 % agarose

Weigh 0.8 g or 1.0 g of agarose and dissolve in 100 mL of 1X TAE buffer to prepare 0.8 % or 1 % agarose respectively. Melt the solution in microwave oven until a clear, transparent solution is obtained. Add ethidium bromide to a final concentration of 0.5 μg mL^{-1} and cast the gel.

C.2 Ethidium Bromide

Add 10.0 mg of ethidium bromide to 1mL of deionized water. Stir on magnetic stirrer for several hours to ensure that the dye has dissolved. Transfer the solution to an amber coloured bottle and store at room temperature.

C.3 Gel Loading Buffer

0.05 % (w/v) Bromophenol blue

40 % (w/v) Sucrose

0.1 M Ethylenediamine tetra acetic acid (EDTA), pH 8.0

0.5 % (w/v) Sodium dodecyl sulphate

C.4 50X Tris Acetate EDTA

Tris base	24.2 g
Glacial acetic acid	5.71 mL
0.5M EDTA	10 mL
Deionized water	100 mL

C.5 10X Tris EDTA (TE) Buffer (pH 8.0)

Tris Chloride	100 mM
EDTA	10 mM

Sterilize for 20 min at 15 psi.

Appendix-D

Sodium Dodecyl Sulphate-Polyacrylamide gel electrophoresis (SDS-PAGE)

D.1 Stock solutions for SDS-PAGE

D.1.1 Acrylamide-bis-acrylamide solution (monomer solution)

Acrylamide	29.0 g
N, N’ methylene bis acrylamide	1.0 g
Deionized water	100 mL

Dissolve acrylamide and N, N’-methylene bis-acrylamide in 80 mL of warm deionized water. Adjust the pH of the solution to 7.0. Make the final volume to 100 mL using deionized water. Store in an amber coloured bottle at room temperature.

D.1.2 Resolving gel buffer (Tris 1.5 M, pH 8.8)

Tris (base)	18.171 g
Deionized water	100 mL

Dissolve tris base in 60 mL of deionized water. Adjust the pH of the solution to 8.8 with 6 N HC1 and make the final volume to 100 mL with deionized water. Store the solution at 4 °C.

D.1.3 Stacking gel buffer (Tris 1.0 M, pH 6.8)

Tris (base)	12.114 g
Deionized water	100 mL

Dissolve tris base in 60 mL of deionized water. Adjust the pH of the solution to 6.8 with 6 N HC1 and make the final volume to 100 mL with deionized water. Store the solution at 4 °C.

D.1.4 10 % ammonium per sulphate (APS)

Ammonium per sulphate	0.1 g
Deionized water	1 mL

D.1.5 10 % Sodium dodecyl sulphate

Sodium dodecyl sulphate	10 g
Deionized water	100 mL

D.1.6 6 N Hydrochloric acid

Concentrated HCl	51 mL
Deionized water	100 mL

D.1.7 1 % Bromophenol blue

Bromophenol blue	0.1 g
Deionized water	10 mL

D.1.8 5X Tris-glycine electrophoresis buffer (pH 8.3)

25 mM Tris base	3.02 g
250 mM Glycine	18.8 g
10 % (w/v) SDS	10 mL
Deionized water	200 mL

Preparation of 1X tank buffer: Make 100 mL of 5X Tris-glycine electrophoresis buffer to 500 mL using deionized water.

D.1.9 2X Sample Solubilizing buffer

1 M Tris HC1 (pH 6.8)	1 mL
Glycerol	2 mL
1 % (w/v) Bromophenol blue	2 mL
10 % (w/v) SDS	4 mL
200 mM β-mercaptoethanol	284 µL
Deionized water	716 µL

D.1.10 Preparation of resolving and stacking gel

Components	12 % Resolving gel (10 mL)	5 % Stacking gel (3 mL)
Monomer	3.98	0.597
1.5 M Tris (pH 8.8)	2.486	-
1.0 M Tris (pH 6.8)	-	0.373
10% (w/v) SDS	0.1	0.03
10% (w/v) APS	0.05	0.015
TEMED	0.005	0.0015
Deionized water	3.381	1.984

D.2 Visualization of SDS-PAGE gels

D.2.1 Coomassie Brilliant Blue Staining Solution

Coomassie Brilliant Blue R-250	0.05 g
Methanol	50 mL
Glacial acetic acid	10 mL
Deionized water	100 mL

D.2.2 Destaining Solution

Methanol	30 mL
Glacial acetic acid	10 mL
Deionized water	100 mL

Appendix-E

Polymerase Chain Reaction

E.1 Primer sets

Primer	Primer sequence	Gene	References
27F	GAGAGTTTGATCCTGGCTCAG	16S rDNA	Studholme et al., 1999
1495R	CTACGGCTACCTTGTTACGA		
aioAF	CCACTTCTGCATCGTGGG	*aioA*	Ghosh et al., 2014
aioAR	TGTCGTTGCCCCAGATGA		
aoxBM1-2F	CCACTTCTGCATCGTGGGNTGYGGNTA	*aoxB*	Quéméneur et al., 2008; 2010
aoxBM2-1R	GGAGTTGTAGGCGGGCCKRTTRTGDAT		
dacr 1F	GCCATCGGCCTGATCGTNATGATGTAYCC	*ACR3*(1)	Achour et al., 2007
dacr 1R	CGGCGATGGCCAGCTCYAAYTTYTT		
dacr 5F	TGATCTGGGTCATGATCTTCCCVATGMTGVT	*ACR3*(2)	
dacr 4R	CGGCCACGGCCAGYTCRAARAARTT		

E.2 PCR reaction mixture

Component	Concentration	Quantity
Template DNA	50 ng μL^{-1}	4 µL
Master mix	2X	25 µL
Forward primer	20 pmol	1 µL
Reverse primer	20 pmol	1 µL
Deionized water	-	19 µL
Total volume	-	50 µL

E.3 PCR reaction cycle

Temperature (ºC)	Step	Time (Min)
95	Hot start	5
95	Denaturation	1
55	Annealing	1
72	Extension	1
72	Final extension	10

Standard curves

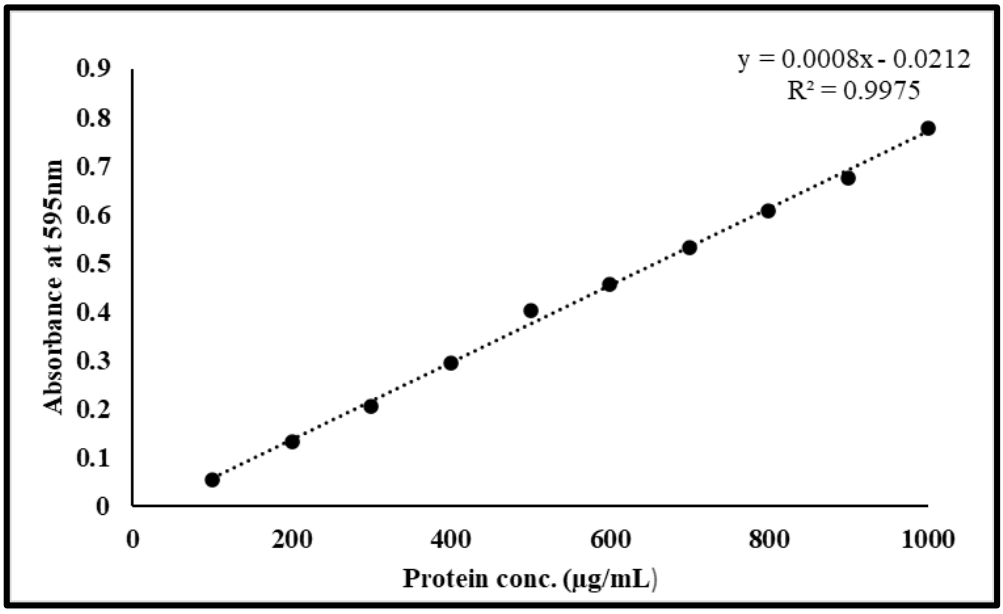

Fig. A: Standard curve for estimation of protein by Bradford assay.

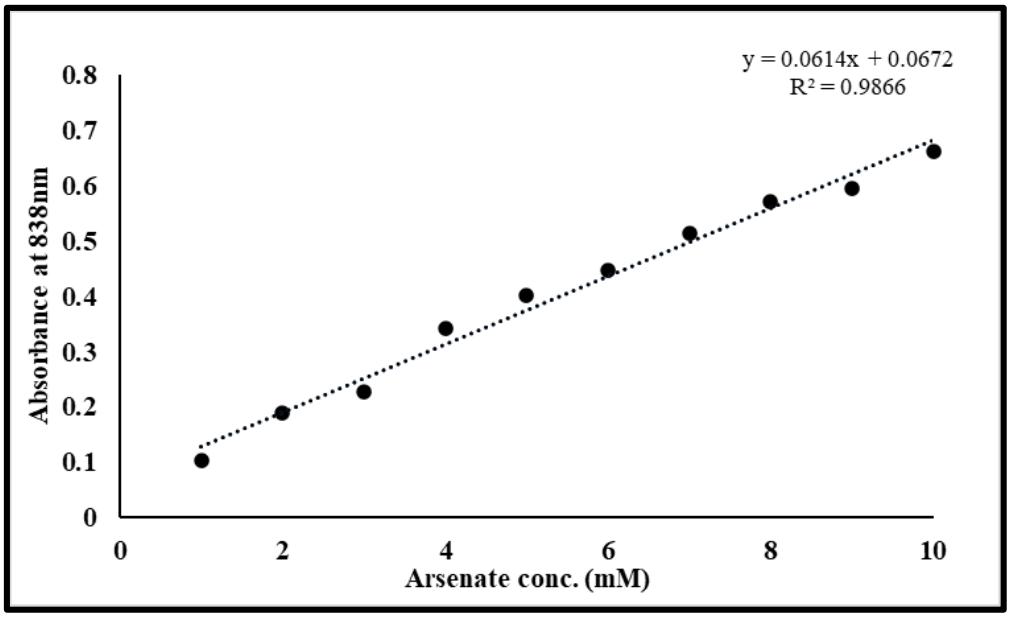

Fig. B: Calibration curve of sodium arsenate for estimation of arsenate using molybdene blue method.

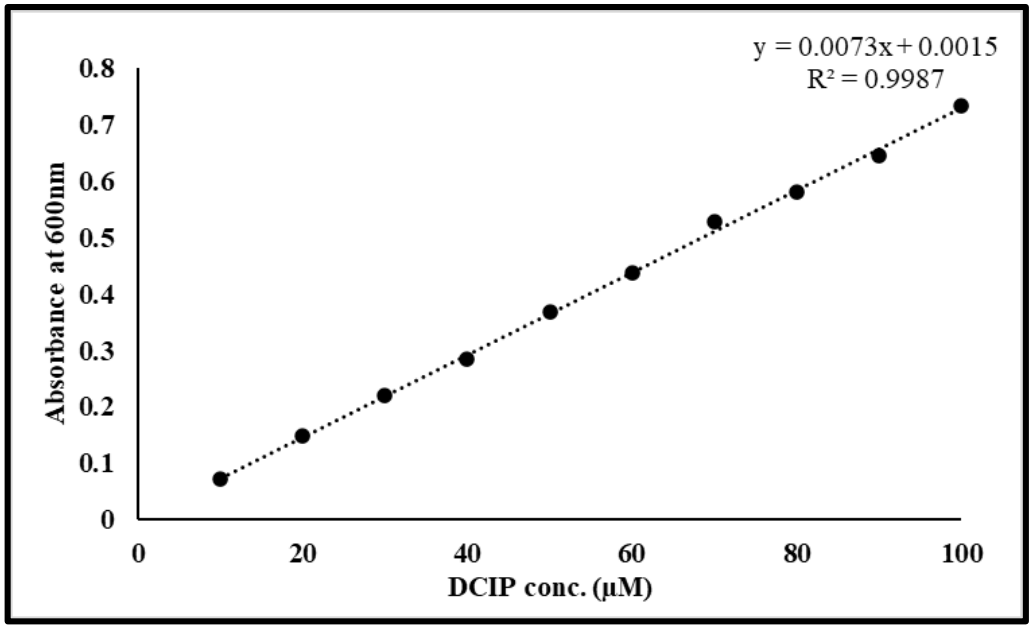

Fig. C: Calibration curve of DCIP for determining enzyme activity.

BIBLIOGRAPHY

- Abbas, S.Z., Riaz, M., Ramzan, N., Zahid, M.T., Shakoori, F.R. and Rafatullah, M. 2014. Isolation and characterization of arsenic resistant bacteria from wastewater. Braz. J. Microbiol. 45(4), 1309-1315.
- Achour, A.R., Bauda, P. and Billard, P. 2007. Diversity of arsenite transporter genes from arsenic-resistant soil bacteria. Res. Microbiol. 158(2), 128-137.
- Aguilar, N.C., Faria, M.C., Pedron, T., Batista, B.L., Mesquita, J.P., Bomfeti, C.A. and Rodrigues, J.L. 2020. Isolation and characterization of bacteria from a brazilian gold mining area with a capacity of arsenic bioaccumulation. Chemosphere 240, 124871.
- Ahmad, A., Richards, L.A. and Bhattacharya, P. 2017. Arsenic remediation of drinking water: an overview. Best practice guide on the control of arsenic in drinking water. Metals and related substances in drinking water series. IWA Publishing, UK, pp.79-98.
- Aksornchu, P., Prasertsan, P. and Sobhon, V. 2008. Isolation of arsenic-tolerant bacteria from arsenic-contaminated soil. Songklanakarin J. Sci. Technol. 30, 95-102.
- Alam, M.O., Shaikh, W.A., Chakraborty, S., Avishek, K. and Bhattacharya, T. 2016. Groundwater arsenic contamination and potential health risk assessment of Gangetic Plains of Jharkhand, India. Expos. Health 8(1), 125-142.
- Ali, H., Khan, E. and Ilahi, I. 2019. Environmental chemistry and ecotoxicology of hazardous heavy metals: environmental persistence, toxicity, and bioaccumulation. J. Chem. https://doi.org/10.1155/2019/6730305.
- Ali, H., Khan, E. and Sajad, M.A. 2013. Phytoremediation of heavy metals—concepts and applications. Chemosphere 91(7), 869-881.

- Ali, W., Isner, J.C., Isayenkov, S.V., Liu, W., Zhao, F.J. and Maathuis, F.J. 2012. Heterologous expression of the yeast arsenite efflux system ACR3 improves *Arabidopsis thaliana* tolerance to arsenic stress. New. Phytol. 194, 716-723.
- Anderson, G.L., Williams, J. and Hille, R. 1992. The purification and characterization of arsenite oxidase from *Alcaligenes faecalis*, a molybdenum-containing hydroxylase. J. Biol. Chem. 267(33), 23674-23682.
- Andres, J. and Bertin, P.N. 2016. The microbial genomics of arsenic. FEMS Microbiol. Rev. 40(2), 299-322.
- Andres, J., Arsene-Ploetze, F., Barbe, V., Brochier-Armanet, C., Cleiss-Arnold, J., Coppee, J.Y., Dillies, M.A., Geist, L., Joublin, A., Koechler, S. and Lassalle, F. 2013. Life in an arsenic-containing gold mine: genome and physiology of the autotrophic arsenite-oxidizing bacterium *Rhizobium* sp. NT-26. Genome Biol. Evol. 5(5), 934-953.
- Argos, M., Kalra, T., Rathouz, P.J., Chen, Y., Pierce, B., Parvez, F., Islam, T., Ahmed, A., Rakibuz-Zaman, M., Hasan, R. and Sarwar, G. 2010. Arsenic exposure from drinking water, and all-cause and chronic-disease mortalities in Bangladesh (HEALS): a prospective cohort study. The Lancet 376(9737), 252-258.
- Arsène-Ploetze, F., Koechler, S., Marchal, M., Coppée, J.Y., Chandler, M., Bonnefoy, V., Brochier-Armanet, C., Barakat, M., Barbe, V., Battaglia-Brunet, F. and Bruneel, O. 2010. Structure, function, and evolution of the *Thiomonas* spp. genome. PLoS Genet. 6(2).
- ATSDR, 2013. Agency for Toxic Substances and Disease Registry (accessed on 23april2019)].Availableonline.http://www.atsdr.cdc.gov/substances/toxsubstance.asp?toxid¼3.

- Bagade, A., Nandre, V., Paul, D., Patil, Y., Sharma, N., Giri, A. and Kodam, K. 2020. Characterisation of hyper tolerant *Bacillus firmus* L-148 for arsenic oxidation. Environ. Pollut. 261, 114124.
- Bagade, A.V., Bachate, S.P., Dholakia, B.B., Giri, A.P. and Kodam, K.M. 2016. Characterization of *Roseomonas* and *Nocardioides* spp. for arsenic transformation. J. Hazard. Mater. 318, 742-750.
- Bahar, M.M., Megharaj, M. and Naidu, R. 2012. Arsenic bioremediation potential of a new arsenite-oxidizing bacterium *Stenotrophomonas* sp. MM-7 isolated from soil. Biodegradation 23(6), 803-812.
- Bahar, M.M., Megharaj, M. and Naidu, R. 2013. Kinetics of arsenite oxidation by *Variovorax* sp. MM-1 isolated from a soil and identification of arsenite oxidase gene. J. Hazard. Mater. 262, 997-1003.
- Bahar, M.M., Megharaj, M. and Naidu, R. 2016. Oxidation of arsenite to arsenate in growth medium and groundwater using a novel arsenite-oxidizing diazotrophic bacterium isolated from soil. Int. Biodeter. Biodegr. 106, 178-182.
- Baker-Austin, C., Dopson, M., Wexler, M., Sawers, R.G., Stemmler, A., Rosen, B.P. and Bond, P.L. 2007. Extreme arsenic resistance by the acidophilic archaeon '*Ferroplasma acidarmanus*' Fer1. Extremophiles 11(3), 425-434.
- Banerjee, S., Datta, S., Chattyopadhyay, D. and Sarkar, P. 2011. Arsenic accumulating and transforming bacteria isolated from contaminated soil for potential use in bioremediation. J. Environ. Sci. Health A 46(14), 1736-1747.
- Battaglia-Brunet, F., Dictor, M.C., Garrido, F., Crouzel, C., Morin, D., Dekeyser, K., Clarens, M. and Baranger, P. 2002. An arsenic (III)-oxidizing bacterial population: selection, characterization, and performance in reactors. J. Appl. Microbiol. 93(4), 656-667.

- Battaglia-Brunet, F., Joulian, C., Garrido, F., Dictor, M.C., Morin, D., Coupland, K., Johnson, D.B., Hallberg, K.B. and Baranger, P. 2006. Oxidation of arsenite by Thiomonas strains and characterization of *Thiomonas arsenivorans* sp. nov. Anton. Leeuw. 89(1), 99-108.
- Bauer, A.W., Kirby, W.M.M., Sherris, J.C. and Turck, M. 1966. Antibiotic susceptibility testing by a standardized single disc method. Am. J. Clin. Pathol. 45, 493-496.
- Belfiore, C., Ordonez, O.F. and Farías, M.E. 2013. Proteomic approach of adaptive response to arsenic stress in *Exiguobacterium* sp. S17, an extremophile strain isolated from a high-altitude Andean Lake stromatolite. Extremophiles 17(3), 421-431.
- Bentley, R. and Chasteen, T.G. 2002. Microbial methylation of metalloids: arsenic, antimony, and bismuth. Microbiol. Mol. Biol. Rev. 66(2), 250-271.
- Bhat, S., Luo, X., Xu, Z., Liu, L. and Zhang, R. 2011. *Bacillus* sp. CDB3 isolated from cattle dip-sites possesses two ars gene clusters. J. Environ. Sci. 23(1), 95-101.
- Bhowmick, S., Pramanik, S., Singh, P., Mondal, P., Chatterjee, D. and Nriagu, J. 2018. Arsenic in groundwater of West Bengal, India: a review of human health risks and assessment of possible intervention options. Sci. Total Environ. 612, 148-169.
- Biswas, R., Majhi, A.K. and Sarkar, A. 2019a. The role of arsenate reducing bacteria for their prospective application in arsenic contaminated groundwater aquifer system. Biocatal. Agric. Biotechnol. 20, 101218.
- Biswas, R., Vivekanand, V., Saha, A., Ghosh, A. and Sarkar, A. 2019b. Arsenite oxidation by a facultative chemolithotrophic *Delftia* spp. BAs29 for its potential

application in groundwater arsenic bioremediation. Int. Biodeter. Biodegr. 136, 55-62.

- Bradford, M.M. 1976. A rapid and sensitive method for the quantitation of microgram quantities of protein utilizing the principle of protein-dye binding. Anal. Biochem. 72(1-2), 248-254.
- Branco, R., Francisco, R., Chung, A.P. and Morais, P.V. 2009. Identification of an aox system that requires cytochrome c in the highly arsenic-resistant bacterium *Ochrobactrum tritici* SCII24. Appl. Environ. Microbiol. 75(15), 5141-5147.
- Bryan, C.G., Marchal, M., Battaglia-Brunet, F., Kugler, V., Lemaitre-Guillier, C., Lièvremont, D., Bertin, P.N. and Arsène-Ploetze, F. 2009. Carbon and arsenic metabolism in *Thiomonas* strains: differences revealed diverse adaptation processes. BMC Microbiol. 9(1), 127.
- Bueno, B.Y.M., Torem, M.L., Molina, F.A.L.M.S. and De Mesquita, L.M.S. 2008. Biosorption of lead (II), chromium (III) and copper (II) by *R. opacus*: Equilibrium and kinetic studies. Miner. Eng. 21(1), 65-75.
- Bundschuh, J., Bhattacharya, P., Sracek, O., Mellano, M.F., Ramírez, A.E., Storniolo, A.D.R., Martín, R.A., Cortes, J., Litter, M.I. and Jean, J.S. 2011. Arsenic removal from groundwater of the Chaco-Pampean plain (Argentina) using natural geological materials as adsorbents. J. Environ. Sci. Health Part A 46(11), 1297-1310.
- Bustaffa, E., Stoccoro, A., Bianchi, F. and Migliore, L. 2014. Genotoxic and epigenetic mechanisms in arsenic carcinogenicity. Arch. Toxicol. 88(5), 1043-1067.

- Cai, L., Liu, G., Rensing, C. and Wang, G. 2009a. Genes involved in arsenic transformation and resistance associated with different levels of arsenic-contaminated soils. BMC Microbiol. 9(1), 4.
- Cai, L., Rensing, C., Li, X. and Wang, G. 2009b. Novel gene clusters involved in arsenite oxidation and resistance in two arsenite oxidizers: *Achromobacter* sp. SY8 and *Pseudomonas* sp. TS44. Appl. Microbiol. Biotechnol. 83(4), 715-725.
- Campos, V.L., Valenzuela, C., Yarza, P., Kämpfer, P., Vidal, R., Zaror, C., Mondaca, M.A., Lopez-Lopez, A. and Rosselló-Móra, R. 2010. *Pseudomonas arsenicoxydans* sp nov., an arsenite-oxidizing strain isolated from the Atacama desert. Syst. Appl. Microbiol. 33(4), 193-197.
- Carapito, C., Muller, D., Turlin, E., Koechler, S., Danchin, A., Van Dorsselaer, A., Leize-Wagner, E., Bertin, P.N. and Lett, M.C. 2006. Identification of genes and proteins involved in the pleiotropic response to arsenic stress in *Caenibacter arsenoxydans*, a metalloresistant beta-proteobacterium with an unsequenced genome. Biochimie 88(6), 595-606.
- Carlin, A., Shi, W., Dey, S. and Rosen, B.P. 1995. The ars operon of *Escherichia coli* confers arsenical and antimonial resistance. J. Bacteriol. 177(4), 981-986.
- Chakrabarti, D., Singh, S.K., Rashid, Md. H., Rahman, Md. M. 2018. Arsenic: Occurrence in Groundwater, Chapter ・January 2018, http://dx.doi.org/10.1016/ B978-0-12-409548-9.10634-7.
- Chang, J.S., Lee, J.H. and Kim, I.S. 2011. Bacterial aox genotype from arsenic contaminated mine to adjacent coastal sediment: Evidences for potential biogeochemical arsenic oxidation. J. Hazard. Mater. 193, 233-242.
- Chang, J.S., Yoon, I.H., Lee, J.H., Kim, K.R., An, J. and Kim, K.W. 2010. Arsenic detoxification potential of aox genes in arsenite-oxidizing bacteria

isolated from natural and constructed wetlands in the Republic of Korea. Environ. Geochem. Health 32(2), 95-105.

- Chauhan, N.S., Ranjan, R., Purohit, H.J., Kalia, V.C. and Sharma, R. 2009. Identification of genes conferring arsenic resistance to *Escherichia coli* from an effluent treatment plant sludge metagenomic library. FEMS Microbiol. Ecol. 67(1), 130-139.
- Chen, C.M., Misra, T.K., Silver, S. and Rosen, B.P. 1986. Nucleotide sequence of the structural genes for an anion pump. The plasmid-encoded arsenical resistance operon. J. Biol. Chem. 261(32), 15030-15038.
- Cheng, H., Hu, Y., Luo, J., Xu, B. and Zhao, J. 2009. Geochemical processes controlling fate and transport of arsenic in acid mine drainage (AMD) and natural systems. J. Hazard. Mater. 165(1-3), 13-26.
- Cleiss-Arnold, J., Koechler, S., Proux, C., Fardeau, M.L., Dillies, M.A., Coppee, J.Y., Arsène-Ploetze, F. and Bertin, P.N. 2010. Temporal transcriptomic response during arsenic stress in *Herminiimonas arsenicoxydans*. BMC Genomics 11(1), 709.
- Corsini, A., Colombo, M., Muyzer, G. and Cavalca, L. 2015. Characterization of the arsenite oxidizer *Aliihoeflea* sp. strain 2WW and its potential application in the removal of arsenic from groundwater in combination with Pf-ferritin. Anton. Leeuw. 108(3), 673-684.
- Costa, P.S., Tschoeke, D.A., Silva, B.S., Thompson, F., Reis, M.P., Chartone-Souza, E. and Nascimento, A.M. 2015. Draft genome sequence of *Micrococcus* sp. strain MS-AsIII-49, an arsenate-reducing isolate from tropical metal-rich sediment. Genome Announc. 3(2), e00122-15.

- Dabrowska, B.B., Vithanage, M., Gunaratna, K.R., Mukherjee, A.B. and Bhattacharya, P. 2012. Bioremediation of arsenic in contaminated terrestrial and aquatic environments. In Environmental chemistry for a sustainable world (pp. 475-509). Springer, Dordrecht.
- Dani, S.U. 2010. Arsenic for the fool: an exponential connection. Sci. Total Environ. 408:1842-1846.
- Das, B., Rahman, M.M., Nayak, B., Pal, A., Chowdhury, U.K., Mukherjee, S.C., Saha, K.C., Pati, S., Quamruzzaman, Q. and Chakrobaorti, D. 2009. Groundwater Arsenic Contamination, Its Health Effects and Approach for Mitigation in West Bengal, India and Bangladesh. Water Qual. Expo. Health. 1 (1), 5-21.
- Das, S., Jean, J.S., Chou, M.L., Rathod, J. and Liu, C.C. 2016. Arsenite-oxidizing bacteria exhibiting plant growth promoting traits isolated from the rhizosphere of *Oryza sativa* L.: implications for mitigation of arsenic contamination in paddies. J. Hazard. Mater. 302, 10-18.
- Daware, V., Kesavan, S., Patil, R., Natu, A., Kumar, A., Kulkarni, M. and Gade, W. 2012. Effects of arsenite stress on growth and proteome of *Klebsiella pneumoniae*. J. Biotechnol. 158(1-2), 8-16.
- Debiec, K., Krzysztoforski, J., Uhrynowski, W., Sklodowska, A. and Drewniak, L. 2017. Kinetics of arsenite oxidation by *Sinorhizobium* sp. M14 under changing environmental conditions. Int. Biodeter. Biodegr. 119, 476-485.
- Dembitsky, V.M. and Levitsky, D.O. 2004. Arsenolipids. Prog. Lipid Res. 43, 403-448.
- Deshmukh, A.B., Bai, S., Aarthy, T., Kazi, R.S., Banarjee, R., Rathore, R., Vijayakumar, M.V., Thulasiram, H.V., Bhat, M.K. and Kulkarni, M.J. 2017.

Methylglyoxal attenuates insulin signaling and downregulates the enzymes involved in cholesterol biosynthesis. Mol. BioSyst. 13(11), 2338-2349.

- Dey, U., Chatterjee, S. and Mondal, N.K. 2016. Isolation and characterization of arsenic-resistant bacteria and possible application in bioremediation. Biotechnol. Rep. 10, 1-7.
- Dey, U., Chatterjee, S. and Mondal, N.K. 2017. Investigation of Bioremediation of Arsenic by Bacteria Isolated from an Arsenic Contaminated Area. Environ. Process. 4(1), 183-199.
- Dombrowski, P.M., Long, W., Farley, K.J., Mahony, J.D., Capitani, J.F. and Di Toro, D.M. 2005. Thermodynamic analysis of arsenic methylation. Environ. Sci. Technol. 39(7), 2169-2176.
- Ebele, B. 2009. Mechanisms of arsenic toxicity and carcinogenesis. Afr. J. Biomed. Res. 3(5), 232-237.
- Ellis, P.J., Conrads, T., Hille, R. and Kuhn, P. 2001. Crystal structure of the 100 kDa arsenite oxidase from *Alcaligenes faecalis* in two crystal forms at 1.64 Å and 2.03 Å. Structure 9(2), 125-132.
- Fahy, A., Giloteaux, L., Bertin, P., Le Paslier, D., Médigue, C., Weissenbach, J., Duran, R. and Lauga, B. 2015. 16S rRNA and As-related functional diversity: contrasting fingerprints in arsenic-rich sediments from an acid mine drainage. Microb. Ecol. 70(1), 154-167.
- Fendorf, S., Michael, H.A. and van Geen, A. 2010. Spatial and temporal variations of groundwater arsenic in South and Southeast Asia. Science 328(5982), 1123-1127.
- Flora, S.J.S. 2011. Arsenic-induced oxidative stress and its reversibility. Free Radical Bio. Med. 51, 257-281.

- Gebel, T. 2000. Confounding variables in the environmental toxicology of arsenic. Toxicology 144(1-3), 155-162.
- Ghosh, D., Bhadury, P. and Routh, J. 2014. Diversity of arsenite oxidizing bacterial communities in arsenic-rich deltaic aquifers in West Bengal, India. Front. Microbiol. 5, 602.
- Goswami, R., Mukherjee, S., Rana, V.S., Saha, D.R., Raman, R., Padhy, P.K. and Mazumder, S. 2015. Isolation and characterization of arsenic-resistant bacteria from contaminated water-bodies in West Bengal, India. Geomicrobiol. J. 32(1), 17-26.
- Gourbal, B., Sonuc, N., Bhattacharjee, H., Legare, D., Sundar, S., Ouellette, M., Rosen, B.P. and Mukhopadhyay, R. 2004. Drug uptake and modulation of drug resistance in *Leishmania* by an aquaglyceroporin. J. Biol. Chem. 279, 31010-31017.
- Green, H.H. 1918. Description of a bacterium which oxidizes arsenite to arsenate, and of one which reduces arsenate to arsenite, isolated from a cattle-dipping Etank. South Afr. J. Sci. 14, 465-467.
- Grund, S.C., Hanusch, K. and Wolf, H.U. 2000. Arsenic and arsenic compounds. In: Ullmann's Encyclopedia of Industrial Chemistry. Wiley-VCH Verlag GmbH & Co. KGaA.
- Guo, H., Liu, Z., Ding, S., Hao, C., Xiu, W. and Hou, W. 2015. Arsenate reduction and mobilization in the presence of indigenous aerobic bacteria obtained from high arsenic aquifers of the Hetao basin, Inner Mongolia. Environ. Pollut. 203, 50-59.
- Hamamura, N., Itai, T., Liu, Y., Reysenbach, A.L., Damdinsuren, N. and Inskeep, W.P. 2014. Identification of anaerobic arsenite-oxidizing and arsenate-reducing

bacteria associated with an alkaline saline lake in Khovsgol, Mongolia. Env. Microbiol. Rep. 6(5), 476-482.

- Han, Y.H., Yin, D.X., Jia, M.R., Wang, S.S., Chen, Y., Rathinasabapathi, B., Chen, D.L. and Ma, L.Q. 2019. Arsenic-resistance mechanisms in bacterium *Leclercia adecarboxylata* strain As3-1: Biochemical and genomic analyses. Sci. Total Environ. 690, 1178-1189.
- Henne, K.L., Turse, J.E., Nicora, C.D., Lipton, M.S., Tollaksen, S.L., Lindberg, C., Babnigg, G., Giometti, C.S., Nakatsu, C.H., Thompson, D.K. and Konopka, A.E. 2009. Global proteomic analysis of the chromate response in *Arthrobacter* sp. strain FB24. J. Proteome Res. 8(4), 1704-1716.
- Holt, J.G., Krieg, N.R. and Sneath, P.H. 1994. Bergey's manual of determinative bacterology.
- Hughes, M.F. 2002. Arsenic toxicity and potential mechanisms of action. Toxicol. Lett. 133(1), 1-16.
- Hughes, M.F., Beck, B.D., Chen, Y., Lewis, A.S. and Thomas, D.J. 2011. Arsenic exposure and toxicology: a historical perspective. Toxicol. Sci. 123(2), 305-332.
- Ianeva, O.D. 2009. Mechanisms of bacteria resistance to heavy metals. Mikrobiolohichnyi zhurnal (Kiev, Ukraine: 1993), 71(6), 54.
- Jain, R., Jha, S., Adhikary, H., Kumar, P., Parekh, V., Jha, A., Mahatma, M.K. and Kumar, G.N. 2014. Isolation and molecular characterization of arsenite-tolerant *Alishewanella* sp. GIDC-5 originated from industrial effluents. Geomicrobiol. J. 31(1), 82-90.
- Jang, Y.C., Somanna, Y. and Kim, H. 2016. Source, distribution, toxicity and remediation of arsenic in the environment–a review. Int. J. Appl. Environ. Sci. 11(2), 559-581.

- Jebeli, M.A., Maleki, A., Amoozegar, M.A., Kalantar, E., Izanloo, H. and Gharibi, F. 2017. *Bacillus flexus* strain As-12, a new arsenic transformer bacterium isolated from contaminated water resources. Chemosphere 169, 636-641.
- Jebelli, M.A., Maleki, A., Amoozegar, M.A., Kalantar, E., Gharibi, F., Darvish, N. and Tashayoe, H. 2018. Isolation and identification of the native population bacteria for bioremediation of high levels of arsenic from water resources. J. Environ. Manage. 212, 39-45.
- Jia, M.R., Tang, N., Cao, Y., Chen, Y., Han, Y.H. and Ma, L.Q. 2019. Efficient arsenate reduction by As-resistant bacterium *Bacillus* sp. strain PVR-YHB1-1: Characterization and genome analysis. Chemosphere 218, 1061-1070.
- Jomova, K., Jenisova, Z., Feszterova, M., Baros, S., Liska, J., Hudecova, D., Rhodes, C.J. and Valko, M. 2011. Arsenic: toxicity, oxidative stress and human disease. J. Appl. Toxicol. 31(2), 95-107.
- Kang, Y.S., Bothner, B., Rensing, C. and McDermott, T.R. 2012. Involvement of RpoN in regulating bacterial arsenite oxidation. Appl. Environ. Microbiol. 78(16), 5638-5645.
- Kashyap, D.R., Botero, L.M., Franck, W.L., Hassett, D.J. and McDermott, T.R. 2006. Complex regulation of arsenite oxidation in *Agrobacterium tumefaciens*. J. Bacteriol. 188(3), 1081-1088.
- Kawa, Y.K., Wang, J., Chen, X., Zhu, X., Zeng, X.C. and Wang, Y. 2019. Reductive dissolution and release of arsenic from arsenopyrite by a novel arsenate-respiring bacterium from the arsenic-contaminated soils. Int. Biodeter. Biodegr. 143, 104712.

- Ke, C., Xiong, H., Zhao, C., Zhang, Z., Zhao, X., Rensing, C., Zhang, G. and Yang, S. 2019. Expression and purification of an ArsM-elastin-like polypeptide fusion and its enzymatic properties. Appl. Microbiol. Biotechnol. 103(6), 2809-2820.
- Khairul, I., Wang, Q.Q., Jiang, Y.H., Wang, C. and Naranmandura, H. 2017. Metabolism, toxicity and anticancer activities of arsenic compounds. Oncotarget 8(14), 23905-23926.
- Khoei, A.J., Joogh, N.J.G., Darvishi, P. and Rezaei, K. 2018. Application of physical and biological methods to remove heavy metal, arsenic and pesticides, malathion and diazinon from water. Turk. J. Fish. Aquat. Sci. 19(1), 21-28.
- Koechler, S., Cleiss-Arnold, J., Proux, C., Sismeiro, O., Dillies, M.A., Goulhen-Chollet, F., Hommais, F., Lièvremont, D., Arsène-Ploetze, F., Coppée, J.Y. and Bertin, P.N. 2010. Multiple controls affect arsenite oxidase gene expression in *Herminiimonas arsenicoxydans*. BMC Microbiol. 10(1), 53.
- Kostal, J., Yang, R., Wu, C.H., Mulchandani, A. and Chen, W. 2004. Enhanced arsenic accumulation in engineered bacterial cells expressing ArsR. Appl. Environ. Microbiol. 70(8), 4582-4587.
- Kruger, M.C., Bertin, P.N., Heipieper, H.J. and Arsène-Ploetze, F. 2013. Bacterial metabolism of environmental arsenic—mechanisms and biotechnological applications. Appl. Microbiol. Biotechnol. 97(9), 3827-3841.
- Kudo, K., Yamaguchi, N., Makino, T., Ohtsuka, T., Kimura, K., Dong, D.T. and Amachi, S. 2013. Release of arsenic from soil by a novel dissimilatory arsenate-reducing bacterium, *Anaeromyxobacter* sp. strain PSR-1. Appl. Environ. Microbiol. 79(15), 4635-4642.

- Kulp, T.R., Hoeft, S.E., Asao, M., Madigan, M.T., Hollibaugh, J.T., Fisher, J.C., Stolz, J.F., Culbertson, C.W., Miller, L.G. and Oremland, R.S. 2008. Arsenic (III) fuels anoxygenic photosynthesis in hot spring biofilms from Mono Lake, California. Science 321(5891), 967-970.
- Kumar, S., Stecher, G. and Tamura, K. 2016. MEGA7: molecular evolutionary genetics analysis version 7.0 for bigger datasets. Mol. Biol. Evol. 33(7), 1870-1874.
- Kumari, N. and Jagadevan, S. 2016. Genetic identification of arsenate reductase and arsenite oxidase in redox transformations carried out by arsenic metabolising prokaryotes–A comprehensive review. Chemosphere 163, 400-412.
- Kumari, N., Rana, A. and Jagadevan, S. 2019. Arsenite biotransformation by *Rhodococcus* sp.: Characterization, optimization using response surface methodology and mechanistic studies. Sci. Total Environ. 687, 577-589.
- Kuroda, M., Ayano, H., Sei, K., Yamashita, M. and Ike, M. 2015. Draft genome sequence of *Bacillus selenatarsenatis* SF-1T, a promising agent for bioremediation of environments contaminated with selenium and arsenic. Genome Announc. 3(1), e01466-14.
- Lenoble, V., Deluchat, V., Serpaud, B. and Bollinger, J.C. 2003. Arsenite oxidation and arsenate determination by the molybdene blue method. Talanta 61(3), 267-276.
- Lett, M.C., Muller, D., Lièvremont, D., Silver, S. and Santini, J. 2012. Unified nomenclature for genes involved in prokaryotic aerobic arsenite oxidation. J. Bacteriol. 194(2), 207-208.

- Li, B., Lin, J., Mi, S. and Lin, J. 2010. Arsenic resistance operon structure in *Leptospirillum ferriphilum* and proteomic response to arsenic stress. Bioresour. Technol. 101(24), 9811-9814.
- Liao, V.H.C., Chu, Y.J., Su, Y.C., Hsiao, S.Y., Wei, C.C., Liu, C.W., Liao, C.M., Shen, W.C. and Chang, F.J. 2011. Arsenite-oxidizing and arsenate-reducing bacteria associated with arsenic-rich groundwater in Taiwan. J. Contam. Hydrol. 123(1-2), 20-29.
- Lieutaud, A., Van Lis, R., Duval, S., Capowiez, L., Muller, D., Lebrun, R., Lignon, S., Fardeau, M.L., Lett, M.C., Nitschke, W. and Schoepp-Cothenet, B. 2010. Arsenite oxidase from *Ralstonia* sp. 22 Characterization of the enzyme and its interaction with soluble cytochromes. J. Biol. Chem. 285(27), 20433-20441.
- Lim, K.T., Shukor, M.Y. and Wasoh, H. 2014. Physical, chemical, and biological methods for the removal of arsenic compounds. BioMed Res. Int. Article ID 503784, 9 pages.
- Lin, Y.F., Yang, J. and Rosen, B.P. 2007. ArsD: an As (III) metallochaperone for the ArsAB As (III)-translocating ATPase. J. Bioenerg. Biomembr. 39(5-6), 453-458.
- Liu, S., Zhang, F., Chen, J. and Sun, G. 2011. Arsenic removal from contaminated soil via bio-volatilization by genetically engineered bacteria under laboratory conditions. J. Environ. Sci. 23, 1544–1550.
- Lloyd, J.R. and Lovley, D.R. 2001. Microbial detoxification of metals and radionuclides. Curr. Opinion. Biotechnol. 12(3), 248-253.
- Lu, X., Zhang, Y., Liu, C., Wu, M. and Wang, H. 2018. Characterization of the antimonite-and arsenite-oxidizing bacterium *Bosea* sp. AS-1 and its potential application in arsenic removal. J. Hazard. Mater. 359, 527-534.

- Lupo, A., Coyne, S. and Berendonk, T.U. 2012. Origin and evolution of antibiotic resistance: the common mechanisms of emergence and spread in water bodies. Front. Microbiol. 3, 18.
- Majumder, A., Bhattacharyya, K., Bhattacharyya, S. and Kole, S.C. 2013. Arsenic-tolerant, arsenite-oxidising bacterial strains in the contaminated soils of West Bengal, India. Sci. Total Environ. 463, 1006-1014.
- Malasarn, D., Keeffe, J.R. and Newman, D.K. 2008. Characterization of the arsenate respiratory reductase from *Shewanella* sp. strain ANA-3. J. Bacteriol. 190(1), 135-142.
- Malik, A.H., Khan, Z.M., Mahmood, Q., Nasreen, S. and Bhatti, Z.A. 2009. Perspectives of low cost arsenic remediation of drinking water in Pakistan and other countries. J. Hazard. Mater. 168(1), 1-12.
- Mallick, I., Bhattacharyya, C., Mukherji, S., Dey, D., Sarkar, S.C., Mukhopadhyay, U.K. and Ghosh, A. 2018. Effective rhizoinoculation and biofilm formation by arsenic immobilizing halophilic plant growth promoting bacteria (PGPB) isolated from mangrove rhizosphere: a step towards arsenic rhizoremediation. Sci. Total Environ. 610, 1239-1250.
- Mallick, I., Hossain, S.T., Sinha, S. and Mukherjee, S.K. 2014. *Brevibacillus* sp. KUMAs2, a bacterial isolate for possible bioremediation of arsenic in rhizosphere. Ecotoxicol. Environ. Saf. 107, 236-244.
- Mallik, S., Virdi, J.S. and Johri, A.K. 2012. Proteomic analysis of arsenite–mediated multiple antibiotic resistance in *Yersinia enterocolitica* biovar 1A. J. Basic Microbiol. 52(3), 306-313.
- Mandal, B.K. and Suzuki, K.T. 2002. Arsenic round the world: a review. Talanta 58(1), 201-235.

- Marchiset-Ferlay, N., Savanovitch, C. and Sauvant-Rochat, M.P. 2012. What is the best biomarker to assess arsenic exposure via drinking water?. Environ. Int. 39(1), 150-171.
- Mazumder, D.G. and Dasgupta, U.B. 2011. Chronic arsenic toxicity: studies in West Bengal, India. Kaohsiung J. Med. Sci. 27(9), 360-370.
- Meliker, J.R., Wahl, R.L., Cameron, L.L. and Nriagu, J.O. 2007. Arsenic in drinking water and cerebrovascular disease, diabetes mellitus, and kidney disease in Michigan: a standardized mortality ratio analysis. Environ. Health 6(1), 4.
- Meng, Y.L., Liu, Z. and Rosen, B.P. 2004. As(III) and Sb(III) uptake by GlpF and efflux by ArsB in *Escherichia coli*. J. Biol. Chem. 279, 18334–18341.
- Mettert, E.L. and Kiley, P.J. 2015. Fe–S proteins that regulate gene expression. Biochim. Biophys. Acta-Molecular Cell Research 1853(6), 1284-1293.
- Meyer, Y., Buchanan, B.B., Vignols, F. and Reichheld, J.P. 2009. Thioredoxins and glutaredoxins: unifying elements in redox biology. Annu. Rev. Genet. 43, 335-367.
- Michalke, K., Wickenheiser, E.B., Mehring, M., Hirner, A.V. and Hensel, R. 2000. Production of volatile derivatives of metal (loid)s by microflora involved in anaerobic digestion of sewage sludge. Appl. Environ. Microbiol. 66(7), 2791-2796.
- Mohapatra, B. and Sar, P. 2018. Genome sequencing and functional analysis of an environmental isolate *Escherichia coli* Cont-1 revealed its genetic basis of arsenic-transformation and niche adaptation. Ecological Genetics and Genomics 9, 34-42.
- Mohapatra, B., Kazy, S.K. and Sar, P. 2019. Comparative genome analysis of arsenic reducing, hydrocarbon metabolizing groundwater bacterium

Achromobacter sp. KAs 3-5T explains its competitive edge for survival in aquifer environment. Genomics 111(6), 1604-1619.

- Mokashi, S.A. and Paknikar, K.M. 2002. Arsenic (III) oxidizing *Microbacterium lacticum* and its use in the treatment of arsenic contaminated groundwater. Lett. Appl. Microbiol. 34(4), 258-262.
- Mondal, P., Majumder, C.B. and Mohanty, B. 2006. Laboratory based approaches for arsenic remediation from contaminated water: recent developments. J. Hazard. Mater. 137(1), 464-479.
- Mukhopadhyay, R., Rosen, B.P., Phung, L.T. and Silver, S. 2002. Microbial arsenic: from geocycles to genes and enzymes. FEMS Microbiol. Rev. 26(3), 311-325.
- Muller, D., Lievremont, D., Simeonova, D.D., Hubert, J.C. and Lett, M.C. 2003. Arsenite oxidase *aox* genes from a metal-resistant β-proteobacterium. J. Bacterial. 185(1), 135-141.
- Muller, D., Médigue, C., Koechler, S., Barbe, V., Barakat, M., Talla, E., Bonnefoy, V., Krin, E., Arsene-Ploetze, F., Carapito, C. and Chandler, M. 2007. A tale of two oxidation states: bacterial colonization of arsenic-rich environments. PLoS Genet. 3(4).
- Nagvenkar, G.S. and Ramaiah, N. 2010. Arsenite tolerance and biotransformation potential in estuarine bacteria. Ecotoxicology 19(4), 604-613.
- Naik, M.M., Shamim, K. and Dubey, S.K. 2012. Biological characterization of lead-resistant bacteria to explore role of bacterial metallothionein in lead resistance. Curr. Sci. 426-429.
- National Research Council (NRC), Arsenic. National Academy Press, Washington, D.C, 1977.

- Naujokas, M.F., Anderson, B., Ahsan, H., Aposhian, H.V., Graziano, J.H., Thompson, C. and Suk, W.A. 2013. The broad scope of health effects from chronic arsenic exposure: update on a worldwide public health problem. Environ. Health Perspect. 121(3), 295-302.
- Niazi, N.K., Bibi, I., Fatimah, A., Shahid, M., Javed, M.T., Wang, H., Ok, Y.S., Bashir, S., Murtaza, B., Saqib, Z.A. and Shakoor, M.B. 2017. Phosphate-assisted phytoremediation of arsenic by *Brassica napus* and *Brassica juncea*: morphological and physiological response. Int. J. Phytoremediat. 19(7), 670-678.
- Nicomel, N.R., Leus, K., Folens, K., Van Der Voort, P. and Du Laing, G. 2016. Technologies for arsenic removal from water: current status and future perspectives. Int. J. Environ. Res. Public Health 13(1), 62.
- Nidheesh, P.V. and Singh, T.A. 2017. Arsenic removal by electrocoagulation process: recent trends and removal mechanism. Chemosphere 181, 418-432.
- Nies, D.H. 1999. Microbial heavy-metal resistance. Appl. Microbiol. Biotechnol. 51(6), 730-750.
- Novick, S.C. and Warrell Jr, R.P. 2000, October. Arsenicals in hematologic cancers. In Seminars in oncology 27 (5), 495-501.
- Nriagu, J.O. and Azcue, J.M. 1994. Arsenic in the environment. Part I: cycling and characterization (Vol. 26, pp. 119-132). New York, NY.: John Wiley & Sons.
- Ohtsuka, T., Yamaguchi, N., Makino, T., Sakurai, K., Kimura, K., Kudo, K., Homma, E., Dong, D.T. and Amachi, S. 2013. Arsenic dissolution from Japanese paddy soil by a dissimilatory arsenate-reducing bacterium *Geobacter* sp. OR-1. Environ. Sci. Technol. 47(12), 6263-6271.
- Oremland, R.S. and Stolz, J.F. 2003. The ecology of arsenic. Science 300, 939-944.

- Oremland, R.S. and Stolz, J.F. 2005. Arsenic, microbes and contaminated aquifers. Trends Microbiol. 13(2), 45-49.
- Oremland, R.S., Hoeft, S.E., Santini, J.M., Bano, N., Hollibaugh, R.A. and Hollibaugh, J.T. 2002. Anaerobic oxidation of arsenite in Mono Lake water and by a facultative, arsenite-oxidizing chemoautotroph, strain MLHE-1. Appl. Environ. Microbiol. 68(10), 4795-4802.
- Oremland, R.S., Saltikov, C.W., Wolfe-Simon, F. and Stolz, J.F. 2009. Arsenic in the evolution of earth and extraterrestrial ecosystems. Geomicrobiol. J. 26(7), 522-536.
- Oust, A., Møretrø, T., Kirschner, C., Narvhus, J.A. and Kohler, A. 2004. FT-IR spectroscopy for identification of closely related lactobacilli. J. Microbiol. Methods 59(2), 149-162.
- Özdemir, S., Kilinc, E., Poli, A., Nicolaus, B. and Güven, K. 2012. Cd, Cu, Ni, Mn and Zn resistance and bioaccumulation by thermophilic bacteria, *Geobacillus toebii* subsp. *decanicus* and *Geobacillus thermoleovorans* subsp. s*tromboliensis*. World J. Microbiol. Biotechnol. 28(1), 155-163.
- Páez-Espino, D., Tamames, J., de Lorenzo, V. and Cánovas, D. 2009. Microbial responses to environmental arsenic. Biometals 22(1), 117-130.
- Palma-Lara, I., Martínez-Castillo, M., Quintana-Pérez, J.C., Arellano-Mendoza, M.G., Tamay-Cach, F., Valenzuela-Limón, O.L., García-Montalvo, E.A. and Hernández-Zavala, A. 2020. Arsenic exposure: A public health problem leading to several cancers. Regul. Toxicol. Pharmacol. 110, 104539.
- Pandey, N. and Bhatt, R. 2015. Arsenic resistance and accumulation by two bacteria isolated from a natural arsenic contaminated site. J. Basic Microbiol. 55(11), 1275-1286.

- Pandi, M., Shashirekha, V. and Swamy, M. 2009. Bioabsorption of chromium from retan chrome liquor by cyanobacteria. Microbiol. Res. 164(4), 420-428.
- Paul, D., Kazy, S.K., Banerjee, T.D., Gupta, A.K., Pal, T. and Sar, P. 2015. Arsenic biotransformation and release by bacteria indigenous to arsenic contaminated groundwater. Bioresour. Technol. 188, 14-23.
- Pereira, E.J., Ramaiah, N., Damare, S. and Furtado, B. 2018. Differential protein analysis of hexavalent chromium stress response in marine *Staphylococcus xylosus*. Curr. Proteomics 15(1), 42-54.
- Philips, S.E. and Taylor, M.L. 1976. Oxidation of arsenite to arsenate by *Alcaligenes faecalis*. Appl. Environ. Microbiol. 32(3), 392-399.
- Prasad, K.S., Subramanian, V. and Paul, J. 2009. Purification and characterization of arsenite oxidase from *Arthrobacter* sp. Biometals 22(5), 711-721.
- Prithivirajsingh, S., Mishra, S.K. and Mahadevan, A. 2001. Detection and analysis of chromosomal arsenic resistance in *Pseudomonas fluorescens* strain MSP3. Biochem. Biophys. Res. Commun. 280(5), 1393-1401.
- Qin, J., Rosen, B.P., Zhang, Y., Wang, G., Franke, S. and Rensing, C. 2006. Arsenic detoxification and evolution of trimethylarsine gas by a microbial arsenite S-adenosylmethionine methyltransferase. Proc. Natl. Acad. Sci. 103(7), 2075-2080.
- Quéméneur, M., Cébron, A., Billard, P., Battaglia-Brunet, F., Garrido, F., Leyval, C. and Joulian, C. 2010. Population structure and abundance of arsenite-oxidizing bacteria along an arsenic pollution gradient in waters of the Upper Isle River Basin, France. Appl. Environ. Microbiol. 76(13), 4566-4570.

- Quéméneur, M., Heinrich-Salmeron, A., Muller, D., Lièvremont, D., Jauzein, M., Bertin, P.N., Garrido, F. and Joulian, C. 2008. Diversity surveys and evolutionary relationships of *aoxB* genes in aerobic arsenite-oxidizing bacteria. Appl. Environ. Microbiol. 74(14), 4567-4573.
- Rahman, F.A., Allan, D.L., Rosen, C.J. and Sadowsky, M.J. 2004. Arsenic availability from chromated copper arsenate (CCA)–treated wood. J. Environ. Qual. 33(1), 173-180.
- Rahman, M.A., Hasegawa, H. and Lim, R.P. 2012. Bioaccumulation, biotransformation and trophic transfer of arsenic in the aquatic food chain. Environ. Res. 116, 118-135.
- Rahman, M.M., Ng, J.C. and Naidu, R. 2009. Chronic exposure of arsenic via drinking water and its adverse health impacts on humans. Environ. Geochem. Health 31, 189-200.
- Rahman, S., Kim, K.H., Saha, S.K., Swaraz, A.M. and Paul, D.K. 2014. Review of remediation techniques for arsenic (As) contamination: a novel approach utilizing bio-organisms. J. Environ. Manage. 134,175-185.
- Rathod, J., Dhanani, A.S., Jean, J.S. and Jiang, W.T. 2019. The whole genome insight on condition-specific redox activity and arsenopyrite interaction promoting As-mobilization by strain *Lysinibacillus* sp. B2A1. J. Hazard. Mater. 364, 671-681.
- Rehman, A., Butt, S.A. and Hasnain, S. 2010. Isolation and characterization of arsenite oxidizing *Pseudomonas lubricans* and its potential use in bioremediation of wastewater. Afr. J. Biotechnol. 9(10), 1493-1498.

- Richey, C., Chovanec, P., Hoeft, S.E., Oremland, R.S., Basu, P. and Stolz, J.F. 2009. Respiratory arsenate reductase as a bidirectional enzyme. Biochem. Biophys. Res. Commun. 382(2), 298-302.
- Rosen, B.P. 1999. Families of arsenic transporters. Trends Microbiol. 7(5), 207-212.
- Rosen, B.P. 2002. Biochemistry of arsenic detoxification. FEBS Lett. 529(1), 86-92.
- Rosen, B.P. and Liu, Z. 2009. Transport pathways for arsenic and selenium: a minireview. Environ. Int. 35(3), 512-515.
- Roychowdhury, R., Roy, M., Rakshit, A., Sarkar, S. and Mukherjee, P. 2018. Arsenic bioremediation by indigenous heavy metal resistant bacteria of fly ash pond. Bull. Environ. Contam. Toxicol. 101(4), 527-535.
- Sacheti, P., Bhonsle, H., Patil, R., Kulkarni, M.J., Srikanth, R. and Gade, W. 2013. Arsenomics of *Exiguobacterium* sp. PS (NCIM 5463). RSC Adv. 3(25), 9705-9713.
- Sadaf, N., Kumar, N., Ali, M., Ali, V., Bimal, S. and Haque, R. 2018. Arsenic trioxide induces apoptosis and inhibits the growth of human liver cancer cells. Life Sci. 205, 9-17.
- Sambrook, J., Fritsch, E.F. and Maniatis, T. 1989. Molecular Cloning: A Laboratory Manual. Cold Spring Harbor Laboratory Press, New York.
- Santini, J.M. and vanden Hoven, R.N. 2004. Molybdenum-containing arsenite oxidase of the chemolithoautotrophic arsenite oxidizer NT-26. J. Bacteriol. 186, 1614-1619.
- Santini, J.M., Sly, L.I., Schnagl, R.D. and Macy, J.M. 2000. A new chemolithoautotrophic arsenite-oxidizing bacterium isolated from a gold mine:

phylogenetic, physiological, and preliminary biochemical studies. Appl. Environ. Microbiol. 66(1), 92-97.

- Santini, J.M., Sly, L.I., Wen, A., Comrie, D., Wulf-Durand, P.D. and Macy, J.M. 2002. New arsenite-oxidizing bacteria isolated from Australian gold mining environments--phylogenetic relationships. Geomicrobiol. J. 19(1), 67-76.
- Sardiwal, S., Santini, J.M., Osborne, T.H. and Djordjevic, S. 2010. Characterization of a two-component signal transduction system that controls arsenite oxidation in the chemolithoautotroph NT-26. FEMS Microbiol. Lett. 313(1), 20-28.
- Satyapal, G.K., Mishra, S.K., Srivastava, A., Ranjan, R.K., Prakash, K., Haque, R. and Kumar, N. 2018. Possible bioremediation of arsenic toxicity by isolating indigenous bacteria from the middle Gangetic plain of Bihar, India. Biotechnol. Rep. 17, 117-125.
- Selvankumar, T., Radhika, R., Mythili, R., Arunprakash, S., Srinivasan, P., Govarthanan, M. and Kim, H. 2017. Isolation, identification and characterization of arsenic transforming exogenous endophytic *Citrobacter* sp. RPT from roots of Pteris vittata. 3 Biotech 7(4), 264.
- Shah, S. and Damare, S.R. 2018. Differential protein expression in a marine-derived *Staphylococcus* sp. NIOSBK35 in response to arsenic (III). 3 Biotech 8(6), 287.
- Shahid, M., Dumat, C., Khan Niazi, N. and Khalid, S. 2018. Global scale arsenic pollution: increase the scientific knowledge to reduce human exposure.
- Shakoor, M.B., Bibi, I., Niazi, N.K., Shahid, M., Nawaz, M.F., Farooqi, A., Naidu, R., Rahman, M.M., Murtaza, G. and Lüttge, A. 2018. The evaluation of

arsenic contamination potential, speciation and hydrogeochemical behaviour in aquifers of Punjab, Pakistan. Chemosphere 199, 737-746.

- Shakoor, M.B., Nawaz, R., Hussain, F., Raza, M., Ali, S., Rizwan, M., Oh, S.E. and Ahmad, S. 2017. Human health implications, risk assessment and remediation of As-contaminated water: a critical review. Sci. Total Environ. 601, 756-769.
- Shen, S., Li, X.F., Cullen, W.R., Weinfeld, M. and Le, X.C. 2013. Arsenic binding to proteins. Chem. Rev. 113(10), 7769-7792.
- Shen, Z., Luangtongkum, T., Qiang, Z., Jeon, B., Wang, L. and Zhang, Q. 2014. Identification of a novel membrane transporter mediating resistance to organic arsenic in *Campylobacter jejuni*. Antimicrob. Agents Chemother. 58(4), 2021-2029.
- Shewale, M., Bhandari, D. and Garg, R.K. 2017. A Review of Arsenic in Drinking Water: Indian Scenario. Int. J. Sci. Res. Sci. Eng. Technol. 3(5), 300-304.
- Shi, K., Li, C., Rensing, C., Dai, X., Fan, X. and Wang, G. 2018. Efflux transporter ArsK is responsible for bacterial resistance to arsenite, antimonite, trivalent roxarsone, and methylarsenite. Appl. Environ. Microbiol., 84(24), e01842-18.
- Silver, S. 1998. Genes for all metals—a bacterial view of the periodic table. J. Ind. Microbiol. Biotechnol. 20(1), 1-12.
- Silver, S. and Phung, L.T. 1996. Bacterial heavy metal resistance: new surprises. Ann. Rev. Microbiol. 50(1), 753-789.

- Silver, S. and Phung, L.T. 2005. Genes and enzymes involved in bacterial oxidation and reduction of inorganic arsenic. Appl. Environ. Microbiol. 71(2), 599-608.
- Singh, A.L. and Singh, V.K. 2015. Arsenic contamination in ground water of Ballia, Uttar Pradesh state, India. J. Appl. Geochem. 17(1), 78-85.
- Singh, J.S., Abhilash, P.C., Singh, H.B., Singh, R.P. and Singh, D.P. 2011. Genetically engineered bacteria: an emerging tool for environmental remediation and future research perspectives. Gene 480(1-2), 1-9.
- Singh, N., Gupta, S., Marwa, N., Pandey, V., Verma, P.C., Rathaur, S. and Singh, N. 2016. Arsenic mediated modifications in *Bacillus aryabhattai* and their biotechnological applications for arsenic bioremediation. Chemosphere 164, 524-534.
- Singh, R., Singh, S., Parihar, P., Singh, V.P. and Prasad, S.M. 2015. Arsenic contamination, consequences and remediation techniques: a review. Ecotoxicol. Environ. Saf. 112, 247-270.
- Singh, S., Kang, S.H., Lee, W., Mulchandani, A. and Chen, W. 2010. Systematic engineering of phytochelatin synthesis and arsenic transport for enhanced arsenic accumulation in *E. coli*. Biotechnol. Bioeng. 105(4), 780-785.
- Singh, S., Mulchandani, A. and Chen, W. 2008. Highly selective and rapid arsenic removal by metabolically engineered *Escherichia coli* cells expressing *Fucus vesiculosus* metallothionein. Appl. Environ. Microbiol. 74(9), 2924-2927.
- Smedley, P.L. and Kinniburgh, D.G. 2002. A review of the source, behaviour and distribution of arsenic in natural waters. J. Appl. Geochem. 17(5), 517-568.

- Sodhi, K.K., Kumar, M., Agrawal, P.K. and Singh, D.K. 2019. Perspectives on arsenic toxicity, carcinogenicity and its systemic remediation strategies. Environ. Technol. Innov. 16, 100462.
- Sousa, T., Branco, R., Piedade, A.P. and Morais, P.V. 2015. Hyper accumulation of arsenic in mutants of *Ochrobactrum tritici* silenced for arsenite efflux pumps. PloS one 10(7), e0131317.
- Srivastava, S., Verma, P.C., Singh, A., Mishra, M., Singh, N., Sharma, N. and Singh, N. 2012. Isolation and characterization of *Staphylococcus* sp. strain NBRIEAG-8 from arsenic contaminated site of West Bengal. Appl. Microbiol. Biotechnol., 95(5), 1275-1291.
- Stolz, J.F., Basu, P. and Oremland, R.S. 2010. Microbial arsenic metabolism: new twists on an old poison. Microbe 5(2), 53-59.
- Stolz, J.F., Basu, P., Santini, J.M. and Oremland, R.S. 2006. Arsenic and selenium in microbial metabolism. Annu. Rev. Microbiol. 60, 107-130.
- Studholme, D.J., Jackson, R.A. and Leak, D.J. 1999. Phylogenetic analysis of transformable strains of thermophilic *Bacillus* species. FEMS Microbiol. Lett. 172(1), 85-90.
- Sun, Y., Polishchuk, E.A., Radoja, U. and Cullen, W.R. 2004. Identification and quantification of *arsC* genes in environmental samples by using real-time PCR. J. Microbiol. Methods 58(3), 335-349.
- Tamaki, S. and Frankenberger, W.T. 1992. Environmental biochemistry of arsenic. In Reviews of environmental contamination and toxicology (pp. 79-110). Springer, New York, NY.

- Tanmoy, P.A.U.L., Chakraborty, A., Islam, E. and Mukherjee, S.K. 2018. Arsenic bioremediation potential of arsenite-oxidizing *Micrococcus* sp. KUMAs15 isolated from contaminated soil. Pedosphere 28(2), 299-310.
- Tsai, S.L., Singh, S. and Chen, W. 2009. Arsenic metabolism by microbes in nature and the impact on arsenic remediation. Curr. Opin. Chem. Biol. 20(6), 659-667.
- Tuli, R., Chakrabarty, D., Trivedi, P.K. and Tripathi, R.D. 2010. Recent advances in arsenic accumulation and metabolism in rice. Mol. Breed. 26, 307-323.
- vanden Hoven, R.N. and Santini, J.M. 2004. Arsenite oxidation by the heterotroph *Hydrogenophaga* sp. str. NT-14: the arsenite oxidase and its physiological electron acceptor. Biochim. Biophys. Acta- Bioenergetics 1656(2-3), 148-155.
- Visioli, G., Marmiroli, M. and Marmiroli, N. 2010. Two-dimensional liquid chromatography technique coupled with mass spectrometry analysis to compare the proteomic response to cadmium stress in plants. J. Biomed. Biotechnol. https://doi.org/10.1155/2010/567510
- Walton, F.S., Harmon, A.W., Paul, D.S., Drobná, Z., Patel, Y.M. and Styblo, M. 2004. Inhibition of insulin-dependent glucose uptake by trivalent arsenicals: possible mechanism of arsenic-induced diabetes. Toxicol. Appl. Pharmacol. 198 (3), 424-433.
- Wang, J., Wu, M., Lu, G. and Si, Y. 2016. Biotransformation and biomethylation of arsenic by *Shewanella oneidensis* MR-1. Chemosphere 145, 329-335.
- Wang, J., Xie, Z., Wei, X., Chen, M., Luo, Y. and Wang, Y. 2020. An indigenous bacterium *Bacillus* XZM for phosphate enhanced transformation and migration of arsenate. Sci. Total Environ. 719, 137183.

- Wang, L., Jeon, B., Sahin, O. and Zhang, Q. 2009. Identification of an arsenic resistance and arsenic-sensing system in *Campylobacter jejuni*. Appl. Environ. Microbiol. 75(15), 5064-5073.
- WHO (World Health Organization), 2014. Arsenic. Environ. Health Criter. 19 Genova.
- Willsky, G.R. and Malamy, M.H. 1980a. Characterization of two genetically separable inorganic phosphate transport systems in *Escherichia coli*. J. Bacteriol. 144(1), 356-365.
- Willsky, G.R. and Malamy, M.H. 1980b. Effect of arsenate on inorganic phosphate transport in *Escherichia coli*. J. Bacteriol. 144(1), 366-374.
- Wu, Y., Feng, S., Li, B. and Mi, X. 2010. The characteristics of *Escherichia coli* adsorption of arsenic (III) from aqueous solution. World J. Microbiol. Biotechnol. 26(2), 249-256.
- Xu, C., Zhou, T., Kuroda, M. and Rosen, B.P. 1998. Metalloid resistance mechanisms in prokaryotes. J. Biochem. 123(1), 16-23.
- Yang, J., Rawat, S., Stemmler, T.L. and Rosen, B.P. 2010. Arsenic binding and transfer by the ArsD As (III) metallochaperone. Biochemistry 49(17), 3658-3666.
- Ye, L., Wang, L. and Jing, C. 2020. Biotransformation of adsorbed arsenic on iron minerals by coexisting arsenate-reducing and arsenite-oxidizing bacteria. Environ. Pollut. 256, 113471.
- Yoon, I.H., Chang, J.S., Lee, J.H. and Kim, K.W. 2009. Arsenite oxidation by *Alcaligenes* sp. strain RS-19 isolated from arsenic-contaminated mines in the Republic of Korea. Environ. Geochem. Health 31(1), 109.
- Zargar, K., Hoeft, S., Oremland, R. and Saltikov, C.W. 2010. Identification of a novel arsenite oxidase gene, *arxA*, in the haloalkaliphilic, arsenite-oxidizing

bacterium *Alkalilimnicola ehrlichii* strain MLHE-1. J. Bacteriol. 192(14), 3755-3762.

- Zhang, Y., Ma, Y.F., Qi, S.W., Meng, B., Chaudhry, M.T., Liu, S.Q. and Liu, S.J. 2007. Responses to arsenate stress by *Comamonas* sp. strain CNB-1 at genetic and proteomic levels. Microbiology 153(11), 3713-3721.
- Zhang, Y.B., Monchy, S., Greenberg, B., Mergeay, M., Gang, O., Taghavi, S. and van der Lelie, D. 2009. ArsR arsenic-resistance regulatory protein from *Cupriavidus metallidurans* CH34. Anton. Leeuw. 96(2), 161-170.
- Zhao, F.J., McGrath, S.P. and Meharg, A.A. 2010. Arsenic as a food chain contaminant: mechanisms of plant uptake and metabolism and mitigation strategies. Ann. Rev. Plant Biol. 61, 535-559.
- Zhu, Y.G., Williams, P.N. and Meharg, A.A. 2008. Exposure to inorganic arsenic from rice: a global health issue?. Environ. Pollut. 154(2), 169-171.
- Zhu, Y.G., Yoshinaga, M., Zhao, F.J. and Rosen, B.P. 2014. Earth abides arsenic biotransformations. Annu. Rev. Earth Planet. Sci. 42, 443-467.

PUBLICATIONS

1. **Mujawar, S.Y.**, Shamim, K., Vaigankar, D.C. and Dubey, S.K. 2019. Arsenite biotransformation and bioaccumulation by *Klebsiella pneumoniae* strain SSSW7 possessing arsenite oxidase (*aioA*) gene. BioMetals 32(1), 65-76.

2. **Mujawar, S. Y.**, Vaigankar, D. C. and Dubey, S. K. 2021. Biological characterization of *Bacillus flexus* strain SSAI1 transforming highly toxic arsenite to less toxic arsenate mediated by periplasmic arsenite oxidase enzyme encoded by *aioAB* genes. BioMetals 1-13.

OTHER PUBLICATIONS

1. Shamim, K., Sharma, J., Mutnale, M., Dubey, S. K. and **Mujawar, S.** 2018. Characterization of a metagenomic serine metalloprotease and molecular docking studies. Process Biochem. 71, 69-75.

2. Vaigankar, D. C., Dubey, S. K., **Mujawar, S. Y.**, D'Costa, A. and Shyama, S. K. 2018. Tellurite biotransformation and detoxification by *Shewanella baltica* with simultaneous synthesis of tellurium nanorods exhibiting photo-catalytic and anti-biofilm activity. Ecotox. Environ. Saf. 165, 516-526.

3. Naik, M. M., Naik, D., Charya, L., **Mujawar, S. Y.** and Vaingankar, D. C. 2019. Application of Marine Bacteria Associated with Seaweed, *Ulva lactuca*, for Degradation of Algal Waste. Proc. Natl. Acad. Sci., India, Sec. B Biol. Sci. 89, 1153-1160.

BOOK CHAPTER PUBLISHED

1. Samant, S., Naik, M. M., Vaigankar, D. C., **Mujawar, S. Y.**, Parab, P. and Meena, S. N. 2019. Biodegradation of seafood waste by seaweed-associated bacteria and application of seafood waste for ethanol production. In: Advances in Biological Science Research (pp. 149-159). Academic Press.

2. Shamim, K., **Mujawar, S. Y.** and Mutnale, M. 2019. Metagenomics- a modern approach to reveal the secrets of unculturable microbes. In: Advances in Biological Science Research (pp. 177-195). Academic Press.

RESEARCH PAPERS PRESENTED IN NATIONAL AND INTERNATIONAL CONFERENCES

1. **Mujawar, S. Y.**, Dubey, S. K. Isolation and characterization of arsenite oxidizing bacteria from battery waste. In International conference on Microbial technology for better tomorrow (17-19th February 2018) held at Dr. D.Y. Patil Arts, Commerce & Science College, Pimpri, Pune, Maharashtra.

2. **Mujawar, S. Y.**, Dubey, S. K. Biological characterization of arsenite oxidizing bacterial strains from terrestrial environments of Goa, India. In International conference on Materials and Environmental Science (7-8th December 2018) held at Shivaji University, Kolhapur (won second prize).

WORKSHOPS AND SYMPOSIA ATTENDED

- Attended national seminar on "Advances in Microbiology and Marine Microbiology" organized by Department of Microbiology, Goa University (13th March 2015).
- Attended 56th Annual Conference of Association of Microbiologists of India and International symposium on "Emerging Discoveries in Microbiology", JNU Delhi (7-10th December 2015).
- Participated in UGC-sponsored "Short Term Course in Research Methodology for Science Students" at Goa University held from 28th November to 3rd December 2016.
- Attended national conference of young researchers on "New Frontiers in Life Sciences and Environment" organized by Faculty of Life Sciences and Environment, Goa University (16-17th March 2017).
- Attended one-day seminar on "New Perspectives in Biosciences" organized by Department of Microbiology, Goa University (7th December 2017).
- Participated in workshop on "Novel Sanitation Approaches and Emerging Trends In Waste Water Treatment Technology" organized by BITS Pilani, K K Birla Goa campus (19-21st December 2017).
- Attended one-day seminar on "Biosafety and Intellectual Property Rights" organized by Department of Biotechnology, Goa University (20th March 2018).
- Attended workshop on "Scientific Manuscript Writing" organized by Department of Biological Sciences, BITS Pilani, K K Birla Goa campus (24th March 2018).

- Participated in one-day seminar cum workshop on “BioTechniques” organized by Department of Biotechnology, Goa University (29th November 2018).
- Attended two-day national seminar on “Recent Trends in Microbial Technology” organized by the Department of Botany, Government College of Arts, Science and Commerce, Quepem-Goa (8-9th February 2019).
- Attended one-day workshop on “Systat and Sigmaplot software” jointly organized by Department of Biological Sciences and Starcom Information Technology Limited, Bengaluru, India at BITS Pilani, K K Birla Goa campus (25th July 2019).
- Attended two-days training in “Genomics and Bioinformatics” organized by RASA Life Science Informatics, Pune (25-26th December 2019).
- Participated in hands-on training in “Molecular Phylogenetics” organized by Department of Zoology, Goa University (7 - 9th February 2020).
- Participated in hands-on workshop on “Modern Laboratory Techniques” organized by Department of Zoology, Goa University (11-14th February 2020).
- Attended two-day national seminar on “Effective Use of Nanotechnology and Nanomaterials for Sustainable Agriculture” organized by Department of Microbiology, PESRSN College of Arts and Science, Ponda, Goa (28-29th February 2020).
- Participated in the webinar on ‘Use of Elsevier Tools for developing Research Workflow and Academic Writing’ organized by the Directorate of Higher Education, Goa, in collaboration with ELSEVIER (18th May 2020).

- Participated in the webinar on “How to Write a Great Research Paper and get it accepted by a Good Journal” organized by the Directorate of Higher Education, Goa in collaboration with ELSEVIER (3rd June 2020).
- Participated in one day webinar on “Successful Research Paper Concept to Submission” held on 22nd June 2020.
- Attended national seminar on “Life and Life Processes: Interdisciplinary Approach for Sustainable Development” organized by Department of Zoology, Goa University (19-21st July 2021).

Biometals (2019) 32:65–76
https://doi.org/10.1007/s10534-018-0158-7

Arsenite biotransformation and bioaccumulation by *Klebsiella pneumoniae* strain SSSW7 possessing arsenite oxidase (*aioA*) gene

Sajiya Yusuf Mujawar · Kashif Shamim · Diviya Chandrakant Vaigankar · Santosh Kumar Dubey

Received: 9 August 2018 / Accepted: 17 November 2018 / Published online: 23 November 2018

Abstract Arsenite oxidizing *Klebsiella pneumoniae* strain SSSW7 isolated from shipyard waste Goa, India showed a minimum inhibitory concentration of 21 mM in mineral salts medium. The strain possessed a small supercoiled plasmid and PCR amplification of arsenite oxidase gene (*aioA*) was observed on plasmid as well as chromosomal DNA. It was confirmed that arsenite oxidase enzyme was a periplasmic protein with a 47% increase in arsenite oxidase activity at 1 mM sodium arsenite. Scanning electron microscopy coupled with electron dispersive X-ray spectroscopic (SEM–EDS) analysis of 15 mM arsenite exposed cells revealed long chains of cells with no surface adsorption of arsenic. Transmission electron microscopy combined with electron dispersive X-ray spectroscopic (TEM-EDS) analysis demonstrated plasma membrane disruption, cytoplasmic condensation and periplasmic accumulation of arsenic. The bacterial strain oxidized 10 mM of highly toxic arsenite to less toxic arsenate after 24 h of incubation. Fourier transformed infrared (FTIR) spectroscopy confirmed the interaction of arsenite with functional groups present on the bacterial cell surface. Sodium dodecyl sulfate-polyacrylamide gel electrophoresis (SDS-PAGE) analysis of 5 mM arsenite exposed cells demonstrated over-expression of 87 kDa and 14 kDa proteins of two subunits aioA and aioB of heterodimer arsenite oxidase enzyme as compared to control cells. Therefore, this bacterial strain might be employed as a potential candidate for bioremediation of arsenite contaminated environmental sites.

Keywords Arsenite · *AioA* gene · Bioremediation · Biotransformation

Introduction

Extensive anthropogenic activities such as mining, combustion of fossil fuels, arsenical pesticides, herbicides, paints, ceramic, glass and pharmaceutical industries have resulted in the release of highly toxic metalloid arsenic in the environment which poses serious threat to all living organisms (Welch et al. 2000; Smedley and Kinniburgh 2002; Cheng et al. 2009; Stolz et al. 2010). Although WHO (1993) has set the permissible limit of 10 µg/l arsenic in drinking

Electronic supplementary material The online version of this article (https://doi.org/10.1007/s10534-018-0158-7) contains supplementary material, which is available to authorized users.

S. Y. Mujawar · K. Shamim · D. C. Vaigankar
Laboratory of Bacterial Genetics and Environmental Biotechnology, Department of Microbiology, Goa University, Taleigao Plateau, Goa 403206, India

S. K. Dubey (✉)
Center of Advanced Study in Botany, Banaras Hindu University, Varanasi, U.P. 221005, India
e-mail: santoshdubey.gu@gmail.com; santosh.dubey@bhu.ac.in

water, many countries still exceed this permissible limit (Chowdhury et al. 2000; Anawar et al. 2002; Mitra et al. 2002; Smedley and Kinniburgh 2002; Mukherjee et al. 2006).

Arsenic usually exists in four oxidation states such as − 3 (arsine), 0 (elemental arsenic), + 3 (arsenite) and + 5 (arsenate) with arsenite and arsenate being the most common forms of arsenic in the environment (Oremland and Stolz 2005). Arsenite is 100 times more toxic than arsenate and acts by interacting with thiol groups of proteins and enzymes inhibiting their functions (Hughes 2002; Rosen 2002; Rai et al. 2011). Arsenic also causes mutagenic and genotoxic effects on humans (Mandal and Suzuki 2002; Chen et al. 2002).

The ubiquity of arsenic in the environment has led microorganisms to develop various transformation mechanisms such as arsenite oxidation, arsenate reduction and arsenite methylation governed by *aio*, *arr, arsC* and *arsM* genes respectively which are located either on chromosomal or plasmid DNA (Silver and Phung 1996; Páez-Espino et al. 2009; Arsene-Ploetze et al. 2010; Bahar et al. 2013; Goswami et al. 2015). These mechanisms are commonly employed by various microorganisms to carry out detoxification or energy generation for their cellular growth and metabolism. The oxidation of highly toxic arsenite to less toxic arsenate encoded by arsenite oxidase enzyme is a key step of detoxification mechanism by microorganisms (Qin et al. 2006; Andreoni et al. 2012; Rauschenbach et al. 2012).

In recent years various bacterial strains capable of arsenite oxidation by arsenite oxidase (*aioA*/*aoxB*) gene have been reported in the genomes of *Acinetobacter junii*, *Acinetobacter baumannii, Geobacillus stearothermophilus, Thiomonas* sp. 3As, *Herminiimonas arsenicoxydans* and *Pseudomonas stutzeri* strain GIST-BDan 2 (Muller et al. 2007; Arsene-Ploetze et al. 2010; Chang et al. 2010; Majumder et al. 2013). In case of *Acinetobacter calcoaceticus* and *Brevibacillus* sp. KUMAs2 the *aioA* gene was present only on plasmid DNA whereas in *Acinetobacter soli,* the *aoxB* gene was located on genomic as well as plasmid DNA (Mallick et al. 2014; Goswami et al. 2015). The *aoxAB/aioAB* genes encode an arsenite inducible periplasmic protein which catalyzes the oxidation of highly toxic arsenite to less toxic arsenate (Silver and Phung 2005; Branco et al. 2009). It consists of two subunits, a small iron-sulfur cluster containing subunit *aoxA/aioB* and a large molybdopterin containing catalytic subunit *aoxB/aioA* (Silver and Phung 2005; Oremland et al. 2009). The *aoxB/aioA* gene acts as a genetic marker for arsenite oxidation (Hamamura et al., 2008; Quemeneur et al. 2008). Two families of arsenite transporters (ArsB and Acr3p) are known in bacteria (Rosen 1999) and Acr3p is divided into two subsets, Acr3(1)p and Acr3(2)p (Achour et al. 2007). Although these transporters have similar sizes and functions, they differ in mechanisms, as well as have different metalloid specificity. ArsB confers resistance to arsenite and antimonite, however Acr3p is highly specific to arsenite (Rosen 1999).

Keeping in view the potential of arsenic toxicity in humans and other life forms it is imperative to remove arsenic present in the environment. The traditional methods to remove arsenic from contaminated environmental sites are expensive, time-consuming and hazardous (Mahimairaja et al. 2005). Therefore, bioremediation of arsenic holds a great potential since it is an eco-friendly method involving microorganisms.

In the present investigation, we characterized one potential arsenite oxidizing bacterial strain from shipyard waste of Goa, India with reference to presence of arsenite oxidase gene, enzyme activity, arsenite uptake, morphological changes, presence of arsenic deposits, protein expression induced by arsenite stress using PCR, SEM, TEM, EDS and SDS-PAGE analysis.

Materials and methods

Isolation of arsenite oxidizing bacteria

Environmental samples were collected from shipyard waste, from Bicholim, Goa, India, in sterile zip-lock bags. Appropriate dilutions of the soil samples were made in 0.85% saline and plated on mineral salt medium (MSM) agar (Mahtani and Mavinkurve 1979) supplemented with 10 mM of sodium (meta) arsenite along with 0.2% glucose as a carbon source. Plates were incubated at 28 °C for 24 h and morphologically distinct bacterial colonies were selected for further studies.

Determination of minimum inhibitory concentration (MIC) of arsenite

Bacterial isolates were spot inoculated on MSM agar plates amended with increasing concentrations of 0–46 mM sodium arsenite along with 0.2% glucose. The plates were checked for visible bacterial colonies after incubation at 28 °C for 24–48 h. The bacterial strains showing highest MIC values were selected for determining MIC in MSM broth. Selected bacterial strains were inoculated in MSM broth supplemented with different concentration of arsenite (0–25 mM) and flasks were incubated at 28 °C, 150 rpm for 24 h. Growth was monitored by recording the absorbance at 600 nm using Biospectrometer (Eppendorf, Germany). The lowest concentration of arsenite which completely inhibited bacterial growth was considered as its MIC value.

Growth behavior of the selected bacterial isolate in presence of sodium arsenite

The selected bacterial strain was inoculated in MSM broth amended with different concentrations of sodium arsenite viz. 5 mM, 10 mM, 15 mM, 20 mM and 21 mM, whereas flask without sodium arsenite was maintained throughout the experiment as control. The flasks were incubated at 28 °C, 150 rpm for 24–30 h and absorbance at 600 nm was recorded after every 2 h using Biospectrometer (Eppendorf, Germany).

Identification of arsenite oxidizing bacterial isolate

The identification of selected bacterial strain was performed by extracting its genomic DNA using Dneasy Blood and Tissue Kit (Qiagen, Hilden, Germany) followed by amplification of 16S rRNA gene using universal eubacterial primers: 27F and 1495R (Studholme et al. 1999). The PCR was carried out using Nexus Gradient Mastercycler (Eppendorf, Germany) and the resulting PCR product was analyzed on 1% agarose gel. The PCR product was purified using PCR clean-up kit (Promega, USA) and sequenced. The nucleotide sequence obtained was subjected to BLAST (tblastn) search analysis using National Center for Biotechnology Information (NCBI) database. The sequence was submitted to GenBank (accession number: MG430351) and its taxonomical relatedness to closely associated genera was determined using the neighbor-joining method with MEGA 7 package (Kumar et al. 2016).

Plasmid profile

The plasmid DNA of the selected bacterial strain was extracted using Gen Elute Plasmid Miniprep kit (Sigma-Aldrich, USA) and was analyzed using 0.8% agarose gel electrophoresis. After electrophoresis gel was visualized under G:BOX gel documentation system (Syngene, UK).

PCR amplification of arsenite oxidase (*aioA*) and transporter (ACR3) genes

The large molybdopterin containing catalytic subunit (aioA) and one of the arsenite transporter (ACR3) genes were PCR amplified with gene-specific primers (Supplementary Table S1) using chromosomal and plasmid DNA separately as templates. The thermal cycler program comprised of an initial denaturation of 5 min at 94 °C, followed by 30 cycles of denaturation at 94 °C for 1 min, annealing at 55 °C for 1 min, extension at 72 °C for 1 min and a final extension at 72 °C for 5 min. The PCR products were analyzed on 1% agarose gel and visualized under G: BOX gel documentation system (Syngene, UK).

Arsenite oxidase enzyme assay

Preparation of cell-free extract

The bacterial cells were grown in MSM broth in presence of 15 mM sodium arsenite. Late log phase cells were harvested by centrifugation at 8000 rpm at 4 °C for 10 min. The cell pellet was washed thrice with washing buffer (20 mM Tris–HCl, 0.1 mM phenylmethylsulfonyl fluoride (PMSF), 0.6 mM EDTA with pH 8.4 and 0.9% NaCl with pH 8.4) and the pellet was resuspended in 10 ml 20 mM Tris–HCl buffer (pH 8.0) containing 0.6 mM PMSF and 0.6 mM EDTA. The cell suspension was incubated with 1 mg ml^{-1} lysozyme at 28 °C for 2 h with occasional stirring. Magnesium sulfate (20 mM), magnesium acetate (100 mM), DNase (100 µg) and RNase (500 µg) (Bangalore GeNei) were added to the cell suspension and incubated at 28 °C for 30 min. The cell suspension was sonicated thrice with 2 min bursts

and 10 min cool-down intervals followed by incubation at 60 °C for 1 min in water bath. Subsequently, the suspension was cooled on ice, followed by centrifugation at 8000 rpm for 10 min and the pH of the clear supernatant was adjusted to 8.4 with 2 M NaOH (Prasad et al. 2009).

Preparation of periplasmic and spheroplast fractions

Bacterial cells grown in MSM broth were harvested by centrifugation at 8000 rpm for 10 min and cell pellets suspended in 20 mM Tris–HCl buffer, 0.1 mM PMSF, 10 mM EDTA pH 8.4 along with 20% sucrose. The outer membrane was lysed using lysozyme (0.5 mg ml^{-1}) at 28 °C for 40 min followed by centrifugation at 8000 rpm for 10 min. The supernatant was collected in a fresh centrifuge tube and cell pellet containing spheroplast was washed twice in buffer containing 20 mM Tris–HC1, 0.1 mM PMSF, 10 mM EDTA (pH 8.4), 20% sucrose and assayed for arsenite oxidase activity.

Enzyme assay

The arsenite oxidase enzyme activity was determined in cell free extract, periplasmic and spheroplast fractions following standard method (Anderson et al. 1992). The enzyme sample was mixed with 1 ml of assay buffer containing 60 µM 2,6-dichlorophenol-indophenol (DCIP), 200 µM sodium arsenite and 50 mM morpholino ethelene diol sulfonic acid (MES) buffer (pH 6.0). The change in absorbance due to reduction of DCIP per minute was monitored at 600 nm for 5 min using Biospectrometer (Eppendorf, Germany). The specific activity of the enzyme was expressed as µmol of DCIP reduced min^{-1} mg^{-1} of protein. Similarly, the effect of arsenite (0.5 and 1 mM) on periplasmic protein was also studied. The protein concentration in the supernatants was determined by Folin Lowry method (Lowry et al. 1951) using bovine serum albumin (Himedia, Mumbai, India) as standard.

Scanning electron microscopy coupled with energy dispersive X-ray spectroscopic (SEM-EDS) analysis

The bacterial isolate was grown in MSM broth supplemented with 15 mM sodium arsenite (test) and without sodium arsenite (control). The flasks were incubated at 28 °C, 150 rpm for 8–20 h and bacterial cells in exponential growth phase (8 and 20 h) were harvested from control and test samples by centrifugation at 8000 rpm, 4 °C for 10 min (Eppendorf, Germany). The pellet obtained was washed thrice with 0.1 M phosphate buffer saline (PBS) with pH 7.4. The washed bacterial cells were evenly spread on a clean grease-free cover slip and fixed overnight using 2.5% glutaraldehyde. After incubation, cells were washed with PBS and were subjected to ethanol gradient of 30%, 50%, 70%, 90% and 100% by incubating for 10 min at each concentration. The samples were analyzed by SEM–EDS (Carl-Ziess, Germany).

Transmission electron microscopy coupled with energy dispersive X-ray spectroscopic (TEM-EDS) analysis

The TEM analysis of the bacterial strain was carried out to evaluate intracellular morphological changes and metal uptake by the cells. Cells grown with 15 mM sodium arsenite were harvested in the exponential growth phase (8 and 20 h) by centrifugation at 8000 rpm for 10 min followed by washing with 0.1 M sodium phosphate buffer (pH 7.2). The pellets obtained were fixed in a mixture of 2.5% glutaraldehyde and 2% paraformaldehyde prepared in 0.1 M sodium phosphate buffer (pH 7.2) for 2–3 h at 4 °C. The fixed bacterial cells were further incubated for 1 h in 1% OsO_4 and propylene oxide followed by graded series of dehydration in ethanol. The samples were then embedded in Epon 812 resins and ultra-thin sectioning (60 nm) was performed. This was followed by examining the samples using transmission electron microscope (TEM-JEOL 2100F, Germany) which were further analyzed for elemental content by EDS. A control without arsenite exposure under similar conditions was also maintained.

Arsenic transformation assay

The arsenite oxidizing ability of bacterial strain was determined qualitatively by silver nitrate test with minor modifications (Lett et al. 2001). The bacterial cells were grown in MSM broth with 15 mM sodium arsenite (test) and without sodium arsenite (control) at 28 °C, 150 rpm for 24 h. One ml culture suspension

was mixed with one ml of 0.1 M $AgNO_3$ and observed for colour change from colourless to light brown.

Quantitative determination of oxidized arsenite (i.e. arsenate) was performed using molybdene blue method with some modifications (Lenoble et al. 2003; Cai et al. 2009). Cells were harvested at 8000 rpm for 10 min and resulting cell pellet was disrupted by sonication (three times for 2 min with 10 min cool-down intervals). The supernatant (0.3 ml) obtained after centrifugation was added to a mixture of 4 ml Milli Q water, 0.4 ml 50% H_2SO_4 (v/v), 0.4 ml of 3% Na_3MoO_4 (w/v) and 0.2 ml of 2% ascorbic acid (w/v). The tubes were incubated at 90 °C in water bath for 20 min. The samples were cooled and final volume was adjusted to 10 ml using Milli Q water. The same protocol was also followed for control sample and absorbance of the samples was measured at 838 nm using Biospectrometer (Eppendorf, Germany). The standard curve of arsenate was used to determine the concentration of arsenate in the test sample.

Fourier transformed infrared (FTIR) spectroscopy

The FTIR samples were prepared using bacterial cells grown with and without 15 mM sodium arsenite. The cell suspension was harvested at 8000 rpm for 10 min followed by washing with 0.1 M PBS (pH 7.4). The cell pellet was dried at 45 °C for 48 h. The dried pellet was subjected to fine grinding in presence of KBr. The IR spectrum was recorded on IR prestige-21 instrument (Shimadzu, Japan) in the region of 4000–400 cm^{-1}.

SDS-PAGE

The bacterial cells were grown with and without 5 mM sodium arsenite and protein profile of extracted protein was studied using standard protocol (Laemmli 1970). Whole cell proteins were extracted and analyzed on 15% sodium dodecyl sulfate-polyacrylamide gel (SDS-PAGE) at a constant voltage of 90 V using BIORAD Mini-PROTEAN Tetra System (BIO-RAD, USA). The gel was stained overnight using freshly prepared 0.05% (w/v) Coomassie Brilliant blue R250 and destained using destaining solution (Sambrook et al. 1989).

Statistical analysis

All the experiments were carried out in triplicates and their mean, as well as standard error were calculated and incorporated as ± in the manuscript.

Results

Isolation of arsenite resistant bacterial strain and determination of MIC of arsenite

Among ten morphologically different arsenite resistant bacterial isolates, strain SSSW7 showed the highest MIC of 46 mM and 21 mM on MSM agar and in MSM broth respectively. The growth pattern of the bacterial strain SSSW7 exposed to sodium arsenite interestingly revealed an extended lag phase at higher concentrations of arsenite. A prominent shift in lag phase with increasing concentrations of sodium arsenite (10, 15, 20 mM) was observed compared to control (Supplementary Fig. 1).

Identification of arsenite oxidizing bacterial isolate

Strain SSSW7 was Gram-negative, non-motile rod which showed oxidase negative and catalase positive reaction. Based on BLAST analysis of 16S rDNA sequence the bacterial strain SSSW7 has been identified as *Klebsiella pneumoniae* (Supplementary Fig. 2) and the sequence has been submitted to Genbank (accession number: MG430351).

Plasmid profile and PCR amplification of arsenite oxidase and arsenite transporter genes

Klebsiella pneumoniae strain SSSW7 possessed a plasmid of > 10 kb in size (Fig. 1a). PCR amplification of *aioA* gene using plasmid and chromosomal DNA as template clearly revealed the presence of arsenite oxidase gene with amplicon size of 1100 bps (Fig. 1b). There was no PCR amplification of ACR3 gene encoding arsenite transporter using genomic as well as plasmid DNA as a template.

Arsenite oxidase assay

Klebsiella pneumoniae strain SSSW7 exhibited highest specific arsenite oxidase activity in the periplasmic

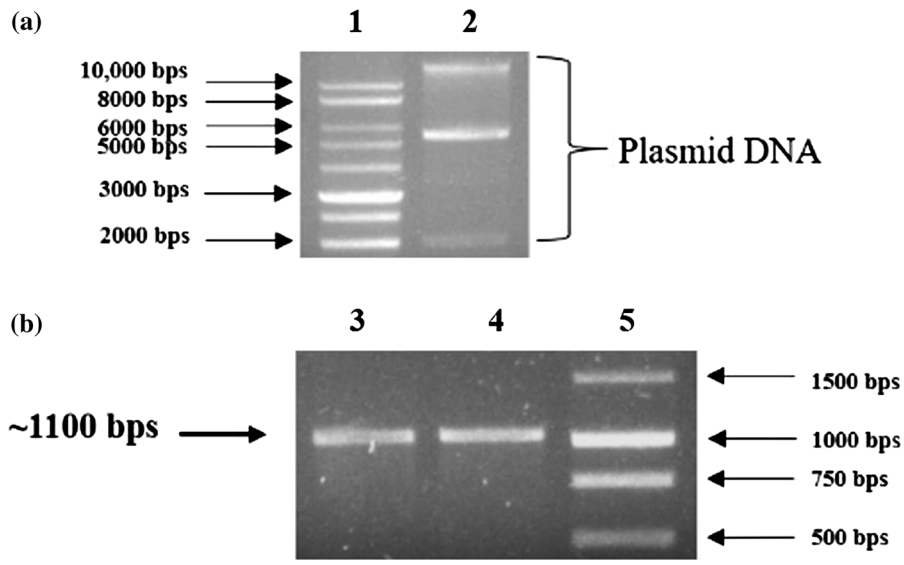

Fig. 1 Plasmid profile and PCR amplification of *aioA* gene of *Klebsiella pneumoniae* strain SSSW7. Lane 1a and 5b: 1 kb DNA markers. Lane 2a: Plasmid DNA of *K. pneumoniae* strain SSSW7. Lane 3b: PCR amplicon of *aioA* gene using chromosomal DNA as template. Lane 4b: PCR amplicon of *aioA* gene using plasmid DNA as template

fraction as the activity was recorded 1.328 µmol DCIP min^{-1} mg^{-1} protein, followed by cell free extract and spheroplast fraction with enzyme activity of 0.58 µmol DCIP min^{-1} mg^{-1} protein and 0.059 µmol DCIP min^{-1} mg^{-1} protein respectively. This clearly shows that arsenite oxidase enzyme is predominant in the periplasmic space. Interestingly, 12% and 47% increase in enzyme activity was observed in presence of 0.5 mM and 1 mM sodium arsenite indicating a high K_m.

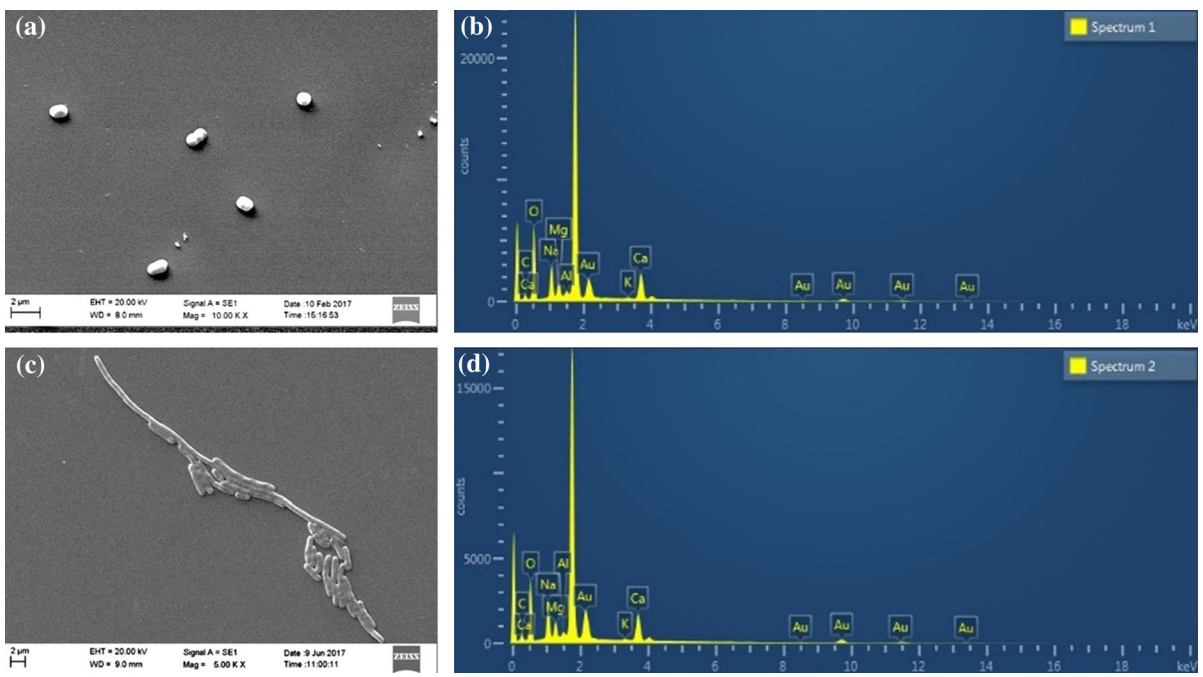

Fig. 2 SEM-EDS micrograph of *Klebsiella pneumoniae* strain SSSW7. **a** Bacterial cells in exponential growth phase (8 h) without exposure to arsenite showing rod shape morphology (control). **b** EDS micrograph of bacterial cells in exponential growth phase (8 h) without arsenite exposure (control). **c** Bacterial cells exposed to 15 mM arsenite in exponential growth phase (20 h) showing interconnected chains of cells. **d** EDS micrograph of bacterial cells in exponential growth phase (20 h) exposed to 15 mM arsenite

SEM-EDS analysis

The scanning electron micrograph of *K. pneumoniae* strain SSSW7 exposed to 15 mM arsenite demonstrated altered morphology from rods to interconnected chains of cells (Fig. 2a, c). The EDS spectrum of the cells exposed to 15 mM arsenite did not reveal any surface adsorption of arsenite (Fig. 2b, d).

TEM-EDS analysis

The intracellular structural analysis of *K. pneumoniae* strain SSSW7 by TEM clearly revealed that arsenite caused disruption of the plasma membrane, condensation of cytoplasm and presence of electron dense deposits throughout the periplasm (Fig. 3a, c). The presence of an arsenic peak in EDS spectrum of cells treated with 15 mM arsenite further confirmed intracellular accumulation of arsenic which was absent in control (Fig. 3b, d).

Arsenic transformation assay

The *K. pneumoniae* strain SSSW7 demonstrated arsenite oxidizing ability since a light brown coloured precipitate of silver-orthoarsenate was formed, indicating oxidation of arsenite to arsenate (Supplementary Fig. 3). Quantitative estimation of arsenate through molybdene blue method revealed that the bacterial strain SSSW7 internalized 10 mM of arsenate within 24 h.

Fourier transformed infrared (FTIR) spectroscopy

The FTIR spectrum analysis of 15 mM arsenite exposed bacterial cells of *K. pneumoniae* strain SSSW7 showed shifting as well as sharpening of many peaks which could be assigned to various functional groups responsible for arsenite accumulation (Fig. 4; Table 1). Arsenite exposed bacterial cells showed spectral changes in the region of

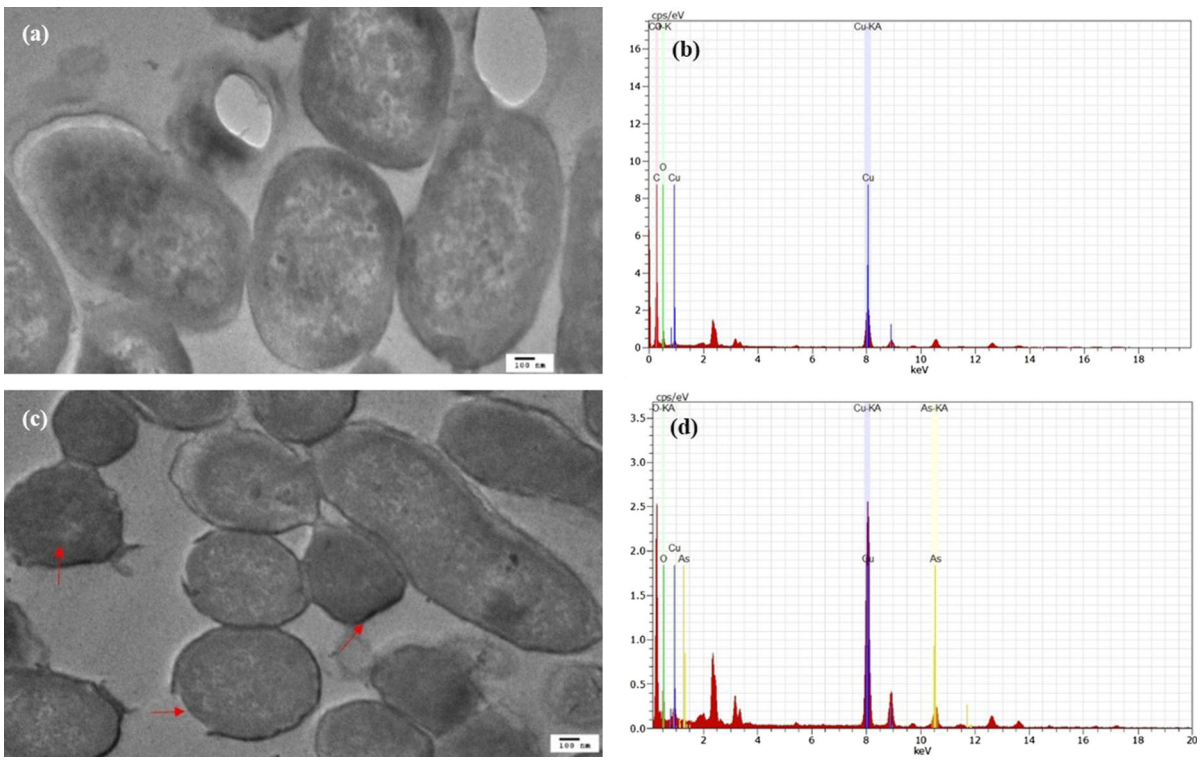

Fig. 3 TEM micrograph of *Klebsiella pneumoniae* strain SSSW7. **a** Bacterial cells in exponential growth phase (8 h) without arsenite exposure showing intact plasma membrane, clear cytoplasm and periplasm (control). **b** EDS micrograph of bacterial cells in exponential growth phase (8 h) without arsenite exposure (control). **c** Bacterial cells exposed to 15 mM sodium arsenite in exponential growth phase (20 h) showing disrupted plasma membrane, condensed cytoplasm and dark periplasm. **d** EDS micrograph of bacterial cells exposed to 15 mM arsenite in exponential growth phase (20 h)

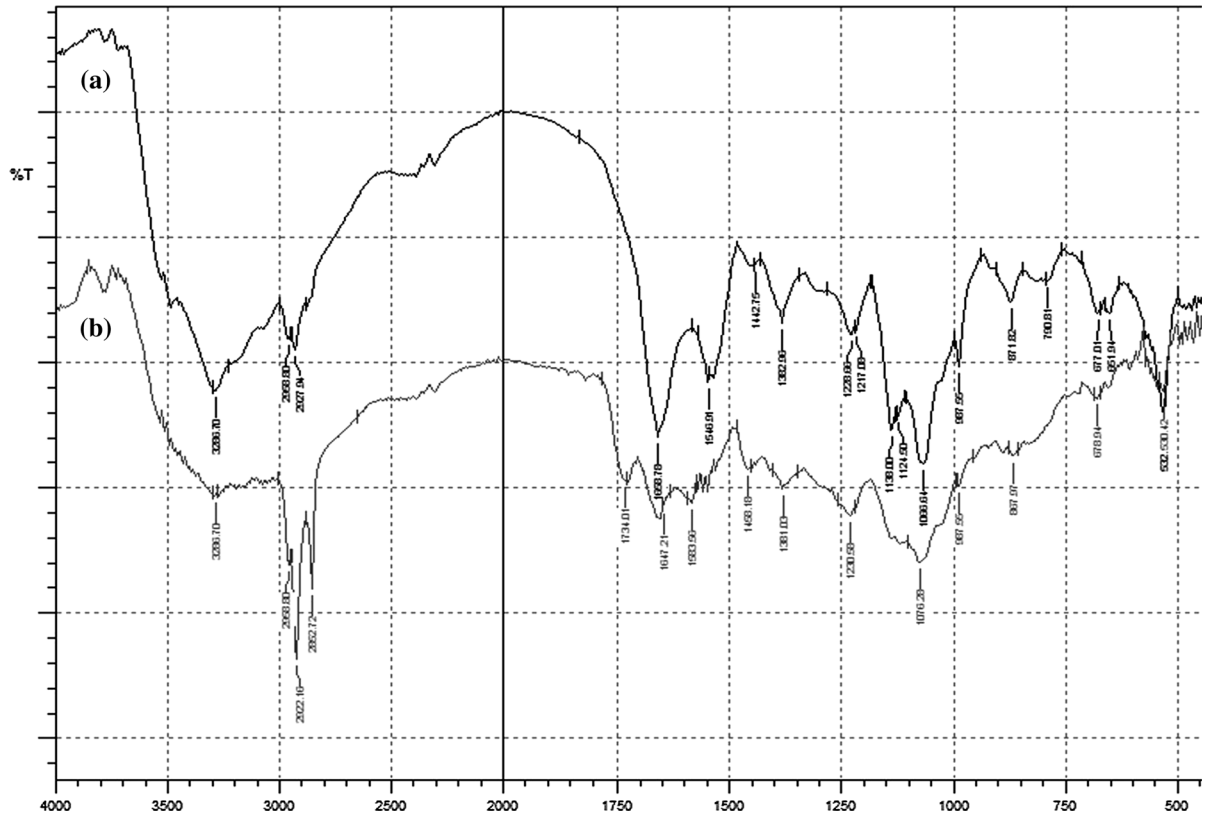

Fig. 4 FTIR spectrum of *Klebsiella pneumoniae* strain SSSW7. **a** Bacterial cells exposed to 15 mM arsenite. **b** Bacterial cells without exposure to arsenite (control)

3300–2800 cm^{-1} which may be attributed to stretching of amide and hydroxyl groups. Shifting of FTIR peaks was observed in the region spanning from 1750–1500 cm^{-1} and 1500–1200 cm^{-1} which showed the interaction of amide linkages from protein and peptides. The sharpening and peak shifts from 1200 to 1000 cm^{-1} was also observed in arsenite exposed cells which may be assigned to C–N stretching of an aliphatic amine and C–O stretching of alcohols, carboxylic acids, esters, and ethers.

SDS-PAGE

The SDS-PAGE analysis of whole-cell proteins of *K. pneumoniae* strain SSSW7 in presence of 5 mM arsenite clearly revealed up-regulation of several proteins as compared to control. Interestingly, two up-regulated proteins of molecular weight 87 kDa and 14 kDa were also observed (Supplementary Fig. 4) which may resemble the two subunits of arsenite oxidase enzyme aioA and aioB respectively.

Discussion

The arsenite resistant bacterial strain SSSW7 isolated from shipyard waste of Goa, India was identified as *K. pneumoniae*. It is interesting to note that *K. pneumoniae* strain SSSW7 exhibited the highest MIC of 21 mM in MSM broth as compared to previously reported bacterial strains. For instance, *K. pneumoniae* strains MNZ4 and MNZ6 tolerated up to 2.3 mM and 2.9 mM sodium arsenite in acetate minimal medium, whereas *K. pneumoniae* strain MR4 showed MIC of 5 mM in Luria–Bertani broth (Daware et al. 2012; Abbas et al. 2014). However, it would be inappropriate to compare the MIC values of present study with previous reports since the media composition alters availability of arsenite in the growth medium. Growth studies revealed extended lag and delayed log phases for this strain at increasing concentrations of arsenite in MSM broth. The slower growth of this bacterial strain exposed to arsenite may be attributed to ensuing

Table 1 Characteristic IR absorption peaks indicating functional groups on the surface of *K. pneumoniae* strain SSSW7

Control (frequency, cm^{-1})	Arsenite-exposed (frequency, cm^{-1})	Band assignment
3296.70	3296.70	N–H stretch of amides and O–H stretch of hydroxyl groups
2922.16	2927.94	C–H stretch of alkanes and O–H stretch of carboxyl acids
2852.72	–	C–H stretch of alkanes, O–H stretch of carboxyl acids
1734.01	1658.78	–C=C– stretch of alkenes
1647.21	1546.91	N–O asymmetric stretch of nitro compounds
1583.56	–	N–H bend of 1° amine
1458.10	1442.75	C–C stretch of aromatics
1381.03	1382.96	–C–H, bend of alkane
1230.58	1228.86	C–O stretch of alcohols, carboxylic acids, esters ethers
–	1138.00	C–N stretch of aliphatic amine and C–O stretch of alcohol carboxylic acids, esters, ethers
1076.28	1066.64	C–O stretch of alcohol carboxylic acids, esters, ethers
987.56	987.56	=C–H bend of alkenes
867.97	871.82	=C–H, bend of alkenes, C–H bend, aromatics
678.94	677.01	C–Br stretch of alkyl halide
651.94	651.94	C–Cl and C–Br stretch of alkyl halide
530.42	532.35	C–Br stretch of alkyl halide

physiological adaptation during extended lag phase leading to increase in doubling time (Paul et al. 2014).

PCR amplification using gene specific primers revealed that *K. pneumoniae* strain SSSW7 possessed *aioA* gene on both plasmid as well as chromosomal DNA. A similar study using *Acinetobacter soli* having *aioA* gene on both plasmid and chromosomal DNA has been reported (Goswami et al. 2015). Many arsenite transforming bacteria possessing arsenite oxidizing gene (*aoxB*) located only on chromosomal or plasmid DNA has been previously reported (Majumder et al. 2013; Mallick et al. 2014; Goswami et al. 2015). Interestingly, the absence of ACR3 gene from the plasmid and chromosomal genome of *K. pneumoniae* strain SSSW7 suggested an intracellular accumulation of arsenite since ACR3 protein has been reported to specifically transport arsenite in bacteria (Wysocki et al. 1997; Achour et al. 2007). Arsenite oxidase assay using different cell fractions further confirmed higher expression of arsenite oxidase enzyme in the periplasmic space. Similarly, arsenite oxidase enzyme is also reported in the periplasm of *Hydrogenophaga* sp strain NT-14, *Rhizobium* NT-26 and *Ochrobactrum triticii* SCII24 (Santini and Vanden Hoven 2004; Vanden Hoven and Santini 2004; Branco et al. 2009).

The exposure of bacterial cells to 15 mM arsenite demonstrated significant morphological alterations which were prominent as compared to control cells (Fig. 2a, c). This could be one of the strategies of bacterial cells to overcome arsenite toxicity since decrease in cell to volume ratio reduces toxicity. Similar morphological alterations have also been observed in arsenite exposed cells of *Acinetobacter lwoffii*, *Pseudomonas resinovorans* and *Acinetobacter calcoaceticus* (Banerjee et al. 2011). The EDS analysis revealed that there was no surface adsorption of arsenite and it may accumulate intracellularly. It was further substantiated by the absence of ACR3 gene which regulates transport of arsenite. Furthermore, TEM analysis of arsenite exposed cells evidently demonstrated structural changes which were similar to previous observations in *Microbacterium oleivorans* strain Ransu-1 and *Acinetobacter* sp. (Goswami et al. 2015). The TEM-EDS analysis of arsenite exposed cells also revealed intracellular accumulation of arsenic in the periplasm which is in agreement with the report of Banerjee et al. (2011). The bacterial strain SSSW7 could oxidize arsenite and showed intracellular accumulation of 10 mM arsenate which was higher than previous reports in bacterial strains (Jain et al. 2014; Naureen and Rehman 2016).

FTIR spectroscopic analysis further revealed interaction of functional groups such as carboxyl, hydroxyl and amino groups on bacterial cell surface with arsenite anions. Similar observations have also been reported in *E. coli* and *Bacillus aryabhattai* strain NBRI014 (Wu et al. 2010; Singh et al. 2016). SDS-PAGE analysis of whole cell proteins of strain SSSW7 exposed to 5 mM arsenite revealed over-expression of 87 kDa and 14 kDa proteins which may resemble with two subunits of arsenite oxidase enzyme. Therefore, it is clear that under stress of arsenite, over-expression of *aioA* gene facilitates transformation of arsenite to arsenate by bacterial cells in order to overcome the arsenite toxicity. This enzyme has been previously reported in *Rhizobium* NT-26 and *Hydrogenophaga* sp. strain NT-14 (Santini and Vanden Hoven 2004; Vanden Hoven and Santini 2004).

Conclusion

The *K. pneumoniae* strain SSSW7 isolated from shipyard waste demonstrated presence of arsenite oxidase gene and periplasmic arsenite oxidase enzyme. It showed high resistance to arsenite and could oxidize 10 mM arsenite to less toxic arsenate within 24 h which was found to be accumulated in the periplasmic space. Therefore, this bacterial strain SSSW7 has potential to bioremediate arsenite present in contaminated environmental sites.

Acknowledgements SM is grateful to University Grants Commission, New Delhi for financial support as Maulana Azad National Fellowship (SRF). The authors are thankful to Areef Sardar from CSIR- National Institute of Oceanography, Goa for EDX analysis; AIRF, Jawaharlal Nehru University, New Delhi for TEM–EDX analysis; B. R. Srinivasan, Head, Department of Chemistry and Rahul Kerkar from Department of Chemistry, Goa University for FTIR analysis. SM is also thankful to Sandeep Garg, Head, Department of Microbiology, Goa University for providing laboratory facilities.

Compliance with ethical standards

Conflict of interest The authors declare that there is no conflict of interest.

References

Abbas SZ, Riaz M, Ramzan N, Zahid MT, Shakoori FR, Rafatullah M (2014) Isolation and characterization of arsenic resistant bacteria from wastewater. Braz J Microbiol 45(4):1309–1315

Achour AR, Bauda P, Billard P (2007) Diversity of arsenite transporter genes from arsenic-resistant soil bacteria. Res Microbiol 158(2):128–137

Anawar HM, Akai J, Mostofa KMG, Safiullah S, Tareq SM (2002) Arsenic poisoning in groundwater: health risk and geochemical sources in Bangladesh. Environ Int 27(7):597–604

Anderson GL, Williams J, Hille R (1992) The purification and characterization of arsenite oxidase from *Alcaligenes faecalis*, a molybdenum-containing hydroxylase. J Biol Chem 267:23674–23682

Andreoni V, Zanchi R, Cavalca L, Corsini A, Romagnoli C (2012) Arsenite oxidation in *Ancylobacter dichloromethanicus* As3-1b strain: detection of genes involved in arsenite oxidation and CO_2 fixation. Curr Microbiol 65:212–218

Arsene-Ploetze F, Koechler S, Marchal M, Coppee JY, Chandler M, Bonnefoy V, Brochier-Armanet C, Barakat M, Barbe V, Battaglia-Brunet F, Bruneel O, Bryan CG, Cleiss-Arnold J, Cruveiller S, Erhardt M, Heinrich-Salmeron A et al (2010) Structure, function and evolution of the *Thiomonas* spp. genome. PLoS Genet 6(2):e1000859

Bahar MM, Megharaj M, Naidu R (2013) Kinetics of arsenite oxidation by *Variovorax* sp.MM-1 isolated from soil and identification of arsenite oxidase gene. J Hazard Mater 262:997–1003

Banerjee S, Datta S, Chattopadhyay D, Sarkar P (2011) Arsenic accumulating and transforming bacteria isolated from contaminated soil for potential use in bioremediation. J Environ Sci Health A 46:1736–1747

Branco R, Francisco R, Chung AP, Morais PV (2009) Identification of an *aox* system that requires cytochrome c in the highly arsenic resistant bacterium *Ochrobactrum tritici* SCII 24. Appl Environ Microbiol 75(5):5141–5147

Cai L, Rensing C, Li X, Wang G (2009) Novel gene clusters involved in arsenite oxidation and resistance in two arsenite oxidizers: *Achromobacter* sp. SY8 and *Pseudomonas* sp. TS44. Appl Microbiol Biotechnol 83:715–725

Chang J, Yoon I, Lee J, Kim K, An J, Kim K (2010) Arsenic detoxification potential of *aox* genes in arsenite oxidizing bacteria isolated from natural and constructed wetlands in the Republic of Korea. Environ Geochem Health 32:95–105

Chen M, Ma LQ, Harris WG (2002) Arsenic concentrations in Florida surface soils. Soil Sci Soc Am J 66(2):632–640

Cheng HF, Hu YN, Luo J, Xu B, Zhao JF (2009) Geochemical processes controlling fate and transport of arsenic in acid mine drainage (AMD) and natural systems. J Haz Mater 165:13–26

Chowdhury UK, Biswas BK, Chowdhury TR, Samanta G, Mandal BK, Basu GC, Chanda CR, Lodh D, Saha KC, Mukherjee SK, Roy S (2000) Groundwater arsenic contamination in Bangladesh and West Bengal, India. Environ health perspect 108(5):393–397

Daware V, Kesavan S, Patil R, Natu A, Kumar A, Kulkarni M, Gade W (2012) Effects of arsenite stress on growth and proteome of *Klebsiella pneumoniae*. J Biotechnol 158(1–2):8–16

Ghosh D, Bhadury P, Routh J (2014) Diversity of arsenite oxidizing bacterial communities in arsenic-rich deltaic aquifers in West Bengal, India. Front Microbiol 5:602

Goswami R, Mukherjee S, Rana VS, Saha DR, Raman R, Padhy PK, Mazumder S (2015) Isolation and characterization of arsenic-resistant bacteria from contaminated water-bodies in West Bengal, India. Geomicrobiol J 32:17–26

Hamamura N, Macur RE, Korf S, Ackerman G, Taylor WP, Kozubal M et al (2008) Linking microbial oxidation of arsenic with detection and phylogenetic analysis of As(III) oxidase genes in diverse geothermal environments. Environ Microbiol 11(2):421–431

Hughes MP (2002) Arsenic toxicity and potential mechanisms of action. Toxicol Lett 133:1–16

Jain R, Jha S, Adhikary H, Kumar P, Parekh V, Jha A, Mahanta MK, Kumar GN (2014) Isolation and molecular characterization of arsenite-tolerant *Alishewanella* sp. GIDC-5 originated from industrial effluents. Geomicrobiol J 31(1):82–90

Kumar S, Stecher G, Tamura K (2016) MEGA7: molecular evolutionary genetics analysis version 7.0 for bigger datasets. Mol Biol Evol 33:1870–1874

Laemmli UK (1970) Cleavage of structural proteins during the assembly of the head of bacteriophage T4. Nature 227:680–685

Lenoble V, Deluchat V, Serpaud B, Bollinger JC (2003) Arsenite oxidation and arsenate determination by the molybdene blue method. Talanta 61:267–276

Lett M, Paknikar K, Lievremont D (2001) A simple and rapid method for arsenite and arsenate speciation. Process Metall 11:541–546

Lowry OH, Rosebrough NJ, Farr AL, Randall RJ (1951) Protein measurement with the Folin phenol reagent. J Biol Chem 193(1):265–275

Mahimairaja S, Bolan NS, Adriano DC, Robinson B (2005) Arsenic contamination and its risk management in complex environmental settings. Adv Agron 86:1–82

Mahtani S, Mavinkurve S (1979) Microbial purification of longifolene: a sesquiterpene. J Ferment Technol 57:529–533

Majumder A, Bhattacharyya K, Bhattacharyya S, Kole SC (2013) Arsenic-tolerant, arsenite-oxidising bacterial strains in the contaminated soils of West Bengal, India. Sci Total Environ 463–464:1006–1014

Mallick I, Hossain SKT, Sinha S, Mukherjee SK (2014) *Brevibacillus* sp. KUMAs2 a bacterial isolate for possible bioremediation of arsenic in rhizosphere. Ecotoxicol Environ Saf 107:236–244

Mandal BK, Suzuki KT (2002) Arsenic round the world: a review. Talanta 58(1):201–235

Mitra AK, Bose BK, Kabir H, Das BK, Hussain M (2002) Arsenic-related health problems among hospital patients in southern Bangladesh. J Health Popul Nutr 20(3):198–204

Mukherjee A, Sengupta MK, Hossain MA, Ahamed S, Das B, Nayak B, Lodh D, Rahman MM, Chakraborti D (2006) Arsenic contamination in groundwater: a global perspective with emphasis on the Asian scenario. J Health Popul Nutr 24:142–163

Muller D, Medigue C, Koechler S, Barbe V, Barakat M, Talla E, Bonnefoy V, Krin E, Arsene-Ploetze F, Carapito C, Chandler M, Cournoyer Cruveiller S, Dossat C, Duval S, Heymann M, Leize E, Lieutaud A, Lievremont D et al (2007) A tale of two oxidation states: bacterial colonization of arsenic-rich environments. PLoS Genet 3(4):e53

Naureen A, Rehman A (2016) Arsenite oxidizing multiple metal resistant bacteria isolated from industrial effluent: their potential use in wastewater treatment. World J Microb Biotechnol 32(8):133

Oremland RS, Stolz JF (2005) Arsenic, microbes and contaminated aquifers. Trends Microbiol 13:45–49

Oremland RS, Saltikov CW, Wolfe-Simon F, Stolz JF (2009) Arsenic in the evolution of earth and extra-terrestrial ecosystems. Geomicrobiol J 26:522–536

Páez-Espino D, Tamames J, de Lorenzo V, Cánovas D (2009) Microbial responses to environmental arsenic. Biometals 22(1):117–130

Paul D, Poddar S, Sar P (2014) Characterization of arsenite-oxidizing bacteria isolated from arsenic-contaminated groundwater of West Bengal. J Environ Sci Health A 49(13):1481–1492

Prasad KS, Subramanian V, Paul J (2009) Purification and characterization of arsenite oxidase from *Arthrobacter* sp. Biometals 22:711–721

Qin J, Rosen BP, Zhang Y, Wang G, Franke S, Rensing C (2006) Arsenic detoxification and evolution of trimethylarsine gas by a microbial arsenite S-adenosyl methionine methyltransferase. Proc Natl Acad Sci USA 103(7):2075–2080

Quemeneur M, Sameron AH, Muller D, Lievremont D, Janzein M, Bertin PN, Garrido F, Joulian C (2008) Diversity surveys and evolutionary relationships of *aoxB* genes in aerobic arsenite oxidizing bacteria. Appl Environ Microbiol 74(14):4567–4573

Rai A, Tripathi P, Dwivedi S, Dubey S, Shri M, Kumar S, Tripathi PK, Dave R, Kumar A, Singh R, Adhikari B, Bag M, Tripathi RD, Trivedi PK, Chakrabarty D, Tuli R (2011) Arsenic tolerance in rice (Oryza sativa) have a predominant role in transcriptional regulation of a set of genes including sulphur assimilation pathway and antioxidant system. Chemosphere 82:986–995

Rauschenbach I, Bini E, Haggblom MM, Yee N (2012) Physiological response of *Desulfurispirillum indicum* S5 to arsenate and nitrate as terminal electron acceptors. FEMS Microbiol Ecol 81(1):156–162

Rosen BP (1999) Families of arsenic transporters. Trends Microbiol 7(5):207–212

Rosen BP (2002) Biochemistry of arsenic detoxification. FEBS Lett 529(1):86–92

Sambrook J, Fritsch EF, Maniatis T (1989) Molecular cloning: a laboratory manual. Cold Spring Harbor Laboratory Press, New York

Santini JM, Vanden Hoven RN (2004) Molybdenum-containing arsenite oxidase of the chemolithoautotrophic arsenite oxidizer NT-26. J Bacteriol 186(6):1614–1619

Silver S, Phung LT (1996) Bacterial heavy metal resistance: new surprises. Ann Rev Microbiol 50(1):753–789

Silver S, Phung LT (2005) Genes and enzymes involved in bacterial oxidation and reduction of inorganic arsenic. Appl Environ Microbiol 71:599–608

Singh N, Gupta S, Marwa N, Pandey V, Verma PC, Rathaur S, Singh N (2016) Arsenic mediated modifications in *Bacillus aryabhattai* and their biotechnological applications for arsenic bioremediation. Chemosphere 164:524–534

Smedley PL, Kinniburgh DG (2002) A review of the source, behaviour and distribution of arsenic in natural waters. Appl Geochem 17(5):517–568

Stolz JF, Basu P, Oremland RS (2010) Microbial arsenic metabolism: new twists on an old poison. Microbe 5:39–53

Studholme DJ, Jackson RA, Leak DJ (1999) Phylogenetic analysis of transformable strains of thermophilic *Bacillus* species. FEMS Microbiol Lett 172:85–90

Vanden Hoven RN, Santini JM (2004) Arsenite oxidation by the heterotroph *Hydrogenophaga* sp. str. NT-14: the arsenite oxidase and its physiological electron acceptor. Biochim Biophys Acta 1656(2–3):148–155

Welch AH, Westjohn DB, Helsel DR, Wanty RB (2000) Arsenic in ground water of the United States: occurrence and geochemistry. Groundwater 38(4):589–604

WHO (1993) Guidelines for drinking water quality. recommendations, 2nd edn. World Health Organization, Geneva

Wu YH, Feng SX, Li B, Mi XM (2010) The characteristics of *Escherichia coli* adsorption of arsenic (III) from aqueous solution. World J Microbiol Biotechnol 26(2):249–256

Wysocki R, Bobrowicz P, Ulaszewski S (1997) The *Saccharomyces cerevisiae ACR3* gene encodes a putative membrane protein involved in arsenite transport. J Biol Chem 272(48):30061–30066

Biometals
https://doi.org/10.1007/s10534-021-00316-x

Biological characterization of *Bacillus flexus strain* SSAI1 transforming highly toxic arsenite to less toxic arsenate mediated by periplasmic arsenite oxidase enzyme encoded by *aioAB* genes

Sajiya Yusuf Mujawar · Diviya Chandrakant Vaigankar · Santosh Kumar Dubey

Received: 13 February 2021 / Accepted: 29 April 2021

Abstract *Bacillus flexus* strain SSAI1 isolated from agro-industry waste, Tuem, Goa, India displayed high arsenite resistance as minimal inhibitory concentration was 25 mM in mineral salts medium. This bacterial strain exposed to 10 mM arsenite demonstrated rapid arsenite oxidation and internalization of 7 mM arsenate within 24 h. The Fourier transformed infrared (FTIR) spectroscopy of cells exposed to arsenite revealed important functional groups on the cell surface interacting with arsenite. Furthermore, scanning electron microscopy combined with electron dispersive X-ray spectroscopy (SEM-EDAX) of cells exposed to arsenite revealed clumping of cells with no surface adsorption of arsenite. Transmission electron microscopy coupled with electron dispersive X-ray spectroscopic (TEM-EDAX) analysis of arsenite exposed cells clearly demonstrated ultra-structural changes and intracellular accumulation of arsenic. Whole-genome sequence analysis of this bacterial strain interestingly revealed the presence of large number of metal(loid) resistance genes, including *aioAB* genes encoding arsenite oxidase responsible for the oxidation of highly toxic arsenite to less toxic arsenate. Enzyme assay further confirmed that arsenite oxidase is a periplasmic enzyme. The genome of strain SSAI1 also carried *glpF*, *aioS* and *aioE* genes conferring resistance to arsenite. Therefore, multi-metal(loid) resistant arsenite oxidizing *Bacillus flexus* strain SSAI1 has potential to bioremediate arsenite contaminated environmental sites and is the first report of its kind.

Keywords Arsenite · Arsenite oxidase · Bioremediation · Metal resistance · WGS

Introduction

Arsenic (As) is a toxic metalloid and ubiquitously present in the environment (Sodhi et al. 2019). Arsenic contamination of terrestrial and aquatic ecosystems has resulted from various natural and anthropogenic activities. Arsenicals are highly toxic due to their carcinogenic, mutagenic and genotoxic potential (Mandal and Suzuki 2002; Zhao et al. 2010). Arsenic toxicity causes severe diseases in humans viz. melanosis, hyperkeratosis, chronic respiratory disorder, miscarriages in women, cardiovascular diseases,

Supplementary Information The online version contains supplementary material available at https://doi.org/10.1007/s10534-021-00316-x.

S. Y. Mujawar · D. C. Vaigankar · S. K. Dubey (✉)
Laboratory of Bacterial Genetics and Environmental Biotechnology, Department of Microbiology, Goa University, Taleigao Plateau, Goa 403206, India
e-mail: santoshdubey.gu@gmail.com; santosh.dubey@bhu.ac.in

S. K. Dubey
Center of Advanced Study in Botany, Banaras Hindu University, Varanasi, Uttar Pradesh 221005, India

Published online: 06 May 2021

gastrointestinal disorders and cancer of bladder, lung, liver, skin and uterus (Rahman et al. 2009; Banerjee et al. 2011; Khairul et al. 2017; Palma-Lara et al. 2020). Conventional methods used for arsenic removal, including filtration, ion exchange and reverse osmosis are expensive, labour-intensive and also generate environmental pollutants (Rehman et al. 2010). Therefore, bioremediation of arsenic contaminated environmental sites employing bacteria is getting more attention due to it's efficient, affordable and eco-friendly advantages.

Bacterial strains possess several strategies to evade toxic arsenic mainly through arsenate reduction, arsenite oxidation and arsenic methylation (Satyapal et al. 2016; Jia et al. 2019; Mujawar et al. 2019). Arsenite is several-fold more toxic than arsenate and biotransformation of arsenite to arsenate is successfully achieved by microorganisms, including bacteria (Jebelli et al. 2018; Mujawar et al. 2019). Arsenite oxidizing bacteria oxidize arsenite to arsenate employing arsenite oxidase encoded by *aio* genes (Bahar et al. 2013; Majumder et al. 2013; Koechler et al. 2015) while arsenate reducing bacteria reduce arsenate to arsenite through pathway encoded by *ars* genes (Guo et al. 2015; Saunders and Rocap 2016; Bermanec et al. 2020). Whereas arsenic methylation involves the reduction of arsenate followed by addition of methyl group generating intermediates viz. monomethyl arsenite, dimethyl arsenate, dimethyl arsenite and trimethyl arsine (Kruger et al. 2013; Thomas and Rosen 2013). The primary role of these processes is to reduce arsenic toxicity to bacterial cells. The oxidation of arsenite by bacterial strains to arsenate is an essential step of detoxification in microorganisms.

Arsenite oxidation has been studied in several bacteria including *Acinetobacter calcoaceticus*, *Acinetobacter soli* (Goswami et al. 2015), *Alcaligenes faecalis* SRR-11 (Chang 2015), *Bacillus* sp., *Aneurinibacillus aneurinilyticus* (Dey et al. 2016), *Bacillus flexus* strain As-12 (Jebeli et al. 2017), *Pseudomonas chengduensis* (Jebelli et al. 2018), *Klebsiella pneumoniae* strain SSSW7 (Mujawar et al. 2019), *Bacillus cereus*, *Lysinibacillus boronitolerans* (Aguilar et al. 2020) and *Bacillus firmus* L-148 (Bagade et al. 2020).

Arsenite oxidation mainly depends on *aio* genes belonging to *aioSRABcytC* operon conferring resistance to arsenite (Kashyap et al. 2006; Muller et al. 2007). It consists of sensor kinase gene *aioS*, regulator gene *aioR*, arsenite oxidase enzyme encoded by *aioAB* gene, c-type cytochrome gene cytC2/*aioC* and molybdopterin biosynthesis gene, chlE/*aioD* (Santini and vanden Hoven 2004; Kashyap et al. 2006; Koechler et al. 2010). The presence of *aioRSABC* operon has been reported in *Rhizobium* sp. strain NT-26 and *Achromobacter* sp. SY8 (Santini and vanden Hoven 2004; Cai et al. 2009a, b). Previously the presence and involvement of *aioR*, *aioS* and *RpoN* sigma factor in arsenite oxidation has been reported in *Agrobacterium tumefaciens* 5A and *Herminiimonas arsenicoxydans* (Koechler et al. 2010; Sardiwal et al. 2010; Kang et al. 2012).

In the present communication, we have identified and biologically characterized arsenite oxidizing bacterial strain from the waste of agro-industry in Tuem, Goa, India which displayed high arsenite resistance, fast arsenite oxidation, peculiar morphological and cytoplasmic alterations along with the presence of genes conferring arsenite oxidation and resistance to multiple metal(loids) in it's genome.

Materials and methods

Isolation of arsenite resistant bacteria

Soil samples were collected in sterile zip-lock bags from agro-industry waste, Tuem, Goa, India. Soil samples were serially diluted in 0.85% saline and plated on mineral salt medium (MSM) agar amended with 10 mM of sodium (meta) arsenite and glucose (0.2%) as a carbon source (Mahtani and Mavinkurve 1979). The agar plates were incubated at 28 °C for 24 h, and morphologically distinct arsenite resistant bacterial colonies were selected for further characterization.

Determination of minimum inhibitory concentration (MIC) of arsenite

Bacterial isolates obtained were spot inoculated on MSM agar plates with increasing arsenite (0–41 mM) concentrations. These plates were incubated at 28 °C for 24 h and checked for visible colonies. Bacterial isolates showing higher MIC value on MSM agar were selected for determining their MIC in liquid medium. To determine MIC in liquid medium selected bacterial isolates were inoculated in MSM broth with increasing arsenite concentrations (0–25 mM), and the flasks

were incubated at 28 °C, 150 rpm for 24 h. Growth was monitored by taking absorbance at 600 nm using Biospectrometer (Eppendorf, Germany). The lowest concentration of arsenite which inhibited growth was considered as MIC.

Identification of arsenite resistant bacterial strain

The selected arsenite resistant bacterial strain SSAI1 was characterized morphologically and biochemically, followed by molecular identification. Genomic DNA of bacterial strain was extracted using Dneasy Blood and Tissue Kit (Qiagen, Hilden, Germany). The amplification of 16S rRNA gene was performed using Nexus Gradient Mastercycler (Eppendorf, Germany) with universal eubacterial primers 27F and 1495R (Studholme et al. 1999). Subsequently, the PCR product was analyzed on 1% agarose gel, purified and sequenced at Eurofins Genomics (Bangalore, India). The identification of the bacterial isolate was performed with BLASTn program, and the sequence obtained was submitted to GenBank. The phylogenetic tree of 16S rRNA gene was constructed by the neighbour-joining method in the MEGA 7 program (Kumar et al. 2016).

Growth behaviour of selected bacterial isolate in the presence of arsenite

The bacterial strain SSAI1 was inoculated in MSM broth amended with different arsenite (0–25 mM) concentration and incubated at 28 °C, 150 rpm for 38 h. Growth of the isolate was determined by recording absorbance at 600 nm at 2 h intervals using Biospectrometer (Eppendorf, Germany). The experiment was carried out in triplicates and the standard deviation was determined.

Fourier transformed infrared (FTIR) spectroscopy

The bacterial strain SSAI1 was inoculated in MSM broth with 10 mM and without arsenite and the flasks were incubated at 28 °C, 150 rpm for 24 h. The cell pellet was obtained by centrifugation at 8000 rpm for 10 min, washed with 0.1 M phosphate-buffered saline (PBS, pH 7.4) and dried in an incubator at 45 °C for 48 h. The dried pellet was ground in the presence of KBr to a fine powder and IR spectrum was recorded in the region of 4000–400 cm^{-1}on IR prestige-21 instrument (Shimadzu, Japan).

SEM-EDAX analysis

Bacterial isolate SSAI1 was grown in MSM broth supplemented with 0.2% glucose along with 10 mM arsenite as a test and without sodium arsenite as control at 28 °C, 150 rpm for 24–48 h. The bacterial cells in exponential phase were harvested by centrifugation at 8000 rpm for 10 min (Eppendorf, Germany) followed by washing with 0.1 M PBS (pH 7.4). Bacterial cells were spread on coverslips, fixed overnight in 2.5% glutaraldehyde and then subjected to drying in acetone series (20–100%). The samples were finally then analyzed by SEM-EDAX (Carl-Ziess, Germany).

TEM-EDAX analysis

Cells grown in the presence (10 mM) and absence of sodium arsenite were harvested in the exponential growth phase by centrifugation at 8000 rpm for 10 min. The pellet obtained was then washed in sodium phosphate buffer (0.1 M, pH 7.2) and fixed in a mixture of glutaraldehyde (2.5%) and paraformaldehyde (2%) prepared in sodium phosphate buffer (0.1 M, pH 7.2) at 4 °C for 2–3 h. The cells were further incubated for 1 h in OsO_4 and propylene oxide (1%) followed by dehydration in graded ethanol series. The samples were embedded in Epon 812 resins, sectioned and analyzed using TEM-EDAX (TEM-JEOL 2100F, Germany).

Arsenite transformation and bioaccumulation

The bacterial strain SSAI1 was grown in MSM broth supplemented with 10 mM sodium arsenite and the flask was incubated at 28 °C, 150 rpm for 24 h. The ability of strain SSAI1 to transform arsenite to arsenate in the culture medium was evaluated using silver nitrate test (Lett et al. 2001). Briefly, culture suspension (1 mL) was mixed with 0.1 M $AgNO_3$ (1 mL) solution and observed for colour change. The quantification of arsenate in the cell was performed using the molybdene blue method as described by Mujawar et al. (2019).

Whole Genome sequencing of strain SSAI1

Genomic DNA from strain SSAI1 was extracted using Dneasy Blood and Tissue Kit (Qiagen, Hilden, Germany) from overnight grown culture. The whole-genome shotgun sequencing was performed through the NextSeq 500 platform at Eurofins Genomics (Bangalore, India). The functional annotation of genes was carried out using Gene Ontology (GO) and Kyoto Encyclopedia of Genes and Genomes (KEGG) databases. The genes associated with metal resistance were identified based on sequence similarity to know metal/metalloid resistance genes in BacMet database.

Preparation of periplasmic and spheroplast fractions

The SSAI1 cells were grown in MSM broth and harvested by centrifugation at 8000 rpm for 10 min. The cell pellet obtained was suspended in suspension buffer containing 20 mM Tris–HCl, 0.1 mM PMSF and 10 mM EDTA (pH 8.4) along with sucrose (20%). The cells were subsequently incubated with 0.5 mg/mL lysozyme at 28 °C for 40 min and centrifuged at 8000 rpm for 10 min. The supernatant constituting periplasm was collected in a fresh centrifuge tube, and the cell pellet containing spheroplast was retrieved, washed twice in the above buffer and finally resuspended in Tris-HC1 buffer. The arsenite oxidase enzyme activity in periplasmic and spheroplast fractions was determined following the method of Anderson et al. (1992). The protein concentration in all the fractions was estimated through Folin Lowry method (Lowry et al. 1951) with bovine serum albumin (Himedia, Mumbai, India) as standard and the specific enzyme activity was defined as µmol DCIP reduced/min′mg protein.

Cross tolerance to other heavy metals and metalloids

The isolate was examined for cross-tolerance to various other heavy metals/metalloids such as Zn, Cr, Pb, Ni, Cu, Fe, Mn, As(V) and Cd. It was grown in MSM broth containing arsenite (5 mM), glucose (0.2%) and varying concentration of different heavy metals/metalloid. The flasks were incubated at 28 °C, 150 rpm for 24 h and growth was checked by measuring optical density at 600 nm using Biospectrometer (Eppendorf, Germany). The lowest metal/metalloid concentration that completely inhibited bacterial growth was considered as the MIC for that metal/metalloid.

Results and discussion

Screening and identification of arsenite resistant bacteria

The soil samples of the sampling site exhibited 27 °C temperature and pH was 7.6. Overall, ten morphologically different arsenite resistant bacterial strains were isolated from agro-industry waste, Tuem, Goa, India. Among all the arsenite resistant bacterial isolates, strain SSAI1 showed the highest MIC of 41 mM arsenite on solid medium and 25 mM arsenite in liquid medium, which lead to it's further characterization. This strain was Gram-positive, with rod-shaped motile cells and demonstrated positive reaction for catalase, oxidase, gelatinase and nitrate reductase. Based on 16S rRNA gene sequence analysis, the strain SSAI1 was identified as *Bacillus flexus* (Fig. 1) and the sequence has been submitted to GenBank (accession number: MH031690). The bacterial strain SSAI1 exhibited high MIC compared to previously isolated arsenite resistant bacterial isolates. For instance, bacterial strain *Alishewanella* sp. GIDC-5 isolated from an effluent treatment plant exhibited MIC of 18 mM, whereas, *Brevibacillus* sp. KUMAs2 isolated from arsenic contaminated soil was reported to tolerate 17 mM arsenite (Jain et al. 2014; Mallick et al. 2014). A recent study on *Bacillus flexus* strain As-12 has reported to tolerate 5 mM arsenite in liquid medium (Jebeli et al. 2017) which is much lower than MIC for strain SSAI1 in the present study. Therefore, the strain SSAI1 with MIC of 25 mM for arsenite is a potential candidate for bioremediation of arsenite contaminated environmental sites.

Growth behaviour of selected bacterial isolate in the presence of arsenite

The *Bacillus flexus* strain SSAI1 showed sigmoidal growth and different concentrations of arsenite significantly influenced its growth which was evident from extended lag phase with increasing arsenite in MSM broth (Fig. 2). A shift in the initiation of log

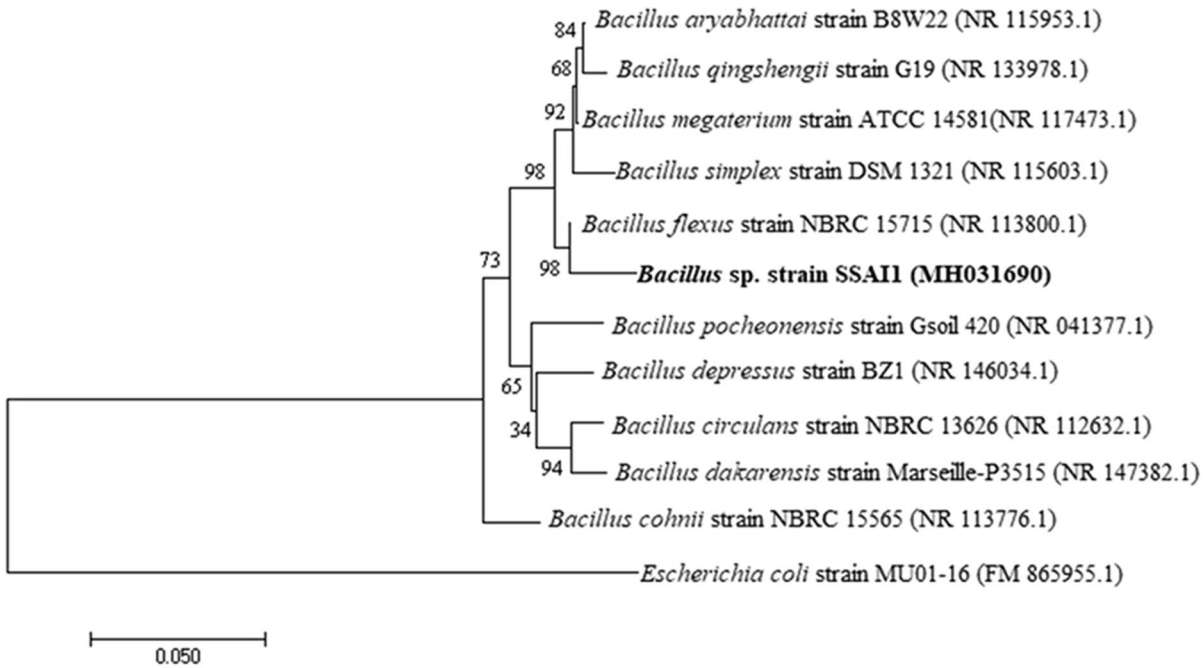

Fig. 1 Phylogenetic tree of 16S rRNA gene sequence of *Bacillus flexus* strain SSAI1 with other strains of *Bacillus* constructed using the neighbour-joining method. (The bootstrap values are based on 1000 replicates)

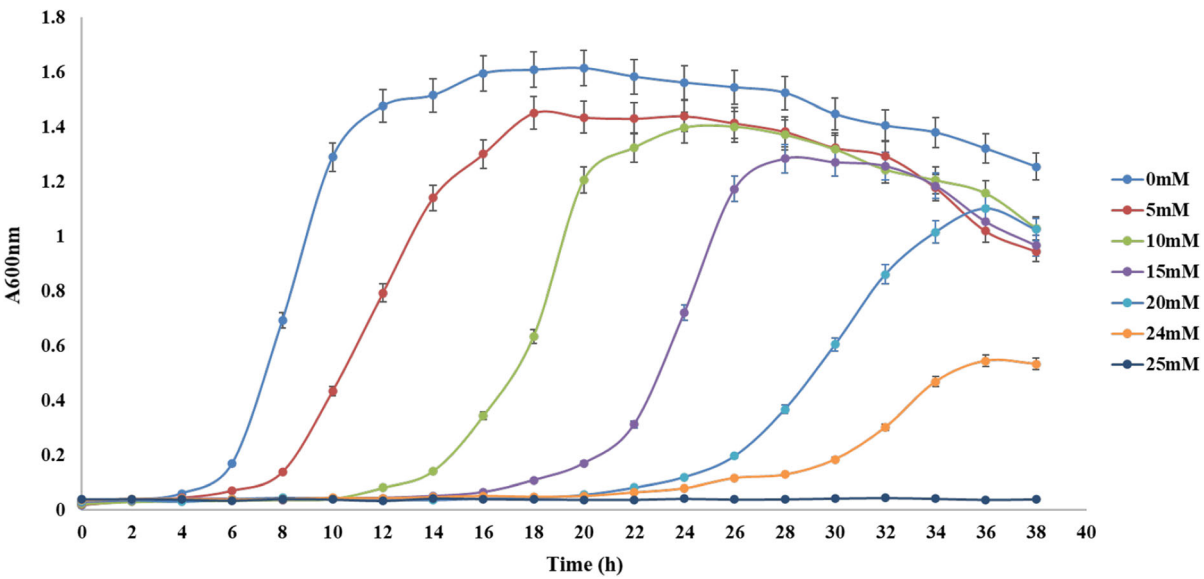

Fig. 2 Growth behaviour of *Bacillus flexus* strain SSAI1 grown in the presence and absence of arsenite

phase was observed from 4 to 6, 12, 16, 20 and 24 h respectively when cells were exposed to 5 mM, 10 mM, 15 mM, 20 mM and 24 mM arsenite respectively.

Fourier transformed infrared (FTIR) spectroscopic analysis

IR spectra analysis of *Bacillus flexus* strain SSAI1 exposed to arsenite indicated shifting and sharpening

of various peaks as compared to control (Fig. 3). These peaks could be assigned to various functional groups present in the biomolecules of bacterial cells involved in arsenite resistance and bioaccumulation (Table 1). A clear peak shift from 3278.99 to 3280.92 cm^{-1} attributed to stretching of carboxylic acids was observed in arsenite treated cells of strain SSAI1. Shifting of peaks was also seen in the regions 1700–1500 cm^{-1} and 1500–1200 cm^{-1} ascribed to proteins, peptides and fatty acids present in bacterial cell wall indicating their interaction with arsenite (Naumann et al. 1991; Oust et al. 2004). Sharpening and peak changes were observed in 1200–900 cm^{-1} region of arsenite exposed cells which can be assigned to stretching of aliphatic amine and alkenes. Spectrum changes obtained in this region are attributed to polysaccharides present within the cell wall indicative of involvement in arsenite interaction (Naumann et al. 1991; Oust et al. 2004). Peak shifts observed from 867.97 to 891.11 cm^{-1} and 530.42 to 534.28 cm^{-1} were assigned to bending of aromatics and stretching of alkyl halides respectively. Therefore, this study clearly revealed arsenite interaction with various functional groups present on the cell wall of arsenite resistant bacterial strain, which provides various metal-binding sites leading to its bioaccumulation (Bueno et al. 2008; Pandi et al. 2009). In *Escherichia coli* involvement of several functional groups viz. alkane, amino, amide and amine in arsenite binding have already been demonstrated (Wu et al. 2010). Similarly, studies on *Bacillus aryabhattai* strain NBRI014 and *Klebsiella pneumoniae* strain SSSW7 have demonstrated the interaction of amino, carboxyl and hydroxyl groups with arsenic (Singh et al. 2016; Mujawar et al. 2019).

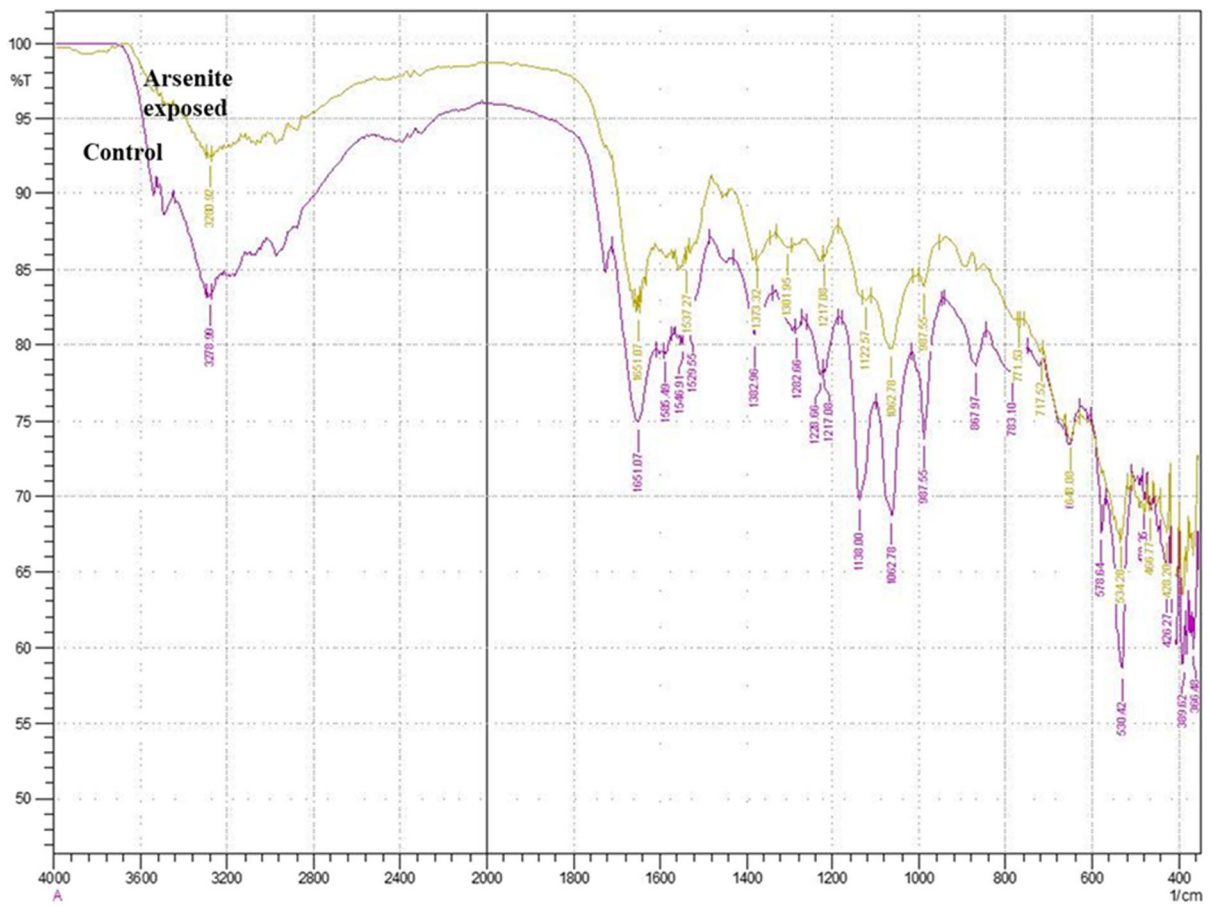

Fig. 3 FTIR spectrum of *Bacillus flexus* strain SSAI1. Purple-Bacterial cells in the absence of arsenite (control), Golden- Bacterial cells exposed to 10 mM arsenite

Table 1 IR peak changes/shifts in *Bacillus flexus* strain SSAI1 exhibiting different functional groups on the surface of bacterial cells

Control cells (cm^{-1})	10 mM arsenite treated cells (cm^{-1})	Functional groups
3278.99	3280.92	O–H stretch of carboxylic acids
1651.07	1651.07	–C=C– stretch of alkenes
1529.55	1537.27	N–O asymmetric stretch of nitro compounds
1382.96	1373.32	–C–H, bend of alkane
1282.66	1301.96	C–N stretch of aromatic amines, C–O stretch of alcohols, carboxylic acids, esters, ethers
1217.08	1217.08	C–N stretch of aliphatic amines
1138	1122.57	C–N stretch of aliphatic amines
1062.78	1062.78	C–N stretch of aliphatic amines
987.55	987.55	=C–H bend of alkenes
867.97	891.11	C–H bend of aromatics
530.42	534.28	C–Br stretch of alkyl halides

SEM-EDAX analysis

SEM analysis of the arsenite exposed cells of *Bacillus flexus* strain SSAI1 displayed unique morphological changes where cells fused forming aggregates (Fig. 4a, c). This may be the possible mechanism of bacterial cells to overcome arsenite toxicity. It has also been reported earlier that *Pseudomonas aeruginosa* RJB-1, *Bacillus circulans* RJB-4 and *Vogesella indigofera RJB*-C demonstrated reduction in their cell size when exposed to arsenite as a resistance strategy to overcome arsenite stress (Banerjee et al. 2011). Similarly, *Acinetobacter* sp., *Pseudomonas resinovorans*, *Lysinibacillus* sp. B2A1 and *Klebsiella pneumoniae* strain SSSW7 formed long interconnected chains of cells in the presence of arsenite (Banerjee et al. 2011; Mujawar et al. 2019; Rathod et al. 2019). Interestingly, EDAX analysis did not reveal any arsenic adsorption peak, confirming no arsenite adsorption at the cell surface and indicating the possibility of it's intracellular accumulation (Fig. 4b, d).

TEM-EDAX analysis

The TEM analysis of the strain SSAI1 exposed to 10 mM arsenite clearly revealed that arsenite adversely affected the plasma membrane's integrity and caused condensation of cytoplasm (Fig. 5a, c). Furthermore, electron-dense deposits throughout the cytoplasm were observed in strain SSAI1 demonstrating intracellular accumulation of arsenic while no such electron-dense regions were observed in untreated control cells (Fig. 5a, c). The presence of specific arsenic peak in the EDAX spectrum of treated cells also confirmed the intracellular accumulation of arsenic (Fig. 5b, d). These results have strengthened our previous findings based on SEM-EDAX analysis. Similar findings have also been reported in *Kocuria flava* strain AB402, *Bacillus vietnamensis* AB403, *Acinetobacter lwoffii* strain RJB-2 and *Klebsiella pneumoniae* strain SSSW7on exposure to arsenite (Banerjee et al. 2011; Mallick et al. 2018; Mujawar et al. 2019).

Arsenite transformation and bioaccumulation

The silver nitrate test confirmed the ability of strain SSAI1 to oxidize arsenite to arsenate as there was formation of light brown silver ortho-arsenate when cells reacted with silver nitrate. The rate of arsenite oxidation of strain SSAI1 as determined by molybdene blue method was pretty fast as it oxidized arsenite to arsenate and internalized 7 mM arsenate within 24 h. The strain SSAI1 was found to be much more efficient in the oxidation of arsenite to arsenate than previously reported strains such as *Stenotrophomonas panacihumi* (500 µM within 12 h), *Variovorax* sp. MM-1 (500 µM within 3 h), *Pseudomonas stutzeri* (1 mM within 25-30 h), *Alcaligenes faecalis* SRR-11 (1 mM

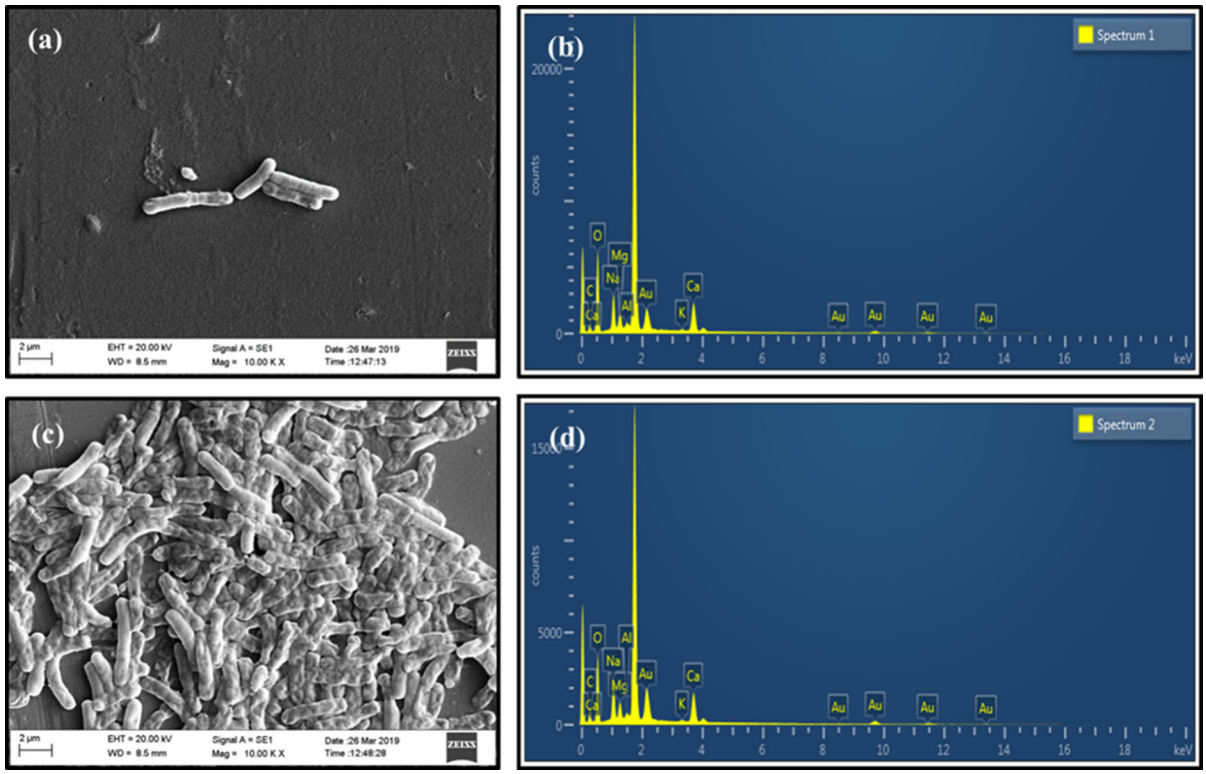

Fig. 4 Scanning electron micrograph showing the effect of arsenite on the morphology of *Bacillus flexus* strain SSAI1 **a** Bacterial cells in the absence of arsenite (magnification: 10,000X), **b** EDAX spectrum of bacterial cells without arsenite, **c** Bacterial cells exposed to 10 mM arsenite (magnification: 10,000X) and **d** EDAX spectrum of bacterial cells exposed to 10 mM arsenite

within 35–40 h), *Achromobacter xylosoxidans* TSL-66 (1 mM within 35-40 h), *Bacillus flexus* strain As-12 (45% after 48 h) and *Pseudomonas chengduensis* As-11 (48% after 72 h) which makes it a more economical candidate for future application of detoxification of arsenite (Chang et al. 2010; Bahar et al. 2012, 2013; Majumder et al. 2013; Chang 2015; Jebeli et al. 2017; Jebelli et al. 2018).

Draft genome of *Bacillus flexus* strain SSAI1

The Whole-genome sequence (WGS) analysis of arsenite oxidizing *Bacillus flexus* strain SSAI1 showed total genome of 4,1,31,040 bps comprising of a single circular chromosome of 4,046,812 bps and 2 plasmids with total genome size of 84,228 bps. Annotation using Prokka version 1.12 identified 4,358 genes with 4269 within the chromosome and 89 genes in the plasmids. Additionally, 108 tRNA and 7 rRNA genes were identified on the chromosome of this strain SSAI1. No rRNA and tRNA encoding genes were found on the plasmids. Gene ontology annotations of the genes on the genome across the categories (biological processes, molecular functions and cellular components) were carried out through WEGO portal and Blast2GO platform (Figs. S1 and S2). Total 1,591 and 9 genes were annotated into 22 and 6 functional pathways categories for chromosomal genome and plasmids, respectively using the KEGG pathway database via KAAS (Table S1).

Identification of arsenite oxidase genes and localization of arsenite oxidase enzyme

It is well known that several genes within the *aio* operons present on the genome of microorganisms confer arsenite resistance (Kashyap et al. 2006; Muller et al. 2007). In order to reveal genes responsible for arsenite resistance, whole-genome sequencing and gene annotations were performed. Interestingly *aioAB*

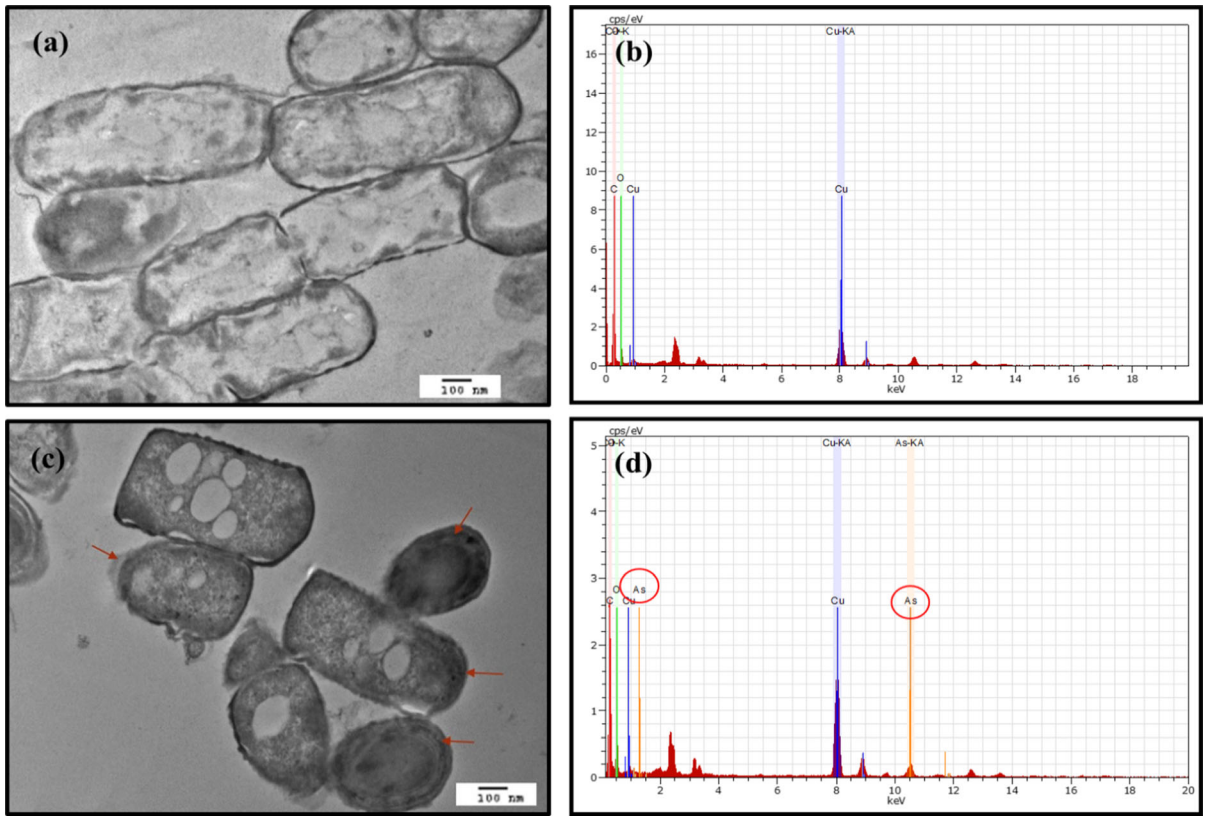

Fig. 5 Transmission electron micrograph of *Bacillus flexus* strain SSAI1. **a** Bacterial cells in the absence of arsenite (magnification: 6000X), **b** EDAX spectrum of bacterial cells without arsenite, **c** Bacterial cells exposed to 10 mM arsenite (magnification: 6000X) and **d** EDAX spectrum of bacterial cells exposed to 10 mM arsenite

genes encoding arsenite oxidase enzyme responsible for the oxidation of highly toxic arsenite to less toxic arsenate was identified from the draft genome of *Bacillus flexus* strain SSAI1. Previously studies on *Acinetobacter* spp., *Geobacillus stearothermophilus*, *Herminiimonas arsenicoxydans*, *Pseudomonas stutzeri*, *Polaromonas* sp. GM1, *P. xanthomarina* S11 and *Thiomonas* sp.3As have showed *aioA* gene-mediated arsenite oxidation (Muller et al. 2007; Arsène-Ploetze et al. 2010; Chang et al. 2010; Majumder et al. 2013; Koechler et al. 2015). Additionally, the strain also showed the presence of *glpF*, *aioS* and *aioE* genes encoding glycerol uptake protein, sensor kinase and oxidoreductase, respectively. Due to structural similarity of glycerol, *glpF* have been reported to transport arsenite and has been identified in many strains such as *Leishmania major*, *E. coli* and *Pseudomonas putida* (Gourbal et al. 2004; Meng et al. 2004; Páez-Espino et al. 2009). Moreover, the presence of *aioR* and *aioS* genes associated with regulation of arsenite oxidation have been characterized in various bacterial strains viz. *Achromobacter* sp. SY8, *Agrobacterium tumefaciens* 5A and *Herminiimonas arsenicoxydans* (Cai et al. 2009a, b; Koechler et al. 2010; Sardiwal et al. 2010; Kang et al. 2012). The presence of *aioE* gene was reported in *Agrobacterium tumefaciens* GW4 and found to be induced by arsenite (Wang et al. 2017). Therefore, the prevalence of *aio* genes in the genome of strain SSAI1 further confirmed the potential of strain SSAI1 to transform arsenite to less toxic arsenate. However, all these genes were located on the chromosome and not on plasmids indicated that chromosomal DNA solely governed arsenite resistance. It is interesting to note that the *aioAB* gene which plays a vital role in arsenite detoxification along with other genes viz. *glpF*, *aioS* and *aioE* involved in arsenite resistance in *Bacillus flexus* strain SSAI1 are being reported for the first time.

The periplasmic fraction of cells showed the highest enzyme activity of 2.168 µmol DCIP/min/

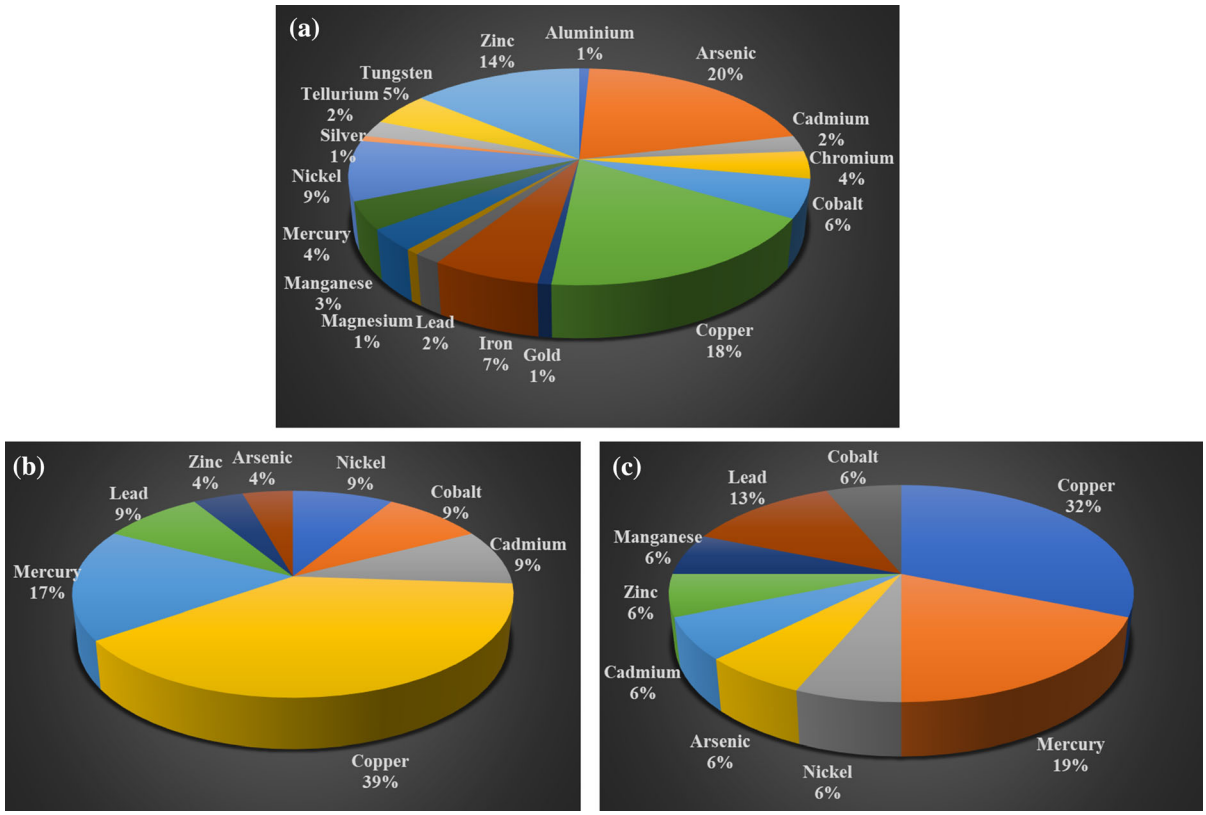

Fig. 6 Graphical representation of metal(loid) resistance gene profile of *Bacillus flexus* strain SSAI1 genome. **a** Chromosomal genome, **b** Plasmid 1 and **c** Plasmid 2

mg protein, followed by spheroplast fraction with enzyme activity of 0.338 µmol DCIP/min/mg protein. This clearly demonstrated that arsenite oxidase is a periplasmic enzyme. The periplasmic arsenite oxidase has also been reported in *Rhizobium* NT-26, *Hydrogenophaga* sp. strain NT-14 and *Ochrobactrum triticii* SCII24 (Santini and Vanden Hoven 2004; Vanden Hoven and Santini 2004; Branco et al. 2009).

Cross tolerance to other metals and metalloids and identification of resistance genes

The *Bacillus flexus* strain SSAI1 showed highest cross tolerance to arsenate (60 mM) while least tolerant to cadmium, nickel and copper (i.e. 2 mM each) compared to other metal ions. The MTCs of this strain SSAI1 for chromium, iron, manganese, zinc and lead were 12, 12, 10, 6 and 4 mM respectively in MSM broth. Many metal and metalloid resistance genes have been confirmed as revealed by WGS analysis of the strain SSAI1 (Table S2). It included resistance genes and operons to aluminium, arsenic, cadmium, chromium, cobalt, copper, gold, iron, lead, magnesium, manganese, mercury, nickel, silver, tellurium, tungsten and zinc (Fig. 6). Besides chromosomal genome, plasmids also possessed genes conferring resistance to nickel, cobalt, cadmium, copper, lead, zinc, arsenic, manganese and mercury (Fig. 6). These genes on chromosomal and plasmid genomes are probably responsible for cross-tolerance in this strain. The presence of large number of other metal/metalloid resistance genes along with arsenic resistance determinants make this arsenite oxidizing strain a suitable candidate for bioremediation of environmental sites contaminated with multiple metals and metalloids.

Nucleotide sequence accession numbers

The complete genome sequences of *Bacillus flexus* strain SSAI1 chromosome and two plasmids viz. plasmid 1 and plasmid 2 have already been deposited

in Genbank with accession numbers CP060274, CP060273 and CP060275 respectively.

Conclusion

In the present investigation arsenite resistant *Bacillus flexus* strain SSAI1 from agro-industry waste of Goa, India has been characterized. This strain showed MIC of 25 mM arsenite in mineral salts medium (MSM) and on exposure to 10 mM arsenite demonstrated rapid arsenite oxidation and internalization of 7 mM arsenate within 24 h. Transmission electron microscopy coupled with electron dispersive X-ray spectroscopic (TEM-EDAX) analysis of arsenite exposed cells clearly demonstrated ultra-structural changes and intracellular accumulation of arsenic. Furthermore, whole-genome sequence analysis of this bacterial strain interestingly revealed presence of large number of metal(loid) resistance genes, along with *aioAB* genes encoding periplasmic arsenite oxidase responsible for oxidation of highly toxic arsenite to less toxic arsenate. The whole-genome sequence of this strain has also clearly demonstrated several other arsenite resistance genes viz. *glpF*, *aioS* and *aioE*. Therefore, multi-metal(loid) resistant arsenite oxidizing *Bacillus flexus* strain SSAI1 has the potential to bioremediate arsenite contaminated environmental sites.

Acknowledgements Ms. Sajiya Yusuf Mujawar is grateful to University Grants Commission, New Delhi for financial support as MANF-SRF (Award Letter No. F1-17.1/2015-16/MANF-2015-17-Goa-50641). The authors are thankful to Mr. Areef Sardar from CSIR-National Institute of Oceanography, Goa for EDAX analysis and AIRF, Jawaharlal Nehru University, New Delhi for TEM-EDAX analysis. The authors are also obliged to Dr. B. R. Srinivasan and Mr. Rahul Kerkar from Department of Chemistry, Goa University for FTIR analysis. The authors are also grateful to Dr. Sandeep Garg, Head, Department of Microbiology, Goa University for providing laboratory facilities.

Author contributions SYM: Conceptualization, experiments, data generation, analysis and writing of the original draft manuscript. DCV: Assisted in experimental work and draft writing. SKD: Experimental designs, verification of data, mentoring of experiments, correction and final editing of the research manuscript.

Declarations

Conflict of interest The authors declare that they have no known competing financial interests or personal relationships that could have appeared to influence the work reported in this paper.

References

Aguilar NC, Faria MC, Pedron T, Batista BL, Mesquita JP, Bomfeti CA, Rodrigues JL (2020) Isolation and characterization of bacteria from a brazilian gold mining area with a capacity of arsenic bioaccumulation. Chemosphere 240:124871

Anderson GL, Williams J, Hille R (1992) The purification and characterization of arsenite oxidase from *Alcaligenes faecalis*, a molybdenum-containing hydroxylase. J Biol Chem 267:23674–23682

Arsène-Ploetze F, Koechler S, Marchal M, Coppée JY, Chandler M, Bonnefoy V, Brochier-Armanet C, Barakat M, Barbe V, Battaglia-Brunet F, Bruneel O (2010) Structure, function, and evolution of the *Thiomonas* spp. genome. PLoS Genet 6(2):e1000859

Bagade A, Nandre V, Paul D, Patil Y, Sharma N, Giri A, Kodam K (2020) Characterisation of hyper tolerant Bacillus firmus L-148 for arsenic oxidation. Environ Pollut 261: 114124.

Bahar MM, Megharaj M, Naidu R (2012) Arsenic bioremediation potential of a new arsenite oxidizing bacterium *Stenotrophomonas* sp. MM-7 isolated from soil. Biodegradation 23(6):803–812

Bahar MM, Megharaj M, Naidu R (2013) Kinetics of arsenite oxidation by *Variovorax* sp. MM-1 isolated from a soil and identification of arsenite oxidase gene. J Hazard Mater 262:997–1003

Banerjee S, Datta S, Chattyopadhyay D, Sarkar P (2011) Arsenic accumulating and transforming bacteria isolated from contaminated soil for potential use in bioremediation. J Environ Sci Health Part A 46(14):1736–1747

Bermanec V, Paradžik T, Kazazić SP, Venter C, Hrenović J, Vujaklija D, Duran R, Boev I, Boev B (2020) Novel arsenic hyper-resistant bacteria from an extreme environment, Crven Dol mine, Allchar, North Macedonia. J Hazard Mater 402:123437

Branco R, Francisco R, Chung AP, Morais PV (2009) Identification of an aox system that requires cytochrome c in the highly arsenic-resistant bacterium *Ochrobactrum tritici* SCII24. Appl Environ Microbiol 75(15):5141–5147

Bueno BYM, Torem ML, Molina FALMS, De Mesquita LMS (2008) Biosorption of lead(II), chromium(III) and copper(II) by *R. opacus*: equilibrium and kinetic studies. Miner Eng 21(1):65–75

Cai L, Liu G, Rensing C, Wang G (2009a) Genes involved in arsenic transformation and resistance associated with different levels of arsenic-contaminated soils. BMC Microbiol 9(1):4

Cai L, Rensing C, Li X, Wang G (2009b) Novel gene clusters involved in arsenite oxidation and resistance in two arsenite oxidizers: *Achromobacter* sp. SY8 and *Pseudomonas* sp. TS44. Appl Microbiol Biotechnol 83(4):715–725

Chang JS (2015) Biotransformation of arsenite and bacterial aox activity in drinking water produced from surface water of floating houses: arsenic contamination in Cambodia. Environ Pollut 206:315–323

Chang JS, Yoon IH, Lee JH, Kim KR, An J, Kim KW (2010) Arsenic detoxification potential of *aox* genes in arsenite-oxidizing bacteria isolated from natural and constructed wetlands in the Republic of Korea. Environ Geochem Health 32(2):95–105

Dey U, Chatterjee S, Mondal NK (2016) Isolation and characterization of arsenic-resistant bacteria and possible application in bioremediation. Biotechnol Rep 10:1–7

Goswami R, Mukherjee S, Rana VS, Saha DR, Raman R, Padhy PK, Mazumder S (2015) Isolation and characterization of arsenic-resistant bacteria from contaminated water-bodies in West Bengal, India. Geomicrobiol J 32(1):17–26

Gourbal B, Sonuc N, Bhattacharjee H, Legare D, Sundar S, Ouellette M, Rosen BP, Mukhopadhyay R (2004) Drug uptake and modulation of drug resistance in *Leishmania* by an aquaglyceroporin. J Biol Chem 279:31010–31017

Guo H, Liu Z, Ding S, Hao C, Xiu W, Hou W (2015) Arsenate reduction and mobilization in the presence of indigenous aerobic bacteria obtained from high arsenic aquifers of the Hetao basin, Inner Mongolia. Environ Pollut 203:50–59

Jain R, Jha S, Adhikary H, Kumar P, Parekh V, Jha A, Mahatma MK, Kumar GN (2014) Isolation and molecular characterization of arsenite-tolerant *Alishewanella* sp. GIDC-5 originated from industrial effluents. Geomicrobiol J 31(1):82–90

Jebeli MA, Maleki A, Amoozegar MA, Kalantar E, Izanloo H, Gharibi F (2017) *Bacillus flexus* strain As-12, a new arsenic transformer bacterium isolated from contaminated water resources. Chemosphere 169:636–641

Jebelli MA, Maleki A, Amoozegar MA, Kalantar E, Gharibi F, Darvish N, Tashayoe H (2018) Isolation and identification of the native population bacteria for bioremediation of high levels of arsenic from water resources. J Environ Manage 212:39–45

Jia MR, Tang N, Cao Y, Chen Y, Han YH, Ma LQ (2019) Efficient arsenate reduction by As-resistant bacterium *Bacillus* sp. strain PVR-YHB1-1: characterization and genome analysis. Chemosphere 218:1061–1070

Kang YS, Bothner B, Rensing C, McDermott TR (2012) Involvement of RpoN in regulating bacterial arsenite oxidation. Appl Environ Microbiol 78(16):5638–5645

Kashyap DR, Botero LM, Franck WL, Hassett DJ, McDermott TR (2006) Complex regulation of arsenite oxidation in *Agrobacterium tumefaciens*. J Bacteriol 188(3):1081–1088

Khairul I, Wang QQ, Jiang YH, Wang C, Naranmandura H (2017) Metabolism, toxicity and anticancer activities of arsenic compounds. Oncotarget 8(14):23905–23926

Koechler S, Cleiss-Arnold J, Proux C, Sismeiro O, Dillies MA, Goulhen-Chollet F, Hommais F, Lièvremont D, Arsène-Ploetze F, Coppée JY, Bertin PN (2010) Multiple controls affect arsenite oxidase gene expression in *Herminiimonas arsenicoxydans*. BMC Microbiol 10(1):53

Koechler S, Arsène-Ploetze F, Brochier-Armanet C, Goulhen-Chollet F, Heinrich-Salmeron A, Jost B, Lièvremont D, Philipps M, Plewniak F, Bertin PN, Lett MC (2015) Constitutive arsenite oxidase expression detected in arsenic-hypertolerant *Pseudomonas xanthomarina* S11. Res Microbiol 166(3):205–214

Kruger MC, Bertin PN, Heipieper HJ, Arsène-Ploetze F (2013) Bacterial metabolism of environmental arsenic—mechanisms and biotechnological applications. Appl Microbiol Biotechnol 97(9):3827–3841

Kumar S, Stecher G, Tamura K (2016) MEGA7: molecular evolutionary genetics analysis version 7.0 for bigger datasets. Mol Biol Evol 33:1870–1874

Lett M, Paknikar K, Lievremont D (2001) A simple and rapid method for arsenite and arsenate speciation. Process Metall 11:541–546

Lowry OH, Rosebrough NJ, Farr AL, Randall RJ (1951) Protein measurement with the Folin phenol reagent. J Biol Chem 193(1):265–275

Mahtani S, Mavinkurve S (1979) Microbial purification of longifolene: a sesquiterpene. J Ferment Technol 57:529–533

Majumder A, Bhattacharyya K, Bhattacharyya S, Kole SC (2013) Arsenic-tolerant, arsenite-oxidising bacterial strains in the contaminated soils of West Bengal, India. Sci Total Environ 463:1006–1014

Mallick I, Hossain ST, Sinha S, Mukherjee SK (2014) *Brevibacillus*sp. KUMAs2, a bacterial isolate for possible bioremediation of arsenic in rhizosphere. Ecotoxicol Environ Saf 107:236–244

Mallick I, Bhattacharyya C, Mukherji S, Dey D, Sarkar SC, Mukhopadhyay UK, Ghosh A (2018) Effective rhizoinoculation and biofilm formation by arsenic immobilizing halophilic plant growth promoting bacteria (PGPB) isolated from mangrove rhizosphere: a step towards arsenic rhizoremediation. Sci Total Environ 610:1239–1250

Mandal BK, Suzuki KT (2002) Arsenic round the world: a review. Talanta 58(1):201–235

Meng YL, Liu Z, Rosen BP (2004) As(III) and Sb(III) uptake by *GlpF* and efflux by *ArsB* in *Escherichia coli*. J Biol Chem 279(18):18334–18341

Mujawar SY, Shamim K, Vaigankar DC, Dubey SK (2019) Arsenite biotransformation and bioaccumulation by *Klebsiella pneumoniae* strain SSSW7 possessing arsenite oxidase (*aioA*) gene. Biometals 32(1):65–76

Muller D, Médigue C, Koechler S, Barbe V, Barakat M, Talla E, Bonnefoy V, Krin E, Arsene-Ploetze F, Carapito C, Chandler M (2007) A tale of two oxidation states: bacterial colonization of arsenic-rich environments. PLoS Genet 3(4):e53

Naumann D, Helm D, Labischinski H, Giesbrecht P (1991) The characterization of microorganisms by Fourier-transform infrared spectroscopy. In: Nelson WH (ed) Modern techniques for rapid microbiological analysis. VCH, New York, pp 43–96

Oust A, Møretrø T, Kirschner C, Narvhus JA, Kohler A (2004) FT-IR spectroscopy for identification of closely related *Lactobacilli*. J Microbiol Methods 59(2):49–162

Páez-Espino D, Tamames J, de Lorenzo V, Cánovas D (2009) Microbial responses to environmental arsenic. Biometals 22(1):117–130

Palma-Lara I, Martínez-Castillo M, Quintana-Pérez JC, Arellano-Mendoza MG, Tamay-Cach F, Valenzuela-Limón OL, García-Montalvo EA, Hernández-Zavala A (2020)

Arsenic exposure: a public health problem leading to several cancers. Regul Toxicol Pharmacol 110:104539

Pandi M, Shashirekha V, Swamy M (2009) Bioabsorption of chromium from retan chrome liquor by cyanobacteria. Microbiol Res 164(4):420–428

Rahman MM, Ng JC, Naidu R (2009) Chronic exposure of arsenic via drinking water and its adverse health impacts on humans. Environ Geochem Health 31:189–200

Rathod J, Dhanani AS, Jean JS, Jiang WT (2019) The whole genome insight on condition-specific redox activity and arsenopyrite interaction promoting As-mobilization by strain *Lysinibacillus* sp. B2A1. J Hazard Mater 364:671–681

Rehman A, Butt SA, Hasnain S (2010) Isolation and characterization of arsenite oxidizing *Pseudomonas lubricans* and its potential use in bioremediation of wastewater. Afr J Biotechnol 9(10):1493–1498

Santini JM, van den Hoven RN (2004) Molybdenum-containing arsenite oxidase of the chemolithoautotrophic arsenite oxidizer NT-26. J Bacteriol 186:1614–1619

Sardiwal S, Santini JM, Osborne TH, Djordjevic S (2010) Characterization of a two-component signal transduction system that controls arsenite oxidation in the chemolithoautotroph NT-26. FEMS Microbiol Lett 313(1):20–28

Satyapal GK, Rani S, Kumar M, Kumar N (2016) Potential role of arsenic resistant bacteria in bioremediation: current status and future prospects. J Microb Biochem Technol 8(3):256–258

Saunders JK, Rocap G (2016) Genomic potential for arsenic efflux and methylation varies among global *Prochlorococcus* populations. ISME J 10(1):197–209

Singh N, Gupta S, Marwa N, Pandey V, Verma PC, Rathaur S, Singh N (2016) Arsenic mediated modifications in *Bacillus aryabhattai* and their biotechnological applications for arsenic bioremediation. Chemosphere 164:524–534

Sodhi KK, Kumar M, Agrawal PK, Singh DK (2019) Perspectives on arsenic toxicity, carcinogenicity and its systemic remediation strategies. Environ Technol Innov 16:100462

Studholme DJ, Jackson RA, Leak DJ (1999) Phylogenetic analysis of transformable strains of thermophilic *Bacillus* species. FEMS Microbiol Lett 172:85–90

Thomas DJ, Rosen BP (2013) Arsenic methyltransferases. In: Kretsinger RH, Uversky VN, Permyakov EA (eds) Encyclopedia of metalloproteins. Springer, New York, pp 140–145

van den Hoven RN, Santini JM (2004) Arsenite oxidation by the heterotroph *Hydrogenophaga* sp. strain NT-14: the arsenite oxidase and its physiological electron acceptor. Biochim Biophys Acta Bioenergetics 1656(2–3):148–155

Wang Q, Han Y, Shi K, Fan X, Wang L, Li M, Wang G (2017) An oxidoreductase *AioE* is responsible for bacterial arsenite oxidation and resistance. Sci Rep 7(1):1–10

Wu Y, Feng S, Li B, Mi X (2010) The characteristics of *Escherichia coli* adsorption of arsenic(III) from aqueous solution. World J Microbiol Biotechnol 26(2):249–256

Zhao FJ, McGrath SP, Meharg AA (2010) Arsenic as a food chain contaminant: mechanisms of plant uptake and metabolism and mitigation strategies. Ann Rev Plant Biol 61:535–559

Terms and Conditions

Springer Nature journal content, brought to you courtesy of Springer Nature Customer Service Center GmbH (“Springer Nature”).
Springer Nature supports a reasonable amount of sharing of research papers by authors, subscribers and authorised users (“Users”), for small-scale personal, non-commercial use provided that all copyright, trade and service marks and other proprietary notices are maintained. By accessing, sharing, receiving or otherwise using the Springer Nature journal content you agree to these terms of use (“Terms”). For these purposes, Springer Nature considers academic use (by researchers and students) to be non-commercial.
These Terms are supplementary and will apply in addition to any applicable website terms and conditions, a relevant site licence or a personal subscription. These Terms will prevail over any conflict or ambiguity with regards to the relevant terms, a site licence or a personal subscription (to the extent of the conflict or ambiguity only). For Creative Commons-licensed articles, the terms of the Creative Commons license used will apply.
We collect and use personal data to provide access to the Springer Nature journal content. We may also use these personal data internally within ResearchGate and Springer Nature and as agreed share it, in an anonymised way, for purposes of tracking, analysis and reporting. We will not otherwise disclose your personal data outside the ResearchGate or the Springer Nature group of companies unless we have your permission as detailed in the Privacy Policy.
While Users may use the Springer Nature journal content for small scale, personal non-commercial use, it is important to note that Users may not:

1. use such content for the purpose of providing other users with access on a regular or large scale basis or as a means to circumvent access control;
2. use such content where to do so would be considered a criminal or statutory offence in any jurisdiction, or gives rise to civil liability, or is otherwise unlawful;
3. falsely or misleadingly imply or suggest endorsement, approval , sponsorship, or association unless explicitly agreed to by Springer Nature in writing;
4. use bots or other automated methods to access the content or redirect messages
5. override any security feature or exclusionary protocol; or
6. share the content in order to create substitute for Springer Nature products or services or a systematic database of Springer Nature journal content.

In line with the restriction against commercial use, Springer Nature does not permit the creation of a product or service that creates revenue, royalties, rent or income from our content or its inclusion as part of a paid for service or for other commercial gain. Springer Nature journal content cannot be used for inter-library loans and librarians may not upload Springer Nature journal content on a large scale into their, or any other, institutional repository.
These terms of use are reviewed regularly and may be amended at any time. Springer Nature is not obligated to publish any information or content on this website and may remove it or features or functionality at our sole discretion, at any time with or without notice. Springer Nature may revoke this licence to you at any time and remove access to any copies of the Springer Nature journal content which have been saved.
To the fullest extent permitted by law, Springer Nature makes no warranties, representations or guarantees to Users, either express or implied with respect to the Springer nature journal content and all parties disclaim and waive any implied warranties or warranties imposed by law, including merchantability or fitness for any particular purpose.
Please note that these rights do not automatically extend to content, data or other material published by Springer Nature that may be licensed from third parties.
If you would like to use or distribute our Springer Nature journal content to a wider audience or on a regular basis or in any other manner not expressly permitted by these Terms, please contact Springer Nature at

onlineservice@springernature.com

Process Biochemistry 71 (2018) 69–75

Contents lists available at ScienceDirect

Process Biochemistry

journal homepage: www.elsevier.com/locate/procbio

Characterization of a metagenomic serine metalloprotease and molecular docking studies

Kashif Shamim[a], Jaya Sharma[a], Milind Mutnale[b], Santosh Kumar Dubey[a,c,*,1], Sajiya Mujawar[a]

[a] Laboratory of Bacterial Genetics and Environmental Biotechnology, Department of Microbiology, Goa University, Goa, India
[b] Laboratory for the Conservation of Endangered Species, CSIR-CCMB, Hyderabad, India
[c] Department of Botany, Institute of Science, Banaras Hindu University, Varanasi, Uttar Pradesh, India

ARTICLE INFO

Keywords:
Serine
Metalloprotease
Metagenomic library
Expression
Next-generation sequencing
In silico docking

ABSTRACT

Functional screening of marine metagenomic library resulted in a single protease positive clone (GUSK-1) containing a 4.0 kbps insert. The DNA insert was sub-cloned using pET-22b expression vector system. Phenylmethylsulfonyl fluoride (PMSF) caused 28% inhibition of protease activity, while 60% inhibition was observed with Disodium ethylenediaminetetraacetic acid (EDTA-Na_2) suggesting it to be a serine metalloprotease. The pH and temperature optima for protease activity were found to be 10 and 70 °C. Bivalent metal cations such as Mg^{2+}, Fe^{2+}, Mn^{2+}, and Ca^{2+} enhanced the protease activity indicating their possible role either at the catalytic site or in the stabilization of the enzyme. Additionally, common organic solvents viz. isopropanol, ethanol, methanol, butanol, chloroform, and benzene also improved the protease activity. Sequence analysis of the DNA insert demonstrated an open reading frame (ORF) of 861 bps encoding 286 amino acids corresponding to a protease belonging to transpeptidase superfamily. In silico docking revealed interesting interactions of this serine metalloprotease with a gp41 protein of HIV-1 and cell adhesion protein of *Listeria monocytogenes*. Therefore, the novel characteristics of this protease make it a potential candidate for various biotechnological and pharmaceutical industries.

1. Introduction

The marine environment is a diverse source of microorganisms with a cell count as high as 10^6–10^9/mL [1]. Since the potential of marine microbes is still underexplored, the community of microbiologists is shifting its focus of research from terrestrial to marine resources [2–4]. Metagenomics has gained a lot of attention as a powerful tool as it can unveil the uncultivable microbial community constituting > 99% of the actual microbial population [5–9]. The marine environment is always under a variety of physiological stresses i.e. temperature, pressure, and salinity that allows the marine microbes to adapt to such extreme conditions leading to the production of novel bioactive molecules [10–14]. These include diverse industrially important enzymes such as proteases, lipases, xylanases, amylases, cellulases, and chitinases.

Protease diversity and specificity are two valuable characteristics which have made them industrially important hydrolytic enzymes. They cover almost 60% of the worldwide sale of enzymes used in various industries viz. detergent, leather, pharmaceutical and cosmetic [15–17]. Interestingly, microbial proteases belonging to alkaline, neutral and acidic categories constitute approximately 45% of the total sale of proteases. Among these alkaline proteases cover around 30% of the total enzyme production worldwide due to their extensive use in detergent, leather, food, feed, textile, organic compound synthesis, pharmaceutical, silk industries and in the removal of proteinaceous wastes from the environment [18–25].

Although cloning and expression of alkaline protease genes have been done extensively through culture-dependent approach [22,24,26], reports on culture-independent approach are few [27,28]. In the present communication, we demonstrate the isolation of a novel serine metalloprotease gene from marine environment of Goa, India using a metagenomic approach and subsequent characterization of the protease enzyme at biochemical as well as at molecular level by employing various bioinformatics tools.

* Corresponding author at: Department of Microbiology, Goa University, Taleigao Plateau, Goa, 403206, India.
E-mail address: santosh.dubey@bhu.ac.in (S.K. Dubey).
[1] Current address: Department of Botany, Institute of Science, Banaras Hindu University, Varanasi, 221005, Uttar Pradesh, India.

https://doi.org/10.1016/j.procbio.2018.05.020
Received 12 February 2018; Received in revised form 24 May 2018; Accepted 25 May 2018
Available online 29 May 2018
1359-5113/

2. Materials and methods

2.1. Sample collection, bacterial strains, plasmid vectors and growth conditions

The sediment samples from various estuarine sites of Goa, India were collected in sterile zip-lock bags and their physiological parameters (moisture content and pH) were recorded. Samples were processed immediately for extraction of metagenomic DNA using our modified method [29]. *Escherichia coli* JM109 (HiMedia, India) was used as cloning host and pUC18 (Merck, India) as a cloning vector, whereas *E. coli* BL-21(DE3) as an expression host and pET-22b as an expression vector. Throughout the experiment, *E. coli* was grown in Luria-Bertani (LB) medium at 37 °C. The medium was supplemented with 50 μg/mL as the final concentration of ampicillin in order to screen positive transformants.

2.2. Construction of metagenomic library and screening of protease positive clones

The metagenomic library was constructed by partial digestion of metagenomic DNA with *Sau* 3A1 followed by ligation of DNA fragments into *Bam* HI cut and dephosphorylated pUC18 vector DNA [30]. The ligation mixture was incubated at 16 °C overnight and subsequently used for transformation of *E. coli* JM109 competent cells by heat shock method [31]. The transformation mix (100 μL) was plated on LB agar plates amended with ampicillin (50 μg/mL) followed by an overnight incubation at 37 °C. Colonies appearing on LB agar plate containing ampicillin (50 μg/mL) were replica plated on (1%) skimmed milk agar plate supplemented with ampicillin (50 μg/mL) to screen protease positive clones.

2.3. Sub-cloning and IPTG induced expression of the protease gene

Recombinant plasmid DNA from protease positive metagenomic clone was extracted and restriction digested with *Bam* HI. Restriction digested sample was electrophoresed on 0.8% agarose gel and DNA insert was purified from the gel using gel extraction kit (Qiagen, Hilden, Germany) followed by its sub-cloning into an expression vector, pET-22b and *E. coli* BL-21 (DE3) as a host. The positive transformant was grown at 37 °C in LB broth supplemented with ampicillin (50 μg/mL). IPTG ranging from 0.2 mM to 1 mM was added to the growth medium after 6 hours (mid-log phase) and was further incubated at 37 °C. The bacterial cells were harvested at 11,000 rpm for 10 min at 4 °C after overnight induction by IPTG.

2.4. Purification of protease enzyme

The enzyme from the cell-free supernatant of the positive clone was purified by ammonium sulfate precipitation method with a range of 30%–80% saturation level and kept overnight at 4 °C on a magnetic stirrer. The precipitate was harvested by centrifugation at 11,000 rpm for 20 min at 4 °C (Eppendorf, Germany). It was re-suspended in 1 ml of 0.1 M sodium carbonate buffer (pH 10) followed by dialysis against the same buffer by keeping it at 4 °C overnight under continuous stirring condition. The enzyme obtained was further purified using a DEAE cellulose column (12 cm × 2.5 cm) pre-equilibrated with 0.1 M sodium carbonate buffer (pH 10.0). The column was washed with the same buffer to remove unbound proteins and the bound protease was eluted by applying a gradient of increasing concentration of NaCl (0–1 M). The eluted fractions were checked for protein by recording the absorbance at 280 nm followed by estimation of protease activity as per Kunitz assay [32] using tyrosine as a standard. All the fractions showing protease activity were pooled together. One unit of enzyme was defined as the amount of enzyme required to liberate 1 μg of tyrosine per minute under standard assay conditions. The protein content of the samples was estimated using Bradford assay [33] taking bovine serum albumin (BSA) as a standard.

2.5. SDS-PAGE and Zymography

The purified protein fraction was analysed by SDS-PAGE to determine the molecular weight of protease using 12% polyacrylamide gel following standard procedure [34] and using a broad range protein molecular weight marker (New England Biolabs, USA). Zymography was carried out to check protease activity using 1% casein co-polymerized with 12% polyacrylamide resolving gel. The electrophoresis was performed at a constant voltage of 100 volts using Mini-PROTEAN Tetra Cell (BIO-RAD, USA). After electrophoresis, the gel was submerged in 2.5% (V/V) Triton X-100 solution and incubated on a rocker at room temperature for 45 min with gentle shaking. Triton X-100 was removed by washing the gel several times with Milli-Q water followed by flooding the gel with a renaturing solution, Tris-Cl (pH 8.0) for 1 hour at 25 °C under gentle agitation. The renaturing solution was decanted after incubation and the gel was incubated overnight at room temperature in the developing buffer (pH 7.5) containing Tris base, NaCl, $ZnCl_2$, $CaCl_2$ and Brij 35. The gel was then stained with Coomassie brilliant blue R-250 for 4 hours followed by de-staining (methanol: water: glacial acetic acid in the ratio of 4:5:1) until clear band indicating protease activity appeared on the gel [35].

2.6. Characterization of protease enzyme

Characterization of protease activity with respect to pH, temperature, metal ions, inhibitors, surfactants and common organic solvents was done. In order to determine optimum pH for protease activity different buffers such as glycine-HCl buffer (pH 2.0, 3.0), sodium acetate buffer (pH 4.0, 5.0, 6.0), sodium phosphate buffer (pH 7.0, 8.0) and glycine-NaOH buffer (pH 9.0–12.8) were used. Whereas for optimum temperature determination, the temperature was varied from 30 °C to 80 °C under standard assay conditions. In order to determine the effect of various metal ions on protease activity, several metal salts with concentration ranging from 1 mM and 5 mM were used viz. $CaCl_2$, $MnCl_2$, $ZnSO_4$, $PbSO_4$, $FeSO_4$, $MgSO_4$, $NiSO_4$ and $CoCl_2$. The enzyme was incubated in respective metal solution for 30 min prior to assay and residual enzyme activity in terms of percentage was estimated considering the control as 100%. Similarly, the effect of various enzyme inhibitors such as β-mercaptoethanol (β-ME), dithiothreitol (DTT), EDTA-Na_2, and PMSF on protease activity at 1 mM and 5 mM was determined. Effect of common organic solvents on enzyme activity at 5% and 10% levels (V/V) was also checked. These solvents included butanol, isopropanol, ethanol, methanol, chloroform, benzene, and toluene. The enzyme was mixed with solvents separately, incubated for 1 hour at 40 °C and residual enzyme activity were recorded. All experiments are performed in triplicates.

2.7. Statistical analysis

Data analysis was carried out using the statistical package, GraphPad Prism version 7.03 (GraphPad Software, La Jolla California, USA). One way ANOVA was used to test the variation between the temperatures and pH with respect to enzyme activity as well as enzyme stability. Results were considered to be statistically significant if $p < 0.05$.

2.8. Sequence analysis of DNA insert

The 4.0 kbps insert was sequenced by employing next-generation sequencing using Illumina MiSeq (Illumina, USA) and the obtained sequenced reads were assembled into one contig (CLC genomics workbench, QIAGEN, Denmark). The sequence reads as FASTQ files were submitted to Sequence Read Archive (SRA) in NCBI. It was

analyzed using NCBI ORF finder to search for the open reading frames present in the DNA sequence.

2.9. Physiochemical properties of protease

The physicochemical characterization of the protease for theoretical measurements was done using ExPASy's ProtParam tool (http://web.expasy.org/protparam/) [36]. The parameters such as amino acid compositions, isoelectric point, molecular weight, total number of positive as well as negative charged residues, instability index, extinction coefficient, Grand Average of Hydropathy (GRAVY) and aliphatic index were determined in the analysis.

2.10. Phylogenetic analysis and homology modeling

The ORF's were subjected to BLAST analysis to determine the identity as well as homology of the sequences [37]. The ORF corresponding to protease was used to deduce the encoded protein. The encoded peptide sequence along with closely related sequences were aligned and evolutionary relatedness of the peptide was inferred using neighbor-joining method in MEGA 7.0 [38].

The three dimensional (3-D) structure of this protein was constructed using the Swiss- Model Server [39]. The constructed model was assessed using several protein model assessment tools at the Swiss-Model server comprising of various local and global quality estimation parameters. This model was further assessed and verified by several programs viz. PROCHECK [41], VERIFY3D [42] and ERRAT [43,44] using the verification server, SAVES. This model was also evaluated using Phyre 2.0 software, which predicts the α and β-strands in the 3-D model [45].

2.11. Protein-protein docking studies

Patchdock server was used as a tool to dock gp41 coat protein (PDB ID: 3U91) of HIV-1 and cell adhesion protein of *Listeria monocytogenes* (PDB ID: 4EZG) with identified metagenomic protease [46]. Structures showing minimum atomic contact energies were downloaded and viewed using PyMOL software.

3. Results

3.1. Metagenomic DNA isolation and library construction

The pH of the collected sediment samples ranged from 7.9 to 8.2 while moisture content ranged from 59 to 65%. The concentration of the extracted DNA ranged from 1185 to 4579 μg/g using our modified method, Shamim et al. [29]. This DNA was used to construct a metagenomic library in *E. coli* JM109 carrying pUC 18. Approximately 25,000 recombinant clones were obtained.

3.2. Screening and sub-cloning of protease positive clone

Functional screening of approximately 25,000 clones of metagenomic library resulted in one protease positive clone i.e. GUSK-1. DNA insert of approx. 4.0 kbps was confirmed by restriction diagnostic analysis of this positive clone with *Bam* HI restriction endonuclease (Supplementary data Fig. 1). Sub-cloning of the protease positive insert in expression vector system resulted in overexpression of protease which was evident from the skimmed milk agar plate supplemented with ampicillin (Supplementary data Fig. 2).

3.3. Purification of protease, SDS-PAGE and zymogram analysis

Maximum protease activity was observed at 70% ammonium sulfate precipitation. This concentrate was purified using DEAE cellulose column and the protein fractions showing good protease activity (Table 1) were pooled together for SDS-PAGE. The purified protease enzyme showed a single band of approximately 40 kDa on SDS-PAGE when compared with protein molecular weight marker. The zymogram analysis revealed single band showing a zone of clearance against dark blue background confirming protease activity. This zone of clearance was a result of casein hydrolysis caused by a protease from a metagenomic marine library (Supplementary data Fig. 3).

Table 1
Purification of serine metalloprotease.

Enzyme Sample	Total enzyme activity (U)	Total Protein content (mg/mL)	Specific enzyme activity (U/mg)	Purification fold
Crude enzyme	121.06	2.25	53.80	–
Purified enzyme	193.46	0.86	224.95	4.18

3.4. Effect of temperature and pH on protease activity

The optimum temperature and pH for maximum enzyme activity of this protease from clone GUSK-1 were observed to be 70 °C and 10 respectively (Supplementary data Figs. 4 and 5). A significant variation was observed at all temperatures and pH using one way ANOVA ($p < 0.0001$; $F = 20106$ and 32114 respectively). Interestingly, this protease showed 100% stability at 70 °C ($p < 0.0001$; $F = 715.9$) for one hour, however, the enzyme activity declined to 78.91% at 80 °C (Supplementary data Fig. 6). It also showed 100% stability at pH 10.0 ($p < 0.0001$; $F = 2363405$) but the enzyme activity declined to 95.83% at pH 12.0 (Supplementary data Fig. 7). This could be due to the alkaline nature of sediment samples that were used for extracting the metagenomic DNA. These interesting characteristics i.e. thermostability and tolerance to high pH mark its potential for industrial applications, especially in detergent and leather industries.

3.5. Effect of metal ions, organic solvents, and inhibitors on enzyme activity

The activity of the protease from a metagenomic marine library was found to be significantly enhanced in presence of most of the bivalent cations used in the study. The maximum increase in enzyme activity was observed in case of Mg^{2+} ions (5 mM) i.e. by 88% followed by Fe^{2+}, Mn^{2+} and Ca^{2+} ions i.e. 63%, 46% and 34% respectively at pH 10 and temperature 70 °C (Supplementary data Table 1) suggesting their possible involvement at the catalytic site of protease in addition to their role in stabilization of the enzyme [47]. The protease activity was slightly inhibited in presence of 5 mM Pb^{2+} (3%) and Co^{2+} (2%).

Protease from the metagenomic marine library also demonstrated a high tolerance to commonly used organic solvents viz. isopropanol, chloroform, ethanol, methanol, butanol, benzene and toluene which was evident from the substantial increase in protease activity in presence of 10% solvents at pH 10 and temperature 70 °C (Supplementary data Table 2). While in case of inhibitors, enzyme activity was significantly inhibited in presence of EDTA-Na_2 (5 mM) as only 40% residual protease activity was observed, confirming it to be a metalloprotease. Moreover, even PMSF (5 mM) was found to inhibit the enzyme activity up to 28% suggesting it to be a serine protease (Supplementary data Table 3). Interestingly, iodoacetate (5 mM), a potent cysteine protease inhibitor enhanced the enzyme activity proving that this protease did not belong to cysteine proteases [25]. Additionally, the enzyme activity got enhanced in presence of 5 mM DTT and β-mercaptoethanol indicating a possible role of these reducing agents in enzyme stability.

3.6. DNA sequence analysis

Next-generation sequencing of the 4.0 kbps DNA insert resulted in a sequence of 4040 bps with 24 ORFs as revealed by ORF finder. The entire DNA sequence has already been submitted to NCBI (Accession No. SRP112498). The nucleotide to protein BLAST (blastx) analysis of ORFs revealed the presence of one ORF encoding protease (ORF 4) which possessed 861 nucleotide pairs encoding for 286 amino acid residues. Other ORFs didn't code for any of the hydrolytic enzymes. The deduced peptide sequence showed a significant homology with a peptidase belonging to transpeptidase superfamily and serine was observed to be a conserved amino acid residue in the catalytic site of enzyme which is one of the characteristic features of transpeptidase superfamily.

3.7. Physicochemical properties of serine metalloprotease

The PostParam analysis of serine metalloprotease resulted in instability index of 41.26, pI value of 5.69, the molecular weight of 31.55 kDa and a total number of positively as well as negatively charged amino acids were 30 and 36 respectively. The extinction coefficient which is in direct correlation with the tryptophan, cysteine, and tyrosine content, was found to be 28085 M^{-1} cm^{-1} at 280 nm for serine metalloprotease. The GRAVY value which predicts the hydrophobicity and solubility of any proteins was −0.099. The higher value of aliphatic index i.e. 94.55 indicates the stability of serine metalloprotease over a wide range of temperature.

3.8. Phylogenetic analysis of serine metalloprotease

Metagenomic serine metalloprotease demonstrated 93% homology with *Shewanella baltica* (WP_006086906.1), *Vibrio* sp. (ANP66759.1 and NP_799737.1), *Thermococcus thioreducens* (WP_055430299.1), *Bacillus* sp. (1WMD_A and AJF89972.1), *Alteromonas* sp. (AAC60459.1) and *Mortierella elongata* (OAQ29870.1) (Fig. 1). The scale bar was found to be 0.2 which indicates 20 amino acid substitutions per 100 positions.

3.9. Model prediction and assessment

In the current study, the best model of protease enzyme (Fig. 2) was chosen using Swiss-Model Server which gave Z-scores of −1.365 [48], QMEAN6 scores of 0.653 [49] and Dfire energy value of −414.90 kJ mol^{1} [50]. The local model quality estimation based on Anolea, Gromos, and QMEAN6 (Supplementary data Fig. 8) also validated the quality of the protease model [51]. The QMEAN Z-score is the degree of nativeness of any given model and it helps in predicting the model quality i.e. whether the provided model is of comparable quality to the experimental structure or not. The analysis of Z-scores of an individual model helps in identification of the geometrical features of that protein model.

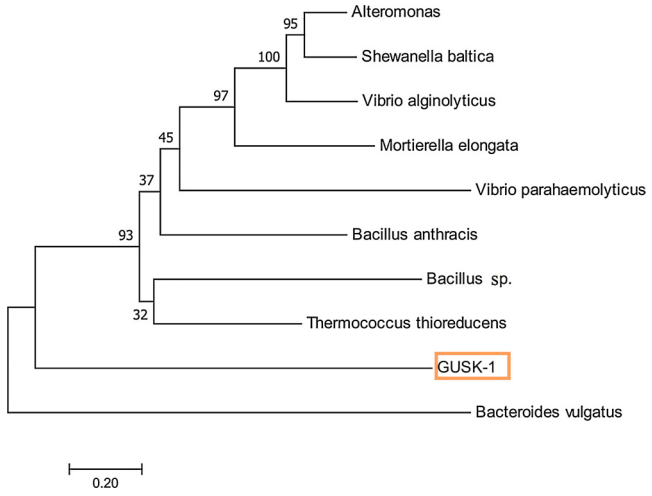

Fig. 1. The phylogenetic tree of serine metalloprotease from metagenomic clone GUSK-1. Evolutionary relationship of the serine metalloprotease from GUSK-1 with serine proteases from other bacterial strains using Maximum Likelihood method in MEGA 7. The bootstrap values are based upon 10000 replicates.

Fig. 2. Best predicted 3-D model of serine metalloprotease using Swiss Model server. The best model of serine metalloprotease was chosen using Swiss Model Server which gave Z-scores of −1.365, QMEAN6 scores of 0.653 and Dfire energy value of −414.90 kJ mol^{-1} respectively.

Further validation of this model using PROCHECK software clearly demonstrated that the amino acid residues located in the most favoured region is 73.2% and amino acid in the disallowed region is only 1.9%. Therefore almost 98.1% of the amino acid residues are in favoured and allowed regions. The analysis of the Ramachandran plot classifies the residues according to their region in the quadrangle. The yellow area of the graph represents the allowed regions while the red area represents the most allowed regions. Glycine is indicated by triangle and rest of the residues are represented by squares (Fig. 3). ERRAT analysis of this model resulted in an overall quality factor of approximately 88.59. The VERIFY3D analysis determined the compatibility of 3D with its own 1D model showing 86.27% match resulting in an average 3D-1D Score of > 0.2. The SAVES software also passed this model for further studies. The evaluation of 3-D model using Phyre 2.0 revealed that α-helix is 49%, β-strand is 14% and only 12% is disordered confirming it to be the best possible model as the disorder percentage is < 50% (Supplementary data Fig. 9).

3.10. In silico docking studies

In silico studies using our serine metalloprotease interestingly revealed docking of the serine metalloprotease (shown in green) with gp41 coat protein (PDB ID: 3U91) of HIV-1 (shown in red) and cell adhesion protein of *L. monocytogenes* (PDB ID: 4EZG). The amino acid residues of the serine metalloprotease SER 74 and SER 138 docked against ARG 20 of the gp41 coat protein of HIV-1 (Fig. 4) whereas GLU 211 and LYS 55 of serine metalloprotease interacted with ASN 103 and SER 218 of cell adhesion protein of *L. monocytogenes* respectively (Fig. 5).

4. Discussion

A metagenomic approach has been employed to isolate and characterize a novel protease from estuarine sediments. The experimental procedures used for extraction of metagenomic DNA from estuarine sediments often lead to co-extraction of humic substances which may cause partial or total inhibition of enzyme-mediated molecular reactions [52] therefore, isolation of pure as well as intact metagenomic DNA from the sediment samples is a major constraint. Our previously published method [29] removes these contaminants and maintains the integrity of the metagenomic DNA for subsequent molecular studies.

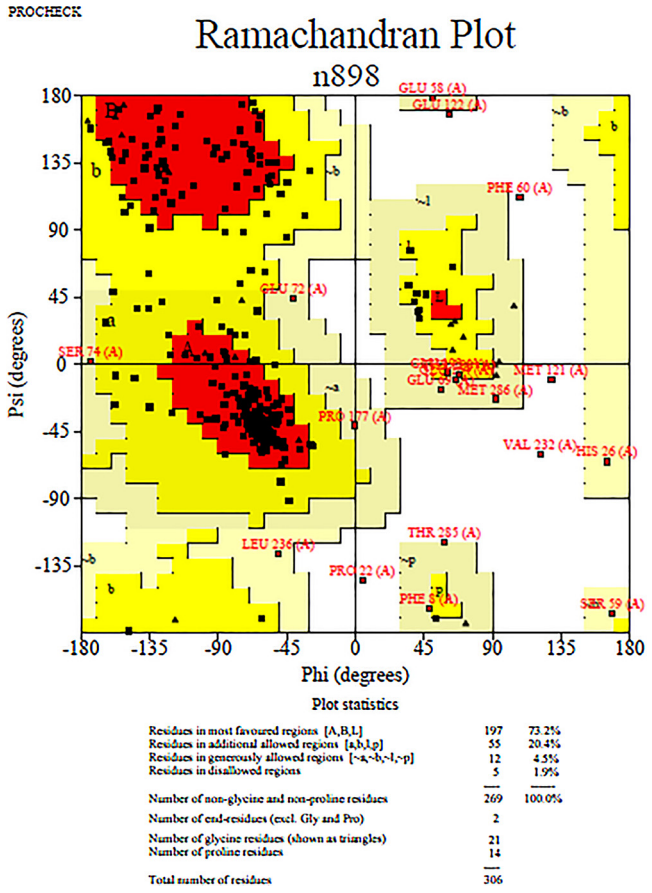

Fig. 3. Ramachandran plot for serine metalloprotease using PROCHECK software. This plot revealed that up to 73.2% amino acid residues were located in the most favoured region confirming the validity of the 3-D model.

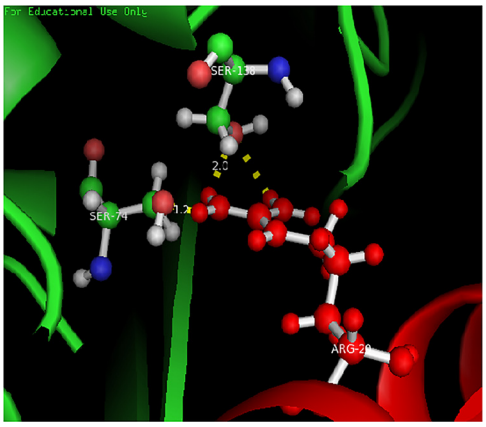

Fig. 4. Docking of serine metalloprotease (in green) with the gp41 coat protein of HIV-1 (in red). Amino acid residue SER 74 and SER 138 of serine metalloprotease are docking with amino acid residue ARG 20 of the coat protein of HIV-1 (For interpretation of the references to colour in this figure legend, the reader is referred to the web version of this article).

Since the previous studies have reported that the cloned genes for protease lied in a range of 0.5 to 2.8 kbps [53], a plasmid cloning vector was chosen for the synthesis of a functional recombinant protein. Functional screening of the metagenomic library resulted in a single protease positive clone, GUSK-1. This could be an indicative of the difference in expression level of diverse taxonomic groups as per the use of expression systems. The optimum IPTG concentration for over-expression of the protease was found to be 1.0 mM. Similar studies

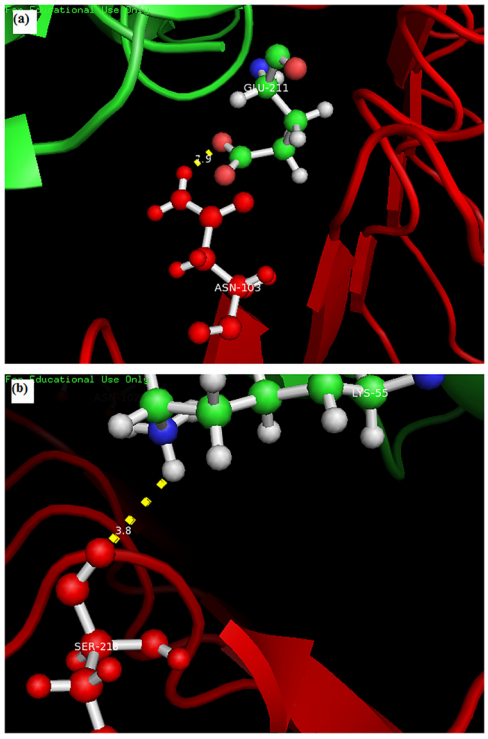

Fig. 5. Docking of serine metalloprotease (in green) with cell adhesion protein of *L. monocytogenes* (in red). **(a)** Amino acid residue GLU 211 of serine metalloprotease docking with amino acid residues ASN 103 of cell adhesion protein of *L. monocytogenes* respectively (For interpretation of the references to colour in this figure legend, the reader is referred to the web version of this article).
(b) Amino acid residue LYS 55 of serine metalloprotease docking with amino acid residues SER 218 of cell adhesion protein of *L. monocytogenes* respectively.

regarding cloning and expression of protease gene have already been reported from various metagenomic libraries [27,28,54–62].

The reported molecular weight of proteases from metagenomic approach ranges from 41–63 kDa [27,54–56,63] indicating the diverse nature of sources in contrary to cultural dependent approach. It is immensely important for a biocatalyst to have a high enzyme activity as well as stability to be a potential candidate for industrial applications [21]. The protease from GUSK-1 clone proved to be thermophilic and alkalophilic in nature as it showed maximum activity as well as stability at high temperature and pH. In earlier reports, alkaline proteases from metagenomic sources have shown different temperature and pH optimas ranging from 42 °C to 55 °C with pH from 8.0 to 10.0 [27,54,56,63]. Moreover, this protease also showed better characteristics than the alkaline proteases reported from cultivable *Bacillus* sp [19,22,64]. demonstrating that the metagenomic approach is an extremely useful tool for isolation of industrially valuable enzymes.

Protease activity was found to increase in presence of most of the bivalent cations used in this study elucidating their possible role at the catalytic site of the enzyme. There are similar reports on the enhancement of enzyme activity in presence of Ca^{2+} ions by metagenomic proteases [54–56,63] and also in case of cultivable bacteria, *Bacillus* sp. JB-99 and *Bacillus cereus* SIU1 [43,65]. On the other hand, common organic solvents significantly enhanced the protease activity which could be due to alterations in the catalytic site attributable to breakage of hydrogen bonds, hydrophobic interactions bringing about some positive conformational changes in the protein structure [39]. Isopropanol (1%) has been reported to enhance the enzyme activity by 25% for alkaline protease from metagenomic sources whereas 2.5% isopropanol enhanced the activity by 10% as compared to that of control [27,54]. This valuable characteristic of a metalloprotease from GUSK-1 i.e.,

increase in enzyme activity in presence of solvents makes it a beneficial candidate for the peptide synthesis industries.

Enzyme inhibitors like EDTA-Na_2 and PMSF are known to inhibit proteases isolated from different metagenomic sources [55,56,63] as well as from *Bacillus lehensis* [25]. The inhibition pattern of the isolated protease was also in line with the above studies and hence was confirmed to be a serine metalloprotease. However, the enzyme activity was also enhanced in presence of 5 mM DTT and β-mercaptoethanol suggesting a possible role of these reducing agents in increasing enzyme stability.

Eventually, the 4.0 kbps DNA insert was sequenced to confirm the identity of the protease to be one from transpeptidase superfamily. Interestingly, we found that protease from a metagenomic marine library showed a significant homology (93%) to the serine proteases from other bacteria.

The instability index was found to be > 40 indicating that serine metalloprotease may remain unstable if not stored in a correct solvent. The GRAVY value indicates a higher enzyme hydrosolubility which corroborates with the residual activity measured in presence of common organic solvents. Similarly, the aliphatic index shows higher value indicating stability of the enzyme at a wide range of temperature thereby supporting our experimental observation [36,66–68].

The evaluation of three-dimensional (3-D) model of a protein provides valuable information for studies related to site-specific inhibitors, disease-associated mutations and site-specific mutagenesis [69]. This further helps in manipulating the cellular and biochemical functions of an enzyme/protein [70]. The 3-D structure of serine metalloprotease from GUSK-1 has been well predicted and evaluated. There is a single earlier report describing the 3-D model of an alkaline metagenomic protease, eventually identified as serine protease from a saline habitat [52].

Proteases play a crucial role in several pathological and pathophysiological processes [71]. Docking studies clearly demonstrated that the protease encoded by the ORF 4 of metagenomic clone GUSK-1 may be useful in designing drugs against HIV-1 and *L. monocytogenes* which are serious human pathogens. In case of HIV-1, combination therapies involve the usage of drugs targeting the HIV- protease and reverse transcriptase. However, a major drawback is that viruses may develop resistance or the drug may even cause side effects in humans. Therefore, there is a need for an alternative approach that can target the virus at an initial stage. This implies that the entry of HIV-1 needs to be blocked which is mediated primarily by two glycoproteins i.e. gp120 and gp41 [72]. On the other hand, *L. monocytogenes* being an intracellular foodborne pathogen mostly targets an immunocompromised host. Listeria adhesion protein (LAP) plays an important role in crossing the barrier via paracellular route [73]. Thus, blocking LAP may serve as a resistance mechanism against *L. monocytogenes*. There has also been a report of a metagenomic metalloprotease showing fibrinolytic activity that could be used to develop therapeutic agents for the treatment of thrombosis [55]. It is interesting to note that there is no report so far about serine metalloprotease from marine environments using metagenomic approach targeting human pathogens viz. HIV-1 and *L. monocytogenes*. Therefore, such environments should be explored for development of novel therapeutics.

5. Conclusion

Microbial diversity is the primary source for biotechnological products, specifically the uncultivable microbial community, which may produce novel enzymes with enhanced properties to meet the increasing commercial demands. In this study, next-generation sequencing (NGS) analysis of the DNA insert clearly revealed an ORF encoding a serine metalloprotease belonging to transpeptidase superfamily.

This serine metalloprotease exhibited tolerance to high temperature, pH, bivalent metal ions and common organic solvents. Additionally, the interesting interactions of this serine metalloprotease with the gp41 coat protein of HIV-1 and cell adhesion protein of *Listeria monocytogenes* suggests its potential role in designing drugs against these human pathogens.

This study on characterization of a thermostable and alkaline serine metalloprotease has clearly verified the significance of metagenomics in exploring novel bioactive compounds valuable for several biotechnological and pharmaceutical industries.

Acknowledgements

The author is grateful to University Grants Commission (U.G.C.), Government of India for financial support as Maulana Azad National Fellowship (SRF) and Department of Microbiology Goa University for providing laboratory facilities.

Appendix A. Supplementary data

Supplementary material related to this article can be found, in the online version, at doi:https://doi.org/10.1016/j.procbio.2018.05.020.

References

[1] W. Fenical, P.R. Jensen, Developing a new resource for drug discovery: marine actinomycete bacteria, Nat. Chem. Biol. 2 (2006) 666–673, http://dx.doi.org/10.1038/nchembio841.
[2] J. Kennedy, J.R. Marchesi, A.D.W. Dobson, Marine metagenomics: strategies for the discovery of novel enzymes with biotechnological applications from marine environments, Microb. Cell Fact. 7 (2008) 27, http://dx.doi.org/10.1186/1475-2859-7-27.
[3] H.S. Lee, K.K. Kwon, S.G. Kang, S.S. Cha, S.J. Kim, J.H. Lee, Approaches for novel enzyme discovery from marine environments, Curr. Opin. Biotechnol. 21 (2010) 353–357, http://dx.doi.org/10.1016/j.copbio.2010.01.015.
[4] A. Trincone, Enzymatic processes in Marine biotechnology, Marine Drugs 15 (4) (2017) 93, http://dx.doi.org/10.3390/md15040093.
[5] J.C. Venter, K. Remington, J.F. Heidelberg, A.L. Halpern, D. Rusch, J.A. Eisen, D. Wu, I. Paulsen, K.E. Nelson, W. Nelson, D.E. Fouts, S. Levy, A.H. Knap, M.W. Lomas, K. Nealson, O. White, J. Peterson, J. Hoffman, R. Parsons, H. Baden-Tillson, C. Pfannkoch, Y.H. Rogers, H.O. Smith, Environmental genome shotgun sequencing of the Sargasso Sea, Science 304 (2004) 66–74, http://dx.doi.org/10.1126/science.1093857.
[6] R.D. Sleator, C. Shortall, C. Hill, Metagenomics, Lett. Appl. Microbiol. 47 (2008) 361–366, http://dx.doi.org/10.1111/j.1472-765X.2008.02444.x.
[7] S. Yooseph, K.H. Nealson, D.B. Rusch, J.P. McCrow, C.L. Dupont, M. Kim, J. Johnson, R. Montgomery, S. Ferriera, K. Beeson, et al., Genomic and functional adaptation in surface ocean planktonic prokaryotes, Nature 468 (2010) 60–66, http://dx.doi.org/10.1038/nature09530.
[8] X.Q. Zhao, Genome-based studies of marine microorganisms to maximize the diversity of natural products discovery for medical treatment, Evid.-Based Complement. Altern. Med. (2011), http://dx.doi.org/10.1155/2011/384572.
[9] M. Ferrer, M. Martínez-Martínez, R. Bargiela, W.R. Streit, O.V. Golyshina, P.N. Golyshin, Estimating the success of enzyme bioprospecting through metagenomics: current status and future trends, Microbial. Biotechnol. 9 (1) (2016) 22–34, http://dx.doi.org/10.1111/1751-7915.12309.
[10] R.J. Andersen, M.S. Wolfe, D.J. Faulkner, Autotoxic antibiotic production by a marine chromobacterium, Mar. Biol. 27 (1974) 281–285, http://dx.doi.org/10.1007/BF00394363.
[11] L. Fernandez-Arrojo, M.E. Guazzaroni, N. Lopez-Cortes, A. Beloqui, M. Ferrer, Metagenomic era for biocatalyst identification, Curr. Opin. Biotechnol. 21 (2010) 725–733, http://dx.doi.org/10.1016/j.copbio.2010.09.006.
[12] F. Berini, C. Casciello, G.L. Marcone, F. Marinelli, Metagenomics: novel enzymes from non-culturable microbes, FEMS Microbiol. Lett. 364 (2017) 15, http://dx.doi.org/10.1093/femsle/fnx211.
[13] D. Dhakal, A.R. Pokhrel, B. Shrestha, J.K. Sohng, Marine rare actinobacteria: isolation, characterization, and strategies for harnessing bioactive compounds, Front. Microbiol. 8 (2017) 1106, http://dx.doi.org/10.3389/fmicb.2017.01106.
[14] E. Nikolaivits, M. Dimarogona, N. Fokialakis, E. Topakas, Marine-derived biocatalysts: importance, accessing, and application in aromatic pollutant bioremediation, Front. Microbiol. 8 (2017) 265, http://dx.doi.org/10.3389/fmicb.2017.00265.
[15] J.W. Fox, J.D. Shannon, J.B. Bjarnason, Proteinases and their inhibitors in biotechnology, Enzym. Biomass Convers. 460 (2009) 62–79, http://dx.doi.org/10.1021/bk-1991-0460.ch006.
[16] N. Romsomsa, P. Chim-anagae, A. Jangchud, Optimization of silk degumming protease production from *Bacillus subtilis* C4 using plackett-Burman design and response surface methodology, ScienceAsia 36 (2010) 118–124, http://dx.doi.org/10.2306/scienceasia1513-1874.2010.36.118.
[17] J.L. Adrio, A.L. Demain, Microbial enzymes: tools for biotechnological processes, Biomolecules 4 (2014) 117–139, http://dx.doi.org/10.3390/biom4010117.
[18] T. Godfrey, S. West, New York.: Macmillan publishers, Industrial Enzymology, 2nd ed., (1996).
[19] R. Gupta, Q. Beg, P. Lorenz, Bacterial alkaline proteases: molecular approaches and industrial applications, Appl. Microbiol. Biotechnol. 59 (2002) 15–32, http://dx.doi.org/10.1007/s00253-002-0975-y.

[20] A. Haddar, R. Agrebi, A. Bougatef, N. Hmidet, A. Sellami-Kamoun, M. Nasri, Two detergent stable alkaline serine-proteases from *Bacillus mojavensis* A21: purification, characterization and potential application as a laundry detergent additive, Bioresour. Technol. 100 (2009) 3366–3373, http://dx.doi.org/10.1016/j.biortech.2009.01.061.

[21] K. Jellouli, A. Bougatef, L. Manni, R. Agrebi, R. Siala, I. Younes, et al., Molecular and biochemical characterization of an extracellular serine-protease from *Vibrio metschnikovii* J1, J. Ind. Microbiol. Biotechnol. 36 (2009) 939–948, http://dx.doi.org/10.1007/s10295-009-0572-5.

[22] D. Jain, I. Pancha, S.K. Mishra, A. Shrivastav, S. Mishra, Purification and characterization of haloalkaline thermoactive, solvent stable and SDS-induced protease from *Bacillus* sp.: a potential additive for laundry detergents, Bioresour. Technol. 115 (2012) 228–236, http://dx.doi.org/10.1016/j.biortech.2011.10.081.

[23] B. D'Costa, K. Shamim, S.K. Dubey, Characterization of thermostable serine protease from *Bacillus altitudinis* strain BR1, J. Sci. Ind. Res. (India) 72 (2013) 166–171.

[24] S. Joshi, T. Satyanarayana, Characteristics and applications of a recombinant alkaline serine protease from a novel bacterium *Bacillus lehensis*, Bioresour. Technol 131 (2013) 76–85, http://dx.doi.org/10.1016/j.biortech.2012.12.124.

[25] M. Baweja, L. Nain, Y. Kawarabayasi, P. Shukla, Current technological improvements in enzymes towards their biotechnological applications, Front. Microbiol. 7 (2016) 965, http://dx.doi.org/10.3389/fmicb.2016.00965.

[26] S.K. Rai, A.K. Mukherjee, Ecological significance and some biotechnological application of an organic solvent stable alkaline serine protease from *Bacillus subtilis* strain DM-04, Bioresour. Technol. 100 (2009) 2642–2645, http://dx.doi.org/10.1016/j.biortech.2008.11.042.

[27] T. Waschkowitz, S. Rockstroh, R. Daniel, Isolation and characterization of metalloproteases with a novel domain structure by construction and screening of metagenomic libraries, Appl. Environ. Microbiol. 75 (2009) 2506–2516, http://dx.doi.org/10.1128/AEM.02136-08.

[28] P.L. Pushpam, T. Rajesh, P. Gunasekaran, Identification and characterization of alkaline serine protease from goat skin surface metagenome, AMB Express 1 (2011) 3, http://dx.doi.org/10.1186/2191-0855-1-3.

[29] K. Shamim, J. Sharma, S.K. Dubey, Rapid efficient method to extract metagenomic DNA from estuarine sediments, 3 Biotech 7 (2017) 182, http://dx.doi.org/10.1007/s13205-017-0846-y.

[30] M.R. Green, J. Sambrook, Detection and Analysis of Protein Expressed from Cloned Genes, 4th ed., Cold Spring Harbor Laboratory, USA, 2012 Available at: http://www.molecularcloning.com/.

[31] D. Hanahan, Studies on transformation of *Escherichia coli* with plasmids, J. Mol. Biol. 166 (1983) 557–580, http://dx.doi.org/10.1016/S0022-2836(83)80284-8.

[32] M. Kunitz, Crystalline soybean trypsin inhibitor : Ii. General properties, J. Gen. Physiol. 30 (1947) 291–310, http://dx.doi.org/10.1085/jgp.30.4.291.

[33] M.M. Bradford, A rapid and sensitive method for the quantitation of microgram quantities of protein utilizing the principle of protein-dye binding, Anal. Biochem. 72 (1976) 248–254, http://dx.doi.org/10.1016/0003-2697(76)90527-3.

[34] U.K. Laemmli, Cleavage of structural proteins during assembly of head of bacteriophage-t4, Nature 227 (1970), http://dx.doi.org/10.1038/227680a0.

[35] C.M. D'Avila-Levy, A.L.S. Santos, P. Cuervo, J.B. De Jesus, M.H. Branquinha, Applications of zymography (substrate-SDS-PAGE) for peptidase screening in a post-genomic era, in: S. Magdeldin (Ed.), Gel Electrophoresis - Advanced Techniques, InTech, China, 2012, pp. 265–288, , http://dx.doi.org/10.5772/36862.

[36] E. Gasteiger, C. Hoogland, A. Gattiker, M.R. Wilkins, R.D. Appel, A. Bairoch, Protein identification and analysis tools in the ExPASy server, The Proteomics Protocols Handbook, Humana press, 2005, pp. 571–607. Available at: https://link.springer.com/protocol/10.1385%2F1-59259-890-0%3A571.

[37] S.F. Altschul, W. Gish, W. Miller, E.W. Myers, D.J. Lipman, Basic local alignment search tool, J. Mol. Biol. 215 (1990) 403–410, http://dx.doi.org/10.1016/S0022-2836(05)80360-2.

[38] S. Kumar, G. Stecher, K. Tamura, MEGA7: molecular evolutionary genetics analysis version 7.0 for bigger datasets, Mol. Biol. Evol. 33 (2016), http://dx.doi.org/10.1093/molbev/msw054 msw054.

[39] T. Schwede, J. Kopp, N. Guex, M.C. Peitsch, SWISS-MODEL: an automated protein homology-modeling server, Nucleic Acids Res. 31 (2003) 3381–3385, http://dx.doi.org/10.1093/nar/gkg520.

[41] R.A. Laskowski, M.W. MacArthur, D.S. Moss, J.M. Thornton, PROCHECK: a program to check the stereochemical quality of protein structures, J. Appl. Crystallogr. 26 (1993) 283–291, http://dx.doi.org/10.1107/S0021889892009944.

[42] D. Eisenberg, R. Lüthy, J.U. Bowie, VERIFY3D : assessment of protein models with three-dimensional profiles, Methods Enzymol. 277 (1997) 397–404.

[43] C. Colovos, T.O. Yeates, Verification of protein structure: patterns of nonbonded atomic interactions, Protein Sci. 2 (1993) 1511–1519.

[44] P.K. Singh, J. Joseph, S. Goyal, A. Grover, P. Shukla, Functional analysis of the binding model of microbial inulinases using docking and molecular dynamics simulation, J. Mol. Model. 22 (2016) 1–7, http://dx.doi.org/10.1007/s00894-016-2935-y90515.

[45] L.A. Kelly, S. Mezulis, C. Yates, M. Wass, M. Sternberg, The Phyre2 web portal for protein modelling, prediction and analysis, Nat. Protoc. 10 (2015) 845–858, http://dx.doi.org/10.1038/nprot.2015-053.

[46] D. Schneidman-Duhovny, Y. Inbar, R. Nussinov, H.J. Wolfson, PatchDock and SymmDock: servers for rigid and symmetric docking, Nucleic Acids Res. 33 (2005) 363–367, http://dx.doi.org/10.1093/nar/gki481.

[47] N. Annamalai, M.V. Rajeswari, R. Thavasi, S. Vijayalakshmi, T. Balasubramanian, Optimization, purification and characterization of novel thermostable, haloalkaline, solvent stable protease from *Bacillus halodurans* CAS6 using marine shellfish wastes: a potential additive for detergent and antioxidant synthesis, Bioprocess. Biosyst. Eng. 36 (2013) 873–883, http://dx.doi.org/10.1007/s00449-012-0820-3.

[48] P. Benkert, M. Biasini, T. Schwede, Toward the estimation of the absolute quality of individual protein structure models, Bioinformatics 27 (2011) 343–350, http://dx.doi.org/10.1093/bioinformatics/btq662.

[49] P. Benkert, T. Schwede, S.C. Tosatto, QMEANclust: estimation of protein model quality by combining a composite scoring function with structural density information, BMC Struct. Biol. 9 (35) (2009), http://dx.doi.org/10.1186/1472-6807-9-35.

[50] H. Zhou, Y. Zhou, Distance-scaled, finite ideal-gas reference state improves structure-derived potentials of mean force for structure selection and stability prediction, Protein Sci. 11 (2002) 2714–2726, http://dx.doi.org/10.1110/ps.0217002.

[51] F. Melo, E. Feytmans, Assessing protein structures with a non-local atomic interaction energy, J. Mol. Biol. 277 (1998) 1141–1152, http://dx.doi.org/10.1006/jmbi.1998.1665.

[52] J.H. Amorim, T.N. Macena, G.V.J. Lacerda, R.P. Rezende, J.C. Dias, M. Brendel, J.C. Cascardo, An improved extraction protocol for metagenomic DNA from a soil of the Brazilian Atlantic rainforest, Genet. Mol. Res. 7 (2008) 1226–1232.

[53] M.K. Purohit, S.P. Singh, A metagenomic alkaline protease from saline habitat: cloning, over-expression and functional attributes, Int. J. Biol. Macromol. 53 (2013) 138–143, http://dx.doi.org/10.1016/j.ijbiomac.2012.10.032.

[54] S. Biver, D. Portetelle, M. Vandenbol, Characterization of a new oxidant-stable serine protease isolated by functional metagenomics, Springerplus 2 (2013) 410, http://dx.doi.org/10.1186/2193-1801-2-410.

[55] D.G. Lee, J.H. Jeon, M.K. Jang, N.Y. Kim, J.H. Lee, J.H. Lee, et al., Screening and characterization of a novel fibrinolytic metalloprotease from a metagenomic library, Biotechnol. Lett. 29 (2007) 465–472, http://dx.doi.org/10.1007/s10529-006-9263-8.

[56] J. Neveu, C. Regeard, M.S. Dubow, Isolation and characterization of two serine proteases from metagenomic libraries of the Gobi and Death Valley deserts, Appl. Microbiol. Biotechnol. 91 (2011) 635–644, http://dx.doi.org/10.1007/s00253-011-3256-9.

[57] M.M. Apolinar-Hernández, Y.J. Peña-Ramírez, E. Pérez-Rueda, B.B. Canto-Canché, C. De Los Santos-Briones, A. O'Connor-Sánchez, Identification and in silico characterization of two novel genes encoding peptidases S8 found by functional screening in a metagenomic library of Yucatán underground water, Gene 593 (1) (2016) 154–161, http://dx.doi.org/10.1016/j.gene.2016.08.009.

[58] C. Jiang, L. Zhang, F. Li, C. Meng, R. Zeng, J. Deng, P. Shen, Q. Ou, B. Wu, Characterization of a metagenome-derived protease from contaminated agricultural soil microorganisms and its random mutagenesis, Folia. Microbiol. 62 (2017) 499, http://dx.doi.org/10.1007/s12223-017-0522-y.

[59] S.G. Devi, A.A. Fathima, M. Sanitha, S. Iyappan, W.R. Curtis, M. Ramya, Expression and characterization of alkaline protease from the metagenomic library of tannery activated sludge, J. Biosci. Bioeng. 122 (2016) 694–700.

[60] M. Faheem, D. Martins-de-Sa, J.F. Vidal, et al., Functional and structural characterization of a novel putative cysteine protease cell wall-modifying multi-domain enzyme selected from a microbial metagenome, Sci. Rep. 6 (2016) 38031, http://dx.doi.org/10.1038/srep38031.

[61] L.S. Morris, J.R. Marchesi, Current functional metagenomic approaches only expand the existing protease sequence space, but does not presently add any novelty to it, Curr. Microbiol. 70 (2015) 19–26, http://dx.doi.org/10.1007/s00284-014-0677-6.

[62] R. Singh, C. Chopra, V.K. Gupta, et al., Purification and characterization of CHpro1, a thermotolerant, alkali-stable and oxidation-resisting protease of Chumathang hotspring, Sci. Bull. 60 (2015) 1252, http://dx.doi.org/10.1007/s11434-015-0834-8.

[63] Y. Zhang, J. Zhao, R. Zeng, Expression and characterization of a novel mesophilic protease from metagenomic library derived from Antarctic coastal sediment, Extremophiles 15 (2011) 23–29, http://dx.doi.org/10.1007/s00792-010-0332-5.

[64] A. Deng, J. Wu, Y. Zhang, G. Zhang, T. Wen, Purification and characterization of a surfactant-stable high-alkaline protease from *Bacillus* sp. B001, Bioresour. Technol. 10 (2010) 7100–7106, http://dx.doi.org/10.1016/j.biortech.2010.03.130.

[65] B. Johnvesly, G.R. Naik, Studies on production of thermostable alkaline protease from thermophilic and alkaliphilic *Bacillus* sp. JB-99 in a chemically defined medium, Process Biochem. 37 (2001) 139–144, http://dx.doi.org/10.1016/S0032-9592(01)00191-1.

[66] J. Kyte, R.F. Doolittle, A simple method for displaying the hydropathic character of a protein, J. Mol. Biol. 157 (1982) 105–132, http://dx.doi.org/10.1016/0022-2836(82)90515-0.

[67] B.K. Shoichet, W.A. Baase, R. Kuroki, B.W. Matthews, A relationship between protein stability and protein function, Proc. Natl. Acad. Sci. U. S. A. 92 (1995) 452–460, http://dx.doi.org/10.1073/pnas.92.2.452.

[68] D.R. Owens, New horizons–alternative routes for insulin therapy, Nat. Rev. Drug. Discovery. 7 (2002) 529–540, http://dx.doi.org/10.1038/nrd836.

[69] S. Fidanova, I. Lirkov, 3D protein structure prediction, Ser. Mat.-Inf. 47 (2) (2009) 33–46.

[70] C. Combet, M. Jambon, G. Deleage, C. Geourjon, Geno3D: automatic comparative molecular modelling of protein, Bioinformatics 18 (2002) 213–214, http://dx.doi.org/10.1093/bioinformatics/18.1.213.

[71] M.B. Rao, A.M. Tanksale, M.S. Ghatge, V.V. Deshpande, Molecular and biotechnological aspects of microbial proteases, Microbiol. Mol. Biol. Rev. 62 (1998) 597–635.

[72] C.J. Teixeira, P. Gomes, R. Gomes, F. Maurel, Viral surface 1162 glycoproteins, gp120 and gp41, as potential drug targets against HIV-1: brief overview one 1163 quarter of a century past the approval of zidovudine, the first anti-retroviral drug, Eur. J. Med. 1164 Chem. 46 (2011) 979–992, http://dx.doi.org/10.1016/j.ejmech.2011.01.046.

[73] O.K. Koo, M.A.R. Amalaradjou, A.K. Bhunia, Recombinant probiotic expressing Listeria adhesion protein attenuates *Listeria monocytogenes* virulence in vitro, PLoS One 7 (2012) e29277, http://dx.doi.org/10.1371/journal.pone.0029277.

Ecotoxicology and Environmental Safety 165 (2018) 516–526

Contents lists available at ScienceDirect

Ecotoxicology and Environmental Safety

journal homepage: www.elsevier.com/locate/ecoenv

Tellurite biotransformation and detoxification by *Shewanella baltica* with simultaneous synthesis of tellurium nanorods exhibiting photo-catalytic and anti-biofilm activity

Diviya Chandrakant Vaigankar[a], Santosh Kumar Dubey[b,*], Sajiya Yusuf Mujawar[a], Avelyno D'Costa[c], Shyama S.K.[c]

[a] Laboratory of Bacterial Genetics and Environmental Biotechnology, Department of Microbiology, Goa University, Taleigao Plateau, Goa 403206, India
[b] Centre of Advanced Study in Botany, Banaras Hindu University, Varanasi, Uttar Pradesh 221005, India
[c] Genetic Toxicology Laboratory, Department of Zoology, Goa University, Taleigao Plateau, Goa 403206, India

ARTICLE INFO

Keywords:
Anti-biofilm
Bioremediation
Estuary
Genotoxicity
Shewanella baltica
Tellurium nanoparticles

ABSTRACT

Tellurite reducing bacterial strain was isolated from Zuari estuary, Goa India which could tolerate 5.5 mM potassium tellurite with a minimum inhibitory concentration of 6 mM. This strain was designated as GUSDZ9 and was identified as *Shewanella baltica* (accession number: MF350629) based on 16S rRNA gene sequencing and BLAST analysis. The Diethyl-dithiocarbamate based colorimetric analysis clearly demonstrated a complete reduction of 2 mM tellurite to elemental tellurium during the late stationary phase. Te Nanoparticles (TeNPs) biosynthesis which initiated at early log phase (i.e. 4 h) was evidently monitored through colour change and a peak due to surface plasmon resonance at 210 nm using UV–Vis spectroscopic analysis. X-ray crystallographic studies and transmission electron microscopy revealed unique nano-rods with a diameter ranging from 8 to 75 nm. Energy dispersive X-ray analysis further confirmed the presence of pure tellurium. The biogenic TeNPs at 10 and 5 μg/mL evidently demonstrated 90% degradation of methylene blue dye and anti-biofilm activity against potential Gram-positive and Gram-negative human pathogens respectively. The alkaline comet assay revealed time and dose-dependent genotoxicity at concentrations higher than 15 μg/mL of TeNPs. This study clearly demonstrated the potential of *Shewanella baltica* strain GUSDZ9 in bioremediation of toxic tellurite through bio-reduction into elemental tellurium and involvement of biogenic TeNPs in the photo-catalytic reduction of methylene blue and anti-biofilm activity. This is the first report of its kind on the synthesis of biogenic TeNPs from *Shewanella baltica* demonstrating photo-catalytic, anti-biofilm activity as well as genotoxicity.

1. Introduction

Estuarine environment is the most common dumping site for industrial, electronic and mining wastes. Consequently, estuaries are heavily contaminated with various persistent toxic metals viz. Cu, Hg, Cd, Pb and metalloids viz. Se, Te, As posing a serious threat to aquatic biota including microorganisms (Tchounwou et al., 2012). During the last several decades, metal and metalloid bioremediation of polluted sites using metal/metalloid resistant microorganisms have been studied extensively (Satyanarayana et al., 2012; Khalilian et al., 2015; Gupta et al., 2016). Tellurium (Te) is a metalloid present at 0.027 ppm concentration in the earth crust. It occurs in the environment as inorganic, unstable telluride [Te^{2-}], water-soluble, toxic tellurate [TeO_4^{2-}] and tellurite [TeO_3^{2-}]; organic form as dimethyl telluride (CH_3TeCH_3) and elemental tellurium (Te°). Industrially Te and its compounds find applications in solar panels, glasses, rubber, photocopying machine, metal alloys, rechargeable batteries, semiconductors in electronics, protein crystallographic analysis and as catalysts in various chemical processes (Chasteen et al., 2009; Naumov, 2010).

Tellurite is highly toxic to microorganisms at concentrations as low as 1 μg/mL (Taylor, 1999). The toxicity of tellurite is of great concern to prokaryotes as well as eukaryotes since its lethal concentration is several folds lower than that of other metals viz. Fe, Hg, Cd, Cu, Cr, Zn, Co and Se which is a metalloid (Chasteen et al., 2009; Presentato et al., 2016). Some microorganisms have evolved resistance mechanisms such as reduction of tellurite to black elemental tellurium, intracellular and extracellular accumulation of reduced tellurium and volatilization by methylation (Trutko et al., 2000; Basnayake et al., 2001; Fuentes et al.,

* Corresponding author.
E-mail address: santosh.dubey@bhu.ac.in (S.K. Dubey).

https://doi.org/10.1016/j.ecoenv.2018.08.111
Received 3 May 2018; Received in revised form 7 August 2018; Accepted 31 August 2018

2007; Chasteen et al., 2009). Few tellurite resistant marine bacteria have already been reported for their possible role in tellurite bioremediation (Rathgeber et al., 2002; Csotonyi et al., 2006; Amoozegar et al., 2008; Ollivier et al., 2008; Kim et al., 2012; Arenas et al., 2014; Borghese et al., 2014; Soda et al., 2018; Valdivia-González et al., 2018).

Bioreduction of soluble tellurite to insoluble elemental tellurium by microorganisms can occur with the formation of nanostructured particles. Since reductive biotransformation and synthesis of nanostructures proceed contextually, the use of estuarine microbes for simultaneous tellurite bioreduction in polluted environments and biogenesis of nanomaterials appears highly promising and economically attractive. Microbially-mediated strategies for nanoparticle synthesis are environment-friendly because they occur in mild reaction conditions avoiding energy-intensive procedures as well as the use of highly toxic stabilizing reagents, which are usually associated with physical and chemical approaches (Xi et al., 2005; Kaushik et al., 2010). There are few strains of bacteria which have been reported to synthesize TeNPs and include *Bacillus* sp., *Rhodococcus aetherivorans, Rhodobacter capsulatus, Bacillus selenitireducens, Sulfurospirillum barnesii* and *Shewanella oneidensis* (Klonowska et al., 2005; Baesman et al., 2007; Kim et al., 2012; Zare et al., 2012; Borghese et al., 2014; Presentato et al., 2016).

Nanoparticles are in high demand in various fields viz. medicine, electronic, catalyst, biosensors, paint, glass, alloy and battery industries (Li et al., 2011). Te in nano-dimensions possesses unique properties such as high surface to volume ratio, piezo-thermoelectrical, photoconductivity, catalytic and non-linear optical characteristics which have attracted the attention of several researchers around the world (Liu et al., 2003; Kurimella et al., 2013). More recently, Te and Cd quantum dots have been reported to have great potential in solar cells and imaging (Liu et al., 2003; Li et al., 2014). Application of nanoparticles in photo-catalytic degradation of toxic and hazardous effluents containing dyes, phenols and pesticides from textile, paper and agro-industries has drawn a lot of attention from environmental scientists. Since current methods employed for the degradation of organic pollutants are laborious and expensive, there is a pressing need for safe, efficient and eco-friendly methods to treat these organic pollutants. Thus, the use of nanoparticles in photo-catalytic degradation of organic pollutants may prove to be a better alternative.

Nanoparticles also find applications in medicine as antimicrobial agents to treat bacterial infections resistant to multiple antibiotics. Over the last few decades, the effectiveness of antibiotic treatment has decreased significantly due to the emergence of bacterial resistance to multiple antibiotics in hospital and community settings. The problem is particularly more serious in the treatment of biofilm-associated microbial infections. Therefore, there is an urgent need to develop novel nanomaterial-based antimicrobials possessing high bactericidal activity against biofilm forming pathogenic microorganisms.

However, with the profound use of nanoparticles in biomedical applications viz. antibacterial therapy and drug delivery, along with enhanced exposure to nanomaterials in everyday life, it is mandatory to investigate the toxicity of these nanoparticles. Under these circumstances, the genotoxicity of nanomaterials is a burgeoning issue in the area of nanotechnology. Although the genotoxicity of chemically-synthesized nanoparticles has been studied extensively, the genotoxicity of biologically-synthesized nanomaterials is scarcely reported (Foldbjerg et al., 2011; Ghosh et al., 2012; De Lima et al., 2013; Lebedová et al., 2017). Moreover, there are no reports on the genotoxicity of TeNPs even though they have been already studied for their antimicrobial and anti-biofilm applications (Lin et al., 2012; Zare et al., 2012; Mohanty et al., 2014; Pugin et al., 2014; Srivastava et al., 2015; Zonaro et al., 2015). Thus, it is highly imperative to study the genotoxic effect of biogenic TeNPs, intended for biomedical and environmental applications.

In the present study, the tellurite reduction potential of *Shewanella baltica* strain GUDSZ9 from Zuari estuary Goa, India, is discussed along with the simultaneous synthesis of TeNPs. We have also studied the potential application of these biogenic TeNPs in photo-catalytic degradation of methylene blue dye, anti-biofilm activity and genotoxicity against human lymphocytes.

2. Materials and methods

2.1. Materials

All the chemicals used for the present study were of certified analytical grade and were procured from Himedia (Mumbai, India) unless specified otherwise.

2.2. Enrichment and isolation of tellurite reducing estuarine bacteria from Zuari estuary, Goa, India

Estuarine surface water was collected from the Zuari estuary Goa, India (Latitude: 15°24'31.03"N, Longitude: 73°53'31.02"E and temperature: 27 °C) using a sterile polycarbonate bottle. One mL of water sample was added to 50 mL Zobell Marine Broth (ZMB) supplemented with 0.5 mM potassium tellurite (K_2TeO_3) and was incubated at 28 ± 2 °C on a shaker at 150 rpm for 48 h. Isolation of tellurite reducing bacteria was done by dilution plating of the enriched sample on Zobell marine agar (ZMA) plates amended with 2 mM K_2TeO_3 and plates were incubated at 28 ± 2 °C for 24 h. Discrete black coloured colonies were re-streaked on ZMA plates without K_2TeO_3 in order to ensure that blackening of the colonies was certainly due to the reduction of K_2TeO_3 to elemental tellurium and not because of bacterial pigment. Morphologically distinct tellurite reducing bacterial colonies were selected for further studies.

2.3. Determination of minimum inhibitory concentration (MIC) of tellurite

Total 20 bacterial isolates were selected and spot inoculated on ZMA plates with increasing concentrations of K_2TeO_3 (0–20 mM). These plates were incubated at 28 ± 2 °C for 24 h and were checked for the appearance of metallic black coloured colonies. The minimum concentration of tellurite at which no visible colonies were obtained was designated as MIC. Ten bacterial isolates with the high MIC on ZMA plates were selected for determining the MIC in ZMB. MIC in liquid medium was determined by inoculating the selected bacterial isolates in ZMB with various concentrations of K_2TeO_3 (0–20 mM). The flasks were incubated at 28 ± 2 °C for 24 h and absorbance at 600 nm was recorded. The lowest concentration of tellurite which inhibited growth was considered as MIC. Out of ten isolates, the bacterial strain exhibiting the highest MIC in ZMB for K_2TeO_3 was considered for further characterization.

2.4. Identification of potential tellurite reducing bacterial strain

The selected tellurite-resistant strain was characterized morphologically and biochemically followed by molecular identification. DNA extraction of the tellurite reducing bacterial strain was carried out using Dneasy® Blood & Tissue Kit (Qiagen, Hilden, Germany). The 16S ribosomal RNA gene (16 S rRNA) was amplified with 27 F (5' AGAGTTTG ATCMTGGCTCAG 3') and 1492R (5' TACGGYTACCTTGTTACGACTT 3') universal eubacterial primers using Nexus Gradient Mastercycler (Eppendorf, Germany). The PCR amplicon was analysed on 1% agarose gel followed by purification using Wizard SVGel and PCR clean-up system (Promega, USA). The 16S rRNA gene was sequenced at Eurofins Genomics Bangalore, India. The DNA sequence was analysed by BLAST (Altschul et al., 1990) and submitted to GenBank. Neighbor-joining method was used for the construction of a phylogenetic dendrogram using MEGA 7 package (Tamura et al., 2013).

2.5. Growth behaviour of potential tellurite reducing bacterial strain

The potential tellurite reducing bacterial strain GUSDZ9 was inoculated in ZMB supplemented with different concentrations (0–6 mM) of K_2TeO_3 under constant shaking at 150 rpm and temperature at 28 ± 2 °C for 48 h. The growth behaviour of the strain at various concentrations of K_2TeO_3 was monitored by recording the absorbance at 600 nm at specific time intervals using UV–Vis spectrophotometer (Shimadzu model-1601, Japan). The experiment was carried out in triplicates and the standard deviation was determined.

2.6. Tellurite uptake studies using selected tellurite reducing bacterial strain

Tellurite uptake was estimated by modified diethyldithiocarbamate (DDTC) colorimetric assay (Turner et al., 1992). The bacterial strain was grown in ZMB with 2 mM K_2TeO_3 and after every 4 h, 0.5 mL culture aliquots were removed and centrifuged at 9727 × g for 10 min. The supernatant (100 µL) was added to the tube containing 0.3 M Tris buffer (pH 7) and 2 mM DDTC and absorbance was recorded at 340 nm in order to determine unreduced tellurite remaining in the supernatant. The assay was carried out in triplicates and the standard deviation was determined.

2.7. TeNPs biosynthesis

The tellurite reducing bacterial strain GUSDZ9 was inoculated in ZMB supplemented with 2 mM K_2TeO_3 and incubated at 28 ± 2 °C under constant shaking at 150 rpm for 24 h. Reduction of K_2TeO_3 by the strain was confirmed by visual observation of black colour which is an indication of tellurite reduction to black elemental Te. Un-inoculated medium with K_2TeO_3 and culture supernatant with K_2TeO_3 were kept as appropriate controls.

2.8. Optimization and time course study of TeNPs biosynthesis using strain GUSDZ9

The tellurite and pH optima for TeNPs biosynthesis was determined at different concentrations of K_2TeO_3 and pH by inoculating overnight grown culture separately in ZMB containing different concentrations of K_2TeO_3 (0.5, 1.0, 1.5, 2.0, 2.5 and 3.0 mM) and pH (5, 6, 7, 8, 9 and 10) respectively. One mL aliquot of culture suspension was withdrawn after 42 h and centrifuged at 9727 × g for 10 min. The pellet obtained was suspended in phosphate buffered saline (PBS), sonicated and centrifuged at 7782 × g for 10 min. The resulting supernatant was centrifuged again at 9727 × g for 30 min and pellet obtained was re-suspended in methanol: chloroform (2:1 v/v). The suspension was monitored using UV–Vis spectrophotometer by recording absorbance at 210 nm which is characteristic for elemental Te. These optimized conditions were maintained for subsequent time course study of TeNPs biosynthesis.

In order to obtain TeNPs, the culture containing TeNPs was harvested by centrifugation at 9727 X g for 10 min and the resultant black coloured pellet was washed thrice with PBS. The cell pellet was re-suspended in methanol: chloroform (2:1 v/v) and sonicated (0.5 pulses for 10 min with 5 min interval). After cell lysis, the suspension was centrifuged at 3502 × g for 10 min, the supernatant was retained and the pellet containing cell debris was discarded. The black colloidal suspension obtained was further harvested at 9727 × g for 30 min and the pellet obtained was subsequently washed twice with deionised water and ethanol. The pellet was dried at 80 °C using an oven in order to get TeNPs.

2.9. Characterization of biogenic TeNPs

2.9.1. UV–Vis spectroscopic analysis

The biogenic TeNPs were suspended in methanol: chloroform solvents (2:1 v/v) and absorbance was recorded in the range of 190–800 nm with methanol: chloroform (2:1 v/v) as blank.

2.9.2. X-ray diffraction analysis

X-ray diffraction pattern for biosynthesized TeNPs was obtained using Rigaku Miniflex X-ray diffractometer operated at 40 keV voltage, 20 mA of current and 1.541 Å of Cu Ka radiation. The data obtained was plotted in Origin 8 software and FWHM (Full Width Half Maxima) was obtained. The crystal size of the nanoparticle was calculated using Scherer's equation as follows: $D = K\lambda/\beta Cos\theta$ where D is the mean grain size, k is constant, λ is the X-ray wavelength for CuKa radiation, β is the FWHM of the diffraction peak in radians and θ is the Bragg's angle.

2.9.3. Transmission electron microscopic analysis

TEM analysis of biogenic TeNPs was carried out by dispersing powdered TeNPs in methanol and mounting on a carbon-coated copper TEM grid (Philips, model- CM200). The machine was operated at an accelerating voltage of 190 keV and images were taken at a resolution of 2.4 Å. The size of TeNPs was calculated using Image J software.

2.9.4. Energy dispersive X-ray analysis

A thin film of powdered TeNPs was placed on a carbon-taped sample holder followed by coating the TeNPs with carbon. The energy dispersive X-ray analysis of the coated sample was carried out using scanning electron microscope (JSM 5800 LV, model- JEOL, Japan) equipped with energy dispersive X-ray analysis operated at 20 keV to determine the elemental composition of the biogenic TeNPs.

2.10. Applications of biogenic TeNPs

2.10.1. Photo-catalytic activity of biosynthesized TeNPs

The photo-catalytic degradation of methylene blue dye using biosynthesized TeNPs was investigated in sunlight. TeNPs (10 µg/mL) was added to a methylene blue solution. This colloidal suspension was incubated in sunlight. The methylene blue solution without nanoparticles was also incubated under similar conditions as a control. The methylene blue degradation was monitored at different time intervals viz. 30, 60, 90, 120, 150, 180, 210 and 240 min by withdrawing 1 mL aliquots of colloidal mixture followed by centrifugation. The supernatant obtained was scanned by UV–Vis spectrophotometer in the wavelength range of 190–800 nm. Absorbance maxima at 664 nm was considered as characteristic for methylene blue and was monitored at various time intervals. The extent of methylene blue dye degradation was calculated using the following formula:

$$\%\text{Decolourization} = (\text{Initial absorbance} - \text{absorbance after treatment}) / \text{Initial absorbance} \times 100$$

2.10.2. Anti-biofilm activity assay of biosynthesised TeNPs

The anti-biofilm activity of biogenic TeNPs against potential human pathogens procured from Goa Medical College, Goa, India was studied using modified crystal violet assay in a 96 well sterile polystyrene microtiter plate as described previously (Baygar and Ugur, 2017). Initially, 300 µL of nutrient broth was added into a sterile polystyrene microtiter plate to which 12 h old pathogenic bacterial cultures viz. *Streptococcus pyogenes, Staphylococcus aureus*, *Klebsiella pneumoniae* and *Escherichia coli* were inoculated separately along with three different concentrations of biogenic TeNPs (5, 10 and 15 µg/mL). Un-inoculated nutrient broth and pathogens grown in nutrient broth without TeNPs were maintained as controls. The microtitre plate was incubated at 37 °C for 48 h under static conditions. Subsequently, the microtiter plate was drained, washed gently with sterile PBS and distilled water to remove unbound cells, followed by drying for 30 min. Crystal violet (0.2% w/v) was added (300 µL) to each well and incubated at 28 °C for 30 min, excess dye was gently washed with sterile distilled water.

Methanol (300 μL) was added to the dried wells of the microtitre plate and absorbance was measured at 660 nm keeping methanol as a blank. The anti-biofilm effect was estimated using the following formula:

% Anti-biofilm activity = (Absorbance of control–absorbance of sample)/absorbance of control × 100; where Absorbance of control corresponds to the bacterial cells grown in nutrient broth without TeNPs. The anti-biofilm assay was carried out in triplicate and the standard deviation was determined.

2.11. Genotoxicity of biogenic TeNPs using comet assay

Genotoxicity of the biogenic TeNPs against human lymphocytes was studied using comet assay. Blood sample (5 mL) was collected from a healthy human blood donor in a heparinized centrifuge tube and was centrifuged at 1953 × g for 15 min. The white buffy coat at the interphase of plasma layer and sedimentary blood cells were collected in a microcentrifuge tube. The blood cell pellet was washed with 0.5 mL of freshly prepared 0.85% NH_4Cl (w/v) in order to remove contaminant red blood cells. Lymphocytes which appeared as a white pellet after subsequent washes were re-suspended in PBS (pH 7) and stored at 4 °C.

The viability of the lymphocytes was ensured by determining the total cell count of lymphocytes prior to the comet assay. The lymphocyte suspension having a cell count of 10^4–10^5 cells/mL were used to study the genotoxic effect of nanoparticles.

Tubes containing lymphocytes (25 μL) were suspended with 15, 20, 25 and 50 μg/mL of biogenic TeNPs separately and were incubated at 37 °C for 0, 1 and 2 h. DNA damage was monitored in the lymphocytes by employing the comet assay (Bausinger and Speit, 2016; D'Costa et al., 2017). Briefly, the lymphocyte suspension exposed to different concentrations of TeNPs was mixed with 150 μL of 0.5% low melting agarose at 37 °C and was overlaid on a frosted slide pre-coated with 1% normal melting agarose. This was gently covered with a coverslip and allowed to solidify at 0 °C. The coverslip was removed gently, followed by placing a layer of 0.5% low melting agarose. After solidification of the final layer, the slide was immersed in freshly prepared lysing solution consisting of 2.5 M NaCl, 100 mM EDTA, 10 mM Tris-HCl, 10% DMSO and 1% Triton X-100 (pH 10) at 4 °C overnight. The slides were then immersed in electrophoresis buffer containing 300 mM NaOH and 1 mM EDTA, pH 10 for 20 min for DNA unwinding. Electrophoresis was carried out for 20 min at 25 V. After electrophoresis, the slides were placed in a cold neutralizing buffer comprising of 0.4 M Tris-HCl, pH 7.5 for 10 min. The slides were then stained with 15 μg/mL ethidium bromide and examined under a BX53 Olympus fluorescence microscope (Japan) at 200× magnification. The images of the comets were captured using ProgRes®Capture Pro 2.7. CASP image analysis software was used to analyse the percent tail DNA as an indicator of single-strand DNA damage. Two slides per specimen (500 comets) were selected for analysis. Lymphocytes exposed to H_2O_2, a known genotoxic agent served as a positive control.

2.12. Statistical analysis

Statistical analysis was performed using graph pad prism 7 software. Data was analysed using the Student *t*-test and one way ANOVA. The significance of the data for each dose against that of the respective controls were analysed by the Student *t*-test. Whereas, one way ANOVA was used to determine variation in the dose-response and time response of the biogenic TeNPs on human lymphocytes. Data were considered as statistically significant at $p < 0.05$.

3. Results and discussion

3.1. Enrichment and isolation of tellurite reducing estuarine bacterial strains

After enrichment of estuarine water sample in ZMB containing 0.5 mM K_2TeO_3, black colouration was observed in the flask indicating the reduction of tellurite to black coloured elemental tellurium. Subsequently, plating the enriched sample on ZMA plates containing 2 mM K_2TeO_3 resulted in the appearance of discrete metallic black colonies after incubation for 24 h (Supplementary Fig. 1). Twenty morphologically diverse bacterial isolates were selected for further studies. These isolates did not show any black pigmentation upon streaking on ZMA plates without K_2TeO_3 (Supplementary Fig. 2). However, it was observed that extent of tellurite reduction was also different in all twenty isolates which was evident from the difference in intensities of the black colour.

The Zuari estuary of Goa is polluted with several metal and metalloids due to extensive shipping and other industrial activities. Interestingly, bacteria from Zuari estuary have already been reported to tolerate high levels of various metal, organo-metal and metalloid pollutants (Khanolkar et al., 2015; Pereira, 2017; Samant et al., 2018; Sunitha et al., 2015). Zuari estuary is also flanked by various electronic and electrical industries. In the present communication, we have confirmed that the bacterial isolates from Zuari estuary are resistant to tellurite, which may be due to exposure of these bacterial isolates to tellurite.

3.2. Determination of MIC of tellurite using selected estuarine bacterial strains

Out of 20 isolates, 10 bacterial isolates exhibiting MIC higher than 15 mM on ZMA were chosen for further studies. In ZMB the estuarine bacterial strain GUSDZ9 showing highest MIC (i.e. 6 mM) was selected for further characterization. The bacterial strain GUSDZ9 showed very high MIC as compared to previously isolated marine tellurite resistant bacterial isolates for instance, bacteria isolated from the Caspian Sea exhibited MIC of 0.8 mM, whereas, marine bacterial strain 14 B isolated from Rehoboth beach, DE, United States was reported to tolerate 0.3–0.4 mM K_2TeO_3 (Ollivier et al., 2008; Zare et al., 2012). A recent study by Valdivia-González et al. (2018) on *Shewanella* spp. has reported MIC values ranging from 0.05 to 1 mM. This is much lower as compared to MIC for strain GUSDZ9. Thus, estuarine strain GUSDZ9 with MIC 6 mM for K_2TeO_3 is a potential candidate which may be used for bioremediation of tellurite contaminated estuarine sites.

3.3. Identification of tellurite reducing estuarine bacterial strain GUSDZ9

The bacterial strain GUSDZ9 was found to be Gram-negative, motile, rod-shaped, oxidase and catalase positive, H_2S producing and facultative anaerobic bacteria. Based on 16 S rRNA gene sequence and comparison of the sequence against GenBank database using NCBI-BLAST search, the strain GUSDZ9 was identified as *Shewanella baltica* (accession number MF350629). The dendrogram analysis has clearly revealed phylogenetic relatedness with other species of *Shewanella* (Fig. 1). Bacteria belonging to genus Shewanella are capable of anaerobic respiration using several electron acceptors. Moreover, the family Shewanellaceae is considered to play a pivotal role in bioremediation of sites contaminated with heavy metals and radioactive wastes (Fredrickson et al., 2008). Although few reports are available on tellurite reducing *Shewanella* spp. viz. *S. oneidensis, S. putrefaciens* and *S. baltica* (Klonowska et al., 2005; Kim et al., 2012, 2013, 2014; Valdivia-González et al., 2018), but *Shewanella baltica* strain GUSDZ9 isolated from Zuari estuary showed a higher level of tellurite reduction as compared to previously reported spp. of *Shewanella*.

3.4. Growth behaviour of tellurite-reducing Shewanella baltica strain GUSDZ9

Growth pattern of *Shewanella baltica* strain GUSDZ9 in presence of different tellurite concentrations (0–6 mM) indicated that the growth of the isolate was adversely affected only at a higher concentration of tellurite (Supplementary Fig. 3). This was evident by the extended lag

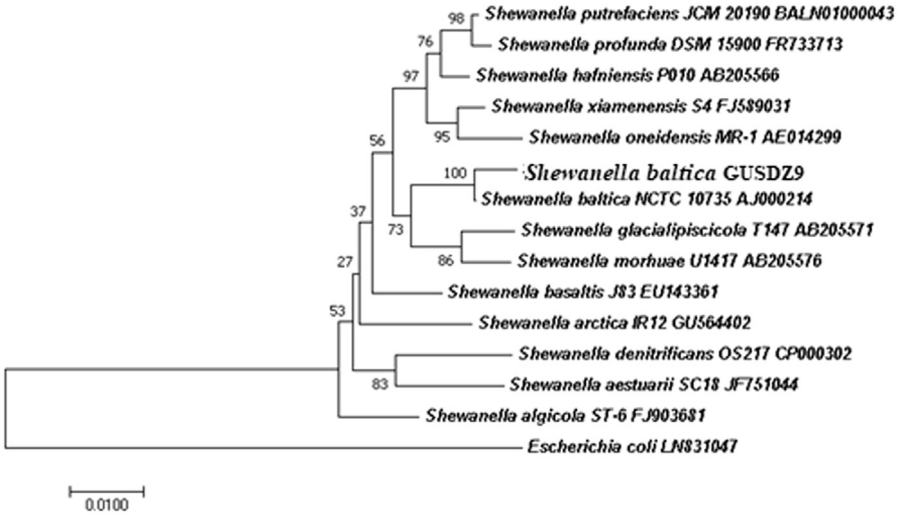

Fig. 1. Phylogenetic tree showing the relatedness of *Shewanella baltica* strain GUSDZ9 with other strains of *Shewanella* constructed using neighbor-joining method (Tamura et al., 2013). The bootstrap values are based on 1000 replicates.

phase at 4.0 and 5.5 mM K_2TeO_3 which is 6 h and 8 h respectively.

3.5. Uptake of tellurite by tellurite reducing Shewanella baltica strain GUSDZ9

Tellurite uptake by *Shewanella baltica* strain GUSDZ9 grown in ZMB with 2 mM K_2TeO_3 was observed during the early log phase of growth (2 h) with a steady increase during mid-log phase (Fig. 2). At mid-log phase (22 h), a 50% reduction of tellurite was observed. However, complete utilization of tellurite was achieved at the end of the stationary growth phase (38 h). The previous study on *Salinococcus* sp. showed a 75% reduction of tellurite after 72 h of bacterial growth supplemented with 0.4 mM K_2TeO_3 (Amoozegar et al., 2008). A similar reduction pattern was also reported in *Rhodococcus* sp. after 120 h while, *Bacillus* sp. BZ showed higher reduction rate (i.e. 80%) after 48 h of bacterial growth (Zare et al., 2012; Presentato et al., 2016). Although, most of the studies pertaining to *Shewanella* spp. on tellurite-reduction have been reported to be more effective under anaerobic conditions, our study showed a higher reduction of tellurite under aerobic conditions. This is in agreement with one recent study which has reported 70–80% tellurite removal under aerobic conditions efficiently (Soda et al., 2018). Knowing the fact that *Shewanella* spp. are facultative anaerobes the bacterial strain GUSDZ9 may also be used for tellurite-reduction under anaerobic conditions.

The present study holds considerable significance since a 100% reduction of 2 mM K_2TeO_3 was achieved at the end of the stationary growth phase (i.e. 38 h) which is the shortest time recorded so far.

3.6. TeNPs Biosynthesis using Shewanella baltica strain GUSDZ9

Reduction of tellurite to elemental tellurium which is tentatively indicated by metallic black colouration was observed in culture supplemented with 2 mM K_2TeO_3. Control flasks without K_2TeO_3 and that of culture supernatant with 2 mM of K_2TeO_3 did not show any black colouration indicting that nanoparticle synthesis is growth dependent and is intracellular (Supplementary fig. 4). Intracellular biosynthesis of

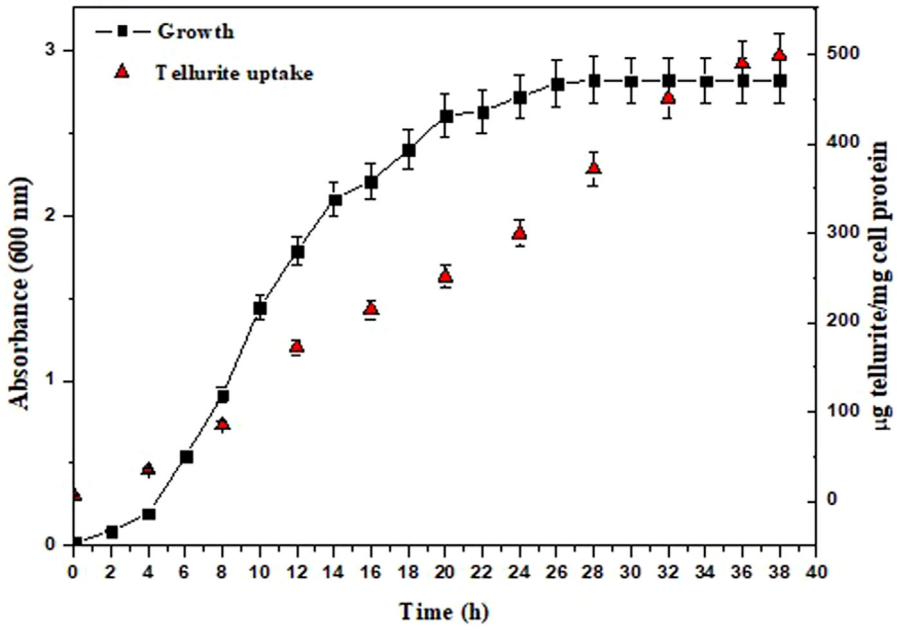

Fig. 2. Growth pattern and tellurite uptake shown by *Shewanella baltica* strain GUSDZ9 in **ZMB with 2 mM K_2TeO_3.**

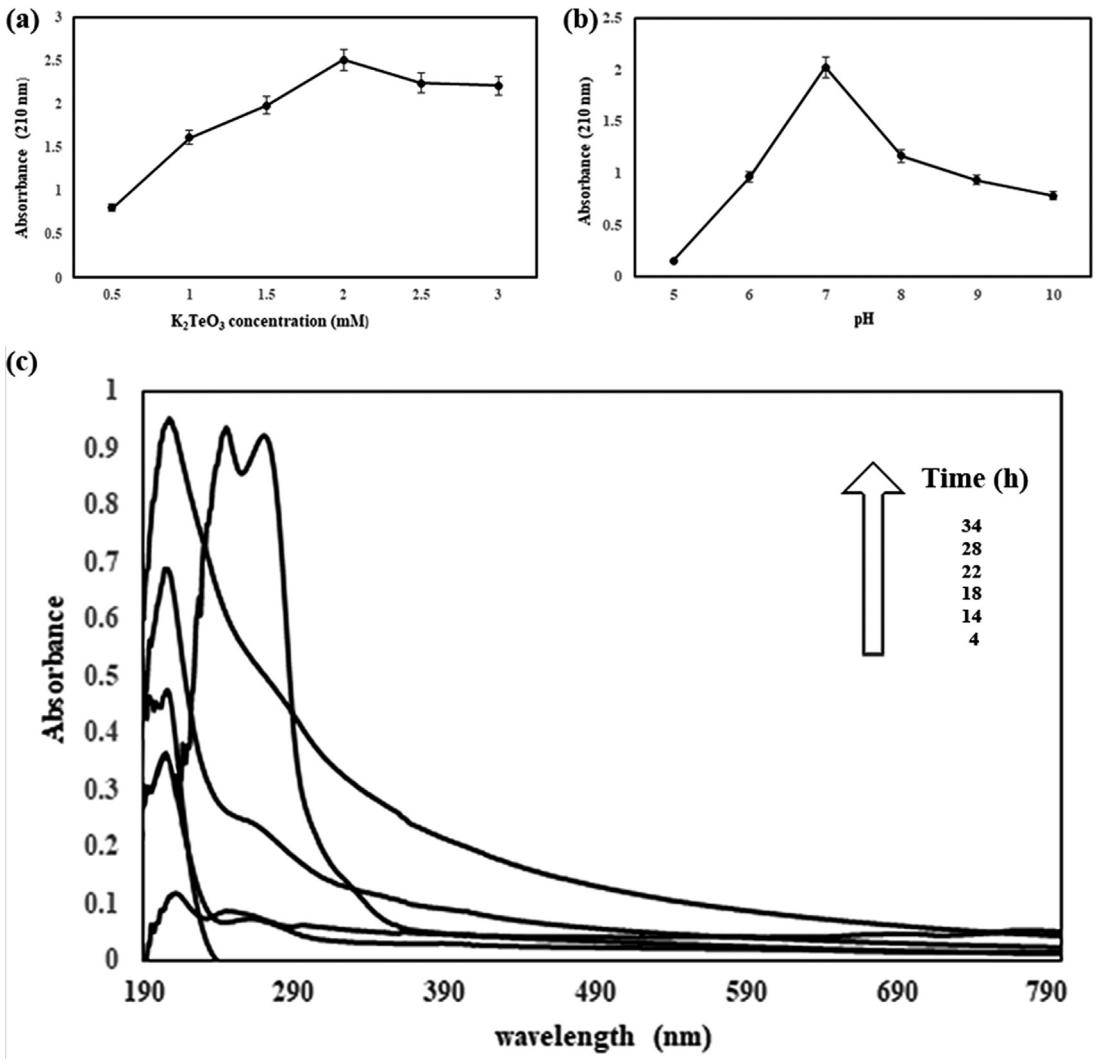

Fig. 3. TeNPs biosynthesis at different: K_2TeO_3 concentrations (a); pH (b); Time course study for TeNPs biosynthesis under optimized conditions (c).

TeNPs has been previously demonstrated in various bacteria viz. *Pseudomonas pseudoalcaligenes* KF707, *Shewanella oneidensis* and *Rhodococcus aetherivorans* (Di Tomaso et al., 2002; Kim et al., 2012; Presentato et al., 2016).

3.7. Optimization and time course study for TeNPs biosynthesis using *Shewanella baltica* strain GUSDZ9

Optimum K_2TeO_3 concentration and pH for TeNPs biosynthesis were found to be 2 mM and 7 respectively (Fig. 3a, b). It was interesting to note that the strain GUSDZ9 could synthesize TeNPs at broad pH range i.e. 6–10 and tellurite concentrations (0.5–3 mM). However, variation in the intensity of black colouration was observed indicating differences in the extent of TeNPs biosynthesis at different pH and K_2TeO_3 concentrations. Time course study of TeNPs interestingly revealed that the biosynthesis was initiated during early log phase (4 h) of bacterial growth which was evident by the change in colour of the media and a distinct peak at 210 nm. Although the reduction of tellurite was initiated during the second hour, no prominent peak was observed at 210 nm since threshold concentration for nanoparticle detection was not achieved. Biosynthesis of TeNPs was found to be time-dependent i.e. there was an increase in absorbance (210 nm) with time (Fig. 3c). However, nanoparticle synthesis was found to be maximum during mid-log to early stationary phase. The optimum time for maximum nanoparticle synthesis was found to 28 h. Even though complete reduction of tellurite was observed at the end of the stationary phase there was a shift in surface plasmon resonance for TeNPs after early stationary phase indicating the formation of TeNPs with a larger diameter. A similar shift in surface plasmon with the formation of larger diameter nanoparticles has been reported (Stoeva et al., 2002). Our strain synthesises TeNPs faster than the previously reported bacterial strain *Pseudomonas pseudoalcaligenes* KF707 (Di Tomaso et al., 2002) since the Te crystallites' synthesis began at the mid-exponential phase.

3.8. Characterization of TeNPs

3.8.1. UV–Vis analysis

An absorption peak at 210 nm by the black colloidal solution due to surface plasmon resonance clearly indicated the presence of TeNPs (Fig. 4a). Similar findings have already been published confirming synthesis of TeNPs (Gautam, Rao, 2004; Zare et al., 2012; Forootanfar et al., 2015).

3.8.2. XRD analysis

The XRD spectrum clearly illustrated characteristic Bragg's peaks at 23.02, 27.5, 38.2, 40.5, 47.0 and 49.65 which corresponds to [100, 101, 102, 110, 200] and [201] of hexagonal phase of Te nanocrystals respectively (Fig. 4b). The average grain size was found to be 57.7 nm. This was in accordance with a standard card of tellurium (ICDD card no. 36) and is also in agreement with the earlier reports (Yuan et al.,

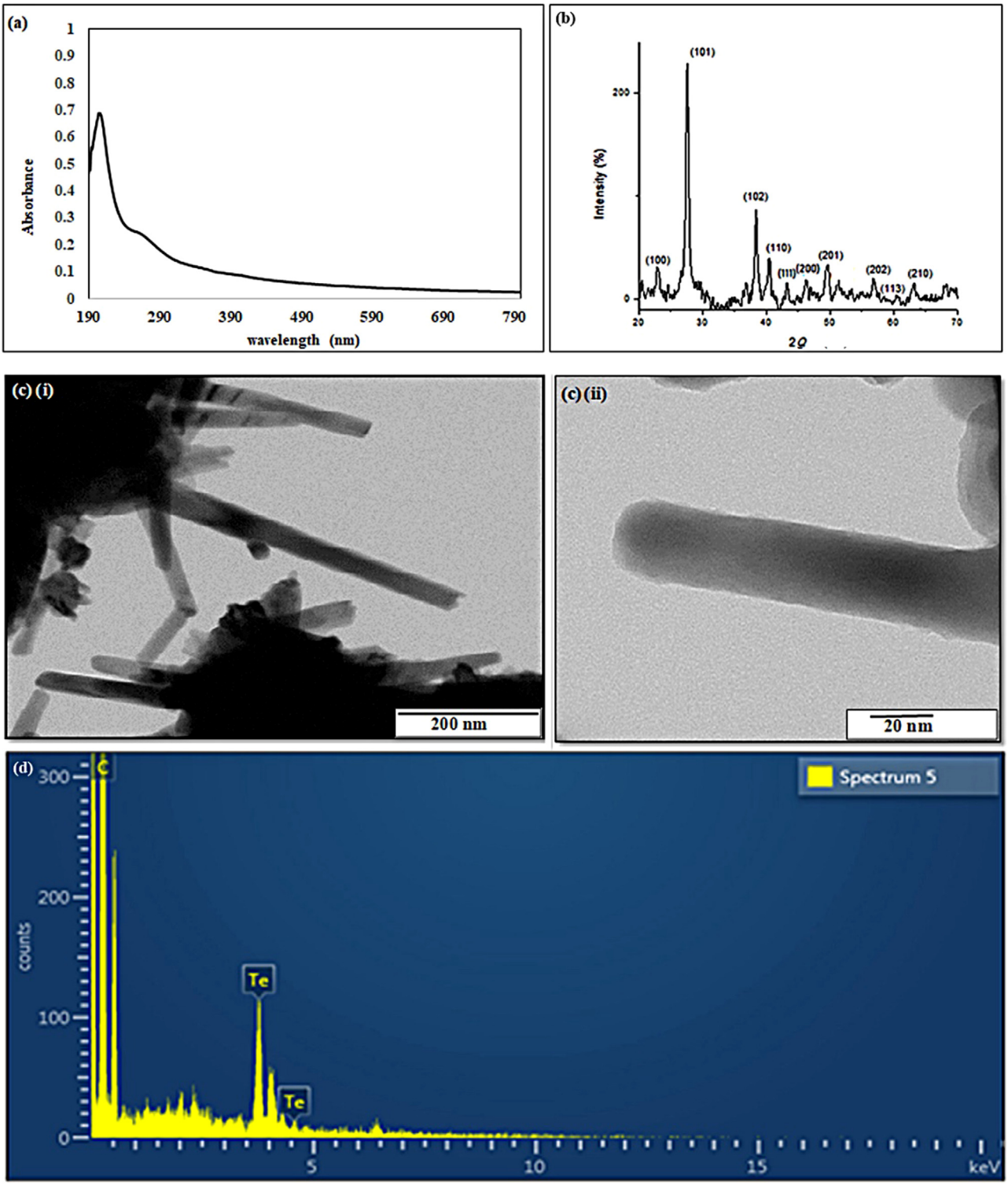

Fig. 4. Characterization of biogenic TeNPs: Absorbance maxima for biosynthesized TeNPs suspended in methanol: chloroform (2:1 v/v) at 210 nm (a); XRD pattern for biosynthesized TeNPs exhibiting characteristics Bragg's angles (b); TEM micrograph of biogenic TeNPs (c) (i) & (ii); EDAX spectrum showing characteristic peak of elemental tellurium at 3.6 keV(d).

2013; Manikandana et al., 2015; Srivastava et al., 2015).

3.8.3. TEM analysis

TEM analysis of nanoparticles revealed unique nano-rod morphology for TeNPs with a diameter in the range of 8–75 nm (Fig. 4c i, ii). Previously, various bacterial isolates have been reported to synthesise Te nano-rods viz. *Bacillus selenitireducens* (10 nm), *Shewanella oneidensis* MR-1 (10–20 nm), *Bacillus* sp. (20 nm), *Shewanella oneidensis* (10–20 nm) and *P. pseudoalcaligenes* (22 nm) (Baesman et al., 2007; Kim et al., 2012; Zare et al., 2012; Mohanty et al., 2014; Forootanfar et al., 2015). However, nano-sphere and needle-shaped TeNPs have also been reported (Di Tomaso et al., 2002; Klonowska et al., 2005). Interestingly, our study is the first evidence demonstrating TeNPs biosynthesis by *Shewanella baltica*.

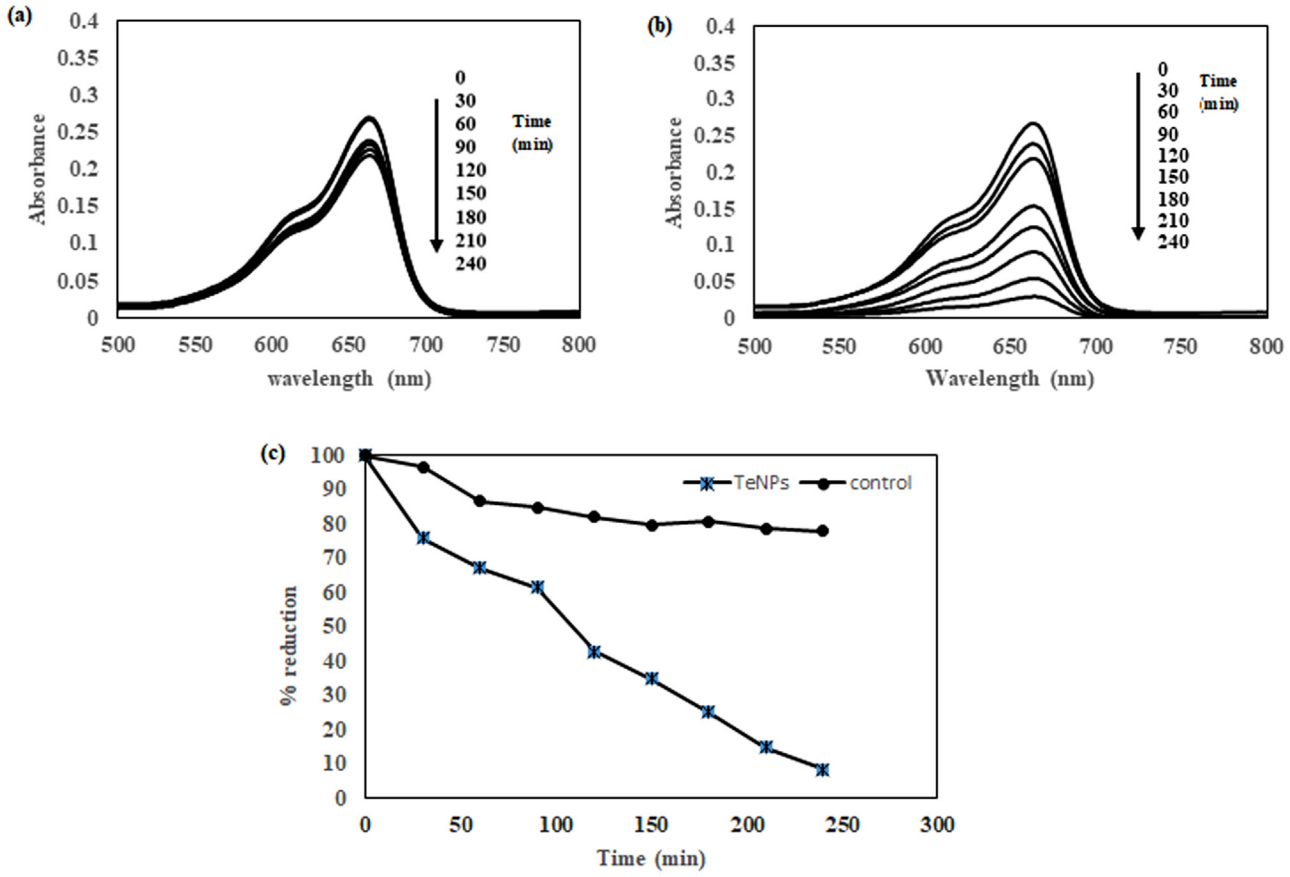

Fig. 5. UV–visible spectra of photo-catalytically degraded methylene blue dye: in absence of TeNPs (a); in presence of TeNPs (b); percent reduction of methylene blue (c).

3.8.4. Energy dispersive X-ray analysis

EDAX analysis of TeNPs clearly revealed a prominent peak of elemental tellurium at 3.6 keV (Fig. 4d). However, the peak due to carbon may be attributed to the carbon taped sample holder as well as coating with carbon.

3.8.5. Photo-catalytic activity of TeNPs

Methylene blue reduction under sunlight demonstrated a gradual change in colour from blue to pale blue. However, in presence of TeNPs as a catalyst, an enhanced decrease in absorbance was observed. In the control flask without Te nanorods, only 20% reduction of methylene blue was observed within 4 h. Whereas, in presence of TeNPs 90% reduction was observed which is very significant (Fig. 5a, b, c). There are various drawbacks associated with current physical and chemical methods employed for the degradation of organic pollutants. However, chemically synthesized TeNPs have already been reported for photocatalysis but there is no report on biogenic TeNPs-mediated photocatalysis (Shanmugam et al., 2015). The use of nanoparticles in photocatalytic degradation is advantageous since it is a reusable and recyclable process which does not require any additional step for disposal (Piella et al., 2013). Thus, biosynthesized TeNPs act as stable photocatalysts to reduce and bioremediate methylene blue dye which is present in the effluents of textile industries. This is the first report showing the photo-catalytic activity of biogenic TeNPs in methylene blue degradation through reduction.

3.9. Anti-biofilm activity assay using TeNPs

Anti-biofilm activity of biogenic TeNPs against clinically important microbial strains clearly demonstrated that these nanoparticles exhibited excellent anti-biofilm activity, which was dose-dependent. It was observed that TeNPs were very effective against *E. coli* wherein 92% of biofilm eradication was achieved at 15 µg/mL, whereas 64% was achieved at 10 µg/mL and 42% at 5 µg/mL concentration of TeNPs. *K. pneumoniae* showed a reduction in biofilm formation by 89%, 47% and 22% when treated with 15, 10 and 5 µg/mL TeNPs respectively. In the case of *S. aureus,* 81% biofilm removal was recorded at 15 µg/mL which was followed by 51% and 22% at 10 and 5 µg/mL of TeNPs respectively. A similar pattern was observed in case of *Streptococcus pyogenes* which recorded 63% biofilm removal at 15 µg/mL whereas, at 10 and 5 µg/mL concentrations, it was 20% and 9% respectively (Fig. 6). There are few reports on the antimicrobial activity of TeNPs (Lin et al., 2012; Zare et al., 2012; Mohanty et al., 2014; Pugin et al.,

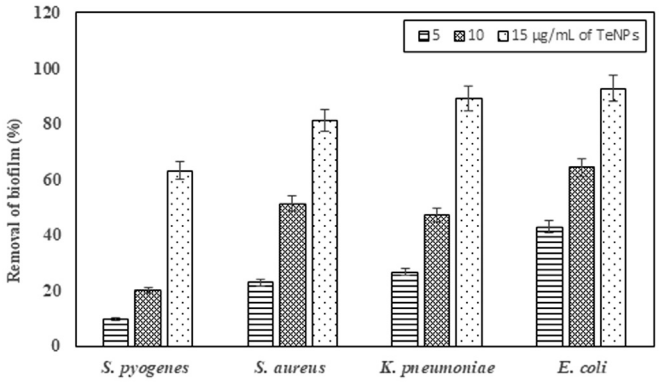

Fig. 6. Anti-biofilm activity of biosynthesized TeNPs against pathogenic clinical isolates.

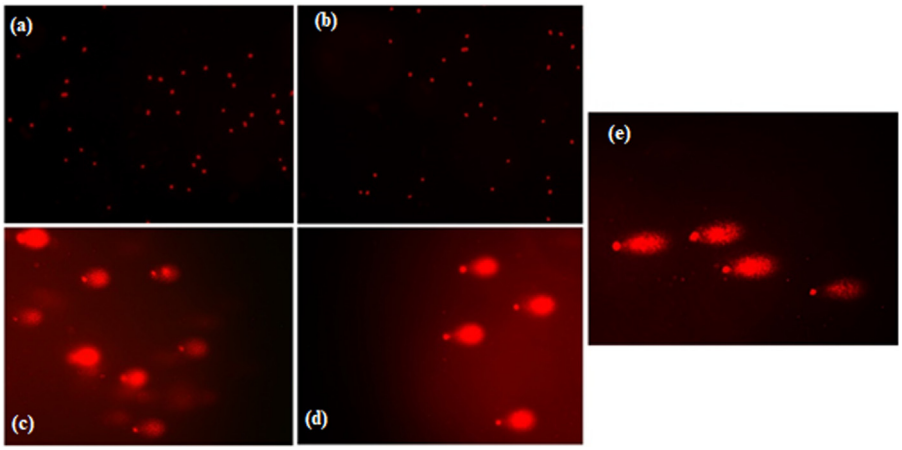

Fig. 7. Comet assay showing lymphocytes cells treated with: 0 μg/mL K_2TeO_3 (a); 15 μg/mL K_2TeO_3 (b); 20 μg/mL (c); 25 μg/mL (d); 50 μg/mL (e).

2014; Srivastava et al., 2015). However, removal of planktonic and biofilm forming bacteria by biogenic TeNPs have also been reported which ensured biofilm eradication at much higher concentrations of TeNPs (Zonaro et al., 2015). Therefore, TeNPs biosynthesised by *Shewanella baltica* strain GUSDZ9 are comparatively more effective in inhibiting potential biofilm forming Gram-positive and Gram-negative human pathogens at very low concentrations. This opens a new arena of applications for TeNPs as coating agents in medical and health-related devices in order to prevent bacterial infections. Furthermore, these TeNPs may also have promising applications in industrial sectors as potential tools to combat biofouling. Additionally, they can also serve as excellent candidates to eradicate biofilm formation in sewage tanks and other sewerage systems.

3.10. Genotoxicity of biogenic TeNPs

The percent (%) DNA damage induced by biogenic TeNPs at 15, 20, 25 and 50 μg/mL concentrations in the human lymphocytes at various time intervals (0, 1 and 2 h) are depicted in the Fig. 7. Interestingly, DNA damage observed at 15 μg/mL concentration of TeNPs with increasing time (1 and 2 h) was found to be insignificant compared to the control thus conferring that biogenic TeNPs do not induce any DNA damage in human cells at this concentration. However, a significant dose-dependent increase in the mean % tail DNA, with respect to the control was observed with time which was proved by the Student's *t*-test. Significant DNA damage was observed at 20 μg/mL (0 h) which increased in a time-dependent manner. A similar trend was also observed with 25 μg/mL concentration wherein 12.1% tail DNA damage was recorded, reaching maxima (30%) for 1 h whereas, at 2 h nearly 47% damage was observed. The highest DNA damage for lymphocytes was recorded at the 50 μg/mL concentration wherein significant % tail DNA recorded was 16%, 41% and 61% at 0, 1 and 2 h of treatments respectively (Fig. 8).

Increase in DNA damage at different concentrations of TeNPs (15, 20, 25 and 50 μg/mL) at all-time intervals (0, 1 and 2 h) was significant (except at 15 μg/mL) which was proved by one way ANOVA ($F = 499.4$, $p < 0.0001$).

Even though TeNPs have been studied for various applications majorly in the biomedical field but there are no reports as far as toxicity on human cells is concerned. Thus, these studies are of immense importance since this is the first ever report demonstrating the genotoxicity of biogenic TeNPs. Based on this study it is also advisable that utmost care must be taken in handling nano-wastes. Since insignificant DNA damage was observed at 15 μg/mL TeNPs, these nanorods can be effectively used to control biofilms inhabiting various medical as well as industrial appliances.

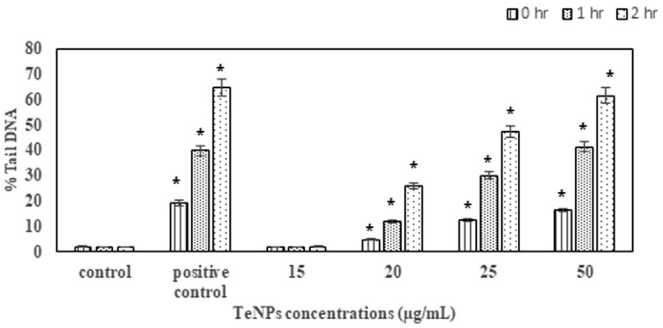

Fig. 8. Percent DNA damage in human lymphocytes exposed to different concentrations of TeNPs. Data are represented as mean ± SD (*$p < 0.0001$).

4. Conclusion

Tellurite-reducing *Shewanella baltica* strain GUSDZ9 isolated from Zuari estuary tolerated 5.5 mM K_2TeO_3 with a MIC of 6 mM in ZMB. Complete reduction of 2 mM K_2TeO_3 within 38 h of bacterial growth was observed using the diethyl-dithiocarbamate method. Interestingly, this strain successfully synthesized Te nanoparticles which was initiated at early log phase (4 h) and was found to be maximum during mid-log phase (28 h) to early stationary phase. A prominent peak of tellurium due to surface plasmon resonance at 210 nm assured the presence of TeNPs. XRD and TEM analysis confirmed the hexagonal tellurium nanocrystals exhibiting nanorod morphology with 8–75 nm average diameter. EDAX analysis further confirmed the elemental tellurium. These biogenic TeNPs also demonstrated 90% reductive degradation of methylene blue dye. TeNPs also exhibited anti-biofilm activity against potential human pathogens at even 5 μg/mL concentration. However, insignificant genotoxicity against human lymphocytes was also observed at 15 μg/mL. Thus, *Shewanella baltica* strain GUSDZ9 can be exploited simultaneously for bioremediation of toxic tellurite to elemental tellurium and TeNPs biosynthesis. We also report for the first time TeNPs biosynthesis by *Shewanella baltica* exhibiting photo-catalytic degradation of methylene blue dye, anti-biofilm activity against human pathogens and genotoxicity towards human lymphocytes.

Acknowledgment

Ms. Diviya Vaigankar is grateful to University Grants Commission, New Delhi for financial support as JRF (Ref. no. F./201718-NFO-2017-18-OBC-GOA-52491, F/2017-18(SA-III)). The authors gratefully acknowledge Mr. Areef Sardar and Mr. Girish Prabhu from CSIR-National Institute of Oceanography, Goa for EDAX and XRD analysis respectively. The authors are also obliged to Prof. Savio Rodriguez, Head,

Department of Microbiology at Goa Medical College, Goa for providing clinical pathogens. Ms. Diviya is also thankful to Prof. Sandeep Garg, Head, Department of Microbiology at Goa University, Goa for extending laboratory facilities. The authors also thank Dr. Milind Naik, Asst. Professor, Department of Microbiology at Goa University for his valuable suggestions.

Conflict of interest

The authors hereby declare no conflict of interest.

Appendix A. Supporting information

Supplementary data associated with this article can be found in the online version at doi:10.1016/j.ecoenv.2018.08.111.

References

Altschul, S.F., Gish, W., Miller, W., Myers, E.W., Lipman, D.J., 1990. Basic local alignment search tool. J. Mol. Biol. 215 (3), 403–410.

Amoozegar, M.A., Ashengroph, M., Malekzadeh, F., Razavi, M.R., Naddaf, S., Kabiri, M., 2008. Isolation and initial characterization of the tellurite reducing moderately halophilic bacterium, *Salinicoccus* sp. strain QW6. Microbiol. Res. 163 (4), 456–465. https://doi.org/10.1016/j.micres.2006.07.010.

Arenas, F.A., Pugin, B., Henríquez, N.A., Arenas-Salinas, M.A., Díaz-Vásquez, W.A., Pozo, M.F., Muñoz, C.M., Chasteen, T.G., Pérez-Donoso, J.M., Vásquez, C.C., 2014. Isolation, identification and characterization of highly tellurite-resistant, tellurite-reducing bacteria from Antarctica. Polar Sci. 8 (1), 40–52. https://doi.org/10.1016/j.polar.2014.01.001.

Baesman, S.M., Bullen, T.D., Dewald, J., Zhang, D., Curran, S., Islam, F.S., Beveridge, T.J., Oremland, R.S., 2007. Formation of tellurium nanocrystals during anaerobic growth of bacteria that use Te oxyanions as respiratory electron acceptors. Appl. Environ. Microbiol. 73 (7), 2135–2143. https://doi.org/10.1128/AEM.02558-06.

Bausinger, J., Speit, G., 2016. The impact of lymphocyte isolation on induced DNA damage in human blood samples measured by the comet assay. Mutagenesis 31 (5), 567–572.

Basnayake, R.S.T., Bius, J.H., Akpolat, O.M., Chasteen, T.G., 2001. Production of dimethyl telluride and elemental tellurium by bacteria amended with tellurite or tellurate. Appl. Organomet. Chem. 15 (6), 499–510. https://doi.org/10.1002/aoc.186.

Baygar, T., Ugur, A., 2017. In vitro evaluation of antimicrobial and antibiofilm potentials of silver nanoparticles biosynthesised by *Streptomyces griseorubens*. IET Nanobiotechnol. 677–681. https://doi.org/10.1049/iet-nbt.2016.0199.

Borghese, R., Baccolini, C., Francia, F., Sabatino, P., Turner, R.J., Zannoni, D., 2014. Reduction of chalcogen oxyanions and generation of nanoprecipitates by the photosynthetic bacterium *Rhodobacter capsulatus*. J. Hazard. Mater. 269, 24–30. https://doi.org/10.1016/j.jhazmat.2013.12.028.

Chasteen, T.G., Fuentes, D.E., Tantaleán, J.C., Vásquez, C.C., 2009. Tellurite: history, oxidative stress, and molecular mechanisms of resistance. FEMS Microbiol. Rev. 33 (4), 820–832. https://doi.org/10.1111/j.1574-6976.2009.00177.x.

Csotonyi, J.T., Stackebrandt, E., Yurkov, V., 2006. Anaerobic respiration on tellurate and other metalloids in bacteria from hydrothermal vent fields in the Eastern Pacific Ocean. Appl. Environ. Microbiol. 72 (7), 4950–4956. https://doi.org/10.1128/AEM.00223-06.

D'Costa, A., Shyama, S.K., Kumar, M.P., 2017. Bioaccumulation of trace metals and total petroleum and genotoxicity responses in an edible fish population as indicators of marine pollution. Ecotoxicol. Environ. Saf. 142, 22–28. https://doi.org/10.1016/j.ecoenv.2017.03.049.

Di Tomaso, G., Fedi, S., Carnevali, M., Manegatti, M., Taddei, C., Zannoni, D., 2002. The membrane-bound respiratory chain of *Pseudomonas pseudoalcaligenes* KF707 cells grown in the presence or absence of potassium tellurite. Microbiology 148 (6), 1699–1708.

De Lima, R., Oliveira, J.L., Murakami, P.S.K., Molina, M.A.M., Itri, R., Haddad, P., Seabra, A.B., 2013. Iron oxide nanoparticles show no toxicity in the comet assay in lymphocytes: a promising vehicle as a nitric oxide releasing nanocarrier in biomedical applications. J. Phys. Conf. Ser. 429. https://doi.org/10.1088/1742-6596/429/1/012021.

Foldbjerg, R., Dang, D.A., Autrup, H., 2011. Cytotoxicity and genotoxicity of silver nanoparticles in the human lung cancer cell line, A549. Arch. Toxicol. 85 (7), 743–750. https://doi.org/10.1007/s00204-010-0545-5.

Forootanfar, H., Amirpour-Rostami, S., Jafari, M., Forootanfar, A., Yousefizadeh, Z., Shakibaie, M., 2015. Microbial-assisted synthesis and evaluation the cytotoxic effect of tellurium nanorods. Mater. Sci. Eng. C 49, 183–189. https://doi.org/10.1016/j.msec.2014.12.078.

Fredrickson, J.K., Romine, M.F., Beliaev, A.S., Jennifer, M., Osterman, L., Pinchuk, G., Reed, J.L., Rodionov, D.A., Jorge, L.M., 2008. Towards environmental systems biology of *Shewanella*. Nat. Rev. Microbiol. 6 (8), 592. https://doi.org/10.1038/nrmicro1947.

Fuentes, D.E., Fuentes, E.L., Castro, M.E., Pérez, J.M., Araya, M.A., Chasteen, T.G., Pichuantes, S.E., Vâsquez, C.C., 2007. Cysteine metabolism-related genes and bacterial resistance to potassium tellurite. J. Bacteriol. 189 (24), 8953–8960. https://doi.org/10.1128/JB.01252-07.

Gautam, U.K., Rao, C.N.R., 2004. Controlled synthesis of crystalline tellurium nanorods, nanowires, nanobelts and related structures by a self-seeding solution process. J. Mater. Chem. 14 (16), 2530–2535.

Ghosh, M., Manivannan, J., Sinha, S., Chakraborty, A., Mallick, S.K., Bandyopadhyay, M., Mukherjee, A., 2012. In vitro and in vivo genotoxicity of silver nanoparticles. Mutat. Res. Gen. Toxicol. Environ. 749 (1), 60–69.

Gupta, A., Joia, J., Sood, A., Sood, R., Sidhu, C., Kaur, G., 2016. Microbes as potential tool for remediation of heavy metals: a review. J. Microb. Biochem. Technol. 8 (4), 364–372. https://doi.org/10.4172/1948-5948.1000310.

Kaushik, N., Thakkar, M.S., Snehit, S., Mhatre, M.S., Rasesh, Y., Parikh, M.S., 2010. Biological synthesis of metallic nanoparticles. Nanomedicine 6, 257–262.

Khalilian, M., Zolfaghari, M.R., Soleimani, M., 2015. High potential application in bioremediation of selenate by *Proteus hauseri* strain QW4. Iran. J. Microbiol. 7 (2), 94–102.

Khanolkar, D.S., Dubey, S.K., Naik, M.M., 2015. Biotransformation of tributyltin chloride to less toxic dibutyltin dichloride and monobutyltin trichloride by *Klebsiella pneumoniae* strain SD9. Int. Biodeterior. Biodegrad. 104, 212–218. https://doi.org/10.1016/j.ibiod.2015.04.030.

Kim, D.H., Kanaly, R.A., Hur, H.G., 2012. Biological accumulation of tellurium nanorod structures via reduction of tellurite by *Shewanella oneidensis* MR-1. Bioresour. Technol. 125, 127–131. https://doi.org/10.1016/j.biortech.2012.08.129.

Kim, D.H., Kim, M.G., Jiang, S., Lee, J.H., Hur, H.G., 2013. Promoted reduction of tellurite and formation of extracellular tellurium nanorods by concerted reaction between iron and *Shewanella oneidensis* MR-1. Environ. Sci. Technol. 47 (15), 8709–8715.

Kim, D.H., Park, S., Kim, M.G., Hur, H.G., 2014. Accumulation of amorphous Cr (III)-Te (IV) nanoparticles on the Surface of *Shewanella oneidensis* MR-1 through reduction of Cr (VI). Environ. Sci. Technol. 48 (24), 14599–14606.

Klonowska, A., Heulin, T., Vermeglio, A., 2005. Selenite and tellurite reduction by *Shewanella oneidensis*. Appl. Environ. Microbiol. 71 (9), 5607–5609. https://doi.org/10.1128/AEM.71.9.5607-5609.2005.

Kurimella, V.R., Kumar, K.R., Sanasi, P.D., 2013. A novel synthesis of tellurium nanoparticles using iron (II) as a reductant. Int. J. Nanosci. Nanotechnol. 4, 209–221.

Lebedová, J., Hedberg, Y.S., Odnevall Wallinder, I., Karlsson, H.L., 2017. Size-dependent genotoxicity of silver, gold and platinum nanoparticles studied using the mini-gel comet assay and micronucleus scoring with flow cytometry. Mutagenesis 33 (1), 77–85. https://doi.org/10.1093/mutage/gex027.

Li, X., Xu, H., Chen, Z.S., Chen, G., 2011. Biosynthesis of nanoparticles by microorganisms and their applications. J. Nanomater. https://doi.org/10.1155/2011/270974.

Li, Z., Sun, Q., Zhu, Y., Tan, B., Xu, Z.P., Dou, S.X., 2014. Ultra-small fluorescent inorganic nanoparticles for bioimaging. J. Mater. Chem. B 2 (19), 2793–2818. https://doi.org/10.1039/C3TB21760D.

Lin, Z.H., Lee, C.H., Chang, H.Y., Chang, H.T., 2012. Antibacterial activities of tellurium nanomaterials. Chem. Asian J. 7 (5), 930–934. https://doi.org/10.1002/asia.201101006.

Liu, Z., Hu, Z., Xie, Q., Yang, B., Qian, Y., 2003. Surfactant-assisted growth of uniform nanorods of crystalline tellurium. J. Mater. Chem. 13 (1), 159–162. https://doi.org/10.1039/b208420a.

Manikandana, M., Dhanuskodia, S., Mathewb, S., Nampoorib, V.P.N., 2015. Nonlinear Optical Property of Tellurium Nanoparticles (Conference paper).

Mohanty, A., Kathawala, M.H., Zhang, J., Chen, W.N., Loo, J.S.C., Kjelleberg, S., Yang, L., Cao, B., 2014. Biogenic tellurium nanorods as a novel antivirulence agent inhibiting pyoverdine production in *Pseudomonas aeruginosa*. Biotechnol. Bioeng. 111 (5), 858–865. https://doi.org/10.1002/bit.25147.

Naumov, A.V., 2010. Selenium and tellurium: state of the markets, the crisis, and its consequences. Metallurgist 54 (3), 197–200. https://doi.org/10.1007/s11015-010-9280-7.

Ollivier, P.R.L., Bahrou, A.S., Marcus, S., Cox, T., Church, T.M., Hanson, T.E., 2008. Volatilization and precipitation of tellurium by aerobic, tellurite-resistant marine microbes. Appl. Environ. Microbiol. 74 (23), 7163–7173. https://doi.org/10.1128/AEM.00733-08.

Pereira, F., 2017. Manganese-Tolerant Bacteria from the Estuarine Environment and their Importance in Bioremediation of Contaminated Estuarine Sites: In Marine Pollution and Microbial Remediation. Springer, Singapore, pp. 153–175. https://doi.org/10.1007/978-981-10-1044-6.

Piella, J., Bastús, N.G., Casals, E., Puntes, V., 2013. Characterizing nanoparticles reactivity: structure-photocatalytic activity relationship. J. Phys. Conf. Ser 429. IOP Publishing, pp. 012040. https://doi.org/10.1088/1742-6596/429/1/012040.

Presentato, A., Piacenza, E., Anikovskiy, M., Cappelletti, M., Zannoni, D., Turner, R.J., 2016. *Rhodococcus aetherivorans* BCP1 as cell factory for the production of intracellular tellurium nanorods under aerobic conditions. Microb. Cell Fact. 15 (1), 204. https://doi.org/10.1186/s12934-016-0602-8.

Pugin, B., Cornejo, F.A., Muñoz-Díaz, P., Muñoz-Villagrán, C.M., Vargas-Pérez, J.I., Arenas, F.A., Vásquez, C.C., 2014. Glutathione reductase-mediated synthesis of tellurium-containing nanostructures exhibiting antibacterial properties. Appl. Environ. Microbiol. 80, 7061–7070. https://doi.org/10.1128/AEM.02207-14.

Rathgeber, C., Yurkova, N., Stackebrandt, E., Beatty, J.T., Yurkov, V., 2002. Isolation of tellurite- and selenite-resistant bacteria from hydrothermal vents of the Juan de Fuca Ridge in the Pacific Ocean. Appl. Environ. Microbiol. 68 (9), 4613–4622. https://doi.org/10.1128/AEM.68.9.4613.

Satyanarayana, T., Johri, B.N., Prakash, A. (Eds.), 2012. Microorganisms in Environmental Management: Microbes and Environment. Springer Science & Business Media, Dordrecht.

Samant, S., Naik, M., Parulekar, K., Charya, L., Vaigankar, D., 2018. Selenium reducing

Citrobacter fruendii strain KP6 from Mandovi estuary and its potential application in selenium nanoparticle synthesis. Proc. Natl. Sci. India Sect. B Biol. Sci. 88 (2), 747–754.

Shanmugam, N., Suthakaran, S., Kannadasan, N., Sathishkumar, K., 2015. Synthesis and characterization of Te doped ZnO nanosheets for photocatalytic application. JO Heterocycl. 105, 15–20.

Srivastava, P., Nikhil, E.V.R., Bragança, J.M., Kowshik, M., 2015. Anti-bacterial TeNPs biosynthesized by haloarcheaon *Halococcus salifodinae* BK3. Extremophiles 19 (4), 875–884. https://doi.org/10.1007/s00792-015-0767-9.

Stoeva, S., Klabunde, K.J., Sorensen, C.M., 2002. Gram-scale synthesis of monodisperse gold colloids by the solvated metal atom dispersion method and digestive ripening and their organization into two- and three-dimensional structures. J. Am. Chem. Soc. 124 (10), 2305–2311.

Sunitha, M.S.L., Prashanth, S., Kishor, P.B.K., 2015. Characterization of arsenic-resistant bacteria and their ars genotype for metal bioremediation. IJSER 6 (2), 304–309.

Soda, S., Ma, W., Kuroda, M., Nishikawa, H., Zhang, Y., Ike, M., 2018. Characterization of moderately halotolerant selenate-and tellurite-reducing bacteria isolated from brackish areas in Osaka. Biosci. Biotech. Biochem. 82 (1), 173–181.

Taylor, D.E., 1999. Bacterial tellurite resistance. Trends Microbiol. 7 (3), 111–115.

Tamura, K., Stecher, G., Peterson, D., Filipski, A., Kumar, S., 2013. MEGA6: molecular evolutionary genetics analysis version 6.0. Mol. Biol. Evol. 30 (12), 2725–2729. https://doi.org/10.1093/molbev/mst197.

Tchounwou, P.B., Yedjou, C.G., Patlolla, A.K., Sutton, D.J., 2012. Heavy Metal Toxicity and the Environment: Molecular, Clinical and Environmental Toxicology. Basel, Springer, pp. 133–164.

Trutko, S.M., Akimenko, V.K., Suzina, N.E., Anisimova, L.A., Shlyapnikov, M.G., Baskunov, B.P., Duda, V.I., Boronin, A.M., 2000. Involvement of the respiratory chain of Gram-negative bacteria in the reduction of tellurite. Arch. Microbiol. 173 (3), 178–186. https://doi.org/10.1007/s002039900123.

Turner, R.J., Weiner, J.H., Taylor, D.E., 1992. Use of diethyldithiocarbamate for quantitative determination of tellurite uptake by bacteria. Anal. Biochem. 204 (2), 292–295. https://doi.org/10.1016/0003-2697(92)90240-8.

Valdivia-González, M.A., Díaz-Vásquez, W.A., Ruiz-León, D., Becerra, A.A., Aguayo, D.R., Pérez-Donoso, J.M., Vásquez, C.C., 2018. A comparative analysis of tellurite detoxification by members of the genus Shewanella. Arch. Microbiol. 200 (2), 267–273. https://doi.org/10.1007/s00203-017-1438-2.

Xi, G., Peng, Y., Yu, W., Qian, Y., 2005. Synthesis, characterization, and growth mechanism of tellurium nanotubes. Cryst. Growth Des. 5 (1), 325–328.

Yuan, Q.L., Yin, H.Y., Nie, Q.L., 2013. Nanostructured tellurium semiconductor: from nanoparticles to nanorods. J. Exp. Nanosci. 8 (7–8), 931–936. https://doi.org/10.1080/17458080.2011.620021.

Zare, B., Faramarzi, M.A., Sepehrizadeh, Z., Shakibaie, M., Rezaie, S., Shahverdi, A.R., 2012. Biosynthesis and recovery of rod-shaped tellurium nanoparticles and their bactericidal activities. Mater. Res. Bull. 47 (11), 3719–3725. https://doi.org/10.1016/j.materresbull.2012.06.034.

Zonaro, E., Lampis, S., Turner, R.J., Junaid, S., Vallini, G., 2015. Biogenic selenium and tellurium nanoparticles synthesized by environmental microbial isolates efficaciously inhibit bacterial planktonic cultures and biofilms. Front. Microbiol. 6, 584. https://doi.org/10.3389/fmicb.2015.00584.

Proc. Natl. Acad. Sci., India, Sect. B Biol. Sci.
https://doi.org/10.1007/s40011-018-1034-5

RESEARCH ARTICLE

Application of Marine Bacteria Associated with Seaweed, *Ulva lactuca*, for Degradation of Algal Waste

Milind Mohan Naik[1] · Diksha Naik[1] · Lakshangy Charya[1] · Sajiya Y. Mujawar[1] · Diviya C. Vaingankar[1]

Received: 23 April 2018 / Revised: 14 June 2018 / Accepted: 15 September 2018

Abstract In the present study, three marine *Ulva lactuca*-associated bacteria capable of producing agarase, λ-carrageenase, amylase, cellulase and protease were isolated from rocky intertidal region of Anjuna beach, Goa, India, and designated as DM1, DM5 and DM15. Based on 16S rRNA sequence analysis and biochemical tests, bacteria were identified as *Vibrio brasiliensis*, *Bacillus subtilis* and *Pseudomonas aeruginosa*. Bacteria DM1, DM5 and DM 15 could able to utilize seaweed waste (*Sargassum* powder) in seawater-based media by releasing reducing sugars, 503.3 ± 17.5 µg/ml, 491.6 ± 20 µg/ml and 376.6 ± 16 µg/ml, respectively, which was confirmed through 3,5-dinitrosalicylic acid method. Therefore, the eco-friendly reuse of seaweed waste is possible by using marine bacteria for the production of reducing sugars in ethanol-producing industry. All three bacterial isolates were found to produce indole acetic acid (IAA) at concentration 98 ± 12 µg/ml, 113.6 ± 13 µg/ml and 121.6 ± 8.5 µg/ml, respectively. Nitrogen fixation by bacterial strains was confirmed when they showed growth on artificial seawater devoid of nitrogen and comprising of 5% carrageenan as a sole source of carbon and gelling agent. Photosynthetic seaweed, *Ulva lactuca,* provides organic carbon and O_2 for associated bacteria and associated bacteria fix atmospheric N_2 and provides iron by siderophore production and synthesize hormone IAA for algal growth during their cooperative association.

Keywords Seaweed · Associated bacteria · Polysaccharide · Enzymes · Cooperative association

Significance statement *Ulva lactuca*-associated marine bacteria were found capable of degrading algal waste and therefore can be used to bioremediate marine sites polluted with algal waste.

Electronic supplementary material The online version of this article (https://doi.org/10.1007/s40011-018-1034-5) contains supplementary material, which is available to authorized users.

✉ Milind Mohan Naik
milindnaik4@gmail.com

Diksha Naik
dikshanaik606@gmail.com

Lakshangy Charya
lakshangyscharya@gmail.com

Sajiya Y. Mujawar
sajiyamujawar@gmail.com

Diviya C. Vaingankar
vaingankardivya@gmail.com

[1] Department of Microbiology, Goa University, Goa, India

Introduction

Marine macroalgae are diverse photosynthetic eukaryotes and play an important ecological role in sustainable productivity of rocky intertidal coastal areas [1]. Marine macroalgal biomass is mainly composed of polysaccharides, and marine heterotrophic bacteria are primarily responsible for cycling of polysaccharide in marine environment [2]. Carrageenan and agar which are component of algal cell wall in marine ecosystem constitute a massive biomass and therefore a valuable carbon source for marine heterotrophic bacteria [2]. Extracellular substances released from marine macroalgae also serve as food for diverse associated bacteria in coastal ecosystems [3]. Macroalgae-associated marine bacteria benefit from organic compounds produced by a host macroalgae, and bacteria, in turn, provide CO_2, minerals, produce auxin and fix atmospheric N_2 and play a crucial role in algal health [2, 4]. Marine environment is a potential source of

Published online: 24 September 2018

microbial enzymes having novel biochemical and functional properties which are very important in industries [4]. Moreover, seaweed-associated bacteria also produce a variety of industrially important enzymes viz. carrageenase, agarases, esterases, cellulase, amylases, phosphatases, lipases, ureases and β-galactosidases inured to be able to assimilate macroalgal organic compounds and play important role in carbon, nitrogen and sulphur cycles [4–8]. Marine bacteria, and in particular those associated with macroalgae, are potential source of novel carbohydrate-active enzymes [5]. Therefore, multiple polysaccharide-degrading bacteria associated with macroalgae play a main role in recycling of carbon from algal complex polysaccharides (CPs) in marine environment [6–8].

Macroalgae contribute significantly to global primary production and are composed of agar and carrageenan, which find their application as constituents in food, personal care, laboratory experiments in microbiology and cosmetic industries owing to their gelling and emulsifying properties [2]. Agar is a polysaccharide and consists of mixture of agarose and agaropectin. In agar, structural repeats are D-galactose and 3,6-anhydro-L-galactose with alternate α-1,3- and β-1,4-linkages, with various residues such as hydroxyl, sulphate and methoxyl. Agar is obtained from the cell walls of Gelidium and Gracilaria [9] and has been extensively used in various laboratory and industrial applications, due to its jellifying properties [10]. There are two types of agarases: α-agarase and β-agarase depending on the cleavage site; α-agarases recognize and cleave α-1,3 linkages of agarose to yield agaro-oligosaccharides, whereas β-agarases identify and cleave β-1,4 linkages of agarose to produce neoagaro-oligosaccharides [5]. Cell walls of marine red seaweeds are also made up of sulphated galactans known as carrageenan, and depending on the number of sulphate ester groups and their position, carrageenans are classified [11]. The most sulphated carrageenan containing at least three sulphates per disaccharide unit is λ-carrageenan (most negatively charged and form highly viscous solutions) followed by *i-iota* (two SO_4 group) and *k*-kappa carrageenan (one SO_4 group). All three carrageenans are made up of linear chains of galactose with alternating α-(1 $\rightarrow$ 3) and β-(1 $\rightarrow$ 4) linkages. Seaweeds also comprise of polysaccharides like starch and cellulose, which are degraded by amylases and cellulases produced by bacteria. Among multiple polysaccharide-degrading (MPD) marine bacteria isolated in recent years which play a significant role in recycling of carbon from complex polysaccharide (CP), *Saccharophagus degradans* and *Microbulbifer* are dominant MPD bacteria [12]. There are ample of reports on marine bacteria producing agarases and carrageenases[13–19], but there are very few reports on marine macroalgae-associated bacteria producing agarases and carrageenases [12, 20]. Cell wall of seaweed comprises array of heterologous polysaccharides and promotes biofilm formation by complex polysaccharide (CP)-degrading bacteria by offering unique econiche [12]. But still the relationship between macroalgae and associated bacteria is poorly understood.

Modification of repeating units of algal polysaccharide with diverse functional groups such as sulphate, methoxy and hydroxyl makes them recalcitrant [12]. Domestic food waste, microbiology laboratory waste and industrial waste containing carrageenan and agar are directly discharged into marine water bodies which persist for long time and affect marine biota, and therefore, there is pressing need to remove these pollutants from marine-polluted sites or treated before discharging into marine environment. Therefore, isolation of multiple polysaccharide-degrading (MPD) marine bacteria is very crucial which serve as potential candidates for eco-friendly degradation of macroalgal waste. In the present study, the authors are investigating marine alga (*Ulva lactuca*)-associated potential agar, carrageenan, starch, cellulose and protein-degrading bacteria for bioremediation of marine environment polluted with algal waste and also to study cooperative association between seaweed *Ulva lactuca* and associated bacteria.

Material and Methods

Collection of Marine Macroalgae

Marine macroalgae (*Ulva lactuca*) [21] were collected from rocky intertidal zone of Anjuna Goa, India, using sterile forceps in sterile Petri plates. *Ulva lactuca* samples were immediately processed to isolate of macroalgae-associated bacteria.

Isolation of Agarase-Producing Marine *Ulva lactuca*-Associated Bacteria

For isolation of *Ulva lactuca*-associated agarase-producing bacteria, *Ulva lactuca* (approx 1 g) was gently rinsed with sterile seawater and then suspended in 50 ml sterile seawater in Erlenmeyer flask and kept on incubator shaker for 1 h at room temperature (RT) with constant shaking at 250 rpm. Algae are removed aseptically from flask, and resultant seawater suspension (0.1 ml) was spread plated on seawater-based agar medium (2% agar without any other added carbon source) and incubated at RT (28 $\pm$ 2 °C) for 24–48 h. Colonies, which showing proper depression in agar plates, were selected as potential agarase-producing marine bacteria. Agarase production was further confirmed by flooding plates with Lugol's iodine and observing zone of clearance around colony [12]. Best

agarase-producing bacteria were selected based on size of zone of clearance after adding Lugol's iodine.

λ-Carrageenase Production by *Ulva lactuca*-Associated Marine Bacteria

Carrageenase production by selected agarase-producing marine *Ulva lactuca*-associated bacteria was checked by spot inoculating bacterial isolates on seawater-based media plate (5% carrageenan as gelling agent without any other added carbon source) and incubated at RT (28 ± 2 °C) for 48 h. Then, agar plate was flooded with phenol red [12].

Production of Cellulase, Amylase and Protease by *Ulva lactuca*-Associated Bacteria

Amylase production by *Ulva lactuca*-associated bacteria was checked by spot inoculating on seawater-based starch agar plate (1.5% agar with 2% starch) and incubated at RT (28 ± 2 °C) for 24 h. After incubation, starch agar plate was flooded with iodine solution. Also, starch utilization was checked in sea water-based broth containing 2% starch as sole, a source of carbon and incubated at RT (28 ± 2 °C) for 24 h with constant shaking at 150 rpm. Cellulase production was checked by spot inoculating on seawater-based agar plates containing 1% carboxymethyl cellulose (CMC) and incubated at RT (28 ± 2 °C) for 48 h. Plates were flooded with 1% (w/v) congo red and allowed to stand for 15 min, and after pouring out excess congo red, plates were flooded with 1 M NaCl solution (decolourization). Excess NaCl solution was discarded after incubating for 15 min. This step was repeated three times to wash off excess unbound congo red. The zone of clearance around colony [22] was observed. Protease activity was checked by spot inoculating on skim milk agar and incubated at RT (28 ± 2 °C), and zone of clearance around bacterial colony was observed.

Identification of Seaweed-Associated Bacteria

Identification of seaweed-associated bacterial isolates was done based on biochemical tests and 16S rDNA sequencing. PCR amplification of 16S rDNA was done using following eubacterial primers: 27F (5′ AGA GTT TGA TCM TGG CTC AG 3′) and 1492R (5′ CGG TTA CCT TGT TAC GAC TT 3′). 16S rDNA sequencing was done at Eurofins Genomics Pvt. Ltd., Bangalore. 16S rDNA sequence was compared against GenBank database using NCBI BLAST search [23].

Nitrogen-Fixing Potential and Auxin-Producing Potential of *Ulva lactuca*-Associated Bacteria

Nitrogen fixation by *Ulva lactuca*-associated bacteria was tested by growing strains DM1, DM5 and DM15 on artificial seawater devoid of nitrogen and containing 5% carrageenan as a sole source of carbon and gelling agent and incubated at RT (28 ± 2 °C) for 48 h [24]. The appearance of colonies on artificial seawater-based media devoid of N_2 after 48 h was observed, which will confirm N_2-fixing ability of isolates, and then plates were flooded with 1% phenol red. See colour change around bacterial colony after flooding with phenol red. Indole acetic acid (IAA) production by seaweed-associated bacteria was tested by inoculating bacterial isolates in Zobell marine broth containing tryptophan and incubated at RT (28 ± 2 °C) for 24 h. After incubation, culture broth was centrifuged at 8000 rpm for 5 min and culture supernatant (1 ml) was mixed with 2 ml Salkowski's reagent (2% of 0.5 M $FeCl_3$ in 35% $HClO_4$ solution) and one drop of orthophosphoric acid and kept in the dark for 30 min. The optical density (OD) was recorded at 530 nm [25, 26]. The concentration of IAA was determined using standard calibration curve of pure IAA following linear regression analysis.

Siderophore Production

Siderophore production by *Ulva lactuca*-associated bacteria was checked by spot inoculating on chrome azurol S agar (CAS) plates and incubated at RT (28 ± 2 °C) for 48 h [27].

Seaweed Waste (*Sargassum* powder) Degradation by *Ulva lactuca*-Associated Bacteria

Sargassum algae were collected from Anjuna beach and sun-dried for 1 month. The dried *Sargassum* samples were ground using mortar and pestle/electronic mixer to make fine powder and used as algal waste. Seawater-based agar was prepared by using 2% ground *Sargassum* powder as carbon source, and 1.5% agar was added as gelling agent. Selected bacterial cultures were spot inoculated and incubated at RT (28 ± 2 °C) for 48 h. The plate was flooded with Lugol's iodine, and zone of clearance around bacterial colony was observed. Seawater-based broth was prepared by using 2% ground *Sargassum* powder as a sole carbon source and sterilized. Broth was inoculated with bacterial culture and incubated for 72 h with constant shaking at 150 rpm. After 72 h incubation, culture broth (5 ml) was centrifuged at 8000 rpm to pellet bacterial cells and supernatant was taken in another tube and reducing sugar was analysed by 3,5-dinitrosalicylic acid (DNSA) method [28], which measures the release of reduced sugar from

algal waste equivalents at 540 nm, with D-galactose as a standard. Appropriate control was kept, and all experiments were performed in triplicate.

Results and Discussion

Isolation of Agarase-Producing Marine *Ulva lactuca*-Associated Bacteria

Twenty-three bacterial colonies which showing proper depression in agar plates were selected as potential agarase-producing marine bacteria. Out of 23 agarase-producing bacteria, only three bacterial isolates which show the best (highest) depression in agar plates were selected for further study and designated as DM1, DM5 and DM15. Agarase production was further confirmed by zone of clearance around colonies, and rest of the plates stained dark brown when plates were flooded with Lugol's iodine. It was also observed that bacterial isolates DM1, DM5 and DM15 showed maximum zone of clearance among 23 isolates and hence selected (Fig. 1).

Carrageenase Production by Marine *Ulva lactuca*-Associated Bacteria

Growth of all three (DM1, DM5 and DM15) selected *Ulva lactuca*-associated bacterial isolates on seawater-based media plate (5% carrageenan as gelling agent without any other added carbon source) was observed after incubation at RT (28 ± 2 °C) for 48 h which confirms utilization (degradation) of carrageenase. This was further confirmed by production of yellow zone around colonies of DM1 and DM5 due to the production of acidic product during carrageenan degradation (Fig. 2) which changed the colour of phenol red from red to yellow. *Microbulbifer* strain CMC-5 showed similar results [12]. Interestingly, bacterial isolate DM15 showed pink colouration around colony when flooded with phenol red which indicate alkaline product formation during degradation of carrageenan which increase the pH and change colour of phenol red from red to dark pink (Fig. 2).

Production of Cellulase, Amylase Protease

All three *Ulva lactuca*-associated bacterial isolates produced amylase, protease and cellulase. Amylase production was confirmed when zone of clearance around bacterial colonies was seen after adding iodine solution, whereas rest of plate stained dark blue. Also, growth in sea water-based broth containing 1% starch as sole source of carbon confirmed amylase production. Cellulase production was detected when zone of clearance was observed around bacterial colonies and rest of plate stained dark red colour (Fig. 3a, b). Protease activity was confirmed when zone of clearance was seen around colonies spot inoculated on skim milk agar due to casein hydrolysis.

Identification of Seaweed-Associated Bacteria

The 16S rDNA sequence analysis was followed by NCBI BLAST search and biochemical tests (Supplementary data 1) by referring to Bergey's manual of systematic bacteriology [29]. The authors confirmed multiple polysaccharide-degrading *Ulva lactuca*-associated bacteria which were identified as *Vibrio brasiliensis* strain DM1, *Bacillus subtilis* strain DM5 and *Pseudomonas aeruginosa* strain

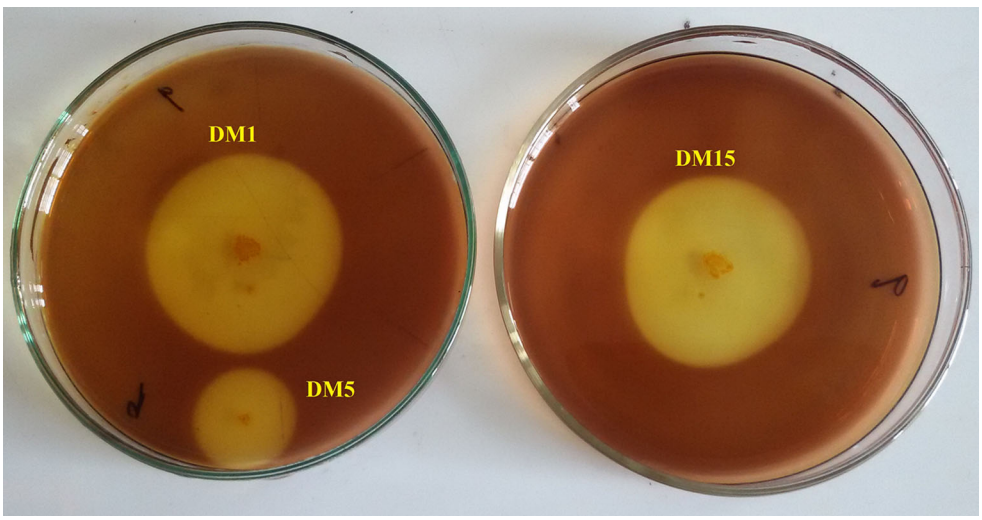

Fig. 1 Agarase production by bacterial strains DM1, DM5 and DM15 on seawater-based agar medium with 2% agar as sole source of carbon

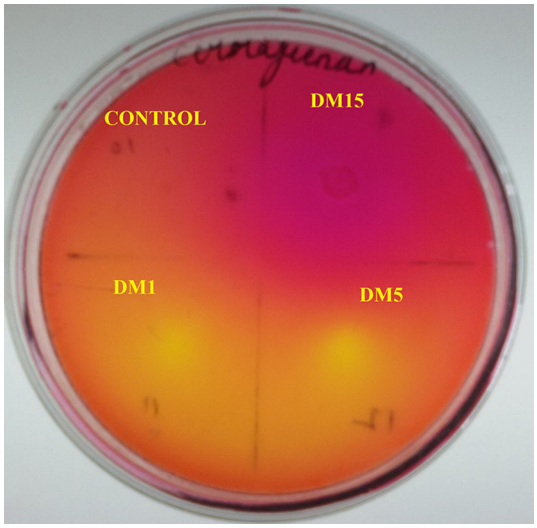

Fig. 2 Carrageenase production by marine *Ulva lactuca*-associated bacterial isolates DM1, DM5 and DM15 on seawater-based agar amended with 5% carrageenan as carbon source and gelling agent

DM15 (GenBank accession nos. MG971393, MG972930 and MG971397, respectively).

Nitrogen-Fixing and Auxin-Producing Potential of *Ulva*-Associated Bacteria

Nitrogen fixation by *Ulva lactuca*-associated bacterial strains DM1, DM5 and DM15 was confirmed when they showed growth on artificial seawater devoid of nitrogen and 5% carrageenan as sole source of carbon and gelling agent when incubated at RT (28 ± 2 °C) for 48 h. *Vibrio brasiliensis* strain DM1 and *Bacillus subtilis* strain DM5 showed yellow colouration around colonies when flooded with phenol red. This is due to breakdown of carrageenan into sugars and subsequently fermentation of sugars producing sufficient acids to which colour of phenol red changed to yellow. *Pseudomonas aeruginosa* strain DM15 showed pink colouration around colonies when flooded with phenol red. *Pseudomonas aeruginosa* strain DM15 breakdowns carrageenan into sugars, but *Psedomonas aeruginosa* DM15 is unable to ferment sugars (oxidative metabolism) and produce acids. Pink colour around DM15 colony is due to ammonium secretion by bacterial cells during nitrogen fixation which increases pH to alkaline and thus colour of phenol red changed from red to pink (Supplementary data 2). Nitrogen-fixing *Paenibacillus* strain and *Azotobacter vinelandii* are capable of secreting ammonium outside cell and changing the pH [30, 31]. Indole acetic acid (IAA) production by seaweed-associated bacteria was confirmed by getting pink colour after adding Salkowski's reagent along with one drop of orthophosphoric acid and keeping it in dark for 30 min. It was further confirmed by specific absorption by IAA at 530 nm. IAA concentration produced by DM1, DM5 and DM15 was determined as 98 ± 12, 113.6 ± 13 and 121.6 ± 8.5 µg/ml, respectively (Fig. 4).

Siderophore Production

All three bacterial isolates showed orange halo around colonies on CAS agar plates, thus confirming siderophore-producing potential of *Ulva lactuca*-associated bacterial isolates. *Ulva lactuca*-associated bacteria producing siderophores may be helping *Ulva lactuca* to uptake iron from seawater during iron-limiting conditions and thus promoting their growth (Fig. 5).

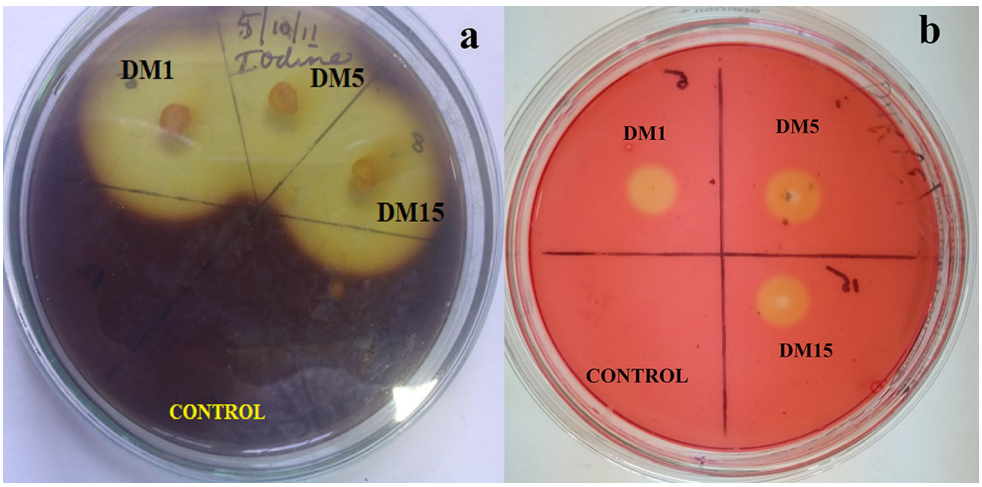

Fig. 3 **a**, **b** Amylase and cellulase production by marine *Ulva lactuca*-associated bacterial isolates DM1, DM5 and DM15 on casein agar, starch agar and CMC agar plates

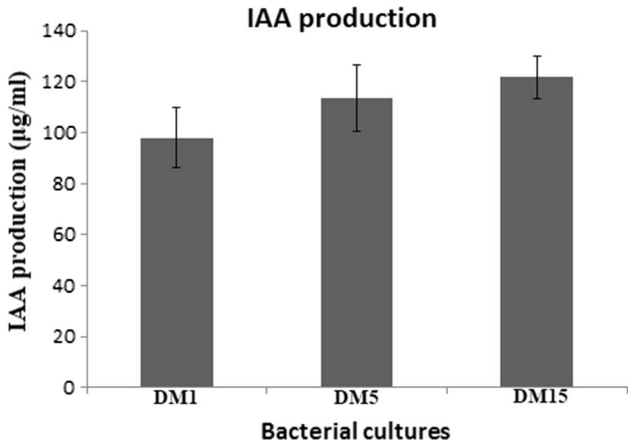

Fig. 4 IAA production by marine *Ulva lactuca*-associated bacterial isolates DM1, DM5 and DM15

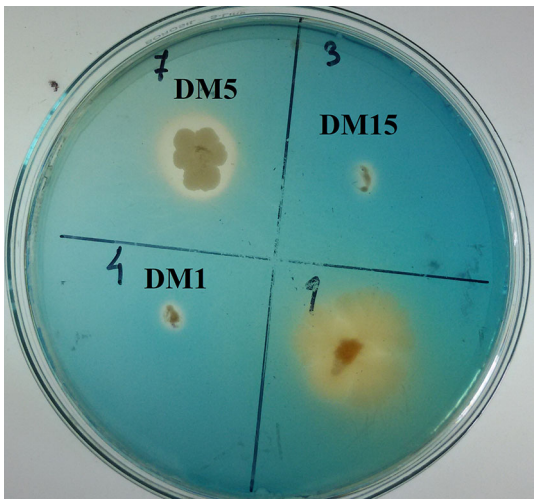

Fig. 5 Siderophore production by marine *Ulva lactuca*-associated bacterial isolates DM1, DM5 and DM15 on CAS agar plates

Seaweed Waste Degradation by Marine *Ulva lactuca*-Associated Bacteria

Potential of seaweed-associated bacteria *Vibrio brasiliensis* strain DM1, *Bacillus subtilis* strain DM5 and *Pseudomonas aeruginosa* strain DM15 for degradation of seaweed waste was confirmed when all three isolates grew on seawater-based agar containing 2% ground *Sargassum* powder as a carbon source and 1.5% agar as gelling agent. Zone of clearance around bacterial colonies after adding Lugol's iodine supported the results (Supplementary data 3). Furthermore, utilization of seaweed powder as a sole source of carbon in seawater-based broth by all three bacterial isolates was confirmed by analysing release of reducing sugar using DNSA method. Through DNSA method, it was confirmed that reducing sugar released after 72 h by DM1, DM5 and DM 15 was 503.3 ± 17.5, 491.6 ± 20 and 376.6 ± 16 µg/ml, respectively (Fig. 6) which is much higher than previous study on *Microbulbifer* Strain CMC-5, isolated from decomposing seaweed by Jonnadula et al. [6]. Jonnadula et al. [6] reported that *Microbulbifer* strain CMC-5 releases only 60 µg/ml reducing sugar from seaweed after 120 h. *Bacillus* sp. SYR4 possessing both agarase and carrageenase activities was studied for its application for reuse of red seaweed waste [17]. When the isolate was cultivated in red seaweed powder medium for 10 days, the reducing sugar released was 24 µg/ml which is much lower than the present report. This confirmed that the *Ulva lactuca*-associated bacterial isolates have better potential for agar waste degradation than previously reported bacterial isolates. Therefore, the eco-friendly reuse of red seaweed waste by these *Ulva lactuca*-associated bacterial isolates appears to be feasible for the production of reducing sugars and could be a valuable resource for ethanol-producing industry.

In recent years, seaweed waste has been increased tremendously owing to two reasons: one is rapid growth of macroalgae due to anthropogenic input of inorganic nutrients (eutrophication); another is culturing of seaweeds on large scale as an industrial resource [32]. Therefore, treatment of seaweed waste using marine bacteria is very crucial for preservation and sustainable development of marine environment. Therefore, *Ulva lactuca*-associated bacterial isolates *Vibrio brasiliensis* strain DM1, *Bacillus subtilis* strain DM5 and *Pseudomonas aeruginosa* strain DM15 can be exploited for degrading multiple polysaccharides or bioremediation of marine environment. Apart from bioremediation of algal waste from marine environments, DM1, DM5 and DM15 isolates producing agarase and carrageenase can be applied to recover DNA from agarose gel, prepare protoplasts, and produce agar/carrageenan-derived oligosaccharides having multiple applications such as improving food quality, antioxidation,

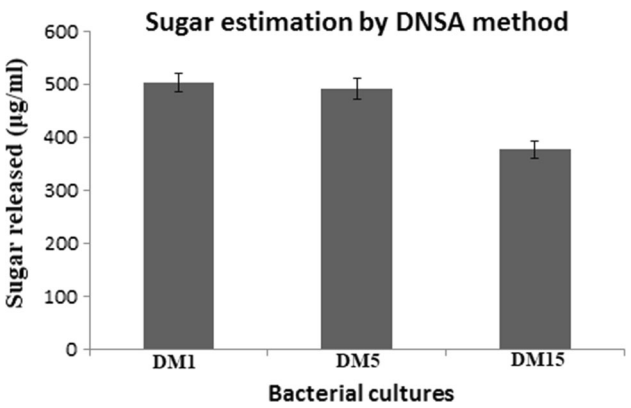

Fig. 6 Sugar released during degradation of algal waste (sargassum) by marine *Ulva lactuca*-associated bacterial isolates DM1, DM5 and DM15 in sea water-based broth

whitening and moisturization [2]. Using agarase and carrageenase enzyme, seaweed waste can also be used for bioethanol production, i.e. for initial hydrolysis of algal waste for reducing sugar production and then fermentation using *Saccharomyces cerevisiae*.

Marine macroalgae are known to hold a large number of associated heterotrophic bacteria which contribute to their survival processes. Macroalgae-bacterial relationship mainly depends on production of organic matter (food) and oxygen which are used by bacteria. Moreover, marine macroalgae-associated bacteria are reported to provide CO_2 and minerals [4]. Some bacteria excrete auxins, siderophores and fix atmospheric N_2 enhancing cell division and growth of macroalgae [1, 4]. Also, it has been reported that macroalgae-associated bacteria produce acyl homoserine lactone (AHL), which plays a great role in growth and development of *Gracilaria dura* [3]. The study also associated all three seaweed marine bacteria which produced a significant amount of algal growth-promoting substance—auxin, fixed atmospheric nitrogen and produced iron-chelating siderophores, whereas, seaweed (*Ulva lactuca*) provided polysaccharide as food for bacteria thus proved their cooperative association.

Conclusion

Three multiple polysaccharide-degrading seaweed (*Ulva lactuca*)-associated bacteria *Vibrio brasiliensis* strain DM1, *Bacillus subtilis* strain DM5 and *Pseudomonas aeruginosa* strain DM15 producing multiple enzymes viz. agarase, carrageenase, amylase, protease and cellulase were isolated. These bacterial strains were found to degrade algal waste and therefore can be used to bioremediate marine sites polluted with algal waste. All three bacterial isolates were found to have potential of fixing atmospheric nitrogen and siderophore production; therefore, the authors can use these bacteria to bioremediate marine sites polluted with algal waste without using biostimulation strategy (addition of NO_3 and Fe to enhance microbial bioremediation). Also, all three bacterial cultures were found positive for IAA, and therefore, the authors conclude that seaweed provides organic carbon and O_2 for bacteria and associated bacteria in turn fix atmospheric N_2 for seaweed in nitrogen-limiting ocean water and also provide hormone IAA and siderophores for algal growth during their cooperative association.

Acknowledgements The authors thank the Science and Engineering Research Board (SERB), Department of Science and Technology, Government of India, for financial support as Young Scientist Project (File Number: YSS/2014/000258). They are also thankful to Prof. S.K. Dubey, Prof. Sandeep Garg and Dr. Shyamalina Haldar (all from), Department of Microbiology, Goa University, Goa.

Compliance with Ethical Standards

Conflict of interest The authors declare that they have no conflict of interest to publish this manuscript.

References

1. Singh RP, Reddy CRK (2016) Unravelling the functions of the macroalgal microbiome. Front Microbiol. https://doi.org/10.3389/fmicb.2015.01488
2. Ficko-Blean E, Préchoux A, Thomas F, Rochat Larocque R, Zhu Y, Stam M, Génicot S, Jam M, Calteau A, Viart B, Ropartz D, Pérez-Pascual D, Correc G, Matard-Mann M, Stubbs KA, Rogniaux F, Jeudy A, Barbeyron T, Médigue C, Czjzek M, Vallenet D, McBride MJ, Duchaud E, Michel G (2017) Carrageenan catabolism is encoded by a complex regulon in marine heterotrophic bacteria. Nat Commun. https://doi.org/10.1038/s41467-017-01832-6
3. Singh RP, Baghel R, Reddy CRK, Jha B (2015) Effect of quorum sensing signals produced by seaweed-associated bacteria on carpospore liberation from *Gracilaria dura*. Front Plant Sci. https://doi.org/10.3389/fpls.2015.00117
4. Comba-González NB, Ruiz-Toquica JS, López-Kleine L, Montoya-Castaño D (2016) Epiphytic bacteria of macroalgae of the genus *Ulva* and their potential in producing enzymes having biotechnological interest. J Mar Biol Ocean. https://doi.org/10.4172/2324-8661.1000153
5. Alvarado R, Leiva S (2017) Agar-degrading bacteria isolated from Antarctic macroalgae. Folia Microbiol 62:409–4016
6. Jonnadula RC, Verma P, Shouche YS, Ghadi SC (2009) Characterization of *Microbulbifer* Strain CMC-5, a new biochemical variant of *Microbulbifer elongatus* type strain DSM6810T isolated from decomposing seaweeds. Curr Microbiol 59:600–607
7. Martin M, Portetelle D, Michel G, Vandenbol M (2014) Microorganisms living on macroalgae: diversity, interactions, and biotechnological applications. Appl Microbiol Biotechnol 98:2917–2935
8. Martin M, Barbeyron T, Martin R, Portetelle D, Michel G, Vandenbol M (2015) The cultivable surface microbiota of the brown Alga *Ascophyllum nodosumis* enriched in macroalgal-polysaccharide-degrading bacteria. Front Miocrobiol. https://doi.org/10.3389/fmicb.2015.01487
9. Song T, Zhang W, Wei C, Jiang T, Xu H, Cao Y, Cao Y (2015) Isolation and characterization of agar-degrading endophytic bacteria from plants. Curr Microbiol 70:275–281
10. Chi WJ, Chang YK, Hong SK (2012) Agar degradation by microorganisms and agar-degrading enzymes. Appl Microbiol Biotechnol 94:917–930
11. Guibet M, Colin S, Barbeyron T, Genicot S, Kloareg B, Michel G, Helbert W (2007) Degradation of λ-carrageenan by *Pseudoalteromonas carrageenovora* λ-carrageenase: a new family of glycoside hydrolases unrelated to κ- and ι-carrageenases. Biochem J 404:105–114
12. Imran Md, Poduval PB, Ghadi SC (2017) Bacterial degradation of algal polysaccharides in marine ecosystem. In: Naik MM, Dubey SK (eds) Marine pollution and microbial remediation. Springer, Berlin, pp 196–202
13. Shieh WY, Simidu U, Maruyama Y (1988) Nitrogen fixation by marine agar-degrading bacteria. J Gen Microbiol 134(1821–1): 825
14. Hu Z, Lin BK, Xu Y, Zhong MQ, Liu GM (2009) Production and purification of agarase from a marine agarolytic bacterium *Agarivorans* sp. HZ105. J Appl Microbiol 106:181–190

15. Vashist P, Nogi Y, Ghadi SC, Verma P, Shouche YS (2013) *Microbulbifer mangrovi* sp. nov., a polysaccharide-degrading bacterium isolated from an Indian mangrove. Int J Syst Evol Microbiol 63:2532–2537
16. Yao Z, Wang F, Gao Z, Jin L, Wu H (2013) Characterization of a κ-carrageenase from Marine *Cellulophaga lytica* strain N5-2 and analysis of Its degradation products. Int J Mol Sci 14:24592–24602
17. Kang S, Kim JK (2015) Reuse of red seaweed waste by a novel bacterium, *Bacillus* sp. SYR4 isolated from a sandbar. World J Microbiol Biotechnol 31:209–217
18. Liu G, Wu S, Jin W, Sun C (2016) Amy63, a novel type of marine bacterial multifunctional enzyme possessing amylase, agarase and carrageenase activities. Sci Rep. https://doi.org/10.1038/srep18726
19. Chauhan PS, Saxena A (2016) Bacterial carrageenases: an overview of production and biotechnological applications. 3 Biotech 6:146–163
20. Singh RP, Reddy CRK (2014) Seaweed–microbial interactions: key functions of seaweed-associated bacteria. FEMS Microbiol Ecol 88:213–230
21. Kerkar V (2004) Addition to the marine algal flora of Goa. Seaweed Res Util 26:19–21
22. Liang YL, Zhang Z, Wu M, Wu Y, Feng JX (2014) Isolation, screening, and identification of cellulolytic bacteria from natural reserves in the subtropical region of China and optimization of cellulase production by *Paenibacillus terrae* ME27-1. BioMed Res Int. https://doi.org/10.1155/2014/512497
23. Altchul SF, Madden TL, Schaffer AA, Zhang J, Zhang Z, Miller W, Lipman DJ (1997) Gapped BLAST and PSIBLAST: a new generation of protein database search programs. Nucleic Acids Res 25:3389–3402
24. Komives CF, Cheung LY, Pluschkell SB, Flickinger MC (2005) Growth of *Bacillus methanolicus* in seawater-based media. J Ind Microbiol Biotechnol 32:61–66
25. Bano N, Musarrat J (2003) Characterization of new *Pseudomonas aeruginosa* strain NJ-15 as a potential biocontrol agent. Curr Microbiol 46:324–328
26. Mohite B (2013) Isolation and characterization of indole acetic acid (IAA) producing bacteria from rhizospheric soil and its effect on plant growth. J Soil Sci Plant Nutr 13:638–649
27. Schwyn B, Neilands JB (1987) Universal chemical assay for the detection and determination of siderophores. Anal Biochem 160:47–56
28. Miller GL (1959) Use of dinitrosalicylic acid reagent for determination of reducing sugar. Anal Chem 31:426–428
29. Bergey DH, Kreig NR, Holt JG (1984) Bergey's manual of systematic bacteriology. Williams & Wilkins, Baltimore
30. Dariush S, Emtiazi G (2010) Ammonium production during the nitrogen-fixing process by wild *Paenibacillus* strains and cell-free extract adsorbed on nano TiO_2 particles. J Microbiol Biotechnol 20:1251–1258
31. Barney BM, Plunkett MH, Natarajan V, Mus F, Knutson CM, Peters JW (2017) Transcriptional analysis of an ammonium-excreting strain of *Azotobacter vinelandii* deregulated for nitrogen fixation. Appl Environ Microbiol. https://doi.org/10.1128/AEM.01534-17
32. Tang JC, Taniguchi H, Chu H, Zhou Q, Nagata S (2009) Isolation and characterization of alginate-degrading bacteria for disposal of seaweed wastes. Lett Appl Microbiol 48:38–43

Chapter 10

Biodegradation of seafood waste by seaweed-associated bacteria and application of seafood waste for ethanol production

Sanika Samant[1], Milind Mohan Naik[2,*], Diviya Chandrakant Vaingankar[2], Sajiya Yusuf Mujawar[4], Prachi Parab[2], Surya Nandan Meena[3]

[1]*Department of Biotechnology, Goa University, Goa, India;* [2]*Department of Microbiology, Goa University, Goa, India;* [3]*Biological Oceanography Division, National Institute of Oceanography, Dona Paula, Goa, India;* [4]*Laboratory of Bacterial Genetics and Environmental Biotechnology, Department of Microbiology, Goa University, Goa, India*

[*]*Corresponding author: milind@unigoa.ac.in; milindnaik4@gmail.com.*

10.1 Introduction

In recent years, seafood waste has increased tremendously, since during the processing of prawns, shrimps, and other shellfish mostly the meat is utilized while the shells, bones, and head portions are thrown as wastes into marine waters [1]. Fish production around the globe has increased tremendously and reached 174 million metric tons in 2017. India is the third largest producer of fishery around the globe and hence produces an enormous amount of fish waste [2]. India generates >2 metric million tons of waste during fish processing, of which 300,000 tons contribute to visceral waste alone [3]. Commercial processing of fish generates a significant amount of waste, which includes viscera, fins, scales, and bones [4]. This huge amount of discards (fishery waste) including solid wastes along with wastewater resulting from fishery processing are unutilized and usually disposed of in landfills, or dumped near shore and into the ocean without any pretreatment, causing environmental pollution, thus severely impacting aquatic biota health ailments [5,6]. Although these wastes are biodegradable, the process is very slow. This results in accumulation of fishery waste over time and pollutes coastal and marine environments due to bad odors and secretion of biogenic amines, thereby affecting marine life [7]. Due to

Advances in Biological Science Research. https://doi.org/10.1016/B978-0-12-817497-5.00010-0

foul odors, seafood waste in the marine environment attracts flies, insects, rodents, and other vermin, creating an unhygienic atmosphere. Fish waste is classified as certified waste because it is comprised of high organic content and is thus even more costly to dispose of [4]. In fish processing industries, acid, alkali, and heat treatments are used to degrade shell waste that is hazardous to the environment [8]. Hence, biodegradation of seafood waste using microorganisms is important as they can be used for polluted environment reclamation without harming natural biota. Bioremediation is ecofriendly and cost-effective as compared to physicochemical methods. Therefore, treatment of prawn shell, shellfish, and fish waste using marine bacteria is crucial for preservation and sustainable development of the marine environment.

The fish processing procedure involves removal of fish bones, scales, heads, and internal organs. Therefore, during the processing of seafood, a large amount of shell and scale waste is discarded from fish markets, seafood restaurants, fish-processing industries, and kitchens. Fish scales consist of protein, calcium phosphate, calcium carbonate, magnesium carbonate, chitin, and pigments [9]. Generally, crustacean shells consist mainly of 30%−50% calcium carbonate, 30%−40% protein, and 20%−30% chitin and calcium phosphate [4,10,11]. Shells also contain carotenoid pigments and a trace amount of lipids. The content of shell components varies with different species and seasons [12]. Therefore, to degrade seafood waste, bacteria possessing protease, chitinase activities, and phosphate and calcium carbonate solubilization properties will be of great importance. There are very few reports on the total degradation of seafood waste by bacteria. Microorganisms possessing proteolytic activity have been applied for the deproteinization of chemically demineralized shells [13]. Purification of chitin from shrimp wastes using microbial deproteination and decalcification activities has been demonstrated [7]. *Lactobacillus plantarum* and *Pseudomonas aeruginosa* were used for deproteinization and demineralization of crab shell and shrimp waste [1]. Two bacterial cultures, *Exiguobacterium acetylicum* and *Bacillus cereus*, were studied for their ability to decompose shrimp shell waste [14]. A *P. aeruginosa* strain, K-187, isolated from soil (in Taiwan) showing protease and chitinase activities when cultured in medium containing shrimp and crab shell wastes as sole carbon sources has been reported [15]. *Serratia marcescens* FS-3 strain exhibiting strong protease activity was isolated from soil toward the seaside of a southwestern region of Korea and was used for degradation of crab (*Chionoecetes opilio*) shell wastes [16].

Most of the above-mentioned studies demonstrate the use of chemicals in the seafood waste treatment process along with the use of microbial enzymes or microorganisms. Also, detail study on complete degradation of crab shell, prawn shell, and fish scale using bacteria has not yet been undertaken. Therefore, the current study focuses on isolation of seaweed-associated bacteria possessing the ability to degrade seafood waste such as scales, crab shell, and prawn shell waste by producing organic acids and hydrolytic enzymes and their

application in bioremediation of seafood waste. Here we also discuss studies on sustainable use of seafood waste for ethanol production.

10.2 Materials and methods

10.2.1 Collection of marine seaweed samples

Live and healthy seaweed samples (*Ulva* sp.) were collected from rocky intertidal regions of Anjuna Beach, Goa, India using sterile forceps in sterile petri plates. The samples were transported to the laboratory immediately under cool conditions for further analysis. *Ulva* sp. samples were processed for isolation of associated bacteria within 24 h.

10.2.2 Enrichment of *Ulva*-associated bacteria

For enrichment of *Ulva* sp.—associated bacteria, seaweed sample was rinsed gently two or three times with sterilized seawater to wash off sand particles and loosely bound bacteria. In order to isolate firmly associated bacteria, *Ulva* sp. was aseptically cut into 5-cm-long pieces and two pieces were inoculated into 50 mL sterile Zobell marine broth (ZMB) in 150-mL Erlenmeyer flask and incubated on shaker for 48 h at room temperature (RT, 28°C ± 2) with constant shaking at 150 rpm to enrich seaweed-associated bacteria.

10.2.3 Isolation of calcium carbonate solubilizing marine *Ulva*-associated bacteria

From enriched ZMB, seaweed pieces were removed aseptically and the broth was serially diluted up to 10^{-8} using sterile saline (2%) and spread plated (0.1 mL) on seawater-based agar containing 1% $CaCO_3$ and 0.4% glucose (pH 7). The plates were then incubated at room RT (28°C ± 2) for 48—72 h. Morphologically different calcium carbonate—solubilizing bacterial colonies showing a highest zone of clearance on agar were selected and purified for further study. These calcium carbonate—solubilizing bacterial cultures were maintained by regular subculturing on Zobell marine agar (HiMedia Laboratories) and stored at 4°C.

10.2.4 Investigating seafood waste (fish, crab, prawn waste) utilizing potential of selected calcium carbonate—solubilizing bacteria

10.2.4.1 Preparation of crab/prawn shell and fish scale powder

Crab shells, prawn shells, and fish scales were obtained from local markets. They were washed with distilled water, sun-dried for 1 week, and ground into a fine powder using an electronic mixer. This powder was then used as fish/crab/prawn waste for degradation studies.

10.2.4.2 Microbial utilization of seafood waste as a sole source of carbon

Seawater-based media was prepared in three different 50 mL conical flasks and 1% sterile crab shell, prawn shell, fish scale powder was added separately into three flasks as a sole carbon and nitrogen source (1.5% agar was added). Media was sterilized and poured into plates. Bacterial isolates were streaked on plates and incubated at RT (28°C ± 2) for 10 days. Plates were observed for bacterial growth.

Calcium-solubilizing bacterial isolates, which also showed the ability to utilize seafood waste as a sole carbon source, were further tested for their potential to produce protease, cellulase, chitinase, agarase, and phosphate-solubilizing activities.

10.2.5 Agarase production by marine *Ulva* sp.—associated bacteria

Bacterial isolates were plated on seawater-based agar medium (2% agar without any other added carbon source) and incubated at RT (28°C ± 2) for 24—48 h. Colonies were observed for depression in agar plates. Agarase production was also tested by flooding plates with Lugol's iodine and observing zone of clearance around colony [17]. Agarase activity was tested to rule out agar utilization by bacteria. The absence of agarase activity confirms the ability of organisms to utilize seafood waste as a sole carbon source.

10.2.6 Production of protease by *Ulva* sp.—associated bacteria

Ulva sp.—associated bacteria, which were found to be utilizing seafood waste as a sole source of carbon, were streaked on skim milk agar (HiMedia Laboratories) plates and incubated for 4 days at RT (28°C ± 2). Positive protease activity was indicated by a clear zone surrounding the bacterial streak/growth.

10.2.7 Phosphate solubilization by acid-producing *Ulva* sp.—associated bacteria

Bacterial isolates were streaked on seawater-based Pikovskaya's agar plates containing 0.05% bromothymol blue (Merck) and incubated at RT (28°C ± 2) for 72 h. Zone of clearance and yellow coloration around bacterial streak indicates phosphate solubilization due to acid production [18].

10.2.8 Cellulase production by *Ulva* sp.—associated bacteria

Bacterial isolates were streaked on seawater-based carboxymethyl cellulose agar (HiMedia Laboratories) and incubated at RT (28°C ± 2). After 4 days of incubation, plates were flooded with 1% Congo red solution (w/v) and allowed

to stand for 10 min. Excess stain was poured out gently and plates were flooded with 1M NaCl solution (destaining). After incubating for 10 min, excess NaCl solution was poured out. This step was repeated two times to wash off excess Congo red stain. Cellulase activity was indicated by a zone of clearance along the bacterial streak [19], whereas the rest of the plate stained dark red.

10.2.9 Production of chitinase by *Ulva* sp.–associated bacteria

Chitinase production by *Ulva* sp.–associated bacteria was checked by streaking on seawater-based agar plates containing 1% colloidal chitin as a sole carbon source and incubated at RT (28°C ± 2) for 4 days. Plates were flooded with 1% Congo red solution (w/v) and were allowed to stand for 10 min. Excess Congo red was discarded gently and plates were flooded with 1M NaCl solution (destaining). Excess NaCl solution was poured out gently after incubating for 15 min. This step was repeated twice to wash off excess Congo red stain. Chitinase activity was indicated by a zone of clearance along streak [20], whereas the rest of the plate stained dark red.

Bacterial isolates exhibiting calcium carbonate solubilizing, protease, chitinase, and cellulase activities were selected for the treatment of fish and shellfish waste by preparing consortia.

10.2.10 Degradation of fish/crab/prawn waste using microbial consortia developed using *Ulva* sp.–associated bacteria

Development of microbial consortia for seafood waste degradation is of utmost importance since improved degradation is achieved using microbial consortia as compared to individual isolates. Before using selected bacterial isolates as consortia for seafood degradation study, these isolates were tested by the cross-inhibition test. Test isolates were inoculated as a line in the center on the surface of Zobell marine agar and incubated at RT (28°C ± 2) for 20 h. Other isolates were inoculated as a perpendicular line to the test isolates, and plates were incubated at RT (28°C ± 2) for 48 h. Positive results were indicated by a zone of inhibition of growth of other isolates. This test was repeated for all the isolates. If bacterial isolates inhibit each other, then they cannot be used in consortia for degradation of seafood waste.

Three selected bacterial isolates were inoculated separately into 50 mL seawater-based broth containing 1% crab shell powder as a sole source of carbon for 4 days at RT (28°C ± 2) with shaking at 150 rpm. Then, 0.1 mL culture broth from each flask was added as inoculum into 100 mL seawater-based media in Erlenmeyer flask (250 mL) containing 2% crab shell powder and incubated at RT (28°C ± 2) with constant shaking at 150 rpm for 4 days. The test was performed in triplicate. Control was maintained containing seawater-based broth supplemented with 2% crab shell powder without

inoculum. After 4 days of incubation, 2 mL culture broth was collected under the aseptic condition and centrifuged at 8000 rpm for 10 min. The supernatant was taken in another tube and used for determining reducing sugars by DNSA method released during degradation of seafood waste [21]. Similar degradation study by consortia was repeated with prawn shell and fish scales in triplicate.

10.2.11 Identification of seaweed-associated bacteria

Three selected seaweed-associated bacteria having the potential of degrading seafood waste were identified by performing biochemical tests and referring to *Bergey's Manual of Systematic Bacteriology* [22] and also by using 16S rDNA gene sequence. Gene coding for 16S rRNA was amplified with universal eubacterial primers: 27F (5′ AGAGTTTGATCMTGGCTCAG 3′) and 1492R (5′ TACGGYTACCTTGTTACGACTT 3′). 16S rRNA sequence data were compared with GenBank database using BLAST.

10.3 Results and discussion

Nine morphologically different calcium carbonate—solubilizing seaweed-associated bacterial isolates showing a highest zone of clearance on agar were selected and purified for further studies. These nine bacterial isolates were designated as PM1, PM2, PM3, PM4, PM5, PM6, PM7, PM8, and PM9 (Fig. 10.1). Only three out of nine bacterial isolates—PM1, PM6, and PM9—were able to utilize crab shells, prawn shells, and fish scale powder as a sole carbon source in seawater-based agar after 10 days of incubation. Also, all three bacterial isolates didn't show growth on seawater-based agar media (agar

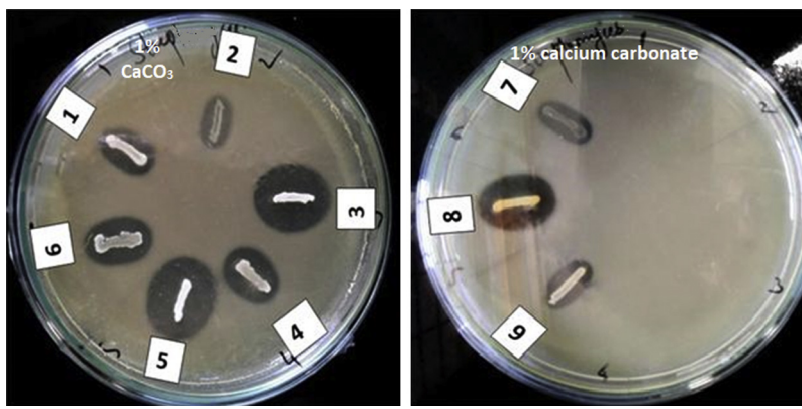

FIGURE 10.1 Calcium carbonate—solubilizing seaweed-associated bacterial isolates showing zone of clearance around colonies when streaked on seawater-based agar comprising 1% $CaCO_3$ and 0.4% glucose.

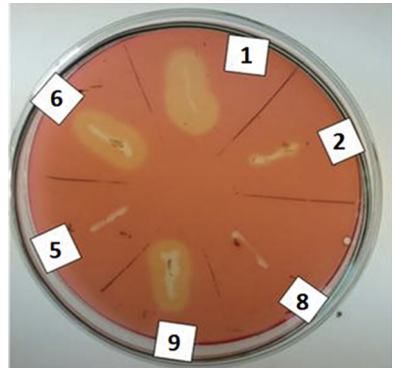

FIGURE 10.2 Seaweed-associated bacteria showing cellulase activity on seawater-based agar plates comprising 1% carboxymethyl cellulose (CMC) as a sole source of carbon.

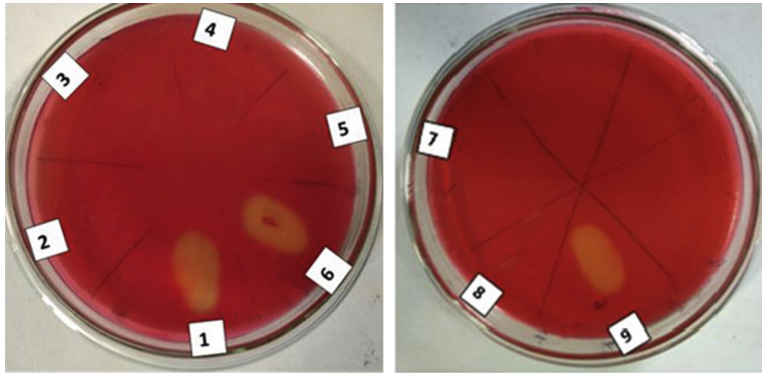

FIGURE 10.3 Seaweed-associated bacteria showing chitinase activity on seawater-based agar plates containing 1% colloidal chitin as a sole carbon source.

as the sole source of carbon), therefore, bacterial isolates PM1, PM6, and PM9 were selected for further studies since the absence of agarase activity confirms that organisms only utilize seafood waste as a sole source of carbon.

All three isolates PM1, PM6, and PM9 were found to be positive for protease, cellulase (Fig. 10.2), and chitinase (Fig. 10.3) activity and also could solubilize phosphate (Fig. 10.4) in seawater-based agar. Crustacean shells consist mainly of 30%−40% protein, 30%−50% calcium carbonate, and 20%−30% chitin and calcium phosphate [9−11]. They also contain carotenoid pigments and a trace amount of lipid resides. Seafood wastes are rich in organic contents such as protein, bioactive peptides, collagen, gelatin, calcium carbonate, and lipid, making the disposal process more complicated and expensive [4]. The content of shell components varies with different species

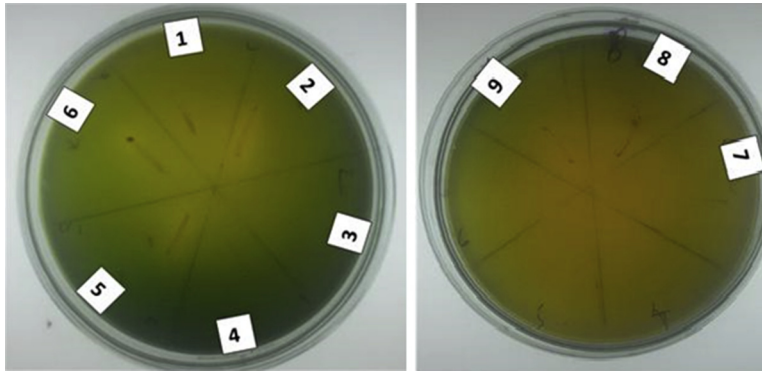

FIGURE 10.4 Seaweed-associated bacteria showing phosphate-solubilizing activity on seawater-based Pikovskaya's agar plates containing 0.05% bromothymol blue.

and seasons [12]. Therefore, to degrade seafood waste bacteria (PM1, PM6, and PM9), which have protease, chitinase activities, phosphate solubilizing and calcium carbonate solubilization properties are of great importance.

Seaweed-associated selected bacterial isolates didn't show any cross-inhibition activity with each other therefore were selected to develop microbial consortia to degrade seafood waste. Microbial consortia (PM1, PM6, and PM9) was developed to enhance degradation of seafood waste, which was evident from the amount of reducing sugars released from crab shell/prawn and fish scales (Fig. 10.5) and was found to be 310 ± 8 μg/mL, 245 ± 14 μg/mL, and 180 ± 15 μg/mL, respectively, after 4 days of incubation. These results confirmed that bacterial consortia have very high seafood waste degradation activity and can be used for bioremediation of seafood waste before discharging into marine waters and also marine sites already polluted with seafood waste. Based on morphology and biochemical tests, bacterial

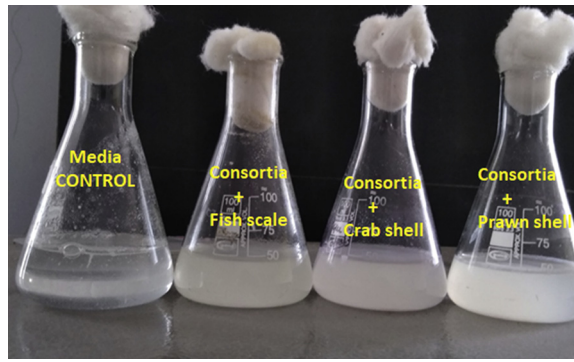

FIGURE 10.5 Seaweed-associated bacteria, when used as microbial consortia (PM1, PM6, and PM9), showed degradation of seafood waste (crab shell, prawn shell, and fish scales).

isolates PM1, PM6, and PM9 were identified as *Bacillus* sp. *Brevibacterium* sp. and *Vibrio* sp., respectively, and through 16S rRNA sequencing, bacterial isolate PM6 was further confirmed as *Brevibacterium iodinum* (accession number MG971400).

Fish production generates a huge amount of solid waste in the form of whole fish waste, fish heads, tails, skin, viscera, bones, blood liver, guts, and some muscle tissue along with wastewater composed of liquid waste produced during fish processing [6]. Improper disposal of seafood wastes generated by fishery-processing industries signifies an increasing environmental and health problem [8]. The intertidal region is exposed to fish, prawn, and crab waste as they get washed toward the shoreline when dumped in the sea during the wave currents. Biodegradation of waste is perhaps the most lucrative and environmentally friendly procedure for waste utilization since chemical treatment method can, in turn, add harmful chemicals (HCl, HNO_3, H_2SO_4, CH_3COOH, and HCOOH) to the environment [9,23]. Fishery waste being collected is in mixed type form near/along the shoreline inhabited by seaweeds, and bacteria associated with seaweeds are adapted to possess enzymes protease, chitinase, phosphate solubilization, and calcium solubilization activity. These properties make them efficient in biodegradation and treatment of fisheries waste containing a mixture of proteins, cellulose, chitin, and minerals, etc. In this study, we have reported for the first time isolation of seaweed-associated bacteria (*Bacillus* sp., *Brevibacterium* sp., *Vibrio* sp.) from the intertidal region of Goa, India, to degrade fish waste efficiently without using any chemical degradation step. Also, first-time detailed studies regarding enzymes (protease, chitinase, and cellulase) and organic acids (demineralization) produced by seafood waste degrading marine bacteria are now underway. Use of marine bacterial consortia for degradation of seafood waste is an ecofriendly and cost-effective method as compared to chemical method. In the near future, genes encoding protease, cellulase, and chitinase from these seaweed-associated bacteria will be used to genetically modify *Escherichia coli* for enhanced degradation of crab shell/prawn shell and fish scale waste as an advance in seafood waste management.

10.4 Application of seafood waste for bioethanol production

The main aim of waste management is to develop advanced biotechnology to biodegrade waste and for sustainable production of biofuel without harming the environment [24]. Application of seafood waste for bioethanol (biofuel) production is a very innovative and ecofriendly concept. The present biotechnology-based concept uses marine bacteria to break down crab shell/fish scales/prawn shell by utilizing them as the sole source of carbon and nutrients and break them down into monomer sugars. The sugars thus produced during degradation of seafood waste can be used to produce bioethanol

in the future, using *Saccharomyces cerevisiae* in a profitable, sustainable, and environmentally friendly manner. Biofuels (ethanol) do not contribute much toward environmental pollution and thus are beneficial over current fuels.

The rapid decline in the world's oil reserves is the main reason behind increasing interest in biofuels as a substitute for fossil fuels. Also, at present ethanol production is mainly done by yeast fermentation (*S. cerevisiae*) by using plant raw material containing very high levels of sugar. Use of plant raw material for biofuel production is economically costly, environmentally damaging, and requires a large cultivable area, therefore, we need an alternative source of raw material [24]. Since a large amount of seafood waste is generated every day, we can use this waste for biofuel production. Here the seafood waste can be first degraded using bacteria possessing calcium carbonate solubilization, cellulase, protease, and chitinase activity to release sugars. The sugars thus released can be used for bioethanol production by fermentation using *S. cerevisiae*. Sugar *N*-acetyl-D-glucosamine (GlcNAc) is the monomer of chitin and released during degradation of seafood waste. Inokuma et al. (2016) used *Scheffersomyces* (*Pichia*) *stipitis* strains for ethanol production by using GlcNAc as the sole carbon source [25]. *S. stipitis* NBRC1687, 10007 and 10063 strains gave 81%, 75% and 82% ethanol yield, respectively, after consuming 50 g/L GlcNAc at 30°C for 96 h. Not much research work has been done in this area to date, and therefore there is great potential for researchers to develop advanced biotechnological methods/processes to efficiently use seafood waste for ethanol (biofuel) production in a sustainable way without damaging the environment.

Acknowledgments

Dr. Milind Naik thanks SERB-DST project (File Number: YSS/2014/000258) and Dr. Shyamalina Haldar, postdoctoral fellow, Department of Microbiology, Goa University.

References

[1] Pal J, Verma HM, Munka VK, Maurya SK, Roy D, Kumar J. Biological method of chitin extraction from shrimp waste an eco-friendly low-cost technology and its advanced application. Int J Fish and Aquat 2014;1(6):104–7.

[2] Varun TK, Senani S, Jayapal N, Chikkerur J, Roy S, Tekulapally VB, et al. Extraction of chitosan and its oligomers from shrimp shell waste, their characterization and antimicrobial effect. Vet World 2017;10(2):170.

[3] Mahendrakar NS. Aqua feeds and meat quality of cultured fish. New Delhi: Biotech Consort India Ltd.; 2000. p. 26–30.

[4] Kumaran E, Mahalakshmipriya A, Rajan S. Effect of fish waste based Bacillus protease in silver recovery from waste X-ray films. Int J Curr Microb Appl Sci 2013;2(3):49–56.

[5] Bozzano A, Sardà F. Fishery discard consumption rate and scavenging activity in the Northwestern Mediterranean Sea. ICES J Mar Sci 2002;59(1):15–28.

[6] Rebah FB, Miled N. Fish processing wastes for microbial enzyme production: a review. 3 Biotech 2013;3(4):255−65.
[7] Xu Y, Gallert C, Winter J. Chitin purification from shrimp wastes by microbial deproteination and decalcification. Appl Microbiol Biotechnol 2008;79(4):687−97.
[8] Arvanitoyannis IS, Kassaveti A. Fish industry waste: treatments, environmental impacts, current and potential uses. Int J Food Sci Technol 2008;43(4):726−45.
[9] Younes I, Rinaudo M. Chitin and chitosan preparation from marine sources. Structure, properties and applications. Mar Drugs 2015;13(3):1133−74.
[10] Knorr D. Use of chitinous polymers in food: a challenge for food research and development. Food Technol 1984;38:85−97.
[11] Arbia W, Arbia L, Adour L, Amrane A. Chitin extraction from crustacean shells using biological methods-a review. Food Technol Biotechnol 2013;51(1):12−25.
[12] Cho YI, No HK, Meyers SP. Physicochemical characteristics and functional properties of various commercial chitin and chitosan products. J Agric Food Chem 1998;46(9):3839−43.
[13] Jung WJ, Jo GH, Kuk JH, Kim KY, Park RD. Extraction of chitin from red crab shell waste by co fermentation with *Lactobacillus paracasei* subsp. *tolerans* KCTC-3074 and *Serratia marcescens* FS-3. Appl Microbiol Biotechnol 2006;71(2):234.
[14] Sorokulova I, Krumnow A, Globa L, Vodyanoy V. Efficient decomposition of shrimp shell waste using *Bacillus cereus* and *Exiguobacterium acetylicum*. J Ind Microbiol Biotechnol 2009;36(8):1123−6.
[15] Wang SL, Chio SH. Deproteinization of shrimp and crab shell with the protease of *Pseudomonas aeruginosa* K-187. Enzym Microb Technol 1998;22(7):629−33.
[16] Jo GH, Jung WJ, Kuk JH, Oh KT, Kim YJ, Park RD. Screening of protease-producing *Serratia marcescens* FS-3 and its application to deproteinization of crab shell waste for chitin extraction. Carbohydr Polym 2008;74(3):504−8.
[17] Imran Md, Poduval PB, Ghadi SC. Bacterial degradation of algal polysaccharides in marine ecosystem. In: Naik MM, Dubey SK, editors. Marine poll microb remed; 2017. p. 196−202.
[18] Mondal D, Islam MS, Hoque MF, Hossain MK, Islam MK, Hossin MS, Ahsan SM. Isolation and screening of potential phosphate solubilizing bacteria (Psb) from tidal saline soils of Bangladesh. Octa J Environ Res 2016;4(3).
[19] Kasana RC, Salwan R, Dhar H, Dutt S, Gulati A. A rapid and easy method for the detection of microbial cellulases on agar plates using Gram's iodine. Curr Microbiol 2008;57(5):503−7.
[20] Krithika S, Chellaram C. Isolation, screening, and characterization of chitinase producing bacteria from marine wastes. Int J Pharm Pharmaceut Sci 2016;8(5):34−6.
[21] Monreal J, Reese ET. The chitinase of *Serratia marcescens*. Can J Microbiol 1969;15(7):689−96.
[22] Garrity GM, Brenner DJ, Kreig NR, Staley JT. Bergey's manual of systematic bacteriology, vol. 2. New York, Berlin, Heidelberg: Springer-Verlag; 2005. p. 685−93.
[23] Kumari S, Rath PK. Extraction and characterization of chitin and chitosan from (Labeo rohit) fish scales. Procedia Mater Sci 2014;6:482−9.
[24] Lozano VMP. Sustainable production of biofuel (bioethanol) from shellfish waste. Universidad de Alicante; 2015. p. 1−8.
[25] Inokuma K, Hasunuma T, Kondo A. Ethanol production from *N*-acetyl-d-glucosamine by *Scheffersomyces stipitis* strains. Amb Express 2016;6:83. https://doi.org/10.1186/s13568-016-0267-z.

Chapter 12

Metagenomics a modern approach to reveal the secrets of unculturable microbes

Kashif Shamim[1], **Sajiya Yusuf Mujawar**[1], **Milind Mutnale**[2]
[1]*Laboratory of Bacterial Genetics and Environmental Biotechnology, Department of Microbiology, Goa University, Goa, India;* [2]*National Centre for Polar and Ocean Research (NCPOR), Vasco-da-Gama, Goa, India*

12.1 Introduction

The most diverse life forms that exist on planet Earth are microorganisms, but still, only 0.1%−1% have been cultivated so far, resulting in creating a great obstacle in understanding the world of microbes. This limitation nowadays has been overcome by the use of data being gathered using metagenomics and single-cell genomic techniques, which bypasses the need for cultivation of microbes in laboratory conditions [1].

The identification of bacterial and archaeal phyla using a small subunit ribosomal RNA database till date has resulted into 89 bacterial and 20 archaeal phyla, which is much less than the expected bacterial phyla of approximately 1500 [2−7]. The lack of data act as an indicator for the incapability of cultivating microorganisms, as the majority of what we have understood so far about microbial life form is based on cultivable organisms. Therefore, the phylogenic information available is being dominated mostly by the Proteobacteria, Actinobacteria, Firmicutes, and Bacteroidetes representing bacteria, with halotolerant and methanogens members of the Euryarchaeota in case of the archaea [3].

The realization of how diverse the untapped microbial community is in any particular environment came from the analysis of RNA (16S rRNA or SSU) genes sequencing directly from various environmental econiches [8]. The outcome of the study revealed that a single cultivable representative was present in less than half of the known microbial phyla [1]. Those phyla that contain exclusively uncultivable microbes are known as Candidate Phyla (CP). This CP is also referred to as microbial dark matter as these microbes account for a large portion of the Earth's biomass as well as biodiversity, but still not

Advances in Biological Science Research. https://doi.org/10.1016/B978-0-12-817497-5.00012-4

much is known about their metabolic and ecological properties. To tap these CP currently proves to be a great challenge to the scientific community, and until we solve the mystery of these CP our knowledge toward microbial communities will be minuscule [9].

Scientists during the last 7 to 8 years have addressed this issue of uncultivable microbes using advanced and newer technologies of genome sequencing. Nowadays the microbial genome from any environmental sample can be directly sequenced using metagenomics and single-cell genomics, but these techniques have their own pros and cons. Shotgun sequencing followed by its assembly in the case of metagenomic approach results in genome fragments from different organisms, which subsequently can be binned into separate genomes using shared features, viz., homology, tetranucleotides, and codon usage. However, the limitation of this technique is that sometimes binning does not reveal the identity of its strains, representing a different composite of genomic fragments from diverse populations [10]. In contrast to the metagenomic approach, single-cell genomics involves the separation of a single cell from the environment followed by its lysis, amplification, and sequencing of the genomic DNA. Although this approach overcomes the drawback of the metagenomic approach, due to limitations in amplification of the entire genome, it often results in fragments representing incomplete genome. These two techniques have contributed quite a lot in recent years in terms of new insights into discovering the hidden uncultivable microbes in any environment [1].

Every microorganism in any environment possesses a unique set of genes within its genome, and the combination of the genomes of all the microbial members in any particular environment is known as metagenome. The metagenome technology, i.e., metagenomics, has helped in accumulating the genomic DNA sequences possessing unique properties for various novel biotechnological applications [11]. The presence of an overwhelming majority of uncultivable microbes in any environment will always result in uncovering the hitherto unknown proteins and sequences pertaining to it, thus making this approach more advantageous over the culture-based traditional approach [12]. The importance of metagenomic approach can be assessed merely based on the fact that nearly one million novel open reading frames encoding microbial enzymes were successfully identified in a single sample of marine prokaryotic plankton obtained from the Sargasso Sea [13].

12.2 History of metagenomic approach

The term *metagenomics* was first coined by a group led by Jo Handelsman [14]. Metagenomics is also known as ecogenomics, community genomics, and environmental genomics [15]. The DNA cloning directly from the environmental sample was first proposed by Pace [16], and as early as 1991, the first

such type of cloning was reported in phage vectors [17]. The construction of the metagenomic library from the mixture of organisms enriched on dried grasses was achieved in similar lines [18]. The library resulted in an expression of cellulolytic activity, which at that time was referred to as zoolibraries (the term was not much used in this field) [18]. The major outcome came from the team led by DeLong that constructed metagenomic libraries from prokaryotes in seawater samples [19]. The library constructed by DeLong resulted into 40 kb clone constituting a 16S rRNA gene, identifying this clone as archaeon that previously had never been cultivated.

When metagenomics became popularized, some aspects of this technology were patented for the first time by biotechnological companies, including Diverse (San Diego, California, USA) and TerraGen Discovery (Vancouver, Canada) in 1996 [13]. Cloning of PCR-generated microbial genes from soil DNA into the partial polyketide synthase gene cluster of recipient *Streptomyces* strain was shown for the first time by TerraGen Discovery company in order to explain the importance of cloning and expression of environmental genes [20,21].

Metagenomics became well known when two different but important research works using this technique were published in 2004. These research works clearly demonstrated the application of random whole-genome shotgun sequencing in understanding the microbial populations present in diverse habitats [22,23]. The research group headed by Tyson [22] used samples from the extreme environment that generated only 76 Mb DNA sequence data and resulted in the complete assembly of genomes of the dominant species along with their metabolic pathway. Whereas the research group of Craig Venter [23] analyzed environmental samples containing a large number of species resulting in a sequence database of 2 Gb. These two projects led to a flood of information in the area of metagenomics as nearly 200 projects with over 450 different environmental samples came into existence within a very short period according to the GOLD database [24].

12.3 Approach, strategies, and tools used in the metagenomic analysis

The metagenomic approach starts with the isolation of metagenomic DNA from an environmental sample followed by its cloning and transformation into a suitable cloning vector and host system (Fig. 12.1A and B). The resulted transformant is then screened for either phylogenetic markers/anchors, such as 16S rRNA gene, or it can be screened for any particular gene of interest using multiplex PCR or hybridization or enzyme substrate reaction or antibiotic production [22,23,25–34]. Each approach has its own strengths as well as weaknesses, but together these approaches have so far broadened our knowledge about the uncultivable microbes, which otherwise would have remained a mystery to us.

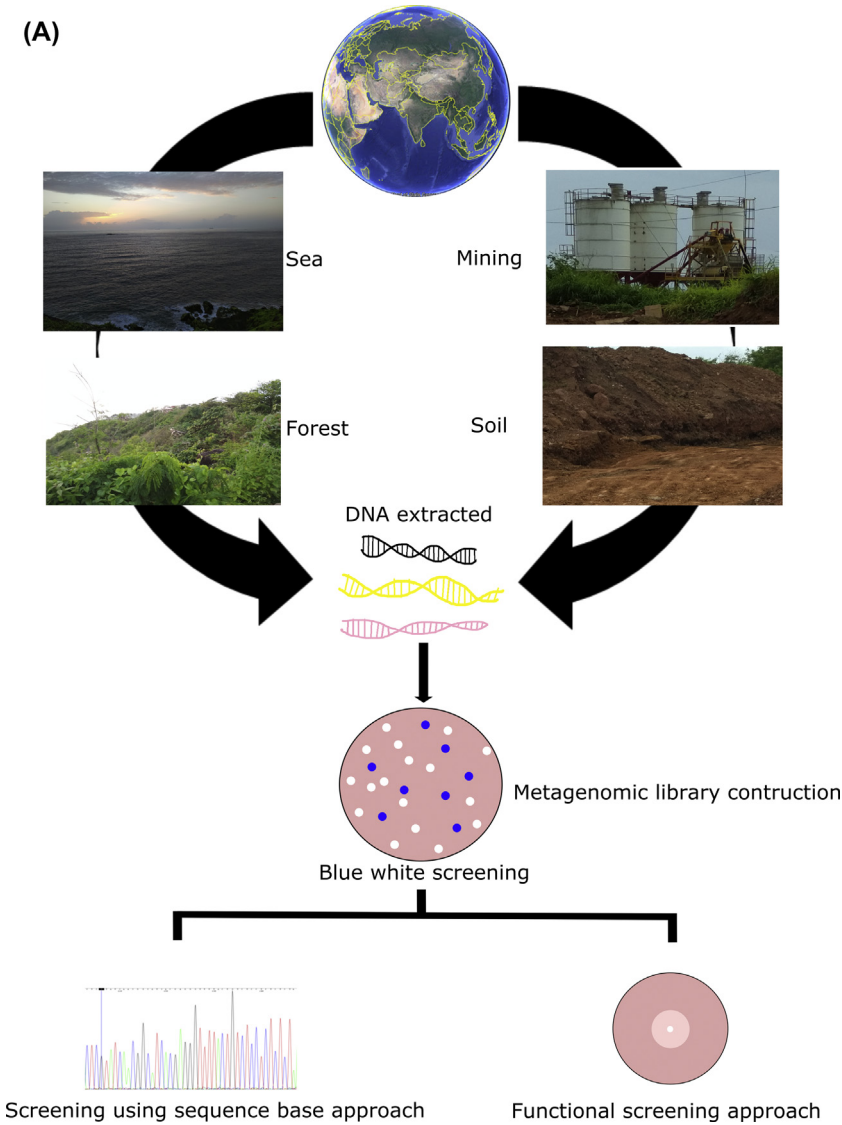

FIGURE 12.1 (A) Schematic representation of metagenomic approach. (B) Cloning and transformation of metagenomic DNA into suitable vector and host.

12.3.1 Isolation of metagenomic DNA

Metagenomic DNA recovery from any environmental sample suitable for metagenomic library construction is a challenging task as various contaminations, viz., humic, fulvic acids, DNases present in soil or sediment samples [35–37], cause major hindrances in downstream process of isolated DNA.

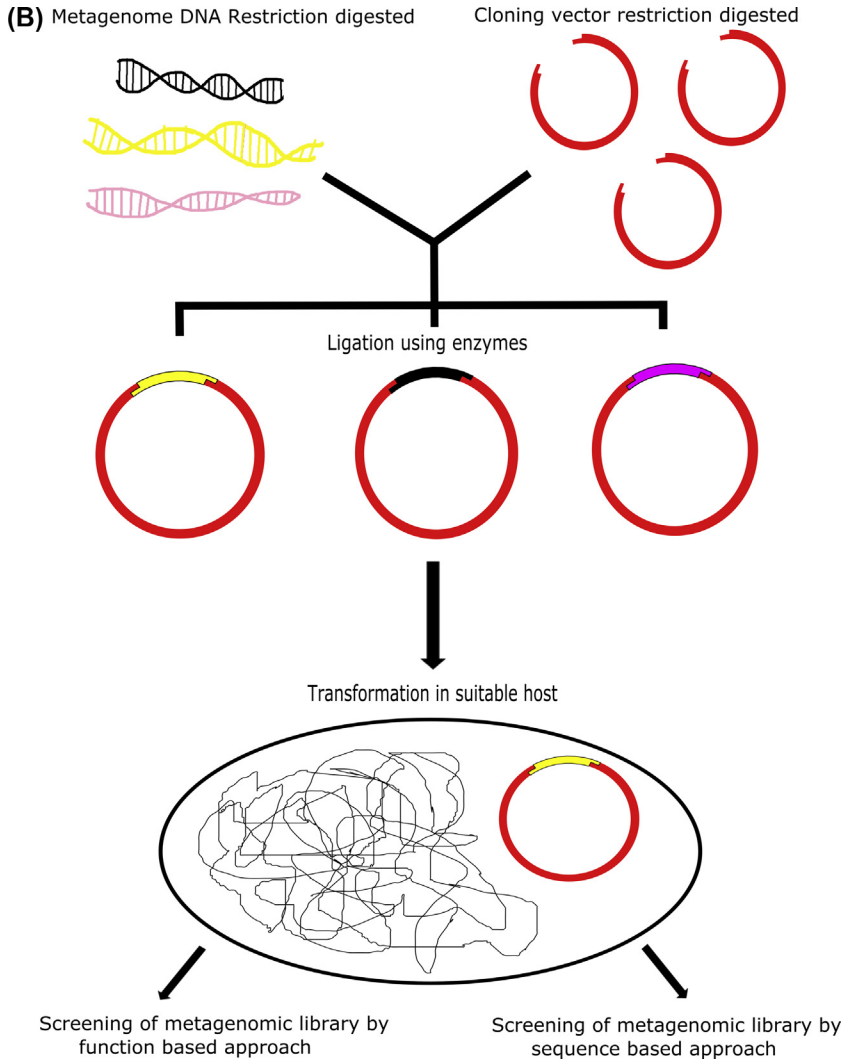

FIGURE 12.1 cont'd

The second drawback in case of isolation of intact high-molecular-weight DNA/metagenomic DNA is there are always chances of DNA getting degraded or sheared in the harsh process of extraction. To ensure the correct representation of any community metagenome, the quality as well as the quantity of extracted metagenomic DNA play an important role [29]. In order to overcome this limitation, several protocols have been devised that are fast, efficient, and yield pure metagenomic DNA from various environmental samples [38–43].

Apart from the above-mentioned protocols for extraction of metagenomic DNA, there are several commercially available kits in the market currently that claim to yield high as well as pure metagenomic DNA from various sources. These kits are easy to use but sometimes require sophisticated equipment in order to carry out the DNA extraction in an efficient manner. Some of the commercially available kits are PowerSoil, UltraClean, and RNA PowerSoil (Mo Bio Laboratories, California, USA); FastDNA Spin kit for soil and FastRNA Pro soil-direct kit (MP Biomedicals, Solon, Ohio, USA); and SoilMaster (Epicentre Biotechnologies, Madison, Wisconsin, USA).

12.3.2 Cloning vector and host

The vector system used in any metagenomic library construction depends upon many criteria such as the desired insert size of the library, screening method or strategy that will be used, quality of the isolated DNA, and vector copy number [44]. The construction of the metagenomic libraries can be classified into two groups: the first type with small insert libraries made in plasmid vector with $<$15 kbps insert size and the second type with large insert made in either cosmid or fosmid with 40 kbps insert size or in bacterial artificial chromosomes (BACs) with $>$40 kbps of insert size. Fosmids and BACs are the vectors that are most commonly used for metagenomic studies due to their capacity to clone larger inserts as well as maintaining the stability of prokaryotic as well as eukaryotic clones [21,45,46].

In most of the cases, the strains of *Escherichia coli* is preferred as a host in cloning and expression studies but there is a limitation in terms of expression of the genes in the *E. coli* host from an organism that is more distantly related to Enterobacteriaceae family. Therefore, in recent years, scientists have successfully tested other host organisms such as *Streptomyces lividans*, *Pseudomonas putida*, *bacillus subtilis*, and *Rhizobium leguminosarum*are for their studies [21,47,48].

12.3.3 Screening of metagenomic clones

Once the metagenomic library is constructed successfully, this library can be screened for either "functional" or "sequence-based" screening procedures [49,50].

Functional metagenomics is based on the expression of genes from the cloned metagenomic DNA in the respective host using specific substrates. This technique is advantageous to explore novel genes encoding various industrially important enzymes and other biomolecules, including antibiotics. There are several limiting factors in functional screening, viz., an expression of the gene(s) inserted in the foreign hosts, availability of substrates, and recognition of regulatory elements such as operators and promoters [51].

The sequence-based metagenomic approach relies on DNA sequencing of the metagenomic library followed by identification of the gene(s) encoding enzymes regulating different metabolic pathways as well as the microbial community structure that defines microbial diversity involved in specific metabolic/degradative pathways. The sequence-based approach requires the use of computers along with their respective software for genome assembly in order to find out the type of organisms as well as functions of different genes in specific samples [17,19,50].

12.3.4 Sequencing and bioinformatics analysis of the metagenomic clones

The complexity of microbiomes can be assessed in an example stated by Hess et al. [52] who estimated that approximately 1000 operational taxonomic units can be present in a single cow rumen, that's why sequencing technology needs to be very sensitive in order to capture the sequences of all the species within any microbiome sample. Nowadays, second- and third-generation sequencing, known as next-generation sequencing, has aided in the analysis of metagenome in a promising manner. The second-generation sequencing consists of Ion Torrent and Illumina, which are able to produce millions of short reads (200−400 bps), whereas third-generation sequencing procedure includes PacBio and ONT produces longer reads, i.e., 6−20 kbps, but they result in fewer reads per run.

The next thing after sequencing is its assembly or genome assembly from the smaller sequenced fragments. The assembling process of any genome from the smaller fragments of sequences is very tedious technique, due to the presence of repetitive elements within the genome. The de novo type of assembler is a reference-free type of strategy for constructing the contiguous sequences known as contigs. The de novo assembly software tools use either overlap layout consensus (OLC) or the de Bruijn graph approach. In the OLC approach, pairwise comparing of all reads are done to find out the regions with significant overlaps, whereas in de Bruijn graph approach a graph is constructed by reading the consecutive k-mers within each read [53]. The de Bruijn graph approach is less expensive than the OLC approach but is more sensitive to sequencing error than that of OLC approach. The list of other software used in the metagenomic analysis is tabulated in Table 12.1.

12.4 Application of the metagenomic approach

In the advancement of culture-independent approach for studying microbial community, we are now evaluating the microorganisms that inhabit each and every ecological niche from the deepest oceans to the gut of almost every organism. This technique has changed the way the bacterial phyla

TABLE 12.1 Commonly used software in metagenomic analysis.

S. No.	Software	Application	Links	References
1	PRINTSEQ	Quality control tool for sequence trimming.	http://prinseq.sourceforge.net/	[54]
2	FastQC	Quality control tool for high-throughput sequence data.	http://www.bioinformatics.babraham.ac.uk/projects/fastqc/	[55]
3	NGS QC toolkit	Tool for quality control analysis performed in parallel environment.	http://www.nipgr.res.in/ngsqctoolkit.html	[56]
4	Mothur	From reads quality analysis to taxonomic classification.	http://www.mothur.org/	[57]
5	Meta-QC-Chain	Parallel environment tool for quality control.	http://www.computationalbioenergy.org/qc-chain.html	[58]
6	QIIME	Quality pretreatment of raw reads, taxonomic annotation, calculus of diversity estimators, and comparison of metaprofiling or metagenomic data.	http://qiime.org/	[59]
7	PICRUSt	Predictor of metabolic potential from taxonomic information.	http://picrust.github.io/picrust/	[60]
8	CARMA	Phylogenetic classification of reads based on Pfam conserved domains.	http://omictools.com/carma-s1021.html	[61]
9	MOCAT	Pipeline that includes quality treatment of metagenomic reads and taxonomic annotation.	http://vm-lux.embl.de/~kultima/MOCAT2/index.html	[62]
10	Parallel-meta	Taxonomic annotation of ribosomal gene markers sequences obtained by metaprofiling or metagenomic reads.	http://www.computationalbioenergy.org/parallel-meta.html	[63]

11	TETRA	Taxonomic classification by comparison of tetranucleotide patterns.	http://omictools.com/tetra-s1030.html	[64]
12	MetaVelvet	De novo assembler of metagenomic short reads.	http://metavelvet.dna.bio.keio.ac.jp/	[65]
13	MetaORFA	Assembly of peptides.	Not available	[66]
14	ProViDE	Analysis of viral diversity in metagenomic samples.	http://metagenomics.atc.tcs.com/binning/ProViDE	[67]
15	MetagenomeSeq	Analysis of differential abundance of 16S rRNA gene in metaprofiling data.	http://bioconductor.org/packages/release/bioc/html/metagenomeSeq.html	[68]
16	MG-RAST	Taxonomic and functional annotation, comparative metagenomics.	http://metagenomics.anl.gov	[69]
17	IMG/M	Functional annotation, phylogenetic distribution of genes and comparative metagenomics.	https://img.jgi.doe.gov/cgi-bin/m/main.cgi	[70]
18	RayMeta	Assembler of de novo metagenomic reads and taxonomy profiler by Ray Communities.	http://denovoassembler.sourceforge.net/	[71]
19	IDBA-UD	Assembler de novo of metagenomic sequences with uneven depth.	http://i.cs.hku.hk/~alse/hkubrg/projects/idba_ud/	[72]

were defined previously by culture-dependent approach as the fact is that approximately 70% of all known bacterial phyla are totally devoid of any cultivable representative [73]. The great diversity among metagenomic 16S rRNA sequences can be easily detected using phylogenetic analysis (Fig. 12.2). In the case of pharmaceutical industries, bacterial strains are well known for the discovery of novel antibiotics to combat the problem of antibiotic-resistant pathogens [74]. To date, more than 10,000 biologically active molecules against serious human pathogens, viz., HIV, cancer, and inflammation have been isolated from known cultured actinomycetes and mostly from a single genus of *Streptomyces* [75]. Therefore, we can truly hypothesize the potential of discovering novel biomolecules from the uncultivable microbes as they are known to outnumber the cultivable microbes.

The industrial application of the metagenomic approach has resulted in the isolation of numerous industrially important enzymes (Table 12.2). In the field of other natural products, viz., drug discovery or metabolites, putative pathways have been reported from various environmental samples, i.e., from soil [93,94], tunicates [95,96], sponges [97] and from insects [98]. But still, the challenge to link these biosynthetic genes to a product has hindered discovery, whereas only in a few cases successful expression or in vitro characterization has been achieved [99,100]. The rate of discovery of newer genes has been accelerated with the advent of the metagenomic approach, and therefore, the application of the metagenomic approach to humankind seems to be endless.

12.5 Conclusion remarks

The viewpoint of microbiologists has been changed after the emergence of the metagenomic approach in recent years. Many concepts defined by cultural microbes have been altered drastically with the discovery of uncultivable microbes. In terms of its application to various biotechnological industries, metagenomics is limitless as it has led to some novel discoveries. This technique had shown a promising future with the advancement of sequencing methods and other bioinformatics analysis tools. There are still more extreme environments, such as thermal vents in the deep sea, the frozen Antarctic region, vertebrate gut microbiomes, cold soils, and plant rhizospheres, that needs to be explored with the help of this technique. Furthermore, this state of art technology, along with its improved methods for analysis, in near future will attract the scientific community of diverse fields. Metagenomics seems to have a very promising future in helping mankind to solve problems and develop a better understanding of the microbial community.

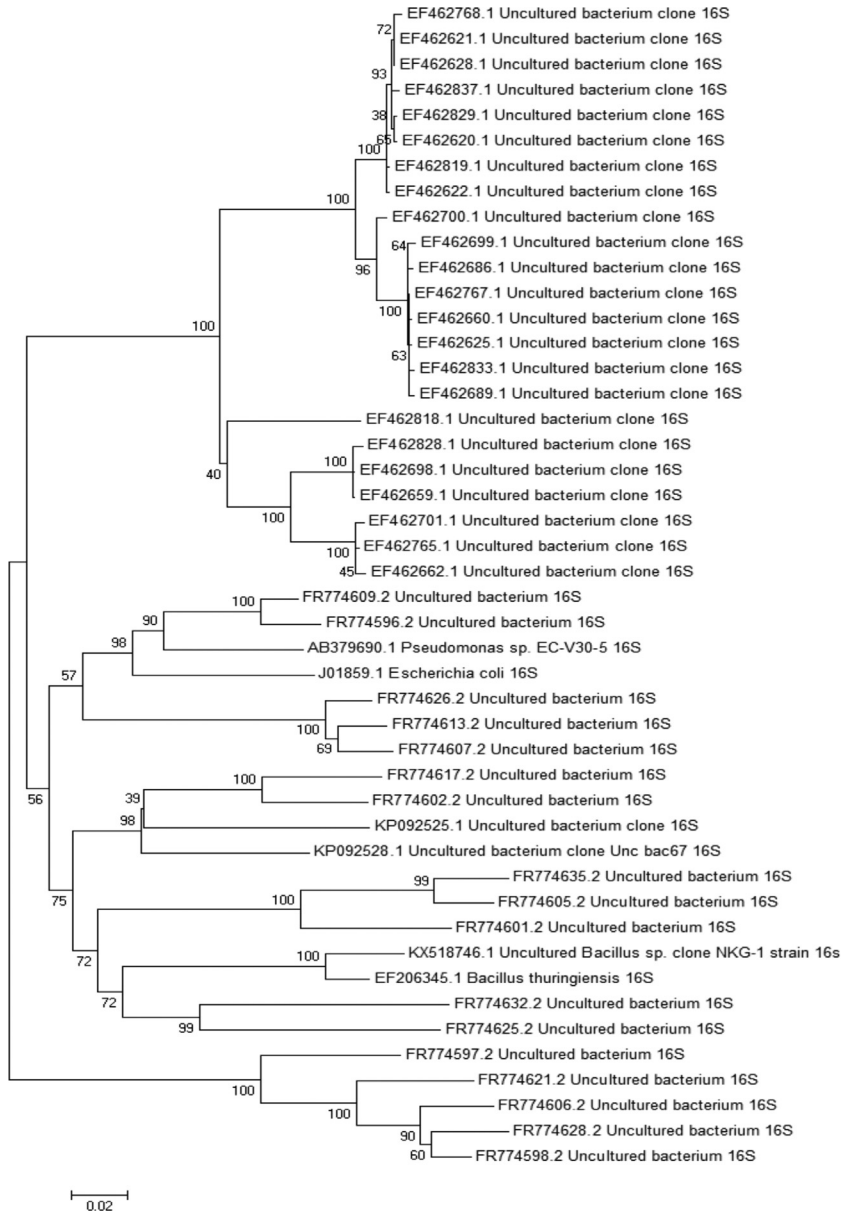

FIGURE 12.2 Phylogenetic analysis showing diversity among unculturable microbes using metagenomic approach.

TABLE 12.2 Various enzymes isolated using metagenomics approach.

S. No.	Source	Gene Name	Host/ Vector	Avg. Insert size (kb)	References
1	Soil	Esterase/lipase	*E. coli*, plasmid	6	[76]
2	Compost	Esterase, amylase, phosphatase, dioxygenase, protease	*E. coli*, plasmid	3.2	[77]
3	Sediment enrichment	Cellulase	*E. coli*, λ phage	6	[78]
4	Loam soil	Oxygenase	*E. coli*, plasmid	5.5	[79]
5	Soil	β-Lactamase	*E. coli*, plasmid	5	[80]
6	Activated sludge treating coke plant wastewater	Extradiol dioxygenase	*E. coli*, fosmid	33	[81]
7	Seawater	Chitinase	*E. coli*, λ phage	5	[82]
8	Glacial ice	DNA polymerase I	*E. coli*, plasmid	4	[83]
9	Soil/sediment enrichment	Dehydratase	*E. coli*, plasmid	4	[28]
10	Cow rumen	Mannanase/ glucanase/ xylanase	*E. coli*, phagemid	3	[84]
11	Sediment	Metalloprotease	*E. coli*	4	[85]

Sequence-based screening

S. No.	Source	Gene Name	Method	References
1	3-Chlorobenzoate enrichment	Benzoate 1,2-dioxygenase, chlorocatechol 1,2-dioxygenase	Degenerate PCR	[86]
2	Grassland soil	Nitrite reductase, nitrous oxide reductase	Probe hybridization	[87]
3	Sediment from hot spring	Pullulanase	Degenerate PCR	[88]

TABLE 12.2 Various enzymes isolated using metagenomics approach.—cont'd

Sequence-based screening				
S. No.	Source	Gene Name	Method	References
4	Bioreactors treating gold-bearing concentrates	Sulfur oxygenase reductase	Degenerate PCR	[89]
5	Deep-sea sediment	Alkane hydroxylase	Degenerate PCR	[90]
6	Marine sponge	Related polyketide synthesis	Degenerate PCR	[91,92]

Acknowledgments

We are thankful to Prof. Santosh Kumar Dubey for his assistance in preparing this chapter, and we are also very grateful to editors Dr. Milind Mohan Naik and Dr. Surya Nandan Meena for giving us the opportunity to contribute a chapter in their prestigious book.

References

[1] Solden L, Lloyd K, Wrighton K. The bright side of microbial dark matter: lessons learned from the uncultivated majority. Curr Opin Microbiol 2016;31:217−26.

[2] Castelle CJ, Wrighton KC, Thomas BC, Hug LA, Brown CT, Wilkins MJ, Frischkorn KR, Tringe SG, Singh A, Markillie LM, et al. Genomic expansion of domain archaea highlights roles for organisms from new phyla in anaerobic carbon cycling. Curr Biol 2015;25.

[3] Rinke C, Schwientek P, Sczyrba A, Ivanova NN, Anderson IJ, Cheng J-F, Darling A, et al. Insights into the phylogeny and coding potential of microbial dark matter. Nature 2013;499(7459):431−7.

[4] Brown CT, Hug LA, Thomas BC, Sharon I, Castelle CJ, Singh A, Wilkins MJ, Wrighton KC, Williams KH, Banfield JF. Unusual biology across a group comprising more than 15% of domain bacteria. Nature 2015;523(7559):208−11.

[5] Baker BJ, Lazar CS, Teske AP, Dick GJ. Genomic resolution of linkages in carbon, nitrogen, and sulfur cycling among widespread estuary sediment bacteria. Microbiome 2015;3:14.

[6] Hug LA, Baker BJ, Anantharaman K, Brown CT, Probst AJ, Castelle CJ, Butterfield CN, et al. A new view of the tree of life. Nat Microbiol 2016:16048.

[7] Yarza P, Yilmaz P, Pruesse E, Glockner FO, Ludwig W, Schleifer KH, Whitman WB, Euzeby J, Amann R, Rossello-Mora R. Uniting the classification of cultured and uncultured bacteria and archaea using 16S rRNA gene sequences. Nat Rev Microbiol 2014;12(9):635−45.

[8] Baker BJ. Omic approaches in microbial ecology: charting the unknown. Microbe 2013;8(9):353−9.

[9] Hedlund BP, Dodsworth JA, Murugapiran SK, Rinke C, Woyke T. Impact of single-cell genomics and metagenomics on the emerging view of extremophile ''microbial dark matter''. Extremophiles 2014;18(5):865−75.
[10] Sharon I, Banfield JF. Genomes from metagenomics. Science 2013;342:1057−8.
[11] Ferrer M, Martinez-Abarca F, Golyshin PN. Mining genomes and 'metagenomes' for novel catalysts. Curr Opin Biotechnol 2005;16:588−93.
[12] Rajendhran J, Gunasekaran P. Strategies for accessing soil metagenome for desired applications. Biotechnol Adv 2008;26(6):576−90.
[13] Lorenz P, Eck J. Metagenomics and industrial applications. Nat Rev Microbiol 2005;3(6):510.
[14] Handelsman J, Rondon MR, Brady SF, Clardy J, Goodman RM. Molecular biological access to the chemistry of unknown soil microbes: a new frontier for natural products. Chem Biol 1998;5(10):R245−9.
[15] Chistoserdova L. Recent progress and new challenges in metagenomics for biotechnology. Biotechnol Lett 2010;32(10):1351−9.
[16] Pace NR. Analyzing natural microbial populations by rRNA sequences. ASM News 1985;51:4−12.
[17] Schmidt TM, DeLong EF, Pace NR. Analysis of a marine picoplankton community by 16S rRNA gene cloning and sequencing. J Bacteriol 1991;173(14):4371−8.
[18] Healy FG, Ray RM, Aldrich HC, Wilkie AC, Ingram LO, Shanmugam KT. Direct isolation of functional genes encoding cellulases from the microbial consortia in a thermophilic, anaerobic digester maintained on lignocellulose. Appl Microbiol Biotechnol 1995;43(4):667−74.
[19] Stein JL, Marsh TL, Wu KY, Shizuya H, DeLong EF. Characterization of uncultivated prokaryotes: isolation and analysis of a 40-kilobase-pair genome fragment from a planktonic marine archaeon. J Bacteriol 1996;178(3):591−9.
[20] Seow KT, Meurer GU, Gerlitz MA, Wendt-Pienkowski EV, Hutchinson CR, Davies JU. A study of iterative type II polyketide synthases, using bacterial genes cloned from soil DNA: a means to access and use genes from uncultured microorganisms. J Bacteriol 1997;179(23):7360−8.
[21] Wang GY, Graziani E, Waters B, Pan W, Li X, McDermott J, Meurer G, Saxena G, Andersen RJ, Davies J. Novel natural products from soil DNA libraries in a *Streptomycete* host. Org Lett 2000;2(16):2401−4.
[22] Tyson GW, Chapman J, Hugenholtz P, Allen EE, Ram RJ, Richardson PM, Solovyev VV, Rubin EM, Rokhsar DS, Banfield JF. Community structure and metabolism through reconstruction of microbial genomes from the environment. Nature 2004;428(6978): 37−43.
[23] Venter JC, Remington K, Heidelberg JF, Halpern AL, Rusch D, Eisen JA, Wu D, Paulsen I, Nelson KE, Nelson W, Fouts DE. Environmental genome shotgun sequencing of the Sargasso Sea. Science 2004;304(5667):66−74.
[24] Liolios K, Chen IM, Mavromatis K, Tavernarakis N, Hugenholtz P, Markowitz VM, Kyrpides NC. The Genomes on Line Database (GOLD) in 2009: status of genomic and metagenomic projects and their associated metadata. Nucleic Acids Res 2009;38 (Suppl. 1):D346−54.
[25] Courtois S, Cappellano CM, Ball M, Francou FX, Normand P, Helynck G, Martinez A, Kolvek SJ, Hopke J, Osburne MS, August PR. Recombinant environmental libraries provide access to microbial diversity for drug discovery from natural products. Appl Environ Microbiol 2003;69(1):49−55.

[26] Diaz-Torres ML, McNab R, Spratt DA, Villedieu A, Hunt N, Wilson M, Mullany P. Novel tetracycline resistance determinant from the oral metagenome. Antimicrob Agents Chemother 2003;47(4):1430−2.

[27] Gillespie DE, Brady SF, Bettermann AD, Cianciotto NP, Liles MR, Rondon MR, Clardy J, Goodman RM, Handelsman J. Isolation of antibiotics turbomycin A and B from a metagenomic library of soil microbial DNA. Appl Environ Microbiol 2002;68(9):4301−6.

[28] Knietsch A, Bowien S, Whited G, Gottschalk G, Daniel R. Identification and characterization of coenzyme B12-dependent glycerol dehydratase-and diol dehydratase-encoding genes from metagenomic DNA libraries derived from enrichment cultures. Appl Environ Microbiol 2003;69(6):3048−60.

[29] Lorenz P, Liebeton K, Niehaus F, Eck J. Screening for novel enzymes for biocatalytic processes: accessing the metagenome as a resource of novel functional sequence space. Curr Opin Biotechnol 2002;13(6):572−7.

[30] Lorenz P, Schleper C. Metagenome-a challenging source of enzyme discovery. J Mol Catal B Enzym 2002;19:13−9.

[31] MacNeil IA, Tiong CL, Minor C, August PR, Grossman TH, Loiacono KA, Lynch BA, Phillips T, Narula S, Sundaramoorthi R, Tyler A. Expression and isolation of antimicrobial small molecules from soil DNA libraries. J Mol Microbiol Biotechnol 2001;3(2):301−8.

[32] Majernık A, Gottschalk G, Daniel R. Screening of environmental DNA libraries for the presence of genes conferring Na+ (Li+)/H+ antiporter activity on *Escherichia coli*: characterization of the recovered genes and the corresponding gene products. J Bacteriol 2001;183(22):6645−53.

[33] Rondon MR, August PR, Bettermann AD, Brady SF, Grossman TH, Liles MR, Loiacono KA, et al. Cloning the soil metagenome: a strategy for accessing the genetic and functional diversity of uncultured microorganisms. Appl Environ Microbiol 2000;66(6):2541−7.

[34] Schloss PD, Handelsman J. Biotechnological prospects from metagenomics. Curr Opin Biotechnol 2003;14(3):303−10.

[35] Tsai YL, Olson BH. Rapid method for separation of bacterial DNA from humic substances in sediments for polymerase chain reaction. Appl Environ Microbiol 1992;58(7):2292−5.

[36] Tebbe CC, Vahjen W. Interference of humic acids and DNA extracted directly from soil in detection and transformation of recombinant DNA from bacteria and a yeast. Appl Environ Microbiol 1993;59(8):2657−65.

[37] Alm EW, Zheng D, Raskin L. The presence of humic substances and DNA in RNA extracts affects hybridization results. Appl Environ Microbiol 2000;66(10):4547−54.

[38] Zhou J, Bruns MA, Tiedje JM. DNA recovery from soils of diverse composition. Appl Environ Microbiol 1996;62(2):316−22.

[39] Yeates C, Gillings MR, Davison AD, Altavilla N, Veal DA. Methods for microbial DNA extraction from soil for PCR amplification. Biol Proced Online 1998;1(1):40−7.

[40] Bürgmann H, Pesaro M, Widmer F, Zeyer J. A strategy for optimizing quality and quantity of DNA extracted from soil. J Microbiol Methods 2001;45(1):7−20.

[41] Amorim JH, Macena TN, Lacerda-Junior GV, Rezende RP, Dias JC, Brendel M, Cascardo JC. An improved extraction protocol for metagenomic DNA from a soil of the Brazilian Atlantic Rainforest. Genet Mol Res 2008;7(4):1226−32.

[42] Sagar K, Singh SP, Goutam KK, Konwar BK. Assessment of five soil DNA extraction methods and a rapid laboratory-developed method for quality soil DNA extraction for 16S rDNA-based amplification and library construction. J Microbiol Methods 2014;97:68−73.

[43] Shamim K, Sharma J, Dubey SK. Rapid and efficient method to extract metagenomic DNA from estuarine sediments. 3 Biotech 2017;7(3):182.

[44] Daniel R. The metagenomics of soil. Nat Rev Microbiol 2005;3(6):470.

[45] Bierman M, Logan R, O'brien K, Seno ET, Rao RN, Schoner BE. Plasmid cloning vectors for the conjugal transfer of DNA from *Escherichia coli* to *Streptomyces* spp. Gene 1992;116(1):43−9.

[46] Shizuya H, Birren B, Kim UJ, Mancino V, Slepak T, Tachiiri Y, Simon M. Cloning and stable maintenance of 300-kilobase-pair fragments of human DNA in *Escherichia coli* using an F-factor-based vector. Proc Natl Acad Sci Unit States Am 1992;89(18): 8794−7.

[47] Martinez A, Kolvek SJ, Yip CL, Hopke J, Brown KA, MacNeil IA, Osburne MS. Genetically modified bacterial strains and novel bacterial artificial chromosome shuttle vectors for constructing environmental libraries and detecting heterologous natural products in multiple expression hosts. Appl Environ Microbiol 2004;70(4):2452−63.

[48] Wexler M, Bond PL, Richardson DJ, Johnston AW. A wide host-range metagenomic library from a wastewater treatment plant yields a novel alcohol/aldehyde dehydrogenase. Environ Microbiol 2005;7(12):1917−26.

[49] Handelsman J. Metagenomics: application of genomics to uncultured microorganisms. Microbiol Mol Biol Rev 2004;68(4):669−85.

[50] Cruz JM, Ortega MA, Cruz JC, Ondina P, Santiago R, Rios-Velazquez C. Unravelling activities by functional-based approaches using metagenomic libraries from dry and rain forest soils in Puerto Rico. In: Current research technology and education topics. Applied microbiology and microbial biotechnology. Badajoz, Spain: Formatex; 2010. p. 1471−8.

[51] Craig JW, Chang FY, Kim JH, Obiajulu SC, Brady SF. Expanding small-molecule functional metagenomics through parallel screening of broad-host-range cosmid environmental DNA libraries in diverse Proteobacteria. Appl Environ Microbiol 2010;76(5):1633−41.

[52] Hess M, Sczyrba A, Egan R, Kim TW, Chokhawala H, Schroth G, Luo S, Clark DS, Chen F, Zhang T, Mackie RI. Metagenomic discovery of biomass-degrading genes and genomes from cow rumen. Science 2011;331(6016):463−7.

[53] Pevzner PA, Tang H, Waterman MS. An Eulerian path approach to DNA fragment assembly. Proc Natl Acad Sci Unit States Am 2001;98(17):9748−53.

[54] Schmieder R, Edwards R. Quality control and preprocessing of metagenomic datasets. Bioinformatics 2011;27(6):863−4.

[55] Andrews S. Babraham bioinformatics-FastQC a quality control tool for high throughput sequence data. 2015.

[56] Patel RK, Jain M. NGS QC Toolkit: a toolkit for quality control of next generation sequencing data. PLoS One 2012;7(2). e30619.

[57] Schloss PD, Westcott SL, Ryabin T, Hall JR, Hartmann M, Hollister EB, Lesniewski RA, Oakley BB, Parks DH, Robinson CJ, Sahl JW. Introducing mothur: open-source, platform-independent, community-supported software for describing and comparing microbial communities. Appl Environ Microbiol 2009;75(23):7537−41.

[58] Zhou Q, Su X, Jing G, Ning K. Meta-QC-Chain: comprehensive and fast quality control method for metagenomic data. Genom Proteom Bioinform 2014;12(1):52−6.

[59] Caporaso JG, Kuczynski J, Stombaugh J, Bittinger K, Bushman FD, Costello EK, Fierer N, Pena AG, Goodrich JK, Gordon JI, Huttley GA. QIIME allows analysis of high-throughput community sequencing data. Nat Methods 2010;7(5):335.

[60] Langille MG, Zaneveld J, Caporaso JG, McDonald D, Knights D, Reyes JA, Clemente JC, Burkepile DE, Thurber RL, Knight R, Beiko RG. Predictive functional profiling of

microbial communities using 16S rRNA marker gene sequences. Nat Biotechnol 2013;31(9):814.

[61] Krause L, Diaz NN, Goesmann A, Kelley S, Nattkemper TW, Rohwer F, Edwards RA, Stoye J. Phylogenetic classification of short environmental DNA fragments. Nucleic Acids Res 2008;36(7):2230−9.

[62] Kultima JR, Sunagawa S, Li J, Chen W, Chen H, Mende DR, Arumugam M, Pan Q, Liu B, Qin J, Wang J. MOCAT: a metagenomics assembly and gene prediction toolkit. PLoS One 2012;7(10). e47656.

[63] Su X, Pan W, Song B, Xu J, Ning K. Parallel-META 2.0: enhanced metagenomic data analysis with functional annotation, high performance computing and advanced visualization. PLoS One 2014;9(3). e89323.

[64] Teeling H, Waldmann J, Lombardot T, Bauer M, Glöckner FO. TETRA: a web-service and a stand-alone program for the analysis and comparison of tetranucleotide usage patterns in DNA sequences. BMC Bioinf 2004;5(1):163.

[65] Namiki T, Hachiya T, Tanaka H, Sakakibara Y. MetaVelvet: an extension of Velvet assembler to de novo metagenome assembly from short sequence reads. Nucleic Acids Res 2012;40(20):e155.

[66] Ye Y, Tang H. An ORFome assembly approach to metagenomics sequences analysis. Comput Syst Bioinformatics Conf 2008;7:3−13.

[67] Ghosh TS, Mohammed MH, Komanduri D, Mande SS. ProViDE: a software tool for accurate estimation of viral diversity in metagenomic samples. Bioinformation 2011;6(2):91.

[68] Paulson JN, Stine OC, Bravo HC, Pop M. Differential abundance analysis for microbial marker-gene surveys. Nat Methods 2013;10(12):1200−2.

[69] Meyer F, Paarmann D, D'Souza M, Olson R, Glass EM, Kubal M, Paczian T, Rodriguez A, Stevens R, Wilke A, Wilkening J. The metagenomics RAST server−a public resource for the automatic phylogenetic and functional analysis of metagenomes. BMC Bioinf 2008;9(1):386.

[70] Markowitz VM, Chen IM, Chu K, Szeto E, Palaniappan K, Grechkin Y, Ratner A, Jacob B, Pati A, Huntemann M, Liolios K. IMG/M: the integrated metagenome data management and comparative analysis system. Nucleic Acids Res 2011;40(D1):D123−9.

[71] Boisvert S, Raymond F, Godzaridis É, Laviolette F, Corbeil J. Ray Meta: scalable de novo metagenome assembly and profiling. Genome Biol 2012;13(12):R122.

[72] Peng Y, Leung HC, Yiu SM, Chin FY. IDBA-UD: a de novo assembler for single-cell and metagenomic sequencing data with highly uneven depth. Bioinformatics 2012;28(11): 1420−8.

[73] Achtman M, Wagner M. Microbial diversity and the genetic nature of microbial species. Nat Rev Microbiol 2008;6(6):431−40.

[74] Wright GD. Antibiotics: a new hope. Chem Biol 2012;19(1):3−10.

[75] Bérdy J. Bioactive microbial metabolites. J Antibiot 2005;58(1):1−26.

[76] Henne A, Schmitz RA, Bömeke M, Gottschalk G, Daniel R. Screening of environmental DNA libraries for the presence of genes conferring lipolytic activity on *Escherichia coli*. Appl Environ Microbiol 2000;66(7):3113−6.

[77] Lämmle K, Zipper H, Breuer M, Hauer B, Buta C, Brunner H, Rupp S. Identification of novel enzymes with different hydrolytic activities by metagenome expression cloning. J Biotechnol 2007;127(4):575−92.

[78] Rees HC, Grant S, Jones B, Grant WD, Heaphy S. Detecting cellulase and esterase enzyme activities encoded by novel genes present in environmental DNA libraries. Extremophiles 2003;7(5):415−21.

[79] Van Hellemond EW, Janssen DB, Fraaije MW. Discovery of a novel styrene monooxygenase originating from the metagenome. Appl Environ Microbiol 2007;73(18): 5832−9.

[80] Gabor EM. Harvesting novel biocatalysts from the metagenome. University Library Groningen; 2004.

[81] Suenaga H, Ohnuki T, Miyazaki K. Functional screening of a metagenomic library for genes involved in microbial degradation of aromatic compounds. Environ Microbiol 2007;9(9):2289−97.

[82] Cottrell MT, Moore JA, Kirchman DL. Chitinases from uncultured marine microorganisms. Appl Environ Microbiol 1999;65(6):2553−7.

[83] Simon C, Herath J, Rockstroh S, Daniel R. Rapid identification of genes encoding DNA polymerases by function-based screening of metagenomic libraries derived from glacial ice. Appl Environ Microbiol 2009;75(9):2964−8.

[84] Palackal N, Lyon CS, Zaidi S, Luginbühl P, Dupree P, Goubet F, Macomber JL, Short JM, Hazlewood GP, Robertson DE, Steer BA. A multifunctional hybrid glycosyl hydrolase discovered in an uncultured microbial consortium from ruminant gut. Appl Microbiol Biotechnol 2007;74(1):113−24.

[85] Shamim K, Sharma J, Mutnale M, Mujawar S, Dubey SK. Characterization of a metagenomic serine metalloprotease and molecular docking studies. Process Biochem 2018;71:69−75.

[86] Morimoto S, Fujii T. A new approach to retrieve full lengths of functional genes from soil by PCR-DGGE and metagenome walking. Appl Microbiol Biotechnol 2009;83(2): 389−96.

[87] Demanèche S, Philippot L, David MM, Navarro E, Vogel TM, Simonet P. Characterization of denitrification gene clusters of soil bacteria via a metagenomic approach. Appl Environ Microbiol 2009;75(2):534−7.

[88] Tang K, Kobayashi RS, Champreda V, Eurwilaichitr L, Tanapongpipat S. Isolation and characterization of a novel thermostable neopullulanase-like enzyme from a hot spring in Thailand. Biosci Biotechnol Biochem 2008;72(6):1448−56.

[89] Chen ZW, Liu YY, Wu JF, She Q, Jiang CY, Liu SJ. Novel bacterial sulfur oxygenase reductases from bioreactors treating gold-bearing concentrates. Appl Microbiol Biotechnol 2007;74(3):688−98.

[90] Xu M, Xiao X, Wang F. Isolation and characterization of alkane hydroxylases from a metagenomic library of Pacific deep-sea sediment. Extremophiles 2008;12(2):255−62.

[91] Fieseler L, Hentschel U, Grozdanov L, Schirmer A, Wen G, Platzer M, Hrvatin S, Butzke D, Zimmermann K, Piel J. Widespread occurrence and genomic context of unusually small polyketide synthase genes in microbial consortia associated with marine sponges. Appl Environ Microbiol 2007;73(7):2144−55.

[92] Fisch KM, Gurgui C, Heycke N, Van Der Sar SA, Anderson SA, Webb VL, Taudien S, Platzer M, Rubio BK, Robinson SJ, Crews P. Polyketide assembly lines of uncultivated sponge symbionts from structure-based gene targeting. Nat Chem Biol 2009;5(7):494.

[93] Chang FY, Brady SF. Cloning and characterization of an environmental DNA-derived gene cluster that encodes the biosynthesis of the antitumor substance BE-54017. J Am Chem Soc 2011;133(26):9996−9.

[94] Feng Z, Kallifidas D, Brady SF. Functional analysis of environmental DNA-derived type II polyketide synthases reveals structurally diverse secondary metabolites. Proc Natl Acad Sci Unit States Am 2011;108(31):12629−34.

[95] Rath CM, Janto B, Earl J, Ahmed A, Hu FZ, Hiller L, Dahlgren M, Kreft R, Yu F, Wolff JJ, Kweon HK. Meta-omic characterization of the marine invertebrate microbial consortium that produces the chemotherapeutic natural product ET-743. ACS Chem Biol 2011;6(11):1244−56.

[96] Schmidt EW, Donia MS, McIntosh JA, Fricke WF, Ravel J. Origin and variation of tunicate secondary metabolites. J Natural Prod 2012;75(2):295−304.

[97] Freeman MF, Gurgui C, Helf MJ, Morinaka BI, Uria AR, Oldham NJ, Sahl HG, Matsunaga S, Piel J. Metagenome mining reveals polytheonamides as posttranslationally modified ribosomal peptides. Science 2012;338:387−90.

[98] Piel J. A polyketide synthase-peptide synthetase gene cluster from an uncultured bacterial symbiont of *Paederus* beetles. Proc Natl Acad Sci Unit States Am 2002;99(22):14002−7.

[99] Brady SF, Chao CJ, Handelsman J, Clardy J. Cloning and heterologous expression of a natural product biosynthetic gene cluster from eDNA. Org Lett 2001;3(13):1981−4.

[100] Long PF, Dunlap WC, Battershill CN, Jaspars M. Shotgun cloning and heterologous expression of the patellamide gene cluster as a strategy to achieving sustained metabolite production. Chembiochem 2005;6(10):1760−5.